ALFRED-WEGENER-INSTITUT
HELMHOLTZ-ZENTRUM FÜR POLAR- UND MEERESFORSCHUNG

807
2026

Berichte
zur Polar- und Meeresforschung
Reports on Polar and Marine Research

Expeditions to Antarctica: ANT-Land 2024/25 NEUMAYER STATION III, Kohnen Station and Field Campaigns

Edited by

Julia Regnery, Peter Köhler, Thomas Matz and Christine Wesche
with contributions of the participants

HELMHOLTZ

Die Berichte zur Polar- und Meeresforschung werden vom Alfred-Wegener-Institut, Helmholtz-Zentrum für Polar- und Meeresforschung (AWI) in Bremerhaven, Deutschland, in Fortsetzung der vormaligen Berichte zur Polarforschung herausgegeben. Sie erscheinen in unregelmäßiger Abfolge.

Die Berichte zur Polar- und Meeresforschung enthalten Darstellungen und Ergebnisse der vom AWI selbst oder mit seiner Unterstützung durchgeführten Forschungsarbeiten in den Polargebieten und in den Meeren.

Die Publikationen umfassen Expeditionsberichte der vom AWI betriebenen Schiffe, Flugzeuge und Stationen, Forschungsergebnisse (inkl. Dissertationen) des Instituts und des Archivs für deutsche Polarforschung, sowie Abstracts und Proceedings von nationalen und internationalen Tagungen und Workshops des AWI.

Die Beiträge geben nicht notwendigerweise die Auffassung des AWI wider.

Herausgeber
Dr. Horst Bornemann

Redaktionelle Bearbeitung und Layout
Susan Amir Sawadkuhi

Alfred-Wegener-Institut
Helmholtz-Zentrum für Polar- und Meeresforschung
Am Handelshafen 12
27570 Bremerhaven
Germany

www.awi.de
www.awi.de/reports

Erstautor:innen bzw. herausgebende Autor:innen eines Bandes der Berichte zur Polar- und Meeresforschung versichern, dass sie über alle Rechte am Werk verfügen und übertragen sämtliche Rechte auch im Namen der Koautor:innen an das AWI. Ein einfaches Nutzungsrecht verbleibt, wenn nicht anders angegeben, bei den Autor:innen. Das AWI beansprucht die Publikation der eingereichten Manuskripte über sein Repositorium ePIC (electronic Publication Information Center, s. Innenseite am Rückdeckel) mit optionalem print-on-demand.

The Reports on Polar and Marine Research are issued by the Alfred Wegener Institute, Helmholtz Centre for Polar and Marine Research (AWI) in Bremerhaven, Germany, succeeding the former Reports on Polar Research. They are published at irregular intervals.

The Reports on Polar and Marine Research contain presentations and results of research activities in polar regions and in the seas either carried out by the AWI or with its support.

Publications comprise expedition reports of the ships, aircrafts, and stations operated by the AWI, research results (incl. dissertations) of the Institute and the Archiv für deutsche Polarforschung, as well as abstracts and proceedings of national and international conferences and workshops of the AWI.

The papers contained in the Reports do not necessarily reflect the opinion of the AWI.

Editor
Dr. Horst Bornemann

Editorial editing and layout
Susan Amir Sawadkuhi

Alfred-Wegener-Institut
Helmholtz-Zentrum für Polar- und Meeresforschung
Am Handelshafen 12
27570 Bremerhaven
Germany

www.awi.de
www.awi.de/en/reports

The first or editing author of an issue of Reports on Polar and Marine Research ensures that he possesses all rights of the opus, and transfers all rights to the AWI, including those associated with the co-authors. The non-exclusive right of use (einfaches Nutzungsrecht) remains with the author unless stated otherwise. The AWI reserves the right to publish the submitted articles in its repository ePIC (electronic Publication Information Center, see inside page of verso) with the option to "print-on-demand".

Titel: Neumayer-Station III aufgenommen während des Landeanflugs durch das Fenster der Polar6 (Foto: Lucas Weis, AWI)

Cover: Neumayer Station III, photographed through the window of Polar6 during the landing approach (Photo: Lucas Weis, AWI)

Expeditions to Antarctica: ANT-Land 2024/25 NEUMAYER STATION III, Kohnen Station and Field Campaigns

---

Edited by

Julia Regnery, Peter Köhler, Thomas Matz and Christine Wesche
with contributions of the participants

Please cite or link this publication using the identifiers

https://epic.awi.de/id/eprint/60770
https://doi.org/10.57738/BzPM_0807_2026

ISSN 1866-3192

ANT-Land 2024/2025

8 November 2024 – 22 February 2025

Neumayer Station III, *Kohnen Station* and Other Field Campaigns in Antarctica

Field Operation Manager *Neumayer Station III*
Thomas Matz and Peter Köhler

Scientific Coordinator
Julia Regnery

Logistical Coordinator
Christine Wesche

Contents

1. ÜBERBLICK UND EXPEDITIONSVERLAUF

Thomas Matz[1], Peter Köhler (Logistics)[1] [1]DE.AWI

Die Sommersaison ANT-Land 2024/25 an der *Neumayer-Station III* kann insgesamt als sehr erfolgreich angesehen werden. Die meisten der geplanten wissenschaftlichen, logistischen und technischen Aufgaben wurden wie vorgesehen abgeschlossen. Der reibungslose Ablauf wurde durch überwiegend günstige Wetterbedingungen während der gesamten Saison unterstützt.

Die An- und Abreise zur Station erfolgte erneut in Zusammenarbeit mit dem Norwegischen Polarinstitut (NPI). Insgesamt wurden sechs Interkontinentalflüge durchgeführt. Wissenschaftler und Techniker reisten gemeinsam mit norwegischen Kollegen von Bremen oder Oslo aus mit Charterflügen und einer Übernachtung in Kapstadt zur norwegischen Antarktisstation *Troll*. Von dort aus erfolgte die Weiterreise zur *Neumayer-Station III* – und die Rückreise am Ende der Saison – mit Flugzeugen vom Typ Basler und Twin Otter (bereitgestellt von White Desert) sowie mit der *Polar 6*. Darüber hinaus führte White Desert zwei Interkontinentalflüge zwischen Kapstadt und Wolf's Fang für den Personaltransport durch.

Insgesamt wurden im Laufe der Saison rund 85 Personen – darunter das 45. Überwinterungsteam – zur *Neumayer-Station III* gebracht.

Der offizielle Saisonstart war am 8. November 2024. In der ersten Saisonhälfte fanden umfangreiche Schulungen und Übergabeverfahren für das neue Überwinterungsteam statt. Aufgrund zunehmend ungünstiger Wetterbedingungen endete die Saison vorzeitig am 22. Februar 2025 mit dem Rückflug über die *Troll-Station* und Kapstadt nach Deutschland.

Trotz des verkürzten Zeitrahmens konnten zahlreiche wissenschaftliche Projekte, Feldkampagnen und dringend notwendige technische Arbeiten erfolgreich abgeschlossen werden. Neben der kontinuierlichen Datenerfassung durch die wissenschaftlichen Observatorien der Station wurden bedeutende Arbeiten auf dem Meereis, im Hinterland, in der Pinguinkolonie und im Rahmen einer groß angelegten Luftkampagne mit der *Polar 6* durchgeführt.

Im Rahmen der Überwachung des Vogelgrippevirus (HPAI: hochpathogene aviäre Influenza) wurde außerhalb der Hauptstation – in einem Wohncontainer – ein spezieller Quarantänebereich für Personen eingerichtet, die engen Kontakt zu Tieren auf dem Meereis hatten. Regelmäßige PCR-Tests stellten sicher, dass das Virus weder eingeschleppt noch verbreitet wurde. Bis zum Ende der Saison wurden keine Fälle des HPAI-Virus festgestellt.

Wie in früheren Berichten an Polar- und Meeresforschung geben die folgenden Kapitel einen Überblick über die Wetterbedingungen der Saison, den Verlauf der technischen Arbeiten und die Logistik. Darüber hinaus werden die jährliche Wartung der Observatorien, weitere wissenschaftliche Projekte an der *Neumayer-Station III* und Feldkampagnen unter Beteiligung des Alfred-Wegener-Instituts (AWI) vorgestellt.

SUMMARY AND ITINERARY

The ANT-Land 2024/25 summer season at *Neumayer Station III* can be considered very successful overall. Most of the planned scientific, logistical, and technical tasks were completed as intended. The smooth course of operations was supported by mostly favorable weather conditions throughout the season.

Travel to and from the station was again carried out in cooperation with the Norwegian Polar Institute (NPI). A total of six intercontinental flights were organized. Scientists and technicians traveled together with Norwegian colleagues from Bremen or Oslo via charter flights, with an overnight stopover in Cape Town, to the Norwegian Antarctic station *Troll*. From there, onward travel to *Neumayer Station III* – and return at the end of the season – took place using Basler and Twin Otter aircraft (provided by White Desert) as well as the *Polar 6*. In addition, White Desert operated two intercontinental flights between Cape Town and Wolf's Fang for personnel transport.

In total, around 85 people – including the 45th overwintering team – were transported to *Neumayer Station III* during the course of the season.

The official start of the season was 8 November 2024. During the first half of the season, extensive training and handover procedures were carried out for the new overwintering team. Due to increasingly unfavorable weather conditions, the season concluded early on 22 February 2025 with the return flight via *Troll* and Cape Town to Germany.

Despite the shortened timeframe, numerous scientific projects, field campaigns, and urgently needed technical work were completed successfully. In addition to the continuous data collection conducted by the station's long-term observatories, significant work was carried out on sea ice, in the hinterland, at the penguin colony, and in the framework of a major airborne campaign using the *Polar 6*.

As part of monitoring for the avian influenza virus (HPAI: Highly pathogenic avian influenza), a dedicated quarantine area was established outside the main station – within a residential container – for individuals who had close contact with animals on the sea ice. Regular PCR testing ensured that the virus was neither introduced nor spread. By the end of the season, no cases of the HPAI virus had been detected.

As in previous reports to Polar and Marine Research, the following chapters will provide an overview of the season's weather conditions, the course of technical operations, and logistics. Additionally, the annual maintenance of the observatories, further scientific projects at *Neumayer Station III*, and field campaigns involving the Alfred Wegener Institute (AWI) will be presented.

2. WEATHER CONDITIONS DURING ANT-LAND 2024/25 AT *NEUMAYER STATION III*

Holger Schmithüsen[1] [1]DE.AWI

Weather conditions at *Neumayer Station III* during ANT-Land 2024/25 (Fig. 2.2.1) were generally well within their climatologically normal range in terms of the basic meteorological parameters listed in Table 2.1. Nevertheless, after a relatively cold November the rest of the season was warmer than the long-term averages by about one standard deviation. This went along with rather calm wind conditions, which were below their long-term averages all through the season. Consequently, drift and white-out events were also less frequent than on average.

With -11.8°C November was 2°C cooler than normal. Night-time temperatures often fell below -20°C, while being between -5°C and -10°C at daytime for most days. The average wind speed during November was recorded to be 8.0 m/s, which is 0.7 STD below its long-term value. Hence, white-out was rather sparse, with an occurrence of 7% of the performed observations. The white-out events occurred during three storm events, one during the first week, one shorter event around 15 November and one towards the end of the month which reached 30 m/s on its peak.

December was dominated by high-pressure influence, with a noteworthy average pressure of 994.1 hPa, which is 1.3 STD above its long-term mean. There was one phase of low-pressure influence with constantly windy conditions reaching above 20 m/s within the first week of December. All white-out events were confined to that period in that month. The rest of the month was characterised by constant changing from calm and cloudy, with some precipitation, to sunny phases.

January, again, was rather calm and warm, but with more sunshine than December. There was only one storm event with wind speeds touching 20 m/s around 15 January.

The calm and warm period continued until the second half of February. On the 18 and 19 February there was one low-pressure system causing wind of around 15 m/s. Towards the end of February there was a second windy period which was longer and more around 20 m/s. This event also brought notable snowfall and accumulation.

Snow accumulation (Fig. 2.2) in 2024 was one of the lowest accumulation years since the respective measurement was started in 2010. With 37 cm of total snow accumulation, it was even slightly below the previous low-accumulation record in 2014 with 38 cm. These two years have a notable offset to the other years, which are all within 65 cm (2022) and 141cm (2021). Both years, 2014 and 2024, are characterised by a lack of accumulation after September. Actually, during ANT-Land 2024/25 there was only one event of persistent snow accumulation, namely the low-pressure passage at the end of February 2025.

Tab. 2.1: Monthly averages of meteorological parameters at *Neumayer Station III*. In parentheses are the long-term mean values for the time since 1981 (1992 for white-out), together with the standard deviation. All values are calculated from the 3 hourly synoptic observations. Note that at 3 UTC white-out is not observed, which biases the frequency of occurrence to too low values.

	Temperature	**Pressure**	**Wind Speed**	**White-Out**
November 2022	**-11.8°C** (-9.8 ± 1.4)°C	**979.9 hPa** (984.4 ± 4.7) hPa	**8.0 m/s** (9.2 ± 1.7) m/s	**7%** (22 ± 12)%
December 2022	**-3.9°C** (-4.8 ± 0.8)°C	**994.7 hPa** (987.1 ± 5.8) hPa	**5.9 m/s** (7.3 ± 1.4) m/s	**0%** (16 ± 10)%
January 2023	**-2.7°C** (-4.1 ± 1.0)°C	**986.0 hPa** (988.9 ± 4.1) hPa	**4.7 m/s** (6.5 ± 1.2) m/s	**0%** (12 ± 8)%
February 2023	**-5.8°C** (-8.0 ± 1.6)°C	**986.6 hPa** (986.8 ± 3.7) hPa	**6.2 m/s** (7.5 ± 1.5) m/s	**0%** (14 ± 9)%

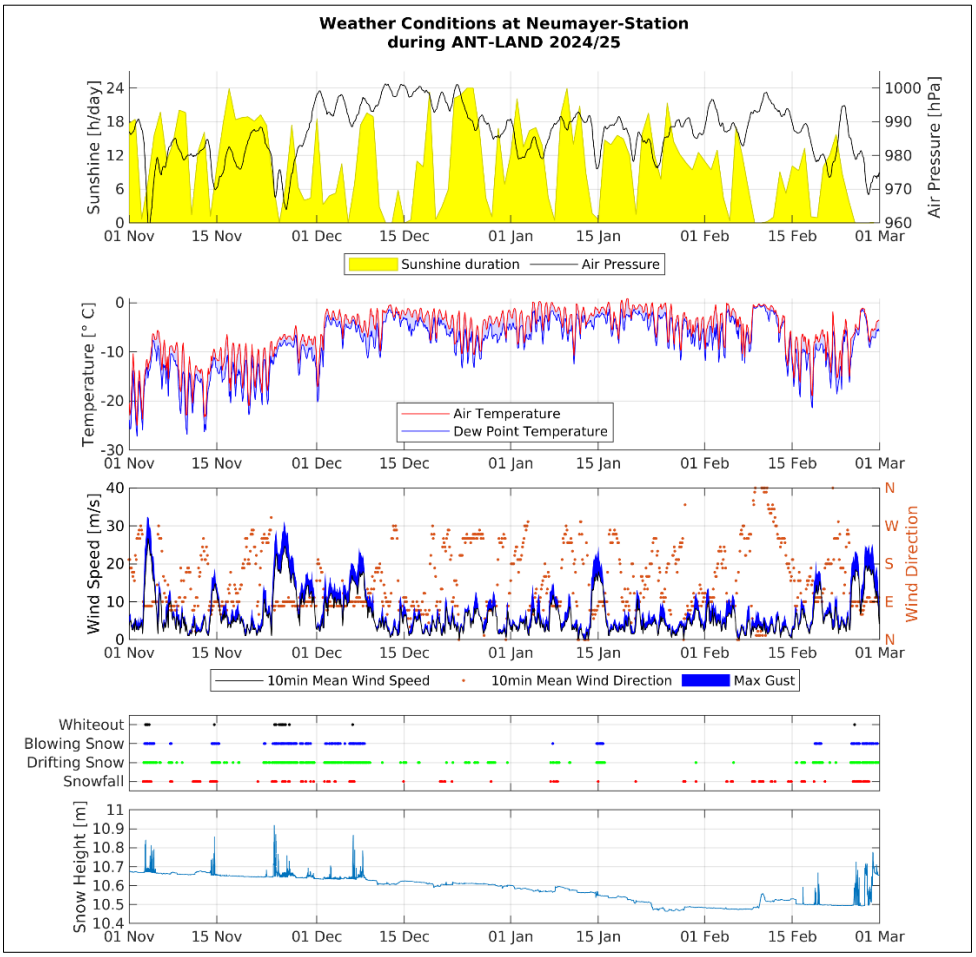

Fig. 2.1: Weather conditions at Neumayer Station III during ANT-Land 2024/25

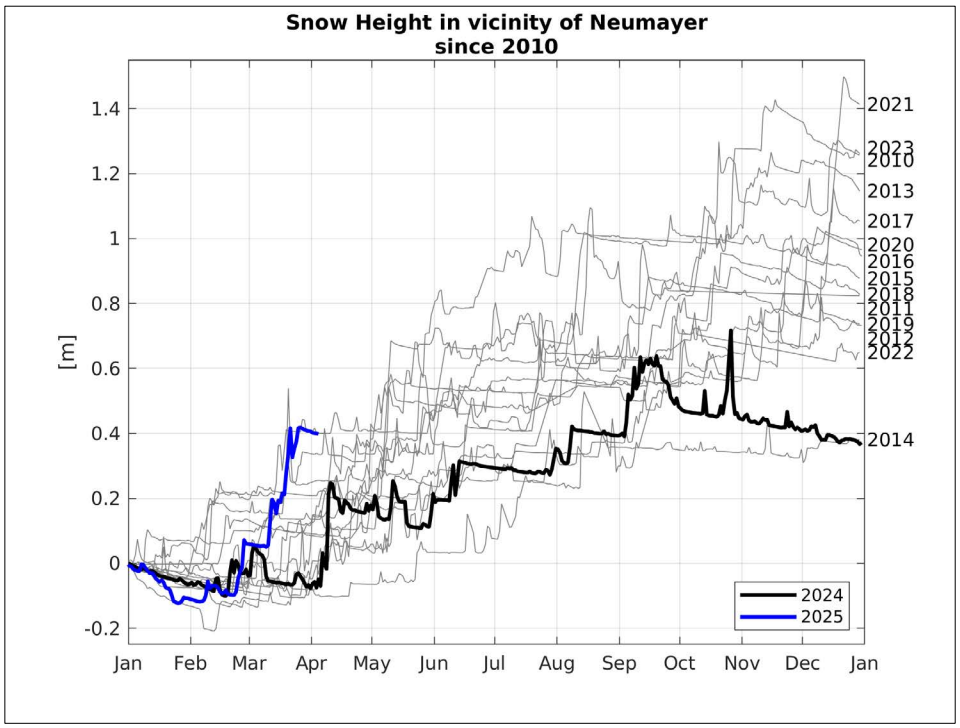

Fig. 2.2: Snow height measured in the vicinity of Neumayer Station III with sensor "Jenoptik SHM30" from 2010 until December 2022, and with its successor "Lufft SHM31 from December 2022 until April 2025. Most recent data is shown in blue, accumulation of 2024 in black, earlier years in grey. All data shown here is relative to the snow height at the beginning of the respective year. Since October 2011 the measurements are conducted near the Spuso (1,500 m south of Neumayer Station III), before the instrument was mounted at the meteorological mast some 300 m south-east of the main station building.

References

Schmithüsen H (2020) Meteorological synoptical observations from Neumayer Station (1981-01 et seq) [Dataset publication series]. Alfred Wegener Institute, Helmholtz Centre for Polar and Marine Research, Bremerhaven. PANGAEA. https://doi.org/10.1594/PANGAEA.911242

Schmithüsen H (2023) Continuous meteorological observations at Neumayer station (1982-03 et seq) [Dataset publication series]. Alfred Wegener Institute, Helmholtz Centre for Polar and Marine Research, Bremerhaven. PANGAEA. https://doi.org/10.1594/PANGAEA.962313

Schmithüsen H (2023) High resolved snow height measurements at Neumayer Station, Antarctica (2010 et seq) [Dataset publication series]. Alfred Wegener Institute, Helmholtz Centre for Polar and Marine Research, Bremerhaven. PANGAEA. https://doi.org/10.1594/PANGAEA.958970

Schmithüsen H, Conrat P (2025) High resolved snow height measurements at Neumayer Station, Antarctica, 2024 [Dataset]. Alfred Wegener Institute, Helmholtz Centre for Polar and Marine Research, Bremerhaven. PANGAEA. https://doi.pangaea.de/10.1594/PANGAEA.979985

3. STATION OPERATIONS

Thomas Matz[1], Peter Köhler (Logistics)[1] [1]DE.AWI

The first flight NPI-F1 together with the Norwegian colleagues took off on 1 November 2024 from Bremen to Oslo, Prague and a landing in Cape Town. With a stopover for refuelling, and 5 hotel nights in Cape Town due to bad weather at *Troll Station*, the first group with 26 scientists, technicians and the field operation manager (FOM) reached *Troll Station* in Antarctica on 7 November 2024. After another night at *Troll Station*, we flew to *Neumayer Station III* on 8 November 2024 and were warmly welcomed by the wintering team for the start of the summer season.

The scientific campaigns and technical work, such as the station elevation (twice), began. In the course of this, further maintenance and repair work by the technical team took place. Technicians from external companies also started with their maintenance of a technical plant and vehicles.

Already on 15 November 2024 the second group with 15 persons reached *Neumayer Station III* with the NPI-F2 flight, including the new wintering team.

The station was occupied by 49 people. Skidoos and sleds were now in full use for trips over the sea ice and to the penguin colony by three different scientific teams.

The training of the new wintering team members began in the individual disciplines. Towards the end of November, maintenance of the outdoor geophysics facilities at Olymp and Watsmann began, interrupted by bad weather. Two Pistenbullys, living containers and technical equipment were deployed.

Contact was made with the previously announced group from SWIDAR RINGS on 8 December 2024. The group of 14 persons travelled with two Twin Otters and two helicopters from *Rothera Station* and spent a few hours at *Neumayer Station III*. After refuelling the aircraft, they continued their flight with the scientific measurements to *Troll Station* and on to Novo Airfield.

The month of December was characterized by various projects and appointments. People departed on the NPIF3 flight and others arrived.

Between these events, the station was handed over to the new wintering team on 16 December 2024.

On the next day, the geophysics team took off on the three-day maintenance of the seismometer station at Utpostane with a Twin Otter from White Desert.

Meanwhile, the supply traverse for the Finnish and Swedish teams to the *WASA/Aboa Station* was being prepared with three snow groomers and lots of equipment on heavy-duty sledges. A colleague from the Finnish logistics who had previously arrived on the F3 flight at *Neumayer Station III* then accompanied the journey to *Aboa Station*. They arrived there safely on 24 December 2024. In the days that followed, equipment was stowed and the Finnish and Swedish colleagues were supported with work on the stations and their power supply. The traverse reached the *Neumayer Station III* on 3 January 2025.

Our meteorology colleagues were able to carry out maintenance on the automatic weather station in December. The journey there took place with snow mobiles. The maintenance of the system on Sörasen was carried out using both Arctic Trucks at the beginning of January.

Another trip was carried out by the geophysics department in the last days of December to maintain the seismometer site at Forstefjell, 240 km away. This trip was also carried out with both Arctic Truck vehicles and sledges. They returned safely to *Neumayer Station III* on New Year's Eve.

All trips by scientists and technicians were supervised and monitored by the Field Operations Manager from *Neumayer Station III*.

In preparation for the return shipment of freight by the cargo ship *Silver Mary* in January, the first containers were stowed towards the end of December/beginning of January, provided the capacity of empty containers allowed.

Neumayer Station III was supplied by *Polarstern*. The ship was announced for 15 January 2025. Due to the approaching bad weather, the supply and thus the arrival of the ship was brought forward. *Polarstern* arrived at the northern point at the ice shelf at around midday on 11 January 2025.Accordingly, preparations were made at *Neumayer Station III* in advance for the safe unloading process and many other coordination measures together with the Shipping company Laeisz. With the start of the unloading on 11 January, the departure on flight WD13 of the old wintering team, scientists from the sea ice campaigns and the change of the Field Operations Manager took place at the same time. The arrival of *Polarstern* began in calm weather, with the unloading of 39 containers. A storm delayed the second supply stage, which included the bulk of the fuel delivery, by several days. This was eventually completed during a night-time transfer without incident end of January. Immediately afterward, the supply ship *Silver Mary* took over 38 containers of returning equipment and waste under significant time pressure.

The expected call of *SA Agulhas II* was repeatedly postponed and ultimately cancelled at short notice. SANAP had previously requested AWI's assistance in transporting a fuel tank container to the SANAP Summer Base. Due to the cancellation, this support could not be carried out. The structural condition of SSS1 remains increasingly critical.

An Austrian film team documented the station’s logistics. Their additional requests were generally supported by the station community.

With the arrival of the WD1 flight crew, the station was fully occupied with 50 people. Due to the condition of the accommodations, the summer camp had to be used to provide additional sleeping space. A four-person traverse to Svea and Kottas, involving glaciological and geophysical tasks, was successfully completed with relatively low effort despite rough, icy snow surfaces.

In terms of science, new observatories were introduced and put into operation. These were presented to station members in talks and site visits, which were met with great interest.

Several feeder flights from ULTIMA and White Desert were also managed, including refuelling stops and weather-related holds. The WD Basler GOOU remained on-site for the final transfers of NPI flights F5 and F6. Favorable weather conditions during this period enabled numerous outdoor activities.

The planned return flight of the summer team posed a logistical challenge. Due to deteriorating weather at *Neumayer Station III*, an early departure was necessary, which would have meant several days of waiting at *Troll Station*. As 70 people were already present there and a gastrointestinal infection was circulating, the Norwegian team agreed to move the team from

the *Neumayer Station III* departure forward by four days – allowing them to travel with flight F5x instead of the originally planned F6.

3.1 General Flight Operations

The intercontinental flights for the ANT-Land 2024/25 summer season to *Neumayer Station III* via *Troll Station* were carried out from the partner Norwegian Polar Institute (NPI). All flights were operated by passenger aircrafts and departed from Europe, Bremen and Oslo via Cape Town to Antarctica. This route was also chosen for the return transport. A few flights ended in Cape Town. The rest of the journey was then via the normal scheduled service to Europe.

Feeder flights from Troll Airfield to *Neumayer Station III*, but also for logistical scientific flights were performed with Basler and Twin Otter aircraft from White Desert. The flights were partly supported by the *Polar 6*.

During the season, a total of six intercontinental flights were offered and used by the NPI to transport personnel and cargo. The Wolf's Fang Runway from White Desert was also used on a few flights to transport some persons and cargo to and from *Neumayer Station III*.

Neumayer Station III was used by British Antarctic Survey personnel travelling through in November to reach *Halley 6 Station* by aircraft.

The *Polar 6* was able to make the jump from *Rothera Station* to *Neumayer Station III* on 17 November 2024. The crew of three stayed until 22 November 2024 and then transferred with *Polar 6* to *Troll Station*.

The scientists and technicians for the flight campaign arrived at Wolf's Fang on White Desert Flight WD06. They were picked up there by *Polar 6*. The aircraft was then equipped with scientific equipment and the measurement flights began.

During the flight campaign, *Polar 6* was stationed at Troll Airfield. From there, different scientific measurement flights were performed. Coordination took place proportionally from *Neumayer Station III*.

With a logistics flight from White Desert, the geophysical science team at *Neumayer Station III* carried out maintenance work on the seismometer site at Utpostane.

About 5 km north of *Neumayer Station III*, a skiway of White Desert was established for the majority of the season once again. This runway was used to allow tourists to visit the Emperor penguin colony at Atka Bay. A large proportion of aircraft movements in the Atka Bay region are due to increased tourist traffic.

3.2 Technical Operations

All preparatory work necessary for the start of the season was carried out by the wintering team in October. This concerns the preparation of the 1,500 m long snow runway for the Basler and Twin Otter ski-equipped aircraft, but also the provision of storage and functional containers were transported from the winter storage to the station for the summer operation.

After the five-day stay at Cape Town and one another day at *Troll Station* due to bad weather, the technical team also arrived at *Neumayer Station III* and work started immediately.

Two station elevations were successfully completed as well as many of the planned maintenance tasks. The outer platforms were routinely raised.

Station maintenance works and repairs

In the months of November and December two station elevations could be carried out as planned. As the station was lifted twice within a summer season, the 32th station elevation started on 10 November 2024 and was completed on 23 December 2024.

In November, the wastewater treatment plant was serviced by a technician from the manufacturer company.

The elevator of the station was serviced and repaired by the technician team.

A major focus was on energy modernization: two wind turbines of the type F144-50 were installed, one of which has already been commissioned. Additionally, the conversion to energy-efficient LED lighting began, with approximately 25% of the station's lighting replaced so far. New control areas were also established, allowing entire sections of the station to be dimmed when occupancy is low, thus saving energy.

In parallel, the entire control system for the air handling units was renewed. This required operating the station intermittently on the emergency diesel generator, which led to several short-term power outages.

Another key project was the installation of the MAGSI observatory. The sensitive measurement equipment was housed in a specialized container and, after successful calibration, has been put into operation for scientific long-term measurements.

Significant work was also done inside the station: the entire wooden flooring on Deck 0 was renewed to improve safety and durability. In addition, the walls in all corridors, various laboratories, and office areas were repainted. These renovation efforts were urgently needed, as the station building has been in nearly continuous use for over 15 years and has experienced considerable wear. The fresh coats of paint not only enhance the station's appearance but also help preserve the interior spaces.

In the tween deck, storage space was significantly expanded with around 500 m² of new shelving installed, greatly improving material logistics and accessibility.

The station's supply was managed through two ship calls, during which approximately 35 to 40 containers each, along with annual supplies of polar diesel and gasoline, were handled. All loading and unloading operations were carried out by the station's technical team. Originally, a single continuous call with *Polarstern* was planned, but due to weather conditions, it had to be split into two separate calls. The subsequent call with the *Silver Mary* was particularly efficient and safe, with smooth and uninterrupted cargo handling. A third call by the *S.A. Agulhas II*, organized by the South African National Antarctic Programme (SANAP), was repeatedly announced but ultimately cancelled at short notice. Cooperation with SANAP continues to be unpredictable, complicating joint logistical planning.

Despite weather-related limitations, the season was technically very successful.

Actions in the terrain, airfield and routes

Around the station terrain maintenance was necessary as every season. Snowdrifts on the outer facilities were removed.

Several times during the season, the 1,500 m long airfield and the taxiway were groomed. The routes to the surrounding scientific measurement facilities such as the Single Penguin Observation and Tracking (SPOT) observatory and the Perennial Acoustic Observatory in the Antarctic Ocean (PALAOA) as well as to the winter storage facility were prepared.

Scientific/technical outdoor facilities

During the ANT-Land 2024/25 summer season, numerous technical measures were successfully implemented around *Neumayer Station III* to support ongoing scientific activities.

A key focus was the relocation of the meteorological observatory. At its new site, a mast was erected, sensors were connected, and the system was commissioned – ensuring improved conditions for long-term atmospheric measurements.

Both the air chemistry platform and the former EDEN platform had to be elevated due to snow accumulation. A working container for the ORACLES project was installed on the raised EDEN platform. In front of it, a protective hangar made from 20-foot containers with a wooden roof was built to safely store the project's helium balloon during storms. The platform was also equipped with an electrical cabinet and a cable reel system to support future operations.

At the magnetic observatory, a new access module was installed, allowing larger equipment to be brought into the tunnel for future maintenance – an important step toward improved serviceability.

The infrasound array measuring fields operated by BGR were elevated by the technical team and serviced by BGR staff. All boxes housing sensitive sensors were replaced during this season.

At the end of the season, all outdoor storage containers were relocated to the winter storage area, which was moved further west to ensure a safe distance from the ice edge. Heavy fuel tanks were placed on snow mounds to allow easier towing by tracked vehicles during the winter.

IT and communication

During the ANT-Land 2024/25 season, the two StarLink systems for internet access which had been provisionally installed last summer for testing purposes were permanently integrated into the station's data network. The connection to the institute in Bremerhaven is now established using StarLink via VPN tunnel. This results in much faster data transfer rates compared to the VSAT system which is still being maintained as a backup. For this purpose, the previously used bandwidth management system (PacketShaper) was decommissioned and replaced by a router with the "ntop nedge" software. The initial operating results are satisfactory.

Updating the hardware and software in the building management system made it possible to revise the connection between these systems and the DSHIP database. The interface was changed from NMEA telegrams to MODBUS/TCP. We expect this to result in simpler and more comprehensible structures and thus more reliable operation.

Extensive routine work was carried out in the station's IT and communications area. This includes the installation of a Wi-Fi link between the station and the EDEN platform (now used for the MAGSI project).

Vehicle Engineering

Throughout the ANT-Land 2024/25 summer season, a technician from the manufacturer Kässbohrer was stationed at *Neumayer Station III* to carry out comprehensive maintenance on the 18 PistenBully 300 Polar vehicles, ensuring their operational readiness.

Once again, vehicle PB29 suffered a major failure, similar to the issues experienced during the 2022/23 season. A serious drivetrain defect was identified, and the vehicle was prepared for return transport in January 2025 on a heavy-duty sled without tracks or snow blade. It will be repaired at the manufacturer's facilities. The damage is currently being assessed in collaboration with Kässbohrer. As a result, maintenance intervals may be shortened in the future, and heavily stressed components of the hydraulic drive will be replaced preventively. Replacement parts that are refurbished by the manufacturer and installed at *Neumayer Station III* will need to be procured.

At the beginning of the season, the two Arctic Truck vehicles were serviced by a company technician and were subsequently deployed on a roughly 1,000 km traverse to geophysical measuring stations, including sites in the Kottas Mountains. They successfully delivered valuable data from remote regions.

During another traverse involving a large living container transported on an extra-wide sled, damage to the sled’s front axle was detected. The container was temporarily transferred to a standard heavy-duty sled. Repairs are planned for the 2025/26 summer season once spare parts are available.

The aging snowmobile fleet was replaced with new vehicles, which arrived at the station in January 2025 along with other supplies during the ship unloading. The old snowmobiles and spare parts were sent back.

For sea ice operations, the remaining older snowmobiles were serviced and repaired as needed in November and December. Minor maintenance work – especially wood and welding repairs – was carried out on their sleds. As in previous seasons, sleds with major damage were replaced entirely.

3.3 Ship Operations

Supply Call of Polarstern and Silver Mary in January 2025

The resupply of *Neumayer Station III* by the research vessel *Polarstern* was originally scheduled for mid-January 2025 but was brought forward to 11 January 2025 due to approaching bad weather. Accordingly, the logistical preparations for unloading at the station were intensified.

On 11 January, unloading began at midday at the northern pier, with medical equipment being delivered simultaneously by helicopter. All procedures were coordinated in detail beforehand between the *Polarstern*, the Field Operations Manager (FOM), and the expedition leader.

On the same day, the exchange of the FOM took place via Wolf’s Fang. The new FOM took over the complex ship supply operations within the first hours of his arrival. Extensive telephone coordination between the FOMs and the technical team ensured a smooth, accident-free operation. Additionally, there were extensive visits by scientists and station personnel to each other’s research sites.

A particular challenge was the rescheduled waste disposal ship *Silver Mary* call on 22 January 2025. During a period of bad weather, containers had to be unloaded and reloaded in time for disposal – a short but significant strain on the technical team.

The previously announced call of the *SA Agulhas* was repeatedly postponed and ultimately cancelled at short notice. SANAP requested assistance from AWI to tow a 20-foot fuel container from the ship's berth to the SANAP Summer Base and exchange it for an old empty container.

3.4 Kohnen Station

Kohnen Station was not opened this summer season.

4. *NEUMAYER STATION III*

4.1 Yearly Maintenance of the Meteorological Observatory Neumayer

Sebastian Berger, Oliver Calek, Pablo Conrat Fuentes, Christian Schröder DE.AWI
not in the field: Holger Schmithüsen*
* holger.schmithuesen@awi.de

Grant-No. AWI_ANT_1

Outline

The Meteorological Observatory Neumayer is an ongoing project that is dedicated to climate monitoring. The observatory is permanently attended by a meteorologist that changes with the station's crew every year. During austral summer major maintenance work is performed.

Objectives

The Meteorological Observatory Neumayer is dedicated to monitor essential climate variables in high quality. The station is part of various international networks, such as the Baseline Surface Radiation Network (BSRN), the Network for the Detection of Atmospheric Composition Change (NDACC), the GCOS Reference Upper Air Network (GRUAN) and the Aerosol, Clouds and Trace Gases Research Infrastructure (ACTRIS).

In order to guarantee high quality time series, the observatory is normally serviced once per year by permanent staff. All instrumentation and operating procedures are checked, and the yearly changing new staff is trained on site.

Fieldwork

In the field season 2024/25 instrumentation and operating procedures of the following atmospheric observations were handed over from one meteorologist to the next:

- 3-hourly synoptic observations
- daily upper-air soundings
- weekly ozone soundings
- continuous surface radiation and meteorological mast measurements
- single column precipitation radar
- ACTRIS components: cloud radar, micro pulse liar and doppler wind lidar

During this season all planned maintenance tasks were carried out. In addition, the meteorological measuring field was set up at a new location approximately 900 m south-east of the station.

- Concerning automatic weather stations (AWS) the following was carried out:
- AWS Søråsen: serviced as planned
- AWS Halfvarryggen: serviced as planned
- AWS Kohnen: not serviced, no Kohnen activities in season 2024/25. Service in season 2025/26 necessary

Within DROMLAN, the Meteorological Observatory of the *Neumayer Station III* continued to support the weather forecasting services offered by StormGeo. This holds for all activities in Dronning Maud Land, especially all aircraft operations. General weather observations and if needed landing weather observations at *Neumayer Station III* for the DROMLAN community were provided as usual.

Data management

Environmental data will be archived, published and disseminated according to international standards by the World Data Center PANGAEA Data Publisher for Earth & Environmental Science (https://www.pangaea.de) within two years after the end of the expedition at the latest. By default, the CC-BY license will be applied. Data from the ACTRIS instruments are archived on the cloudnet portal (https://cloudnet.fmi.fi/).

Furthermore, data is supplied to various international networks, mainly those organised within the World Meteorological Organisation (WMO).

This expedition was supported by the Helmholtz Research Programme “Changing Earth – Sustaining our Future” Topic 1, Subtopic 1 and 2; Topic 2, Subtopic 1, 2 and 3.

In all publications based on this expedition, the **Grant No. AWI_ANT_1** will be quoted and the following publication will be cited:

Alfred-Wegener-Institut Helmholtz-Zentrum für Polar- und Meeresforschung. (2016a). *Neumayer III and Kohnen Station* in Antarctica operated by the Alfred Wegener Institute. Journal of large-scale research facilities, 2, A85. http://dx.doi.org/10.17815/jlsrf-2-152.

4.2 Long-term Trace Gas and Aerosol Observations at *Neumayer Station III*

Zsófia Jurányi[1*], Alexander Schulz[1], Lukas Weis[1], Tim Bösch[1]
not in the field: Olaf Eisen[1,2], Valerie Reppert[1,2]
* zsofia.juranyi@awi.de

[1]DE.AWI
[2]DE.Uni-Bremen

Grant-No. AWI_ANT_2

Objectives

The air masses over Antarctica are the cleanest in the Earth's atmosphere, making it an ideal natural laboratory for studying atmospheric conditions similar to those before industrialization. This unique environment allows for research on the background composition and natural biogeochemical cycle of aerosols. Nowadays, minor anthropogenic emissions arising from fossil fuel combustion during research and tourism activities have to be considered as well.

The primary mission of the Neumayer Trace Gas and Aerosol Observatory is to collect continuous, year-round data on key gaseous and particulate trace components in the coastal Antarctic troposphere. Long-term atmospheric monitoring is essential for understanding the current Southern Ocean climate system and its main driving forces. Another aspect of studying atmospheric chemistry in Antarctica is the need to interpret records of archived trace compounds in ice cores and their relation to environmental conditions. Provided the present atmospheric chemistry and the physical-chemical processes of air to snow transfer are well characterized, we can use such records to derive information about climate, composition and chemistry of the paleo-atmosphere.

The Neumayer Trace Gas and Aerosol Observatory is one of only very few comparable clean air laboratories operated in Antarctica partly established since 1983. There is a strong scientific cooperation with the meteorological observatory. Both observatories are part of the GAW (Global Atmosphere Watch) global station network.

Part I Atmospheric measurements: Aerosol and trace gases

Fieldwork

The necessary fieldwork could be completed to run successfully the observatory for another year. In the summer season the operation of the observatory was taken over by the new air-chemistry overwinterer Lukas Weis from Tim Bösch. The on-site training of Lukas was successfully completed by Tim and by the observatory supervisor.

The following installations, repairs and maintenance were performed by Zsófia Jurányi and Alexander Schulz, with the help of Lukas Weis:

- Installation of the new data logging system (DT85) to replace the old system (DT800) which broke during 2024 (including the on-site substitute)
- Thorough checking of the grounding of the different systems (no problems could be found)

- Adaptation of the DT85 programming
- Installation of the SP2-XR (single-particle soot photometer, extended range) instrument to measure BC concentration (unfortunately the instrument broke down after one day of operation, no repair was possible)
- Set-up and calibration and communication testing of the new integrating Nephelometer Acoem Aurora NE-300, to run parallel at least one year and then to replace the currently running, almost 30 years old Nephelometer (TSI 3563)
- Installation of the LAS (Laser Aerosol Spectrometer) which was back in Germany in 2024 for service, unfortunately the instrument broke down shortly after the installation (no repair was possible, instrument was sent back to Germany).
- Installation of 2 naneos Partector Pro instruments to test the capability of the miniature sensors for low concentration measurements for future mobile Antarctic applications
- Measurements with 2 naneos Partector Pro instruments during a geophysics and glaciology traverse to the Kottas Mountains to measure the aerosol concentration and size distribution for the first time from the Neumayer Station III towards the Antarctic Plateau.
- Succesfull integration of the ozone monitor O3AWI3 into the data acquisition system, demounting the O3AWI2 instrument
- Installation of the MAX-DOAS controller and replacement of the acquisition computer. Was successful, however after that a new (until then not known) problem was discovered, that the cooling of the system was not functioning anymore. Attempts to repair was not successful.
- Spontanous collaboration with Michael Hartje to identify systematic electromagnetic disturbances within the Neumayer Station III electric installation – a fully controlled black-out scenario had been conducted to identify potential influence on local electromagnetic emissions from the trace gas and aerosol observatory instrumentations – report will be provided by that project
- Collaboration with the projects VACCINE and ORACLES
- Other small repairs and maintenances to enable optimal operation over the winter season

Preliminary (expected) results

We completed an in-depth evaluation and validation of the established long-term observations (LTO) from the year 2024. Like in previous years, the outcome of the completed analysis revealed the high quality of the measured time series including among others: aerosol number concentration, aerosol number size distribution, black carbon (BC) concentration, aerosol scattering coefficients, surface ozone concentration with generally negligible data gaps, occasionally caused by short temporary instrumental problems or routine service operations.

The following graphs (Fig. 4.2.1 to 4.2.5) show exemplarily the obtained validated time series of these parameters for the year 2024. Further information on metadata can be found in data sets archived in PANGAEA (e.g.: https://doi.pangaea.de/10.1594/PANGAEA.945533):

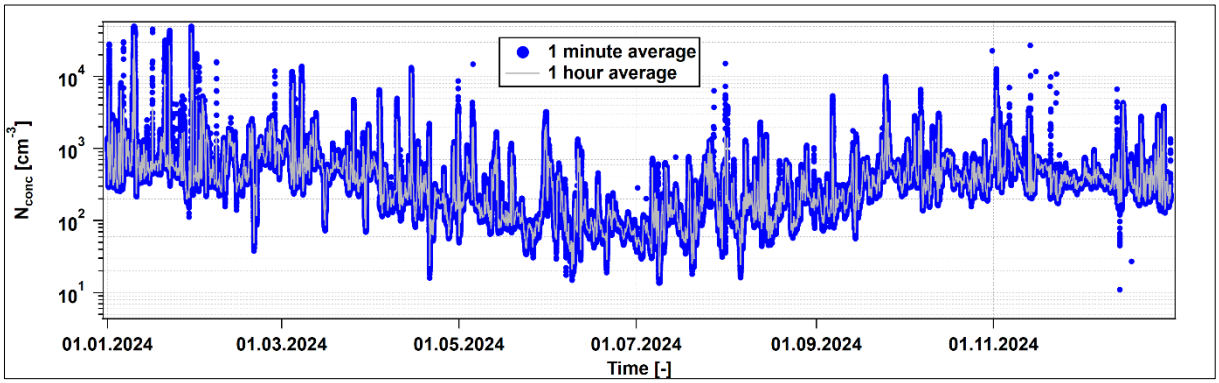

Fig. 4.2.1: Time series of the aerosol number concentration (N_{conc}) at Neumayer Station III during the year 2024, as measured by a TSI type CPC 3775 condensation particle counter. This instrument detects all particles above the lower 50 % cut-off diameter of 4 nm. The blue markers show the original 1-minute data, whereas the grey line shows the 1-hour averages.

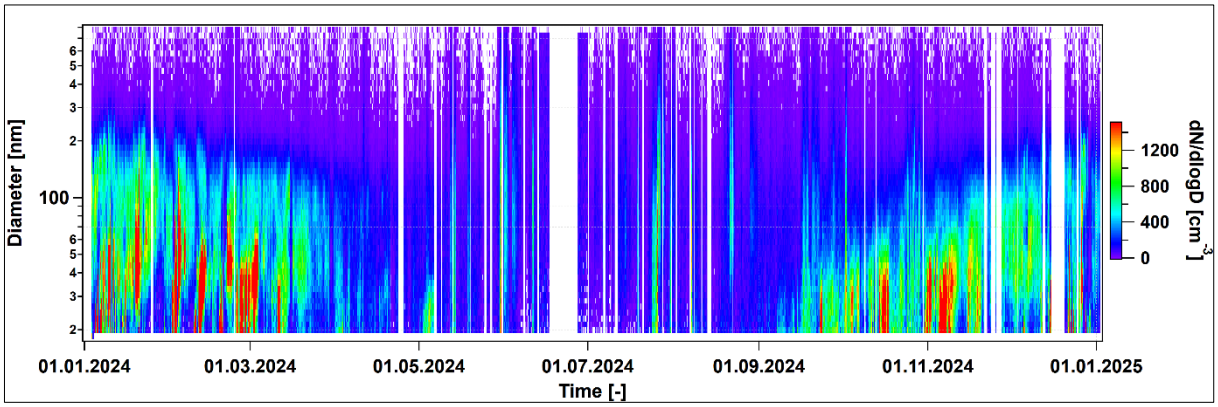

Fig. 4.2.2: Time series of the aerosol number size distribution at Neumayer Station III during the year 2024, as measured by an electrical classifier (TSI 3081) and a condensation particle counter (CPC 3776). The graph shows 1-hour averages, the original data has a time resolution of 10-minutes.

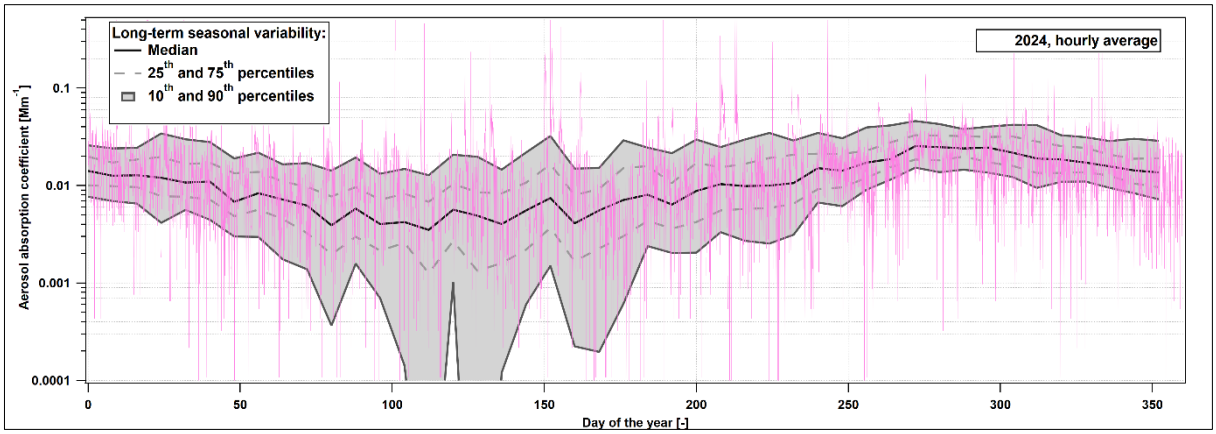

Fig. 4.2.3: The seasonal variability of the absorption coefficient as measured by the multi-angle absorption photometer (MAAP) in the year 2024 (pink line). The black/grey lines and shading show the long-term statistics.

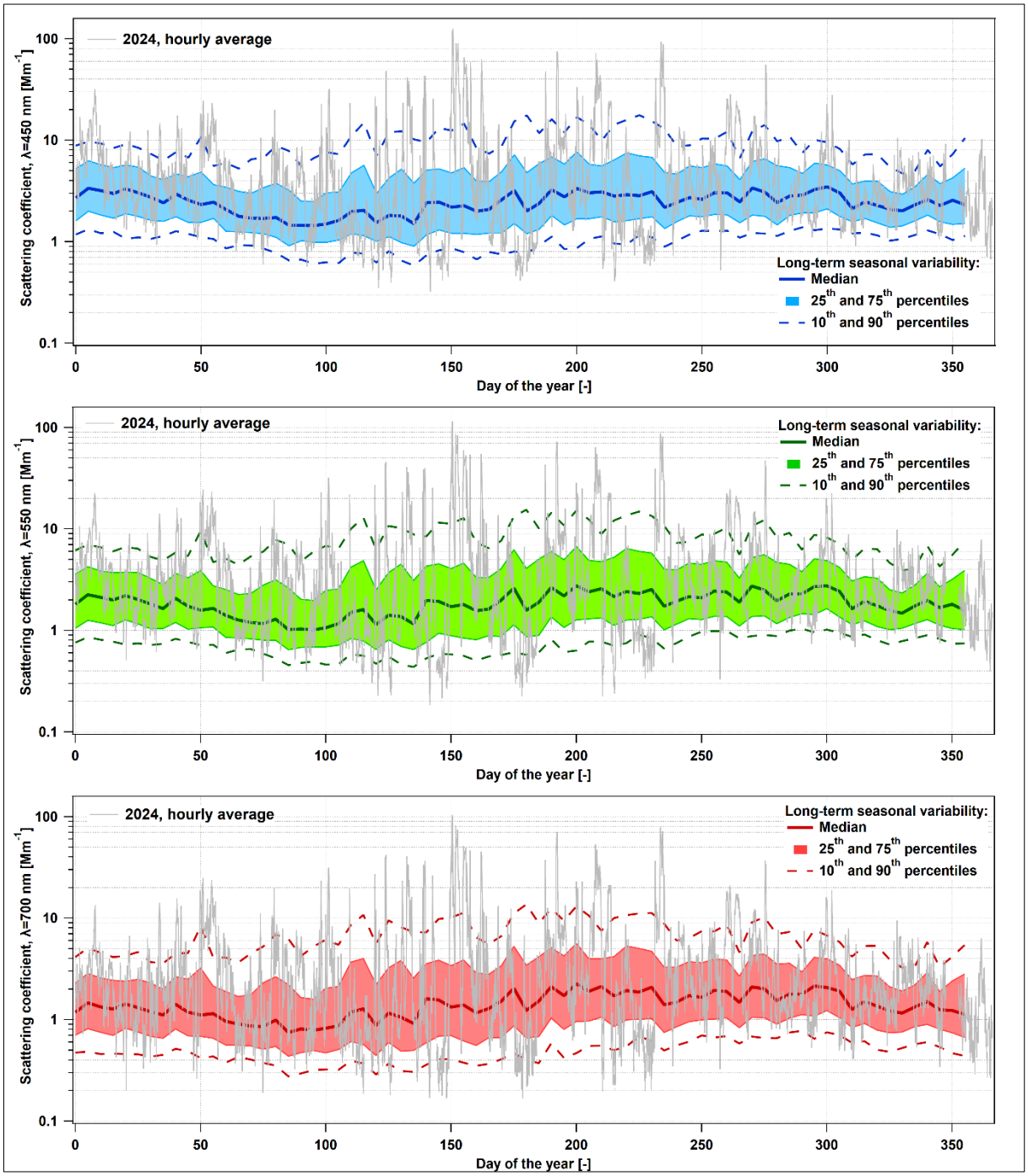

Fig. 4.2.4: The seasonal variability of the scattering coefficient as measured by a 3-wavelength integrating nephelometer (TSI 3563) in the year 2024 (grey lines). The colored lines and shaded areas show the long-term statistics. The three different panels belong to the measurements at the 3 different wavelengths of light (450, 550 and 700 nm). The presented data shows 1-hour averages, the original data has a 1-minute time resolution.

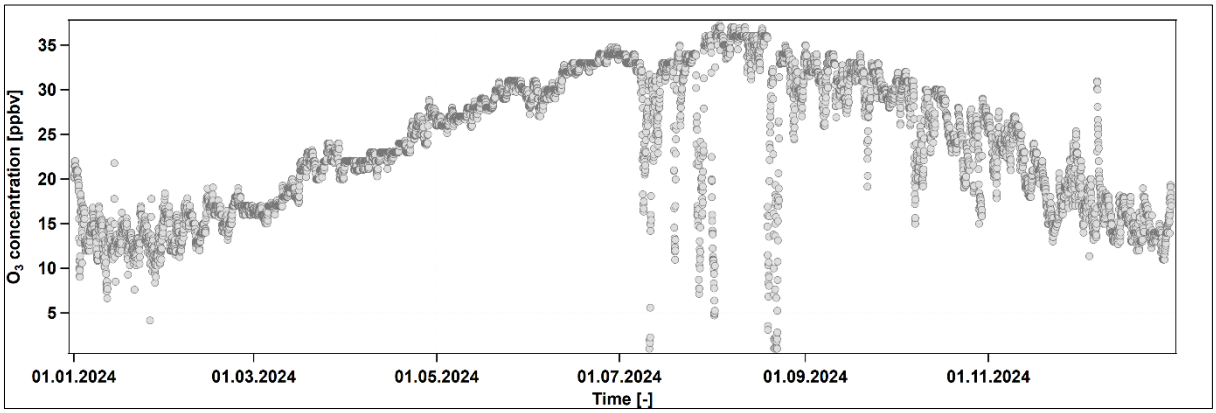

Fig. 4.2.5: Time series of the ozone concentration (ppbv: parts per billion by volume) at Neumayer Station III for the year 2024 (measured with an UV photometer O3 41M, Environnement). Presented data are one-hour averages based on originally one-minute data.

Data management

In the meanwhile, we archived the long-term observations from the year 2024 after thorough evaluation in the GAW repository. The submitted data are available at NILU/EBAS under: https://ebas-data.nilu.no/ (note: accept policies, select “Germany” – “Neumayer” and desired data).

Environmental data will be archived, published and disseminated according to international standards by the World Data Center PANGAEA Data Publisher for Earth & Environmental Science (https://www.pangaea.de) within two years after the end of the expedition at the latest. By default, the CC-BY license will be applied. The 2024 data is currently under validation for the submission to the PANGAEA database.

This expedition was supported by the Helmholtz Research Programme “Changing Earth – Sustaining our Future” Topic 1, Subtopic 2.

In all publications based on this expedition, the **Grant No. AWI_ANT_2** will be quoted and the following publication will be cited:

Alfred-Wegener-Institut Helmholtz-Zentrum für Polar- und Meeresforschung. (2016a). *Neumayer III* and *Kohnen Station* in Antarctica operated by the Alfred Wegener Institute. Journal of large-scale research facilities, 2, A85. http://dx.doi.org/10.17815/jlsrf-2-152

Part II Snow accumulation and glaciological studies

Work in field

In order to put impurity content retrieved in snow, firn and ice cores into the glaciological context, it is important to have a reliable record of the surface mass balance. To this end the long-time observation of snow accumulation measurement at stake fields were continued and conducted bi-weekly at the Pegelfeld Süd and weekly at the Pegelfeld SpusoIII. In addition, monthly measurements of density in snow pits were performed near the SpusoIII until December 2024, but will be reduced to yearly measurements at the beginning of summer from 2025 on.

Preliminary (expected) results

With the completion of the year 2024 the snow surface accumulation measurements at the Pegelfeld Süd completed 33 years of measurement. After the two years 2021 and 2023 with considerably higher than normal snow accumulation at the surface, in 2023 with a total of 164 cm at Pegelfeld Süd and 156 cm at Pegelfeld Spuso, the year 2024 showed average accumulation rates at Pegelfeld Süd (1.11 m/a) and Spuso (0.98 m/a) (Fig. 4.2.6). Currently, a PhD thesis is in progress to evaluate the whole record in terms of interannual variations, seasonal shifts and relation to large-scale circulation and climate change, continuing the results from a previous MSc thesis (Reppert, 2024).

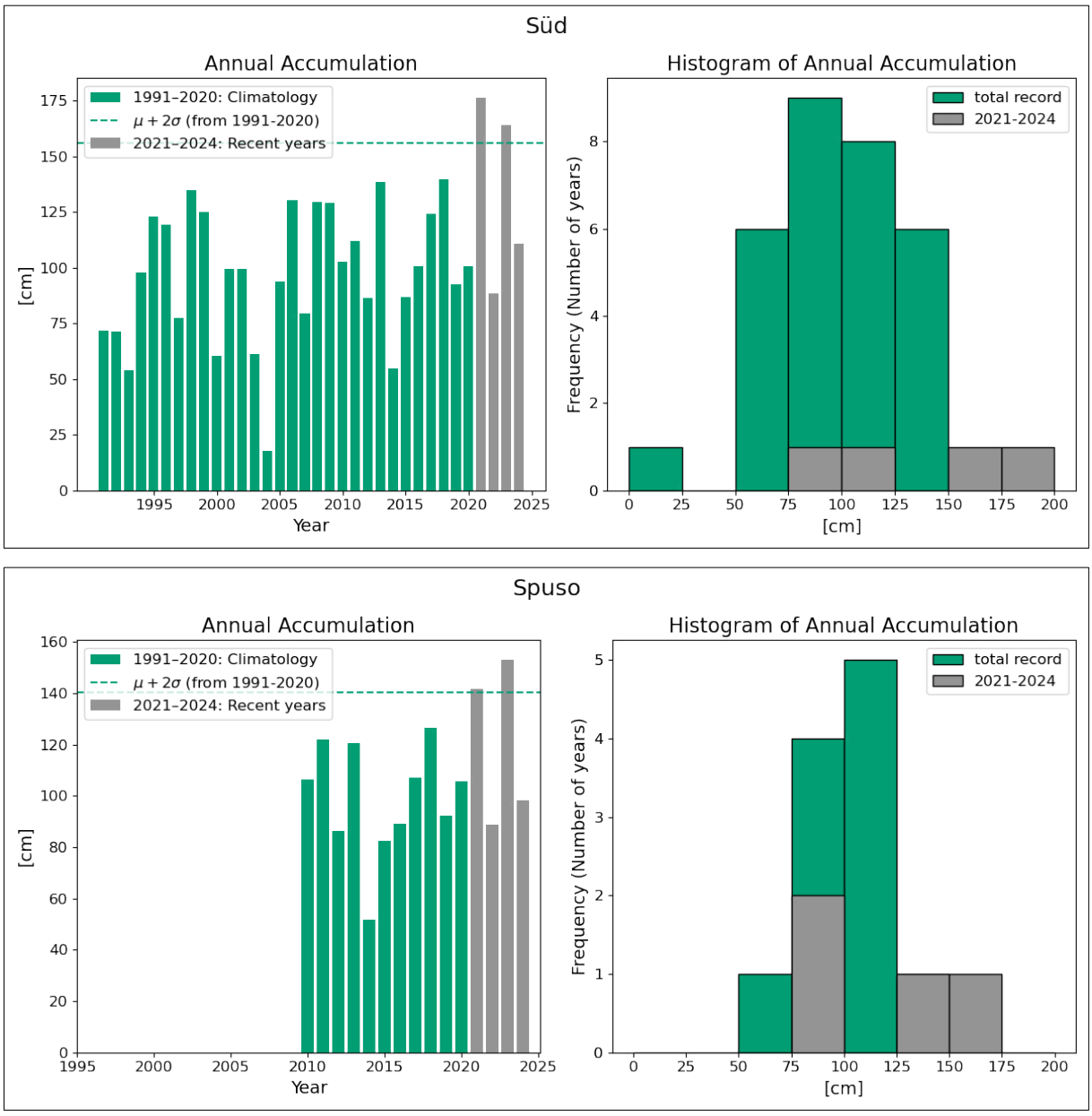

Fig. 4.2.6: Time series of annual snow accumulation at Pegelfeld Süd (top) and Pegelfeld Spuso near Neumayer Station III (bottom). The graphs on the left show the variation over time while the graphs on the right show the histogram distribution. For details of data homogenization see Reppert (2025).

Data management

The semi-automatic workflow has been implemented to incorporate the metadata of newly acquired density measurements directly into registry.o2a-data.de (formerly sensor.awi.de).

To homogenize the data accessibility for the glaciological measurements, a Jupyter notebook based on Python has been developed to make the data easily readable (i.e. convert from the xls format to ASCII), formatted in the same way and include standard graphic displays. The notebook is currently available on AWI's gitlab. After data processing and quality checking, which is currently in progress, the corrected data and derived products will be published in the overarching bibliography of the long-term observatory Glaciology at *Neumayer Station III* at https://doi.pangaea.de/10.1594/PANGAEA.971649.

- The surface snow density record is currently being updated with the 2024 values and is available at https:/doi.org/10.1594/PANGAEA.963323
- The specific surface mass balance record is currently being updated with the 2024 values and is available at https:/doi.org/10.1594/PANGAEA.972104

This expedition was supported by the Helmholtz Research Programme "Changing Earth – Sustaining our Future" Topic 2, Subtopic 3.

In all publications based on this expedition, the **Grant No. AWI_ANT_2** will be quoted and the following publication will be cited:

Alfred-Wegener-Institut Helmholtz-Zentrum für Polar- und Meeresforschung. (2016a). *Neumayer III* and *Kohnen Station* in Antarctica operated by the Alfred Wegener Institute. Journal of large-scale research facilities, 2, A85. http://dx.doi.org/10.17815/jlsrf-2-152

References

Reppert V (2025) Climate Signals from NEUMAYER, Coastal Dronning Maud Land, Antarctica: A 33-Year Statistical Analysis of Snow Accumulation in a Stake Farm / H. Bornemann and S. Amir Sawadkuhi (editors), Berichte zur Polar- und Meeresforschung = Reports on polar and marine research, Bremerhaven, Alfred-Wegener-Institut Helmholtz-Zentrum für Polar- und Meeresforschung, 792, 89 p. https://doi.org/10.57738/BzPM_0792_2025

4.3 The Geophysical Observatory

Jölund Asseng[1], Amelie Nüsse[1], Andrey Jakovlev[1], [1]DE.AWI
Johanna Brehmer-Moltmann[1], Jozef Müller[1], [2]DE.GFZ
Jürgen Matzka[2]
Not in the field: Vera Schlindwein*[1], Tanja Fromm[1]
* Vera.Schlindwein@awi.de

Grant-No. AWI_ANT_3

Objectives

The Geophysical Observatory at *Neumayer Station III* allows long-term observations with different geophysical instruments and contributes to worldwide networks collecting geophysical data for the scientific community. Due to its location at the coast line of Antarctica, the observatory provides valuable data points for geophysical networks with sparse data coverage in the southern hemisphere where the spacing between data points easily becomes hundreds or thousands of kilometres. The closest stations with winter capacities are *SANAE IV* (230 km) and *TROLL* (420 km) to the east. *Halley Station*, 780 km to the west, is only occupied during summer. In contrast to datasets acquired as part of short-term projects, the observatory provides continuous, long-term time series that allow revealing slow and small changes otherwise undetectable.

The observatory operates instruments for the following disciplines or tasks: a) seismology (Fromm et al. 2018; Eckstaller et al. 2006), b) geomagnetism (GFZ 2016) and c) GNSS recordings.

a) Seismology

The primary objective of the seismographic observations at *Neumayer Station III* is to complement the worldwide network of seismographic monitoring stations in the southern hemisphere. Within Antarctica only eleven broad-band seismometers provide data in real time, three of them are operated by AWI. A focus of the AWI network is the detection of local and regional earthquakes within Antarctica. Recently, interest in seismological data from ice covered regions has drastically increased, as seismometers also record cryogenic events giving information about processes of ice dynamics (e.g. Aster et al. 2017).

The local seismographic network at *Neumayer Station III* comprises the station VNA1 near *Neumayer Station III* itself and two remote stations VNA2 and VNA3 on the ice rises Halvfarryggen and Søråsen, respectively. In addition, the seismic broad-band station VNA2 is part of a small aperture array with 15 vertical seismometers placed on three concentric rings in a total diameter of almost 2 km. Other unattended seismographic broadband stations (KOHN, WEI, SVEA, UPST, DS4, NVL) record data at logistically feasible locations (see Fig. 4.3.1).

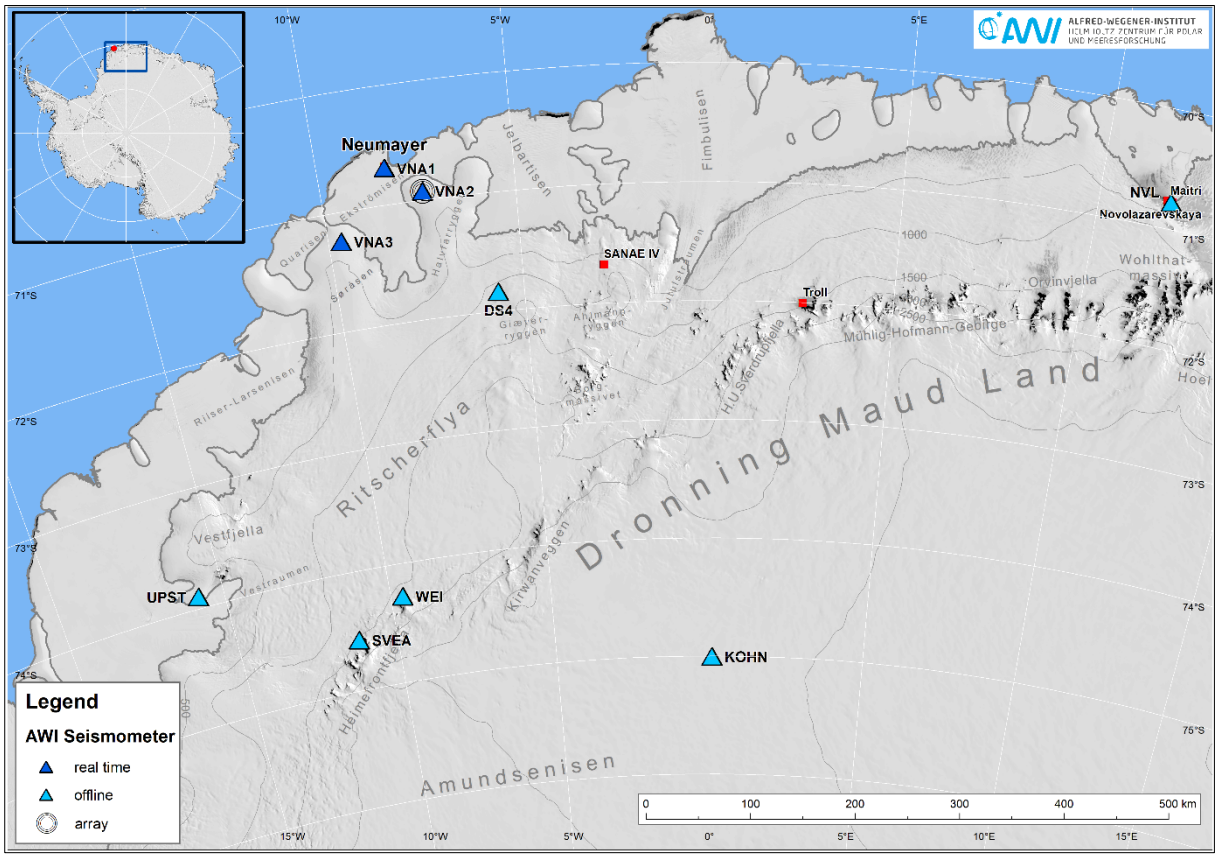

Fig. 4.3.1: Map showing the active seismometer stations in Dronning Maud Land of the AWI network during 2024

b) Geomagnetism

The Geomagnetic Observatory at *Neumayer Station III* was built in 2009 and since November 2024 the observatory data comes from a new location about 157 m to the south of the original location. A detailed description of the new observatory can be found in the field work section. Declination and inclination of the geomagnetic field are regularly measured manually using a non-magnetic theodolite with a single-axis fluxgate sensor mounted on the telescope. For declination measurements, the knowledge of the geographic north direction is necessary. Since there is no stable reference for geographic north, it has to be determined periodically by a gyro compass. Since 2014 the observatory is a certified member of the INTERMAGNET network, with its high standards for data quality, its traceable specifications for measuring and recording and exchanging data. It is one of only five INTERMAGNET observatories in Antarctica and the only one on an ice shelf.

c) GNSS recordings

We continuously record GNSS data since the beginning of July 2012 with a dual-band receiver situated on the roof of *Neumayer Station III*. At first, we used an Ashtech Z-12 receiver until June 2020. Since February 2020, a Novatel PwrPak7 is installed in combination with the VP6235 VeraPhase dual band GNSS antenna. GNSS data provides valuable information for

higher atmospheric research and reveal characteristics of the Ekström ice shelf dynamics. During the winter of 2021 we increased the sample rate of the receiver to 50 Hz and added support for GLONASS, Galileo and Beidou.

Fieldwork

In summer season 2024/25 AWI seismometer stations VNA2, VNA3, DS4, WEI, UPST and SVEA were visited for maintenance and data collection. The seismographic station NVL at the Russian station *Novolazarevskaya* is not accessible.

The geomagnetic fieldwork consisted of taking manual theodolite measurements of the declination and inclination of the magnetic field every three days and gyro measurements for the determination of geographic North on a monthly basis.

A completely new magnetic observatory (Fig. 4.3.2) has been built and equipped during the season 2023/24 and started operation at the end of February 2024. It ran in parallel to the old observatory from February 2024 to January 2025. Then the operation of the old observatory was finally stopped. The official transition in data registration to the new observatory took place on 1 November 2024.

Similar to the old magnetic observatory, the new observatory hosts a GSM-90 Overhauser proton-magnetometer, a 3-component fluxgate sensor (FGE) and a non-magnetic theodolite with a single-axis fluxgate sensor mounted on the telescope. The geographic north reference will be determined periodically by a new gyro compass (GYROMAX AK-2M nT on LEICA TS07). Additionally, a second 3-component fluxgate sensor (GEOMAG 02) and a second FGE were installed. The length of the observatory trench is 62 m. This enables a greater distance between sensors and magnetic parts and thus guarantees a high quality of magnetic measurements and angle determinations for declination measurements.

The available space in the trench was also used to install two 3-component broad-band seismometers to substitute the seismometer in the old observatory in the future.

Fig. 4.3.2: The new magnetic observatory

Fig. 4.3.3: 3D model of the new observatory

At the snow pit of MICAS-S station the entrance was raised to maintain accessibility.

Preliminary results

- A total of 7,828 earthquakes were located in the year 2024. 2,614 of these earthquakes were associated with earthquakes listed in international catalogues. In addition, 5,214 earthquakes were located by AWI (Fig. 4.3.4).
- 7,284 of all earthquakes have been detected in and around Antarctica. Nearly all of these regional earthquakes (7073) were located by AWI (Fig. 4.3.5).
- During 2024, Neumayer Station III moved 156.8 m from 70°39'36.79”S, 8°17'3.42”W to 70°39'31.82”S, 8°17'6.28”W.
- The total magnetic field intensity decreased by around 60 nT in 2024. This decrease is largely attributable to the regional weakening of the Earth magnetic field in the South Atlantic Magnetic Anomaly. The strong geomagnetic storms in 2024, on 10 May and 10 October, together with further geomagnetic storms, can also be seen in the Fig. 4.3.6.

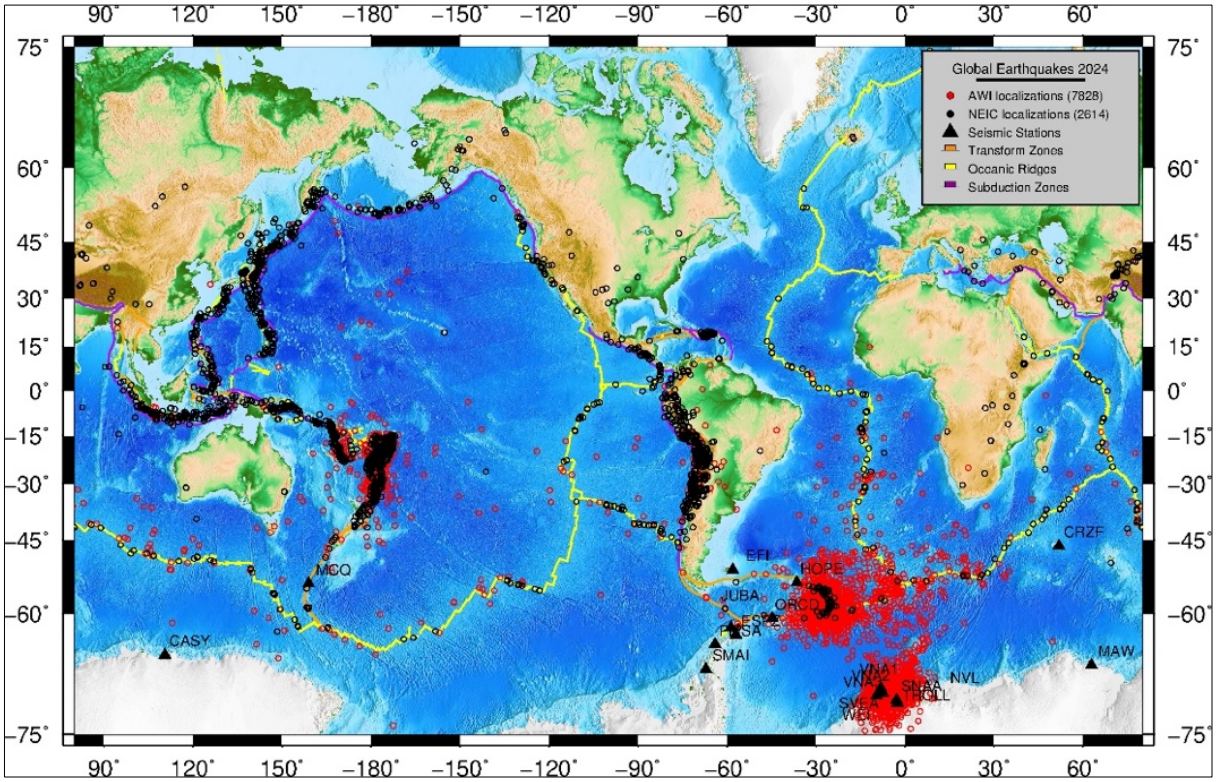

Fig. 4.3.4: Map showing seismic events recorded by the AWI network in 2024

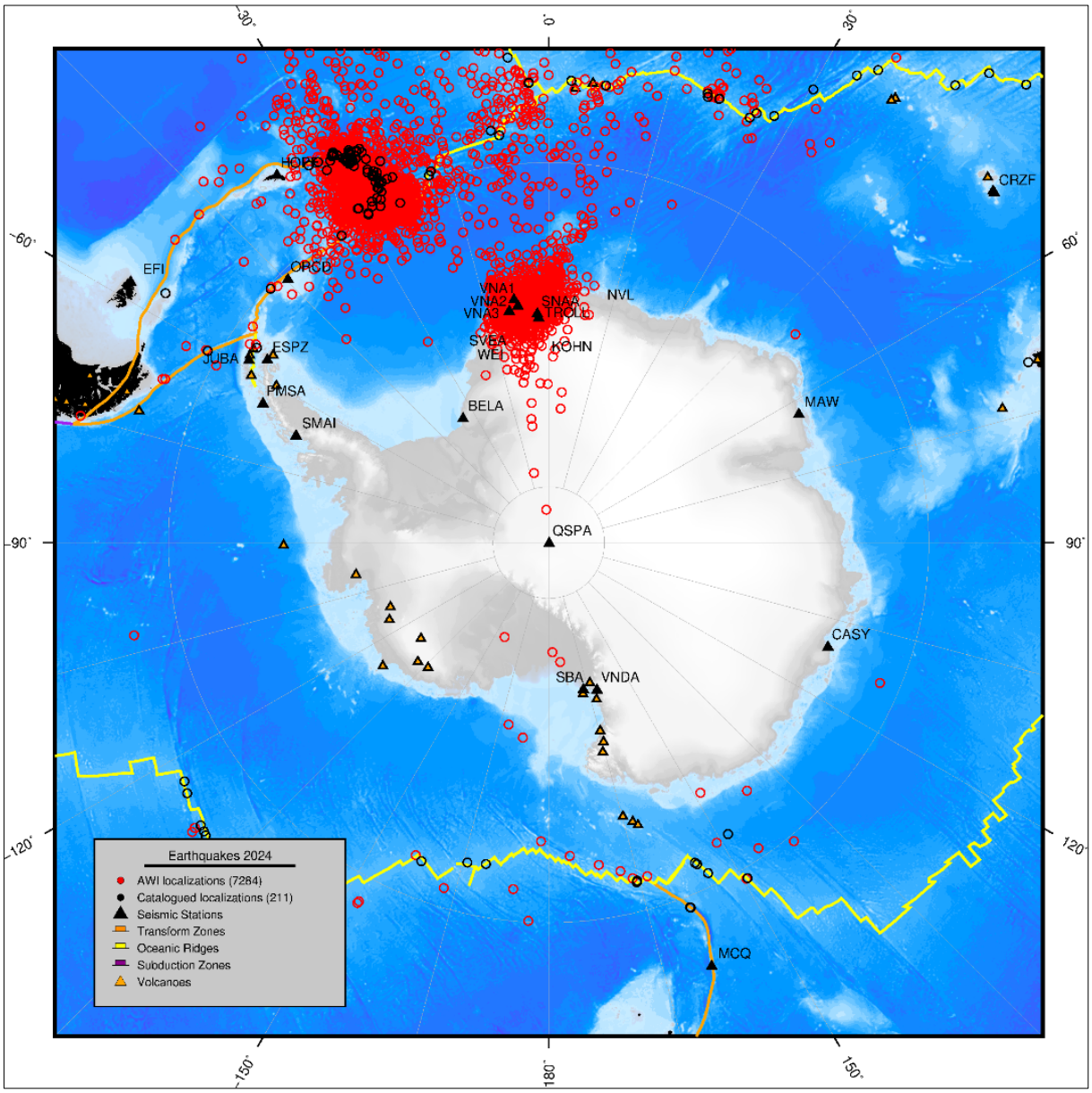

Fig. 4.3.5: Regional earthquakes in 2024

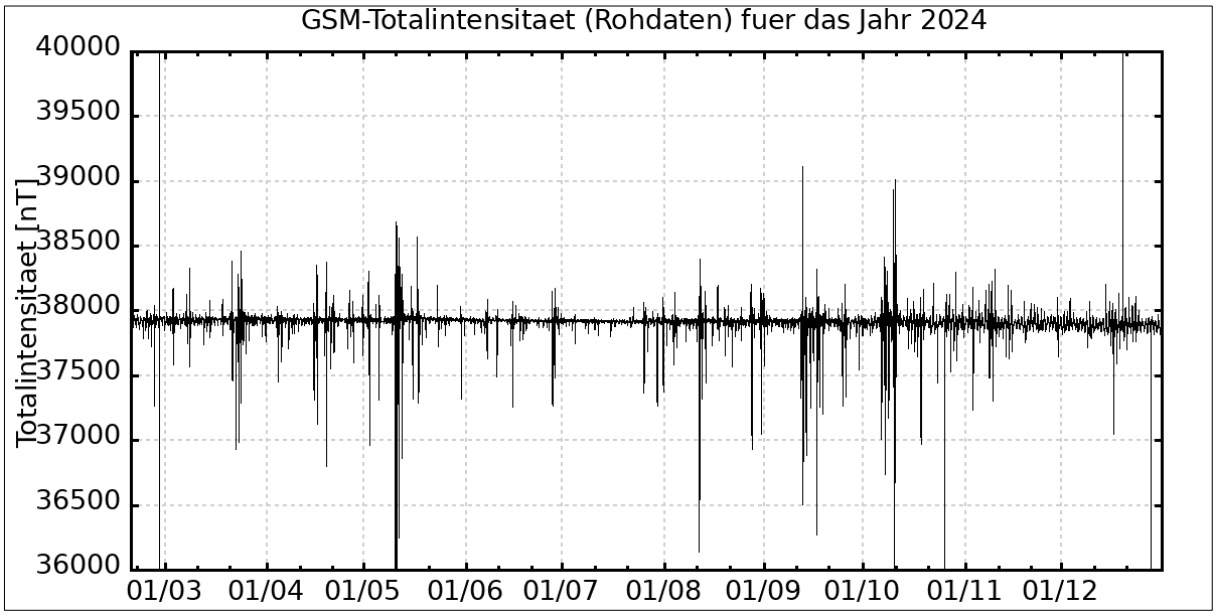

Fig. 4.3.6: Total Intensity of the geomagnetic field at Neumayer Station III, recorded by the Overhauser GSM-19 in 2024

Data management

- Seismological waveform data can be accessed via Geofon (https://geofon.gfz-potsdam.de/doi/network/AW). Information about arrivals and events can be retrieved from ISC (http://www.isc.ac.uk/).
- Data from the geomagnetic observatory can be accessed via INTERMAGNET (https://intermagnet.github.io) and SuperMAG (http://supermag.jhuapl.edu/)
- GPS data in Rinex format are available on request.

This expedition was supported by the Helmholtz Research Programme “Changing Earth – Sustaining our Future” Topic 2, Subtopic 3.

In all publications based on this expedition, the **Grant No. AWI_ANT_3** will be quoted and the following publication will be cited:

Alfred-Wegener-Institut Helmholtz-Zentrum für Polar- und Meeresforschung (2016). *Neumayer III* and *Kohnen Station* in Antarctica operated by the Alfred Wegener Institute. Journal of large-scale research facilities, 2, A85. http://dx.doi.org/10.17815/jlsrf-2-152.

References

Aster RC & Winberry JP (2017) Glacial seismology. Reports on Progress in Physics, 80(12), 126801, https://doi.org/10.1088/1361-6633/aa8473

Eckstaller A, Müller C, Ceranna L & Hartmann G (2006) The Geophysics Observatory at Neumayer Stations (GvN and NM II) Antarctica. Polarforschung 76 (1-2):3–24, https://doi.org/10.2312/polarforschung.76.1-2.3

Fromm T, Eckstaller A & Asseng J (2018) The AWI Network Antarctica – Alfred-Wegener Institute, Germany. Summary of the Bulletin of the International Seismological Centre 22–36:2309-236X, https://doi.org/10.5281/zenodo.1156983

GFZ German Research Centre for Geosciences (2016) Geomagnetic Observatories. Journal of large-scale research facilities 2:A83. http://dx.doi.org/10.17815/jlsrf-2-136

4.4 CTBTO – IS27 Infrasound Station

Torsten Grasse[1], Gernot Hartmann[1], Mathias Hoffmann*[1], Amelie Nüsse[2], Andrey Jakovlev[2], Johanna Brehmer-Moltmann [2], Jozef Müller[2]
* mathias.hoffmann@bgr.de

[1]DE.BGR
[2]DE.AWI

Grant-No. AWI_ANT_4

Objectives

In accordance with the Comprehensive Nuclear Test Ban Treaty (CTBT), the IS27 Infrasound Station is operated at the German *Neumayer Station III* Antarctic Research Base as one of 60 global distributed elements of the infrasound network of the International Monitoring System (IMS). Infrasound stations measure micropressure fluctuations in the atmosphere, and thus are primarily focused on the monitoring of compliance with the CTBT with respect to atmospheric nuclear explosions. The proximity of the VNA seismic array enables seismo-acoustic studies. The IS27 array is situated approximately 3 km southwest of the *Neumayer Station III* (Fig. 4.4.1). It comprises nine elements (Fig. 4.4.2), each equipped with a microbarometer and a data acquisition system (Fig. 4.4.3). The array is arranged on a spiral at regularly increasing radii from the centre point. The aperture of this array is approximately 2 km. The central array control system is installed in the *Neumayer Station III*. IS27 commenced operations in 2003.

Fieldwork

IS27 must operate continuously with at least 98% data availability within one year. This is a requirement for a CTBTO IMS station. Routine maintenance of the array is essential to ensure high reliability and is normally carried out annually during the Austral summer, between November and February. It involves checking the condition of the equipment, installing hardware and software upgrades and carrying out any necessary repairs. The nine elements were successfully brought to the surface without incident, thanks largely to the efforts of the AWI construction team. The focus of this year's cruise was a major upgrade of the measurement system. We replaced the data acquisition, sensor, power supply, radio transmitter and the field box itself with newer parts.

Preliminary (expected) results

Data availability and quality for year 2024 met the requirement set by the CTBTO. All data were qualified for data processing at CTBTO.

Waveform data from IS27 contributed to several recently conducted atmospheric research studies (see references).

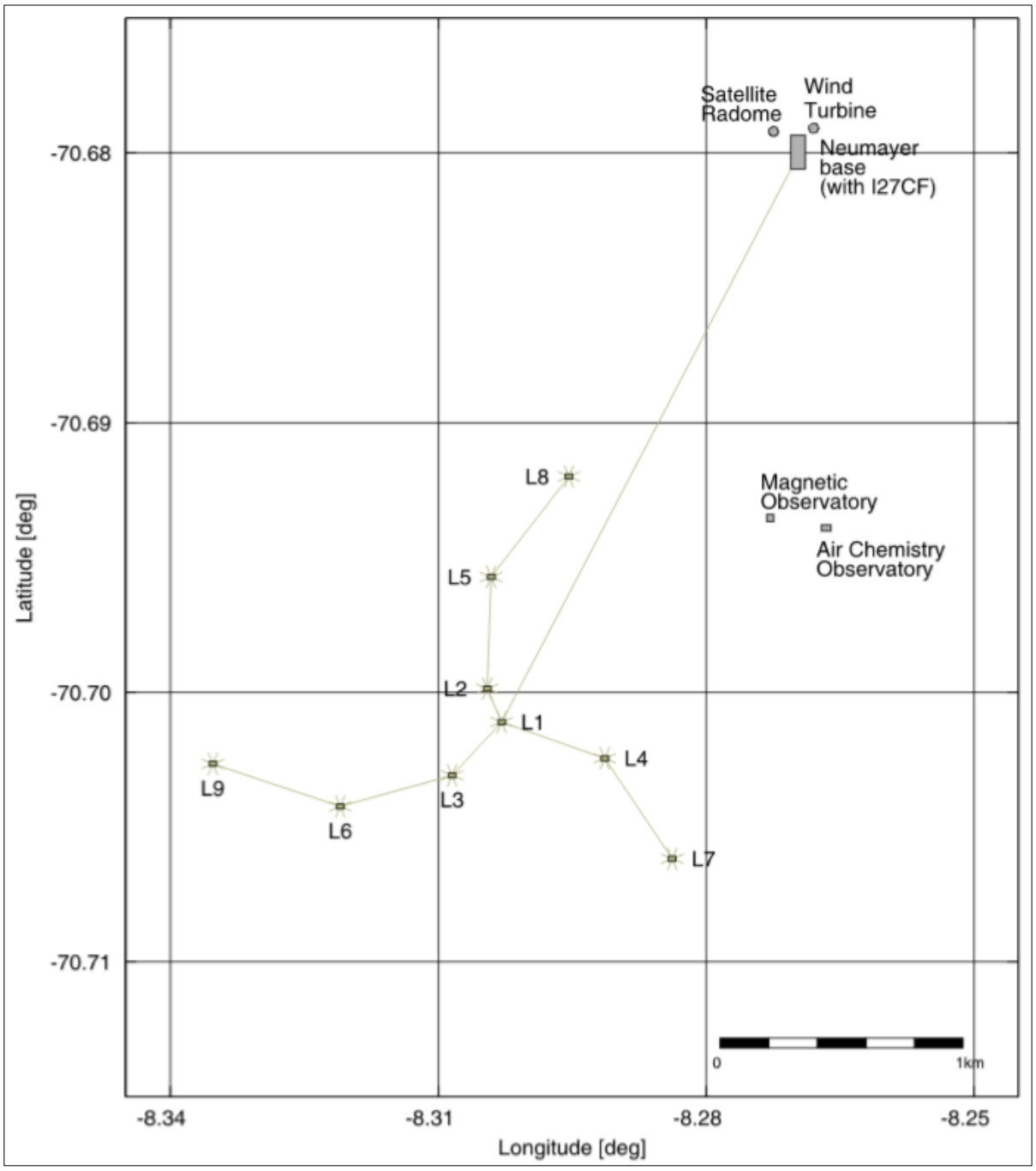

Fig. 4.4.1: Map showing the location and layout of the Infrasound Array IS27 with reference to Neumayer Station III.

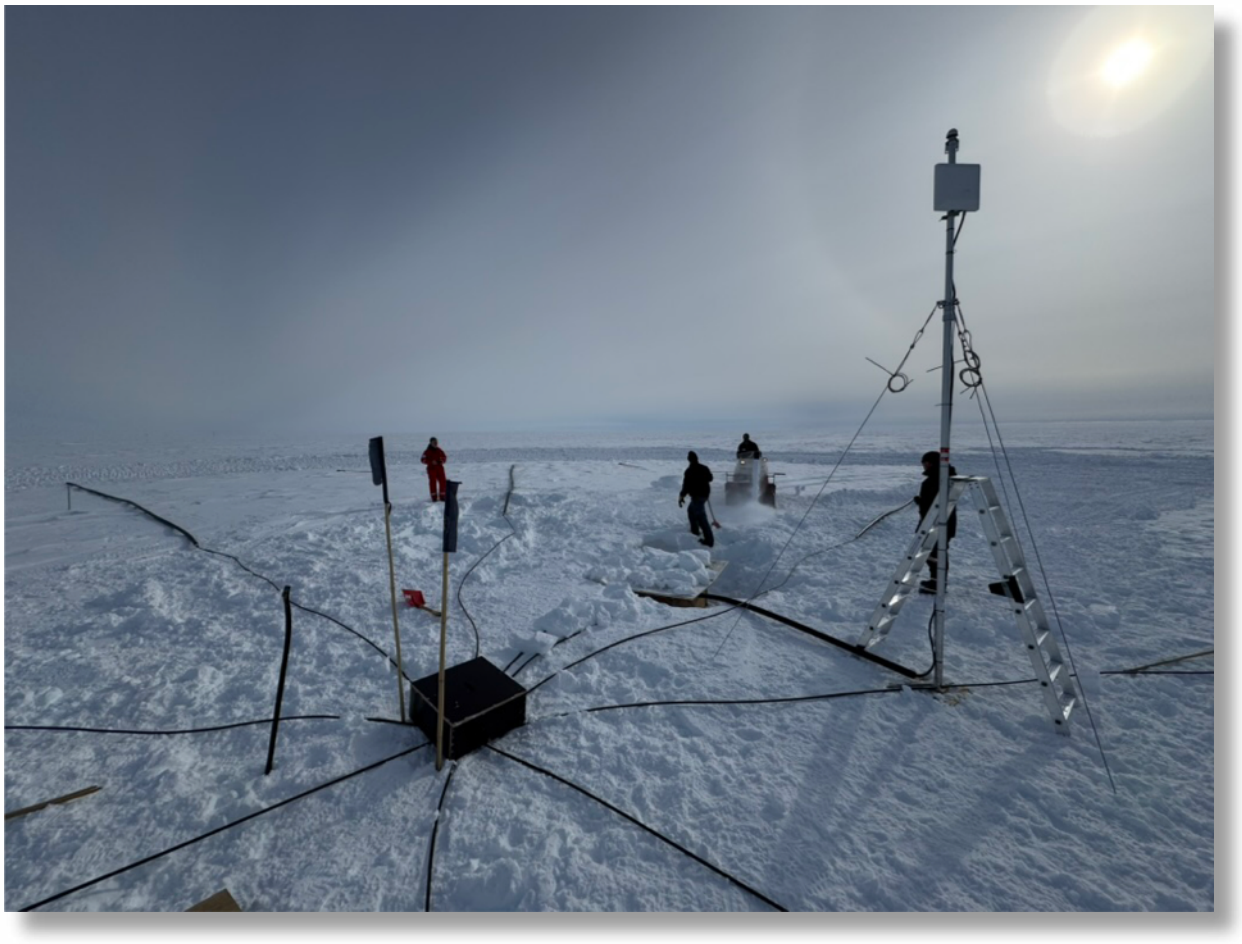

Fig. 4.4.2: One of the nine renewed infrasound elements that has just been placed on the snow surface. A centrally positioned manifold connects eight air intake pipes that make up the wind noise reduction system. The field box containing the sensor and electronics is buried nearby in the snow. A WiFi link connects each element to the base at Neumayer Station III.

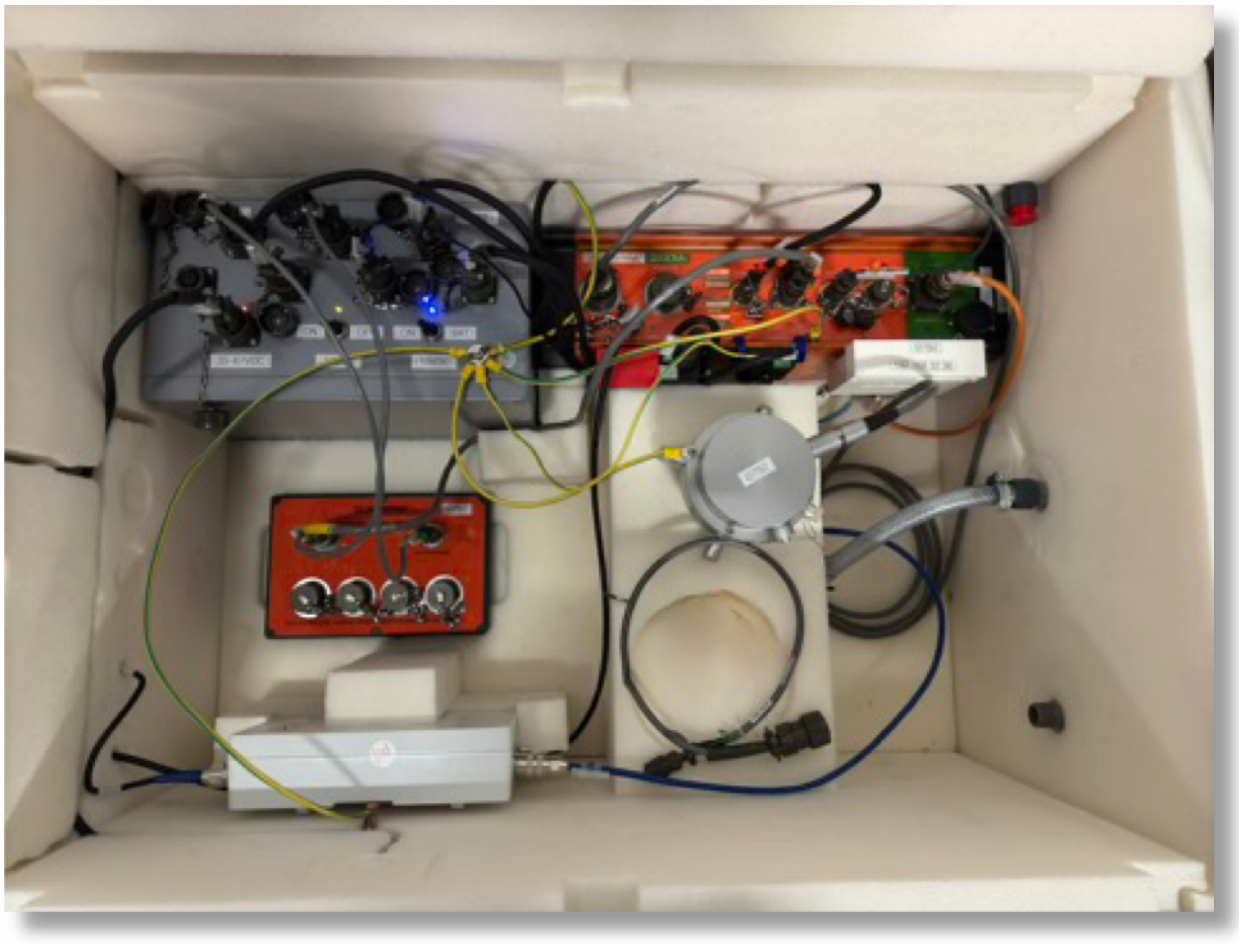

Fig. 4.4.3 The insulated field box contains the microbarometer (centre), the data acquisition system (orange), the power supply (grey) and a communication unit (white). One element is also equipped with a weather station, which is connected to the acquisition system by the red box.

Data management

Archived data, as well as real-time infrasound waveform data and associated metadata, are publicly available. Such data can be accessed via the BGR FDSN Webservice (https://eida.bgr.de/info).

In all publications based on this expedition, the **Grant No. AWI_ANT_4** will be quoted and the following publication will be cited: Alfred-Wegener-Institut Helmholtz-Zentrum für Polar- und Meeresforschung (2016a). *Neumayer III* and *Kohnen Station* in Antarctica operated by the Alfred Wegener Institute. Journal of large-scale research facilities, 2, A85. http://dx.doi.org/10.17815/jlsrf-2-152

References

De Carlo M, Hupe P, Le Pichon A, Ceranna L & Ardhuin F (2021) Global microbarom patterns: A first confirmation of the theory for source and propagation. Geophysical Research Letters 48:e2020GL090163. https://doi.org/10.1029/2020GL090163

De Negri R, Rose K, Matoza RS, Hupe P & Ceranna L (2022) Long-Range Multi-Year Infrasonic Detection of Eruptive Activity at Mount Michael Volcano, South Sandwich Islands. Geophys. Res. Lett. 49:e2021GL096061. https://doi.org/10.1029/2021GL096061

Hupe P, Ceranna L, Le Pichon A, Matoza RS & Mialle P (2022) International Monitoring System infrasound data products for atmospheric studies and civilian applications. Earth Syst. Sci. Data 14:4201–4230. https://doi.org/10.5194/essd-14-4201-2022

Hupe P (2022) BGR Report 2022, Geo-Wissen: Druckwellen des Unterseevulkans vor Tonga umrunden den Globus. https://www.bgr.bund.de/DE/Gemeinsames/Produkte/Downloads/Taetigkeitsberichte/Report2022.pdf

Hupe P, Steinberg A, Donner S, et al. (2022) Der Vulkanausbruch von Tonga am 15. Januar 2022 – ein Jahrhundertereignis! DGG-Newsletter #011. https://dgg-online.de/WordPress_01/wp-content/uploads/2022/05/DGG-Newsletter_BGR_Tonga-Vulkan.pdf

Hupe P, Ceranna L, Pilger C, Le Pichon A, Blanc E & Rapp M (2019) Mountain-Associated Waves and their relation to Orographic Gravity Waves. Meteorologische Zeitschrift. https://doi.org/10.1127/metz/2019/0982

Hupe P, Ceranna L & Le Pichon A (2019) How Can the International Monitoring System Infrasound Network Contribute to Gravity Wave Measurements? Atmosphere 10:399. https://doi.org/10.3390/atmos10070399

Hupe P (2019) Global infrasound observations and their relation to atmospheric tides and mountain waves. Dissertation, LMU München: Faculty of Physics. https://doi.org/10.5282/edoc.23790, https://edoc.ub.uni-muenchen.de/23790/

Hupe P, Ceranna L & Pilger C (2018) Using barometric time series of the IMS infrasound network for a global analysis of thermally induced atmospheric tides. Atmospheric Measurement Techniques 11(4):2027–2040. https://doi.org/10.5194/amt-11-2027-2018

Kristoffersen SK, Le Pichon A, Hupe P & Matoza RS (2022) Updated Global Reference Models of Broadband Coherent Infrasound Signals for Atmospheric Studies and Civilian Applications. Earth and Space Science 9:e2022EA002222. https://doi.org/10.1029/2022EA002222

Le Pichon A, Blanc E, Hauchecorne A (2019) Infrasound Monitoring for Atmospheric Studies, Springer. https://doi.org/10.1007/978-3-319-75140-5

Le Pichon A, Ceranna L, Pilger C, Mialle P, Brown D, Herry P & Brachet N (2013) The 2013 Russian fireball largest ever detected by CTBTO infrasound sensors. Geophys. Res. Lett. 40:3732–3737. https://doi.org/10.1002/grl.50619

Matoza RS, Fee D, Assink JD et al. (2022) Atmospheric waves and global seismoacoustic observations of the January 2022 Hunga eruption, Tonga. Science 377(6601):95-100. https://doi.org/10.1126/science.abo7063

Pilger C, Ceranna L & Bönnemann C (2017) Monitoring Compliance with the Comprehensive Nuclear-Test-Ban Treaty (CTBT), Contributions by the German National Data Center. Schweizerbart Science Publishers, Stuttgart, Germany. ISBN 978-3-510-96858-9

Pilger C, Ceranna L, Ross JO, Le Pichon A, Mialle P & Garcés MA (2015) CTBT infrasound network performance to detect the 2013 Russian fireball event. Geophys. Res. Lett. 42:2523– 2531. https://doi.org/10.1002/2015GL063482

Pilger C & Ceranna L (2018) BGR Report 2018, Titelstory: Lauschen für den Frieden. https://www.bgr.bund.de/DE/Gemeinsames/UeberUns/Taetigkeitsbericht/taetigkeitsbericht_node.html

Vergoz J, Hupe P, Listowski C et al. (2022) IMS observations of infrasound and acoustic-gravity waves produced by the January 2022 volcanic eruption of Hunga, Tonga: A global analysis. Earth and Planetary Science Letters 591:117639. https://doi.org/10.1016/j.epsl.2022.117639

4.5 AFIN – Antarctic Fast Ice Network

Amelie Nüsse[1], Andrey Jakovlev[1]
not in the field: Stefanie Arndt*[1,2], Mara Neudert[1]
* stefanie.arndt@awi.de

[1]DE.AWI
[2]DE.Uni-Hamburg

Grant-No. AWI_ANT_5

Objectives

Sea ice fastened to coasts, icebergs and ice shelves (fast ice) is of crucial importance for climate and ecosystems. At the same time, it is not represented in climate models and many processes affecting its energy- and mass balance are currently only poorly understood. Near Antarctic ice shelves, this fast ice exhibits two unique characteristics that distinguish it from most other sea ice:

1. Ice platelets form and grow in super cooled water masses, which originate from cavities below the ice shelves. These crystals rise to the surface, where they accumulate beneath the solid sea ice cover. Through freezing of interstitial water, they are incorporated into the sea ice fabric as platelet ice.

2. A thick and highly stratified snow cover accumulates on the fast ice, altering the response of the surface to remote sensing and affecting sea ice energy and mass balance.

At the same time, fast ice is ideal to monitor sea ice and its seasonal evolution, because it may be accessed from nearby stations. In order to improve our understanding of sea ice processes and mass balance, we perform a continuous measurement programme on the fast ice of Atka Bay, Antarctica. This work contributes to the international Antarctic Fast Ice Network (AFIN), which was initiated as legacy project under the International Polar Year (IPY) and is set out to establish an international network of fast-ice monitoring stations around the Antarctic coastline. The monitoring programme at *Neumayer Station III* started in 2010 (Arndt et al. 2020).

Fieldwork

Sea ice conditions

The first sea ice measurements were conducted on 9 June 2024, but only at the first three measurement points, ATKA03-ATKA11 (Fig. 4.5.1). The second half of the measurement transect was completed on 14 June 2024. In the following months, the entire transect was sampled once per month (Tab. 4.5.1). The last measurement took place on 19 December 2024.

By the end of the year, the area of sea ice that could be traversed was significantly reduced due to increasing cracks. On 4 January 2025, the sea ice was completely closed off due to the growing crack structures and associated potential instabilities. By mid to late January, the fast ice had completely broken up and drifted out of the bay.

Conducted measurement principles

Manual measurements of sea ice and snow thickness

Manual measurements of sea ice and sub-ice platelet layer thickness, freeboard, and snow depth (drillings and stake measurements) were conducted across Atka Bay. As in previous years, six fixed sampling sites along a 25-km-long transect across Atka Bay have been revisited monthly between annual formation and end of December (Fig. 4.5.1).

All conducted drill hole measurements within the AFIN work are summarized in Table 4.5.1.

Continues sea ice thickness transects by means of an electromagnetic induction sounding system (EM)

In addition to the manual sea ice and snow thickness measurements, a ground-based electromagnetic induction sounding device GEM-2 (Geonics Limited, Mississauga, Ontario, Canada) was operated from which we can derive total sea ice thickness (sea ice thickness plus snow depth) as well as the sub-ice platelet layer thickness.

In winter, the measurements were conducted along with the borehole measurements along the AFIN standard transect. However, due to technical issues, the system could not be used on every measurement trip (Tab. 4.5.1).

In December 2024, extensive additional E-W and N-S transects were defined and surveyed in order to obtain a comprehensive description of the thickness of the sub-ice platelet layer and consolidated fast ice for the whole bay.

All conducted GEM-2 measurements are summarized in Table 4.5.1.

Deployment of autonomous ice tethered platforms (buoys)

To measure sea ice and snow thickness throughout the seasonal cycle on an hourly basis, two autonomous ice-tethered platforms (buoys) were deployed on the fast ice in Atka Bay near ATKA11 (see Fig. 4.5.1) on 27 June 2024. One Snow Buoy (2024S120) measured snow accumulation, while one Ice Mass Balance buoy (IMB, 2024T125) recorded sea ice growth over the course of the year.

Unfortunately, the thermistor chain buoy did not survive the breakup of the bay on 21 January 2025, and has not transmitted any data since then. In contrast, the Snow Buoy drifted with the ice in the Antarctic Coastal Current towards the Weddell Sea. As it was located on a small ice floe, it did not survive the summer melt and has not transmitted any data since 9 February 2025.

CTD profiling

To describe the water mass properties in the vertical water column, a Conductivity-Temperature-Depth (CTD) sensor suit was lowered from the ice bottom down to the ocean floor. The CTD was deployed during the standard transect surveys at some the sampling sites.

All CTD measurements are summarized in Table 4.5.1.

Ice coring

To draw conclusions about the ice growth processes in Atka Bay, one ice core was taken at each of the drill hole sampling sites along the AFIN standard transect in the E-W direction in November. The cores were drilled using an ice corer with a diameter of 0.09 m, stored in core bags after retrieval, and kept frozen at -20°C. The cores were then shipped with *Polarstern* to Bremerhaven. On board the ship, ice texture analysis, salinity measurements, and sample filtering for later biological analysis were performed. The melted samples were poured into sampling vials, which were filled completely and tightly sealed. The vials will be shipped at 4°C to the AWI ISOLAB Facility in Potsdam, where they will be analyzed for stable water isotopes.

All taken ice cores are summarized in Table 4.5.1.

Tab. 4.5.1: Overview of all conducted measurements within the framework of AFIN. The sampling sites/transects are marked in Fig. 4.5.1.

Date	Drilling	GEM	CTD	Ice cores
09.06.24	ATKA03-11 (3p)	Along whole transect		
14.06.24	ATKA16-24 (3p)	Along whole transect		
27.06.24			ATKA11	
14.07.24	ATKA (6p)		ATKA11	
12.08.24	ATKA (6p)	Along whole transect	ATKA11, ATKA24	
13.09.24	ATKA (6p)	Along whole transect	ATKA03, ATKA11, ATKA24	
06.10.24	ATKA03-11 (3p)	Along whole transect	ATKA03, ATKA11	
11.10.24	ATKA16-24 (3p)	Along whole transect	ATKA24	
19.11.24	ATKA (6p)	Along whole transect	ATKA03, ATKA11, ATKA24	6 ice cores (1 core per sampling site)
10.12.24		Several north-to-south transects		
19.12.24	ATKA (6p)	Along whole transect	ATKA03, ATKA11, ATKA24	
27.12.24		Additional east-to-west transect		

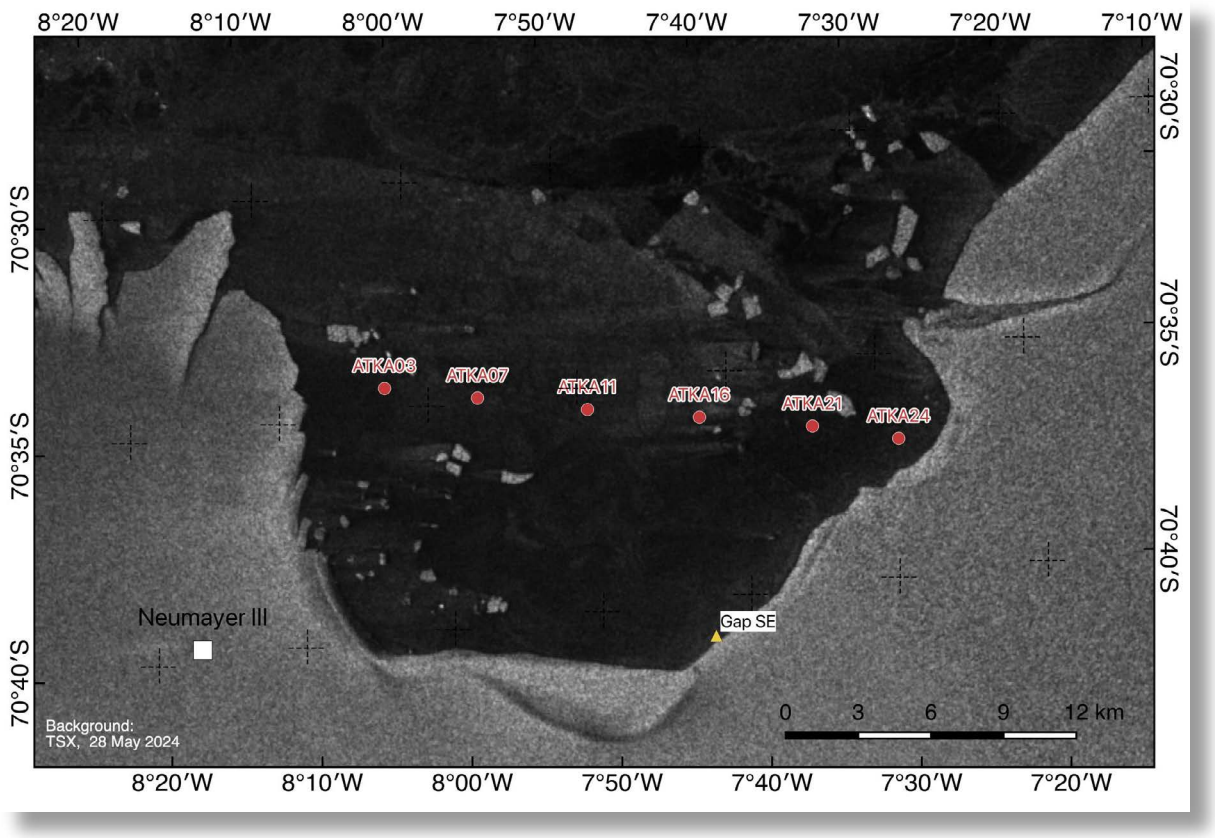

Fig. 4.5.1: Overview on the measurement sites in Atka Bay for the season 2024. ATKA03-24 denote the routinely measurement sites of AFIN. Numbers (03-24) state the distance to the western shelf ice edge (E-W transects). Background: TerraSAR-X image recorded on 28 May 2024.

Preliminary (expected) results

Fast ice, sub-ice platelet ice and snow thickness

Fig. 4.5.2 summarizes all measurements of snow, sea ice, and sub-ice platelet layer thickness, as well as the observed freeboard throughout the season. The snow layer reached annual maximum thickness values of approximately 0.44 m in the east at ATKA24 and 1.10 m in the west at ATKA03. The latter was due to a rather rough surface and the close proximity to icebergs.

The mean annual maximum thickness of the fast ice is 1.86 ± 0.17 m, with an average annual platelet ice accumulation of 4.18 ± 1.03 m. Both the average maximum thickness of the fast ice and the sub-ice platelet layer are comparable to the measurements from previous years.

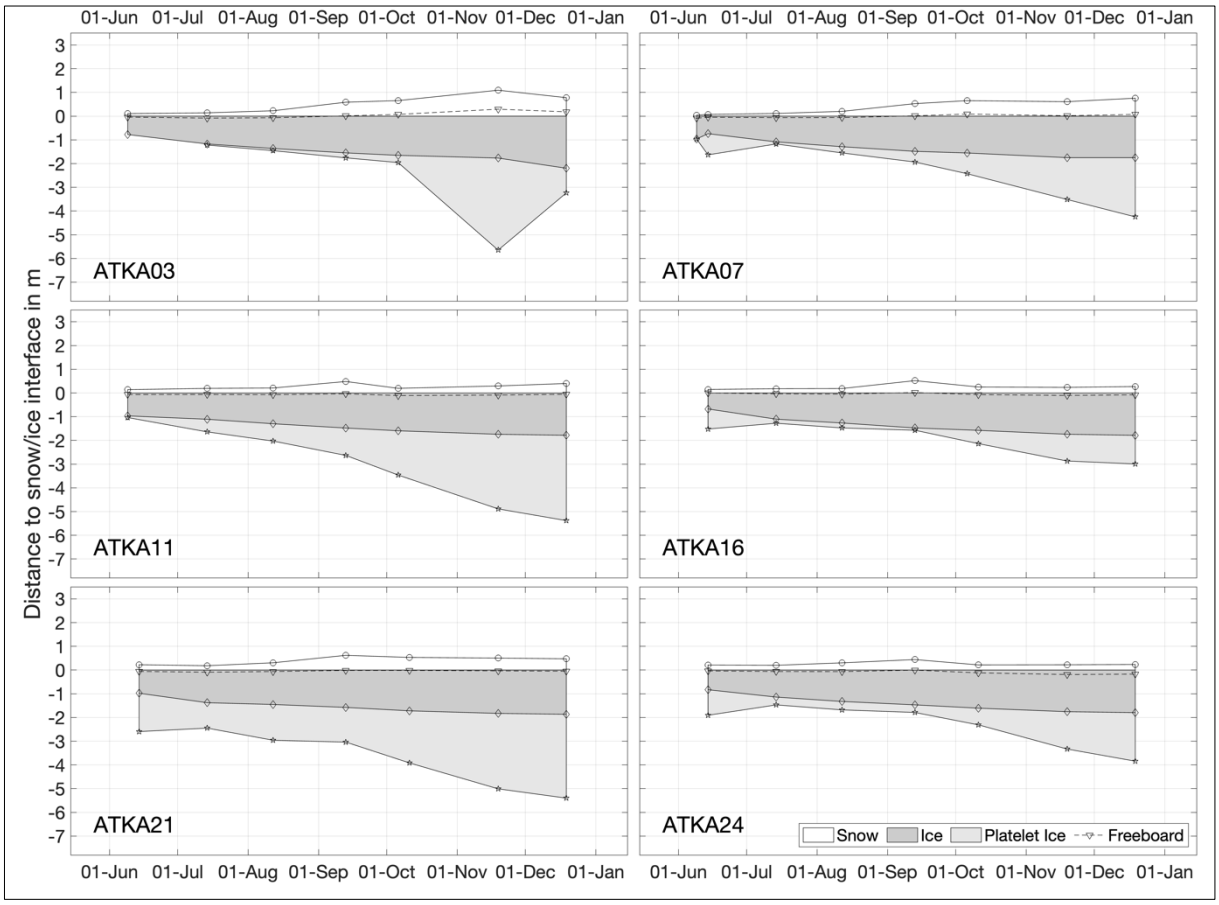

Fig. 4.5.2: Overview of all manual snow depth, sea ice and sub-ice platelet layer thickness as well as freeboard measurements for the six sampling sites along the standard AFIN transect (Fig. 4.5.1) in 2024.

Figure 4.5.3 depicts the snow accumulation recorded by the Snow Buoy 2022S121 (at ATKA11) from 27 June 2024 to 9 February 2025. In mid-July, a strong storm resulted in an immediate increase in snow height of approximately 0.2 m from the initial snow thickness of 0.15 m at the end of June during the deployment. Subsequent storms until early September appeared to redistribute the snow without significantly altering the overall snow budget. Over the month of September, strong storm and snowfall activities caused an increase of up to 0.80 m; however, the snow mass was redistributed after reaching the maximum until the end of the month and stabilized at around 0.3 m. Another strong storm event at the end of November caused another abrupt increase in snow height to 0.5–0.6 m. Afterward, the summer melt and slight redistribution led to a steady loss of snow, bringing it down to roughly 0.3 m. Subsequently, the buoy either sank or flipped due to summer sea ice melt or the decay of ice in the ice edge zone on 9 February 2025.

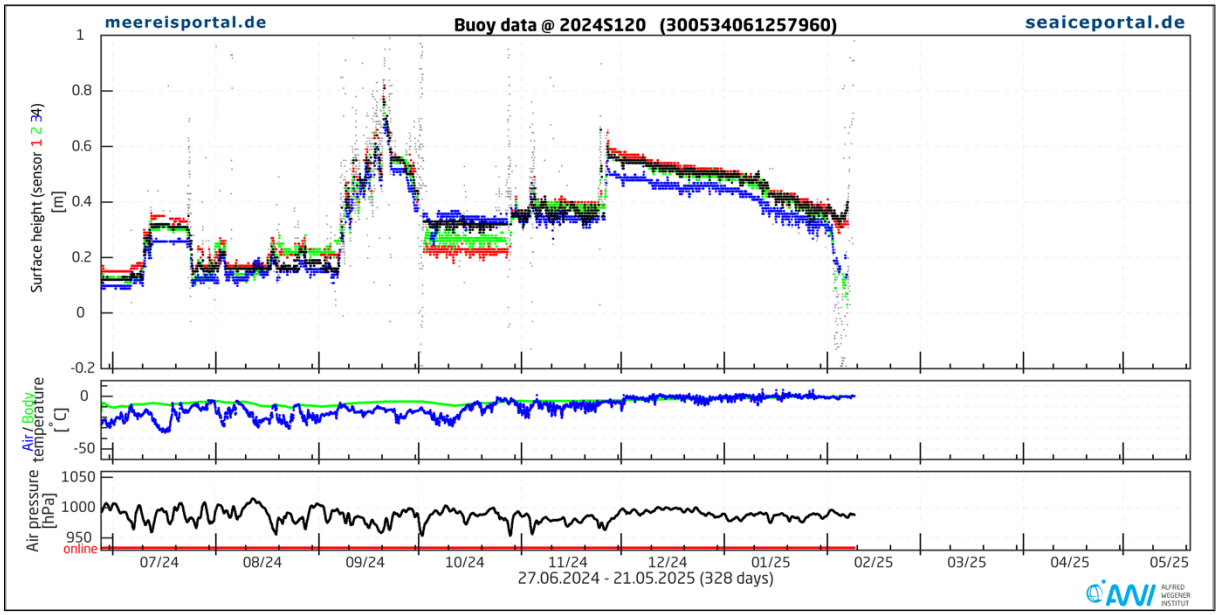

Fig. 4.5.3: Time series of snow accumulation along with the respective meteorological conditions for Snow Buoy 2024S120, deployed on 27 June 2024 at ATKA11 (Fig. 4.5.1, data.meereisportal.de).

CTD Profiles

A total of 16 CTD casts were conducted across the standard transect covering the whole seasonal cycle from June to December 2024.

Future work will focus on elaborating the detailed relationships between the seasonal and regional platelet ice distribution, the pack ice conditions in front of the bay, and the water mass distribution beneath the fast ice in Atka Bay.

Data management

All manual drilling measurements are already post-processed and will be published in PANGAEA within one year. By default, the CC-BY license will be applied.

All sea ice thickness data from electromagnetic induction sounding as well as CTD data will be released following its analysis in the home laboratories after the expedition or depending on the completion of competing obligations (e.g. PhD projects), upon publication as soon as the data are available and quality-assessed. Data submission will be to the PANGAEA database. By default, the CC-BY license will be applied.

All buoy positions and raw data are available in near real time through the sea ice portal www.meereisportal.de. At the end of their lifetime (end of transmission of data), all data will be finally processed and made available in PANGAEA. The Snow Buoys report their position and atmospheric pressure directly into the Global Telecommunication System (GTS). Furthermore, all data are exchanged with international partners through the International Programme for Antarctic Buoys (IPAB).

This expedition was supported by the Helmholtz Research Programme “Changing Earth – Sustaining our Future” Topic 2, Subtopic 1.

In all publications based on this expedition, the **Grant No. AWI_ANT_5** will be quoted and the following publication will be cited:

Alfred-Wegener-Institut Helmholtz-Zentrum für Polar- und Meeresforschung. (2016a). *Neumayer III and Kohnen Station* in Antarctica operated by the Alfred Wegener Institute. Journal of large-scale research facilities, 2, A85. http://dx.doi.org/10.17815/jlsrf-2-152

References

Arndt S, Hoppmann M, Schmithüsen H, Fraser AD & Nicolaus M (2020) Seasonal and interannual variability of landfast sea ice in Atka Bay, Weddell Sea, Antarctica. The Cryosphere 14:2775–2793. https://doi.org/10.5194/tc-14-2775-2020

4.6 CHOICE @ Neumayer – Consequences of Longterm-Confinement and Hypobaric Hypoxia on Immunity in the Antarctic Environment at *Concordia Station* and *Neumayer Station III*

Not in the field: Alexander Choukér*[1], [1]DE. Med.Uni-Muenchen
Dominique Moser[1]
*Alexander.Chouker@med.uni-muenchen.de

Grant-No. AWI_ANT_6

Objectives

The overarching goal of the field study, CHOICE@Neumayer, is to explore the dynamic relationship between stress and the immune system and its ramifications on the well-being of the wintering crews stationed at *Neumayer Station III* in Antarctica. This research endeavor is intricately connected to prior and ongoing scientific inquiries conducted in Antarctica (*Concordia*, known as CHOICE_III) and in space (International Space Station (ISS), referred to as IMMUNO and IMMUNO_2 and Immunity Assay). Led by the Hospital of the Ludwig Maximilian University of Munich, “Laboratory of Translational Research – Stress and Immunity” an international research team endeavors to delve into the following aspects at *Neumayer Station III:*

a) Scrutinizing how the immune system reacts to prolonged periods of isolation and confinement, elucidating potential stress-induced, neuroendocrine, and metabolic alterations. b) Assessing the consequential impact of these changes on the overall health of the participants in field.

For the winterover-season 2024, after a baseline data collection in the fall of 2023, the examinations of all nine subjects started on the station in February 2024 to run the CHOICE@Neumayer observation in a monthly period over the winter. The study has been completed by 8 subjects and ended by the last time point in March 2025 for the post-collection in Berlin (joint activity and kindly organized by Prof. Dr. Alexander Stahn). Blood, saliva, urine, hair and stool samples were collected and also questionnaires were filled in.

Preliminary (expected) results

The ongoing investigations conducted in the extreme exposome of the Antarctic environment elicits distinctive stress and immune responses. These studies aim to deepen our understanding and strengthen the statistical significance of any significant environmental and sex-specific differences observed. Notably, gender disparities have been identified as independent of heightened psychological stress, with potential links to environmental factors. However, the origins and implications of these gender differences require further elucidation, and efforts to investigate them are currently underway, necessitating a large sample size. The present analyses of samples collected from the recent and previous overwintering seasons focus on evaluating the impact of fresh food on the immune system at both the transcriptional and functional levels, as well as on the microbiome profile. Findings regarding the latter indicate a dynamic shift in microbiome diversity during missions, which subsequently recovers upon return to Europe and that seem differentially changed as a function of oxygen tension / altitude. Further immune functional phenomics analyses are currently in progress with these

data collected in the Winterover 2024. Moreover, immune-allergy and stress surveys (via an App) were also implemented in this season and 61 person*timepoint assessments were completed.

Data management

All samples and documentation which have been collected along the study time-points are considered confidential as they are considered “medical research data” that is subject to data protection regulation and has to follow the rules and regulations of the institutional ethical board (Ethikkommission an der Medizinischen Fakultät der LMU). Once the samples are analyzed and anonymized, data batches can be made available upon request and reconsideration of the topics of interest if covered by the ethical approval (a re-iteration the ethical board might be necessary).

Molecular data (viral DNA and transcriptome/RNA data) will be archived, published and disseminated within one of the repositories of the International Nucleotide Sequence Data Collaboration (INSDC, www.insdc.org) comprising of EMBL-EBI/ENA, GenBank and DDBJ).

In all publications based on this expedition, the **Grant No. AWI_ANT_6** will be quoted and the following publication will be cited:

In all publications based on this expedition the following publication will be cited:

Alfred-Wegener-Institut Helmholtz-Zentrum für Polar- und Meeresforschung. (2016a). *Neumayer III and Kohnen Station* in Antarctica operated by the Alfred Wegener Institute. Journal of large-scale research facilities, 2, A85. http://dx.doi.org/10.17815/jlsrf-2-152.

4.7 Neuromayer – Neurophysiological Changes in Human Subjects During Long-Duration Over-Wintering Stays at *Neumayer Station III* in Antarctica

Not in the field: Alexander Stahn*[1], Anika Friedl-Werner[1], Katharina Brauns[1], Poppy Barsby[1], Stefan Hetzer[2], Simone Kühn[3], Bernhard Riecke[4]
* alexander.stahn@charite.de

[1]DE.CHARITE
[2]DE.BCAN
[3]DE.MPIB-Berlin
[4]CA.SFU

Grant-No. AWI_ANT_11

Outline

The project will help to find predictive indicators and biomarkers for resilience and adaptation in individuals and teams, and to aid in selection and individualized countermeasure development with the goal to maintain and optimize performance capability and behavioral health during long-duration missions. The project is based on a close cooperation between Charité – Universitätsmedizin Berlin and AWI, Helmholtz Institute for Polar and Marine Research. The study is voluntary, approved by the Charité Ethics Committee, and all subjects provide written informed consent prior to their participation. All data collection is performed in accordance with the Declaration of Helsinki and GDPR.

Objectives

The overarching objective of the project is to investigate the effect of long-duration Antarctic stays on crew health and behavior. To this aim we have optimized a set of measures combining cutting-edge imaging technologies, molecular markers and behavioral and operational measures. Our primary outcome are structural and functional brain changes assessed by MRI before and after the winter-over. In addition, we also assess behavior and cognitive performance with sensitive but unobtrusive state-of-the-art cognitive and psychosocial measurement tools. These measures will be performed before, after and during the winter-over. The test battery is based on a number of well-validated paradigms and specifically targets spatial cognition, i.e., the ability to process information of our location in spatial environments. We also draw and subsequently freeze blood samples from the crew members before, during and after the campaign, which will later allow for the identification and time course of biological markers of vulnerability to the effects of prolonged exposure to Antarctic overwintering. To parse out the effects of reduced sensory stimulation from other stressors during long duration space missions such as social isolation, crew conflicts, sleep and circadian disorders, and reduced physical activity levels we will administer various surveys to capture individual responses the expedition.

Fieldwork

Data has been collected in crew members at *Neumayer Station III* since ANT-Land 2018/19. Data collections in field are optimized to limit crew burden and maximize scientific return.

Preliminary (expected) results

It is expected that the multiple stressors associated with long-duration overwintering lead to neurobehavioral changes as assessed by structural and functional brain imaging, key neurotrophins and behavior (e.g., mood and cognitive performance). We also expect that resilience will reflect inter-individual differences in sensitivity to the stressors associated with prolonged Antarctic missions, led considerable changes in brain structure, cognitive performance, and neurotrophins that are key to learning, memory formation, and brain plasticity. Future work foresees to verify whether such changes can be observed across multiple crews and are comparable to isolation studies conducted in standardized conditions, i.e. dedicated habitats to mimic isolation and confinement associated with prolonged spaceflight.

Data management

Data will be analyzed at the PI's laboratory at Charité and his partners. Data will be pseudonymized and stored on a central server that is backed up and managed by the universities' IT programs. Results will be publicly disclosed by submission to peer-reviewed journals with authorships that accurately reflects the contributions of those involved. De-identified data will be made available as long as all personal information can be protected. We will carefully attend to any characteristic that might make the data fields identifiable (e.g., campaign, analog, mission length and/or sex).

In all publications based on this expedition, the **Grant No. AWI_ANT_11** will be quoted and the following publication will be cited:

Alfred-Wegener-Institut Helmholtz-Zentrum für Polar- und Meeresforschung. (2016a). *Neumayer III and Kohnen Station* in Antarctica operated by the Alfred Wegener Institute. Journal of large-scale research facilities, 2, A85. http://dx.doi.org/10.17815/jlsrf-2-152.

References

Stahn AC, Gunga HC, Kohlberg E, Gallinat J, Dinges D & Kühn S (2019) Brain changes in response to long Antarctic expeditions. New England Journal of Medicine 381(23): 2273–2275 https://doi.org/10.1056/NEJMc1904905

4.8 Quasi-Long-Term Observatory Glaciology@NM

Olaf Eisen[1,2*] (not in the field), Ole Zeising[1], Filip Heitmann[1], Jölund Asseng[1], Julia Regnery[1], Johanna Brehmer-Moltmann[1], Jozef Müller[1], Lukas Weis[1], Andrey Jakovlev[1], Amelie Nüsse[1] not in the field: Daniel Steinhage[1], Reinhard Drews[5], Tore Hattermann[3], Tanja Fromm[1], Frank Pattyn[4]
* oeisen@awi.de

[1]DE.AWI
[2]DE.UNI-Bremen
[3]NO.NPolar
[4]BE.ULB
[5]DE.UNI-Tuebingen

Grant-No. AWI_ANT_8

Outline

This project provides long-term time series of glaciological obervables at *Neumayer Station III* and its hinterland. It consists of three sub-projects, which will be described in the following order in chapters Objectives and Fieldwork:

The sub-project “MIMO-EIS (Monitoring melt where Ice Meets Ocean – Continuous observation of ice-shelf basal melt on Ekström Ice Shelf, Antarctica)” monitors the temporal variation of the basal melt in the center of the Ekströmisen on sub-daily times scales. In addition, it investigates spatial variations of annually averaged basal melt rates.

In the sub-project “NM surface mass balance”, surface accumulation and surface layer density were regularly observed at the two stake farms Pegelfeld Süd and Pegelfeld Spuso as part of the Airchemistry Observatory at the *Neumayer Station III*. Results are described in Chapter 4.2 – Part II of this volume.

As part of the conventional density observations, the sub-project “GNSS–RR (Global Navigation Satellite System – Reflecto/Refractometry)” aims at developing a methodology deriving automated and continuous specific surface mass balance time series for fast moving parts of ice sheets and shelves (>10 m/a).

The sub-project “Kottaspegel” investigates the spatio-temporal variation of the snow accumulation along the traverse route between *Neumayer Station III* and Kottas camp, if possible, also to *Kohnen Station*. Snow accumulation is determined from reading of snow height at bamboo stakes in annual to bi-annual intervals, which is relevant to provide ground-truth measurement for satellite and regional climate modelling approaches.

Objectives

Antarctic mass balance is mainly controlled at the surface and the edges, where the interaction of ice shelves with the ocean water underneath is one of the key processes for the future development. Especially for the Antarctic ice sheet, mass loss through ice shelves is the dominant component of loss in the mass budget. The quasi-longterm observatory Glaciology@NM provides continuous monitoring system of surface mass balance and basal melting of the Ekström Ice Shelf (EIS) as well as its inflowing part of the grounded ice sheet.

Regarding the ice-ocean interaction of EIS we determine the interannual and seasonal variability of basal melt rates to improve our understanding of the processes of ice-ocean interaction along the DML coast. To this end, an Autonomous phase-sensitive Radio-Echo Sounding (ApRES) was deployed in the center of EIS in 2020, at the flank of the main bathymetric trough, as part of the sub-project MIMO-EIS. Data is retrieved annually and is used as validating constraints in numerical ocean-modelling runs as well as satellite-based analyses. The project will extend a chain of already available and ongoing ApRES observations on other ice shelves in the Dronning Maud Land Region, like Roi Baudouin and Fimbul, and thus increase our observational and potentially monitoring capabilities in this region. The continuous system has been extended with discrete repeat measurements as well as a second pilot system next to the grounding line of EIS.

The second component concerns the surface mass balance. Apart from weekly and bi-weekly snow height readings at several stake farms since 1990, providing a temporally resolved variation on snow accumulation, a continuous stake line with a distance of 500 m or 1,000 m has been operated on an annual to tri-annual basis along the traverse route to the Kottas mountains and further to *Kohnen Station* (Kottaspegel). Those readings provide the spatial variation of multi-annual surface accumulation.

The third component concerns the determination of density, required to convert snow accumulation to mass. While conventional measurements in snow pits are carried out once a year at *Neumayer Station III* as well as along the Kottaspegel traverse route, the implementation of a GNSS-RR near *Neumayer Station III* enables us to obtain a continuous time series of density. After a successful initial two-year pilot study, the system is now in operational use as part of the Neumayer Meteorological Observatory (Chapter 4.1 of this volume). It will be extended to further stations over the next years.

All components together provide an essential understanding of the processes determining the basal and surface mass balance around EIS and towards the polar plateau. These provide unique ground-truthing observations to calibrate, e.g., regional climate models, as well as observations derived from satellite remote sensing. At the same time the time series capture the changing climate conditions in this part of Antarctica, as contiuous observations serve as an early warning system (please compare Part II of Chapter 4.2 of this volume).

Fieldwork

In the summer season 2024/25, the team arrived at *Neumayer Station III* on 12 January 2025. The traverse equipment for Kottaspegel and maintenance of MIMO-EIS was prepared immediately afterwards.

MIMO-EIS

After failure and repair of an autonomous pRES (ApRES) system following the summer season 2023/24, the device was set up on 22 April 2024 at site MIMO-EIS-E (Latitude 71.426385 °S, Longitude 8.330166 °W), near the Kottas-Pegel location KP180 approx. 90 km south of the *Neumayer Station III*, by the overwinterer team.

The ApRES system at the site MIMO-EIS-8 was dug out by a team of two people (Ole Zeising and Filip Heitmann) over four hours, dismounted on 17 January 2025 and data downloaded. The station was raised to the new level of the surface redeployed by a team of two persons

(Ole Zeising and Filip Heitmann) and put in operation in the autonomous (ApRES) mode on 19 January 2025 with new antennas, separated by 10 m. The system records measurements every hour with data storage in joint files about every four hours (5 MB limit for file size). Additional pRES re-measurements with different antenna polarizations were performed on 18 January 2025 and 19 January 2025 at seven locations: MIMO-EIS-4 to MIMO-EIS-8, MIMO-EIS-A, MIMO-EIS-B and MIMO-EIS-C (Tab. 4.8.1). All polarimetric pRES sites, initially marked with two bamboo poles, were re-marked with two new poles, as the exact positioning of the antennas is key for obtaining useful data.

Measurements at all stations were conducted using Hilux (MIMO-EIS-5 to MIMO-EIS-8, MIMO-EIS-A, MIMO-EIS-B and MIMO-EIS-C) and snowmobile (MIMO-EIS-4) as vehicles.

The ApRES system at the site MIMO-EIS-E was serviced by a team of two persons (Ole Zeising and Filip Heitmann) on 24 January 2025. The ApRES was dug out over a couple of minutes and the data downloaded. The station was redeployed with a new ApRES device (multi-channel ApRES) and put in operation in the autonomous mode on the same day at the site MIMO-EIS-E (position in Tab. 4.8.1.) with an antenna separation of 10 m. Transfer to and from the site was accomplished using two snowmobiles as vehicles and took 10 hours in total (transit outbound 3 h, deployment 3 h, transit inbound 4 h). The system has been working since then and is sending regularly the state of health data.

A new ApRES system was installed at MIMO-EIS-4 on 26 January 2025 by a team of four persons (Ole Zeising, Filip Heitmann, Johanna Brehmer-Moltmann and Jozef Müller). The system consists of two bow-tie antennas, separated by 10 m. Transfer to and from the site was accomplished using two snowmobiles as vehicles.

Kottaspegel

The measurements along the traverse commenced on 29 January 2025, reaching Kottas Camp on 1 February 2025. Measurements along the traverse were performed by four persons (Ole Zeising, Filip Heitmann, Jölund Asseng and Julia Regnery) with the Hilux setup, i.e., a two-person team in each vehicle.

In total, 1,072 out of 1,155 envisaged stake readings were obtained at 748 locations, of which 148 stakes newly deployed and 83 stakes not found (i.e. buried).

At the end of each day, a snow core was drilled with an electric drill to obtain snow density (Tab. 4.8.2). The snow corer had an inner diameter at the core cutters of 9.05 cm weighed with a spring scale. The length of the corer was 111 cm and the barrel filled completely for each drilling.

GNSS-RR

No particular tasks for the sub-project GNSS-RR were carried out in the 2024/25 field season for the station at the snow height mast (SHM); any maintenance of the SHM, as part of the meteorological, is described in Chapter 4.1 of this volume.

In addition, a new GNSS-RR system from the company ANavS was deployed next to Pegelfeld Süd (coordinates: 70.68005° S, 8.45085° W) on 20 January 2025. The system transmits state of health and pre-calculated values of snow accumulation and snow water content (SWE) via an Iridium link. In April 2025 the system started to show some irregularities.

Tab. 4.8.1: Position of pRES measurements on Ekströmisen and preliminary values for the long-term average basal melt rates a_b.

Station	Latitude 2023/24 °	Longitude 2023/24 °	Latitude 2024/25 °	Longitude 2024/25 °	a_b m/a	Comments
MIMO-EIS-4	-70.64553	-8.20752	-70.64417	-8.20834	4.45	
MIMO-EIS-5	-70.74210	-8.82374	-70.74074	-8.82714	0.54	
MIMO-EIS-6	-70.80622	-8.62781	-70.80435	-8.63090	0.78	
MIMO-EIS-7	-70.82906	-8.72208	-70.82711	-8.72543	0.44	
MIMO-EIS-8	-70.82006	-8.74226	-70.81811	-8.74529	0.51	
MIMO-EIS-A	-70.76142	-8.87338	-70.75947	-8.87706	0.43	
MIMO-EIS-B	-70.87354	-8.88296	-70.87196	-8.88646	0.57	
MIMO-EIS-C	-70.68173	-8.45302	-70.67983	-8.45482	0.84	
MIMO-EIS-E	-71.4264	-8.3302	-71.42537	-8.33012	0.32	22 April 2024 to 24 January 2025

Tab. 4.8.2: Location of density measurements performed with the snow corer

Date	CoreID	Lat °	Lon °	Mean density kg/m^3	Core depth cm
30.01.2025	DMLKO_25_SC01	-71.425595	-8.330090	533	111
30.01.2025	DMLKO_25_SC02	-72.309605	-8.976373	476	111
31.01.2025	DMLKO_25_SC03	-73.231186	-9.697895	392	111
01.02.2025	DMLKO_25_SC04	-74.120145	-9.750193	420	111

MIMO-EIS

Preliminary analysis of the **repeated pRES measurement**, matching pairs measured at different seasons, and taking into account strain thinning and firn compaction, yield average basal melt rates (Tab. 4.8.1). Please note that the individual results at each site are a result of multiple measurements at different polarisations.

Since its deployment, the **ApRES systems operating in unattended mode at MIMO-EIS-4**, **MIMO-EIS-8**, and **MIMO-EIS-E** have been sending state-of-health messages regularly via an Iridium link in its Lagrangian frame of reference. Analysis of the continuous ApRES data is ongoing. A peer-reviewed manuscript is under review to publish the findings at MIMO-EIS-8 (Zeising et al. 2025).

Given our experience from now the several winters of ApRES measurements on Ekströmisen, the operation of the system with a 105 Ah Pb battery, securely stored in a Zarges box, and two 16 GB SD cards (one being the mirror of the other) are sufficient to allow more than one year of unattended operation at 1 h measurement intervals.

Kottaspegel

The compilation and analysis of data regarding actual snow accumulation at each of the measured points has not been completed due to work on this report. Table 4.8.2 summarizes the calculated snow core densities along the traverse.

Fig. 4.8.1: Left: Photograph of ApRES at station MIMO-EIS-8 after maintenance on 19 January 2025 Right: Photograph of wooden sheet above ApRES at station MIMO-EIS-8

Fig.4.8.2: Left: Photograph of ApRES at station MIMO-EIS-E after maintenance on 24 January 2025 Right: Photograph of wooden sheet above ApRES at station MIMO-EIS-E

Fig. 4.8.3: Left: Photograph of ApRES at station MIMO-EIS-4 after maintenance on 26 January 2025 Right: Photograph of wooden sheet above ApRES at station MIMO-EIS-4

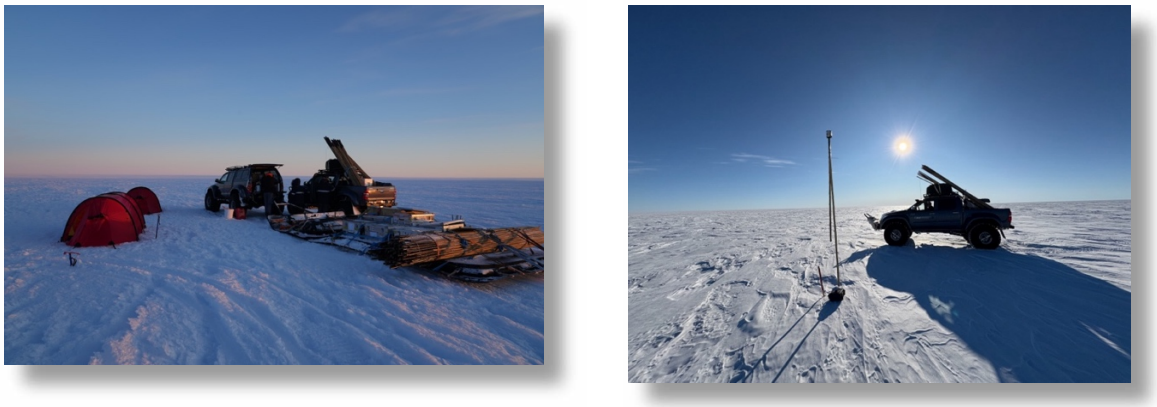

Fig. 4.8.4: Accumulation stake measurements: Left: Setup of Hilux train Right: Measuring the height of a bamboo stake higher than 2 m with an extension and a wireline device, which automatically records GPS positions.

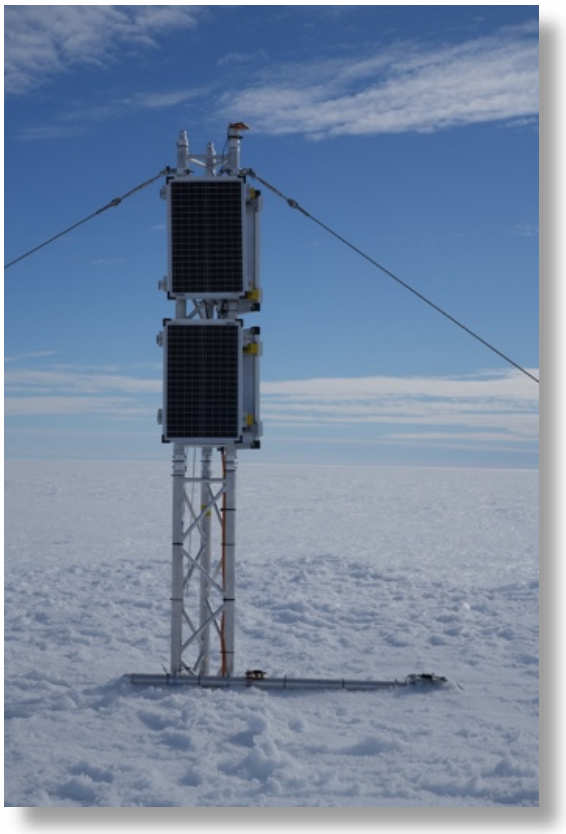

Fig. 4.8.5: Photograph of the ANavS GNSS-RR station near Pegelfeld Süd

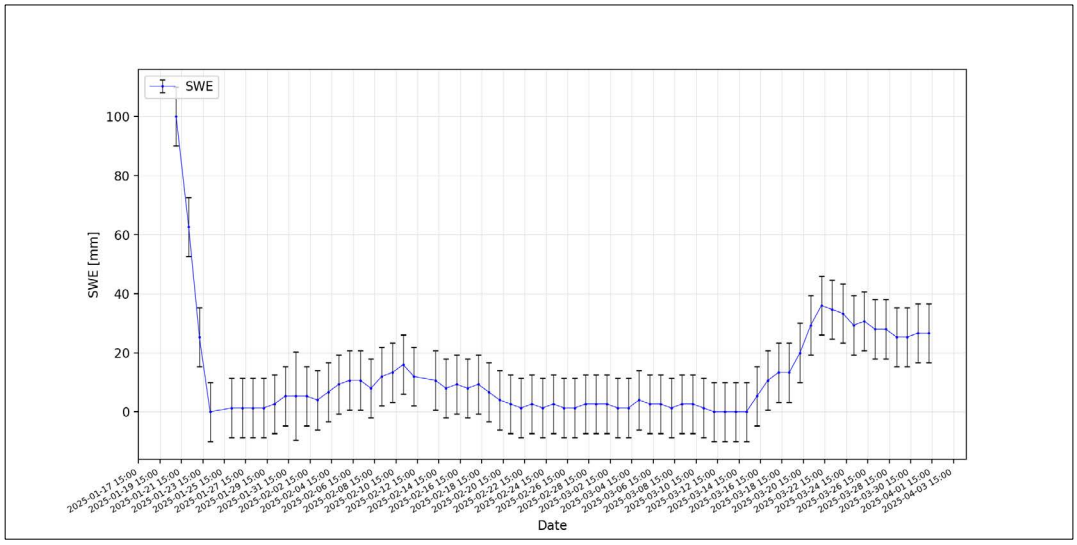

Fig. 4.8.6: Data series of SWE at the ANavS GNSS-RR station near Pegelfeld Süd

Data management

Environmental data will be archived, published and disseminated according to international standards by the World Data Center PANGAEA Data Publisher for Earth & Environmental Science (https://www.pangaea.de) within two years after the end of the expedition at the latest.

By default, the CC-BY license will be applied. The overarching bibliography of all datasets created within the long-term Observatory Glaciology at *Neumayer stations* is available at https://doi.pangaea.de/10.1594/PANGAEA.971649. Metadata for MIMO-EIS are already available in registry.o2a-data.de (ID 8403, item: Phase-sensitive Radio Echo Sounding System, event labels NMEIS?_24). Previous results from MIMO-EIS are available at https://doi.pangaea.de/10.1594/PANGAEA.972121.

Metadata for density measurement performed during the Kottaspegel traverse and at *Neumayer Station III* for the 2024/25 season will be made available in registry.o2a-data.de with a new ID – previous corer IDs 8363 (AWI single tube snowpack sampler) and 5065 (Ice Corer Kovacs Mark II). The already quality checked density data is available in at https://doi.org/10.1594/PANGAEA.963323.

For the GNSS-RR sub-project, the Python code for preprocessing, processing, analyzing, and visualizing the GNSS-RR data is provided on GitHub https://github.com/lasteine/GNSS_RR.git and archived in Zenodo under https://doi.org/10.5281/zenodo.10135417. Collected and analyzed multifrequency and multisystem GNSS data have been made publicly available at PANGAEA (https://doi.org/10.1594/PANGAEA.958973).

Any other data will be submitted to an appropriate long-term archive that provides unique and stable identifiers for the datasets and allows open online access to the data.

This expedition was supported by the Helmholtz Research Programme “Changing Earth – Sustaining our Future” Topic 2, Subtopic 3.

In all publications based on this expedition, the **Grant No. AWI_ANT_8** will be quoted and the following publication will be cited:

Alfred-Wegener-Institut Helmholtz-Zentrum für Polar- und Meeresforschung (2016a). *Neumayer III and Kohnen Station* in Antarctica operated by the Alfred Wegener Institute. Journal of large-scale research facilities, 2, A85. http://dx.doi.org/10.17815/jlsrf-2-152.

References

Zeising O, Hattermann T, Kaleschke L, Berger S, Drews R, Ershadi MR, Fromm T, Pattyn F, Steinhage D & Eisen O (2025) Weakening of meltwater plume reduces basal melting in summer at Ekström Ice Shelf, Antarctica, The Cryosphere. https://doi.org/10.5194/egusphere-2024-2109

4.9 Maintenance of the PALAOA3 Observatory

Stefanie Spiesecke[1], [1]DE.AWI
Olaf Boebel[1]
not in the field: Elke Burkhardt[1],
Karolin Thomisch[1],
Ilse van Opzeeland[1*]
*Ilse.van.opzeeland@awi.de

Grant-No. AWI_ANT_12 and AWI_PS146_01

Objectives

PALAOA (the Perennial Acoustic Observatory in the Antarctic Ocean) located on the Ekström Ice Shelf since 2005, collected continuous underwater recordings from a coastal Antarctic environment using a hydrophone deployed at ca. 160 m depth. With the ice shelf advancing by about 150 m per year, the position was constantly changing.

Upon our arrival at *Neumayer Station III* on PS129 it was observed that the hydrophone was ripped off during a calving event. During a helicopter flight to the PALAOA site on 23 March 2022, the recording box was retrieved and the electronics, including the data storage, were taken back to *Polarstern*. Analyzing the recovered acoustic data revealed that the calving event took place on the 27 February 2022 at approx. 08:16 UTC.

In January 2024, during ANT-Land 2023/24 three new hydrophones were successfully deployed under the ice shelf, using hot water drilling. The former recording unit, an aluminum box, containing a modified SonoVault electronics and battery supply, was again set up for further recordings. The hydrophone cable was inserted into a protective hose, leading to the box (80 cm x 60 cm x 60 cm), which is recessed into the snow and covered with a wooden board and snow. It includes a Reson input module EC6073 for the active hydrophone (Reson TC4032) and a SonoVault electronics module, similar to those used in the moored recorders. For the power supply, four 90 Ah, 12 V batteries are included, two batteries in a row and those rows in parallel, supplying both, the hydrophone and the recording electronics. Storage capacity is 4.4 TB (35 x 128 GB SDXC). With a sampling rate of 96 kHz at 24 bit and a file size corresponding to of 600 s (10 min) the PALAOA system will be serviced by the *Neumayer Station III* overwintering team every 3-4 months.

Shortly after the deployment the northernmost hole (PALAOA-N), originally 1 km from the ice edge, was not safe to service anymore, due to substantial calving events after which the bore hole with hydrophone was now situated 350 m away from the ice edge. The recording electronics were therefore moved to the second bore hole (PALAOA-C), now 1.3 km away from the edge. Unfortunately, data from this hydrophone position, contained clipping, during certain periods, presumably originating from high flow noise and strumming at the hydrophone and/or cable. However, this problem could not be solved with the available technical means during the overwintering period.

During PS146, the *Polarstern* offloading time frame at *Neumayer Station III*, spanning the 11 to 13 January 2025, was used for amendments to improve recording quality at PALAOA-C.

Fieldwork

To facilitate the work on site at PALAOA-C, a living container, generator and skidoo were provided. First, a filter was installed to remove the high amplitude low frequency noise which had been resulting in the clipping of recordings. After several test runs, it was decided to use a RESON VP2000 filter module and install it between the input module and the recording unit with a high pass filter of 50 Hz (low pass = 1 MHz, output gain = 0 dB). A gain setting of level 1 was then set for a test run. Weather related logistics required *Polarstern* to leave the Nordanleger and return on 23 January 2025. This period functioned as a longer test run to check the recordings for further clipping events. Following this check, a setting of level 2 (+12 dB) was settled upon for the time being. With support of the overwintering team, the quality of the recordigns will be monitored allowing further adjustments in the settings to be made if required.

Data management

Passive acoustic data (of data processing Level 1+, see also Thomisch et al, 2023a; 2023b) acquired by the PALAOA LTO will be archived, published and disseminated according to international standards by the World Data Center PANGAEA Data Publisher for Earth & Environmental Science (https://www.pangaea.de; Felden et al. 2023) within two years after the end of the expedition at the latest. By default, a CC-BY 4.0 license will be applied. Quality controlled data will be made available through the OPUS (Open Portal to Underwater Soundscapes; www.opus.aq) applying FAIR principles, following the working group's standard operating procedures (Thomisch et al, 2023a; 2023b).

This expedition was supported by the Helmholtz Research Programme "Changing Earth – Sustaining our Future" Topic 6, Subtopic 4.

In all publications based on this expedition, the **Grant No. AWI_ANT_12** will be quoted and the following publication will be cited:

Alfred-Wegener-Institut Helmholtz-Zentrum für Polar- und Meeresforschung. (2016a). *Neumayer III* and *Kohnen Station* in Antarctica operated by the Alfred Wegener Institute. Journal of large-scale research facilities, 2, A85. http://dx.doi.org/10.17815/jlsrf-2-152

References

Felden J, Möller L, Schindler U et al. (2023). PANGAEA - Data Publisher for Earth & Environmental Science. Sci Data 10:347. https://doi.org/10.1038/s41597-023-02269-x

Thomisch K, Spiesecke S & Boebel O (2023a) Standard operating procedures: Featuring Passive Acoustic Data by The Open Portal to Underwater Soundscapes (OPUS), Glossary. https://doi.org/10.5281/zenodo.7620763

Thomisch K, Spiesecke S & Boebel O (2023b) Standard operating procedures: Featuring Passive Acoustic Data by The Open Portal to Underwater Soundscapes (OPUS), Part I: Data preparation and standardization. https://doi.org/10.5281/ZENODO.7680029

4.10 SPOT – Single Penguin Observation and Tracking

Daniel P. Zitterbart*[1,2], Alexander Winterl[1], [1]DE.FAU
Loïcka Baille[2] , Aymeric Houstin[2], Gaël Bardon[3] [2]EDU.WHOI
Not in the field: Céline Le Bohec[3,4], Sebastian [3]MCO.CSM
Richter[1], Ben Fabry[1] [4]FR.CNRS
*dzitterbart@whoi.edu

Grant-No. AWI_ANT_13

Outline

SPOT is a long-term remote-controlled observatory to monitor emperor penguins continuously throughout the year for biophysical, ecological and behavioral studies.

Objectives

Continuous data collection over prolonged time periods is the cornerstone of behavioral and ecological studies. Such data can be used to analyze a large scale of behavioral and ecological problems, from an individual animal to population trends. Time lapse imaging has gained significant interest within the last decade and is now a standard tool due to the large availability of low-cost digital cameras (Kucera & Barrett 1993; Newbery & Southwell 2009; Lynch, Alderman & Hobday 2015) as well as the steadily increasing capability of image processing software (Dell et al. 2014; Gerum et al. 2016). However, in remote and climatically harsh locations such as Antarctica, data acquisition and physical access to the observation system can be challenging. We implemented a remote-controlled and energetically self-sufficient observatory (Fig. 4.10.1) specifically designed to operate in Antarctic conditions.

The observatory is designed with the aim to investigate the population and behavioral ecology of emperor penguins (Zitterbart et al. 2011, 2014; Gerum et al. 2013). The challenges in observing emperor penguin colonies are that those are poorly accessible, and their mating and breeding behavior can only be observed during the coldest and darkest months, with wind speeds up to 150 km/h and temperatures as low as -50°C. Therefore, the observatory needs to be autonomous and remotely controllable, as well as require little maintenance. As emperor penguins do not build nests, and incubate their single egg on their feet, the whole colony can move within an area of several km^2. In order to observe such a large area, we installed seven stationary wide-angle cameras for panoramic overview images, and a steerable 29-megapixel camera mounted on a pan-and-tilt unit as well as a long wave thermal imaging camera. Both, the thermal and the color camera, are equipped with a telephoto lens for either high-resolution images, stitched panoramic images, or video recordings of the colony.

SPOT was deployed in the Austral summer season 2012/2013 at Atka Bay (70°37.0'S, 8°9.4'W), approximately 8 km north of *Neumayer Station III*, on the Ekström shelf ice (Richter et al. 2018). Since 2013, we have been collecting wide-angle overview images at a rate of 1 frame per minute to determine the colony position, and when visibility conditions permit daily panoramic images stitched from high-resolution images to count penguins, and on-demand high-resolution video recordings of the colony at 5 frames per second (fps).

Fig. 4.10.1: SPOT Penguin Observatory in 2025 with new wind turbines

Fieldwork

Data collection throughout the winter 2024 went without major problems. In 2024, the penguin colony was situated again in front of SPOT compared to 2022 and 2023, leading to successful data collection for phenology and abundance estimates. Overview cameras recording the position and density of the colony were operational throughout the year. The high-resolution RGB camera was operational throughout the year and recorded images on demand when daylight, penguin's position was favorable and the power reserves of SPOT observatory enough. The thermal imaging camera was operated when possible, in conjunction with the RGB camera.

During the summer campaign in 2024/2025, we replaced both Windside wind turbines which were over 5 years old with a new model. We are trailing a V150 (h-rotor) and a Air30 (v-rotor) for survivability. Both turbines are designed to provide more power in lower-wind regimes then the Windside turbines, to allow SPOT to be powered throughout the Antarctic winter.

Preliminary (expected) results

We have been operating SPOT now for 13 breeding seasons with increasing success, which is reflected in annual operation time and data collected. Whilst during the first 2 years we had hardware failure of different components, this has not occurred since the winter of 2015. The operation is conducted completely remotely with support from the overwintering team in case it is needed. Most assistance is needed to grease the wind generators every 3 months, as well as to de-ice the overview cameras, which do not have a dedicated heating, especially in autumn when rare freezing fog is possible. Counts throughout the seasons 2018 to 2020 clearly show the arrival pattern as well as the occupation peak of the colony when presumably the whole population is present in May. SPOT phenology and population data is now being used by the international emperor penguin scientist community to ground truth satellite imagery for continent wide emperor penguin abundance assessments (Larue et al. 2024). Using SPOT data, we developed a new method to estimate Emperor penguin breeding success from satellite imagery (Winterl et al. 2024).

Data management

All data recorded by SPOT is transferred annually to the AWI Pangea Data storage repository and stored in the long-term archive.

In all publications based on this expedition, the **Grant No. AWI_ANT_13** will be quoted and the following publication will be cited:

Alfred-Wegener-Institut Helmholtz-Zentrum für Polar- und Meeresforschung. (2016a). *Neumayer III and Kohnen Station* in Antarctica operated by the Alfred Wegener Institute. Journal of large-scale research facilities, 2, A85. http://dx.doi.org/10.17815/jlsrf-2-152

References

LaRue M, Iles D, Labrousse S, Fretwell P, Ortega D, Devane E, Horstmann I, Viollat L, Foster-Dyer R, Le Bohec C, Zitterbart D, Houstin A, Richter S, Winterl A, Wienecke B, Salas L, Nixon M, Barbraud C, Kooyman G, Ponganis P, Ainley D, Trathan P & Jenouvrier S (2024) Advances in remote sensing of emperor penguins: first multi-year time series documenting trends in the global population. Proc R Soc B 291:20232067. https://doi.org/10.1098/rspb.2023.2067

Dell AI, Bender JA, Branson K, Couzin ID, De Polavieja GG, Noldus LPJJ, Pé Rez-Escudero A, Perona P, Straw AD, Wikelski M & Brose U (2014) Automated image-based tracking and its application in ecology, Trends in Ecology & Evolution 29(7):417–428. https://doi.org/10.1016/j.tree.2014.05.004

Gerum RC, Richter S, Fabry B & Zitterbart DP (2016) ClickPoints: an expandable toolbox for scientific image annotation and analysis (T. Poisot, Ed.). Methods in Ecology and Evolution. 8(6):750–756. https://doi.org/10.1111/2041-210X.12702

Gerum RC, Fabry B, Metzner C, Beaulieu M, Ancel A & Zitterbart DP (2013) The origin of traveling waves in an emperor penguin huddle. New Journal of Physics,15:125022. https://doi.org/10.1088/1367-2630/15/12/125022

Kucera TE & Barrett RH (1993) THE TRAILMASTER? CAMERA SYSTEM FOR DETECTING WILDLIFE. Wildlife Society Bulletin 21:505–508.

Lynch TP, Alderman R & Hobday AJ (2015) A high-resolution panorama camera system for monitoring colony-wide seabird nesting behaviour (H. Schielzeth, Ed.). Methods in Ecology and Evolution 6(5):491–499. https://doi.org/10.1111/2041-210X.12339

Newbery KB & Southwell C (2009) An automated camera system for remote monitoring in polar environments. Cold Regions Science and Technology 55(1):47–51. https://doi.org/10.1016/j.coldregions.2008.06.001

Richter S, Gerum R, Schneider W, Fabry B, Le Bohec C & Zitterbart DP (2018) A remote-controlled observatory for behavioural and ecological research: A case study on emperor penguins, Methods in Ecology and Evolution 9 (5):1168–1178. https://doi.org/10.1111/2041-210X.12971

Winterl A, Richter S, Houstin A, Barracho T, Boreau M, Cornec C, Couet D, Cristofari R, Eiselt C, Fabry B, Krellenstein A, Mark C, Manika A, Menard D, Moriany J, Pottier S, Schloesing E, Le Bohec C & Zitterbart DP (2024) Remote sensing of emperor penguin abundance and breeding success. Nat Commun 15:4419. https://doi.org/10.1038/s41467-024-48239-8

Zitterbart DP, Richter S, Spiekermann G, Behrens LK, Regnery J, Fontes RP, Hänssler T, König-Langlo G, Weller R & Fabry B (2014) Short Note Are environmental factors responsible for changed breeding behaviour in emperor penguins? Antarctic Science 26(5):563-564. https://doi.org/10.1017/S0954102014000285

Zitterbart DP, Wienecke B, Butler JP & Fabry B (2011) Coordinated movements prevent jamming in an emperor penguin huddle. PLoS ONE 6:e20260. https://doi.org/10.1371/journal.pone.0020260

4.11 MARE – Monitor the Health of the Antarctic Using the Emperor Penguin as a Sentinal

Gaël Bardon[1], Aymeric Houstin[2],
Alexander Winterl[3], Loïcka Baille[2],
Dev Vaibhav[2], Daniel P. Zitterbart[2,3]
not in the field: Céline Le Bohec*[1,4]
* celine.lebohec@cnrs.fr

[1]MCO.CSM
[2]US.WHOI
[3]DE.FAU
[4]FR.CNRS

Grant-No. AWI_ANT_14

Outline

Operation of a long-term Emperor Penguin Life Observatory in Atka Bay (on land and at sea) to evaluate the dynamics and trends of this population, and, ultimately, the amplitude of the adaptive capacities of the species.

Objectives

The main goal of MARE is to assess the vulnerability of Antarctic ecosystems using a sentinel species of Polar Regions: the Emperor penguin (*Aptenodytes forsteri*), which stands at the forefront of the impacts of climate warming. Until 2017, the general biology of the entire species (e.g. all parameters concerning the breeding, life-history, and demography) was based on the monitoring of a single colony (a colony that our team is also monitoring electronically and through camera systems within the framework of the IPEV 137 project at Pointe Géologie in Terre Adélie). Yet, to evaluate the overall trend of a species and the amplitude of its adaptive capacities, it is crucial to monitor over the long-term more than one population breeding in different ecosystems. This is especially true considering that the species is at high risk of extinction in a very near future according to climatic scenarios (Trathan et al. 2020; LaRue et al. 2024; Jenouvrier et al. 2025). In that context, this second worldwide Life Observatory of emperor penguins (started in 2017 in Atka Bay; that aims to be embedded in an Integrated East Antarctic Marine Research (IEAMaR) Observatory, Gutt et al. 2022) aims to measure the species' adaptive potential to climate change and associated fluctuations in prey abundance and distribution.

WP1

Since 2017, each year and over several decades, 300 five-month-old emperor penguin chicks from Atka Bay colony (out of the approx. 7'000 chicks present each year at the end of the breeding cycle) are marked with small Passive Integrated Transponders (PIT) in order to monitor birds of known-age and -history throughout their life. Microtagged individuals are detected and identified, year after year, with Mobile Identification Systems (MIS), i.e. Radio-Frequency Identification (RFID)-antenna-sledges temporarily deployed on access passageways to birds' breeding sites and RFID-antenna mounted on ECHO-Rover.

WP2

Gathering knowledge on the distribution at sea of the upper-level species is fundamental to help us to define and map marine biological 'hotspots' and/or Marine Protected Areas (MPA). Since 2017, emperor penguins from Atka Bay colony are equipped, over regular intervals and at different stages of their life cycle, with miniaturized multi-sensor biologgers to understand how this species uses the space at sea during the breeding/wintering season, their migration, and their wintering at-sea habitats, and to explore their foraging strategies.

In addition, through yearly collection of biological samples we aim at monitoring the diet and trophic level (and their yearly variability) on which emperor penguins are foraging. Gastroliths collected in dead chicks (stomach contents of dead birds) aim to improve the geologic characterization of the foraging grounds and thus the glacial-geologic history of the Ekströmisen region. Moreover, prevalence and yearly variability of microplastics and contaminants is monitored through the analyses of these biological samples.

Fieldwork

The ANT-Land 2024/2025 summer season for MARE program ran from 8 November 2024 to 11 January 2025 on the Atka Bay emperor penguin colony.

A total of 300 five-month-old emperor penguin chicks from the colony of Atka Bay were microtagged. Each chick was also measured (flippers and beak), weighed, blood sampled, and temporarily marked before release to avoid accidental recapture.

Three RFID antenna sledges (Fig. 4.11.1) were deployed along key access routes used by emperor penguins moving between the sea and their breeding colony. Some were also positioned to intercept natural colony movements caused by wind shifts. These antennas enabled the identification of microtagged individuals and the collection of longitudinal capture-mark-recapture data for population dynamics modelling.

Fig. 4.11.1: Deployment of a LittleLeonardo-Ausoms-VHF datalogger on a breeding adult emperor penguin at Atka Bay

Eighteen breeding emperor penguins were successfully equipped with dataloggers and VHF transmitters. Four types of devices were deployed:

- CatsCam: sounds, video, depth, and accelerometers;
- LittleLeonardo + Ausoms: video, depth, and accelerometers; sounds;
- Axytreck: GPS, depth, and accelerometers;
- Custom LoRA loggers: GPS.

After identifying adults feeding their chicks at the periphery of the colony, we isolated adult-chick pairs in a corral outside the colony. Chicks were measured, weighed, temporarily marked, and RFID-tagged as part of the cohort marking. Adults were measured (flippers and beak), externally equipped with data-loggers using Tesa-tapes and Colson-ties, and temporary marked before release (for identifying the bird for the recapture/retrieval of the equipment). Visual monitoring and VHF antenna tracking were conducted throughout the season to locate equipped birds and recover the devices.

Three automated LoRa-connected VHF antennas were installed early in the season, enabling continuous monitoring of tagged individuals and real-time detection of their presence or absence at the station (Fig. 4.11.2).

Fig. 4.11.2: LoRa-connected autonomous VHF antenna installed near the colony for real-time tracking of tagged individuals

All deployed devices were successfully recovered, except for one. All four systems performed as expected, providing hours of underwater video and audio, GPS tracks of 10 foraging trips, and the first dataset from the custom LoRa loggers.

New tests were also conducted with the ECHO rover. After being returned at the end of the ANT-Land 2023/2024 season, ECHO was upgraded with tracks instead of wheels to improve its mobility on ice. The new configuration significantly enhanced its manoeuvrability. Tests were carried out to evaluate ECHO's ability to approach the colony slowly and autonomously without causing disturbance. Some mechanical noise was detected due to the new track system, a challenge we'll be working to overcome next season(s). Data collected during these tests will help improve ECHO's approaches and its ability to scan RFID tags.

Colony census, key phenological and breeding parameters, chick mortality, and major environmental constraints were monitored throughout the season. This year, the census was conducted using drone imagery, allowing for more accurate and automated counts via deep learning-based tools (Fig. 4.11.3).

A total of 149 emperor penguin chicks were found dead and collected for biometry between 8 November 2024 to 10 January 2025.

In the context of the global outbreak of HPAI (Highly Pathogenic Avian Influenza), the colony was closely monitored for abnormal mortality or disease symptoms. No signs of infection were observed during the season. One individual (dead or alive) was tested each day of handling using oral swabs; all samples tested negative for HPAI.

Acoustic recorders (AudioMoth) were deployed around the colony to build a vocal database for acoustic capture-mark-recapture analyses and to study the colony's soundscape. Three recorders were continuously operated at the locations of the RFID antennas.

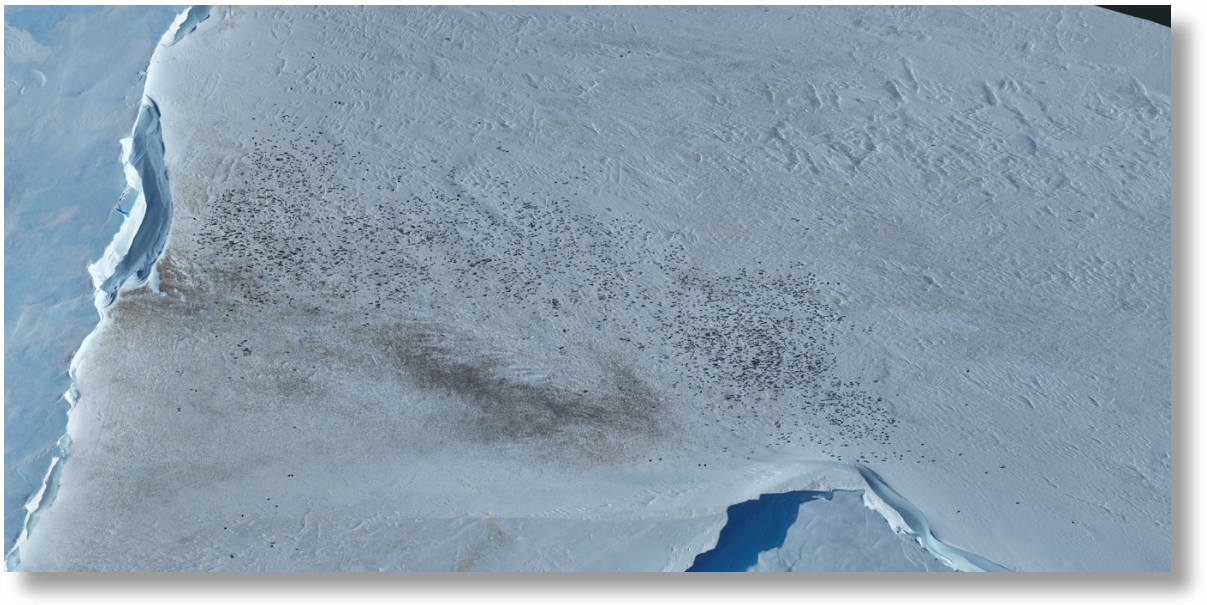

Fig. 4.11.3: High-resolution drone imagery used for colony-wide census and phenological monitoring of the emperor penguin population

Preliminary (expected) results

The primary on-land objective of the MARE Program is to model the population dynamics and trends of the Atka Bay emperor penguin colony. This is achieved through the annual microtagging of fledging chicks and their identification using the MIS systems (a combination of RFID-antenna sledges and the ECHO Rover), a process initiated during the 2021/2022 season. This objective relies on long-term data collection based on the capture-mark-recapture method. Age-specific vital rates–such as survival and breeding success–required to feed population models will only become available after at least 10 years of electronic monitoring. For reference, emperor penguins in the Pointe Géologie colony typically begin breeding at an average age of five years, the first analysis of this population's vital traits (i.e. juvenile survival) was published this year, after 15 years of monitoring (Le Scornec et al. 2025).

Following the first detections in the 2022/23 season, we identified 21 different previously PIT-tagged emperor penguins during the 2024/25 season (from November to mid-January; please see Tab. 4.11.1). This high detection rate is encouraging and suggests the potential for robust survival analyses. The next step is to double the number of detection systems at the site, allowing for continuous monitoring throughout the full breeding season (April to January).

As for the phenology and census of the Atka Bay emperor penguin colony during the 2024/25 season: unlike the previous two seasons, the majority of the colony settled on sea ice. Only a small group of approximately 1,000 individuals remained on the shelf ice throughout the season. Drone imagery significantly improved the efficiency and accuracy of the census. Less than one hour of flight time was sufficient to cover the entire colony, enabling near-daily monitoring. Combined with ongoing phenological data collection at Atka Bay, these high-resolution datasets now allow for the refinement of phenological models. This is essential for more accurate tracking of colony size and population trends in emperor penguins, as demonstrated in our recent publication in Nature Communications (Winterl et al. 2024).

Following the first deployment of CatsCam devices on wild emperor penguins during the Ant-Land 2022/23 summer season, five additional individuals were equipped during the 2024/25 season. The video data collected has already yielded promising results. Notably, we documented, for the first time to our knowledge, a group of emperor penguins feeding at the base and along the side of an iceberg (Fig. 4.11.4). This novel observation provides new insights into emperor penguin foraging ecology. These preliminary findings mark the beginning of a broader analysis: the hours of recorded footage will be used to study collective foraging strategies, in collaboration with Drs. A. Thiebault and I. Charrier (University of Paris-Saclay).

The successful deployment of automatic VHF antennas–connected to the station via LoRa–significantly reduced the need for direct observation during the field season. Since VHF technology is widely used for tracking wild individuals across various taxa in ecological research, this technological advancement represents a major improvement in monitoring efforts and should be published in the coming years.

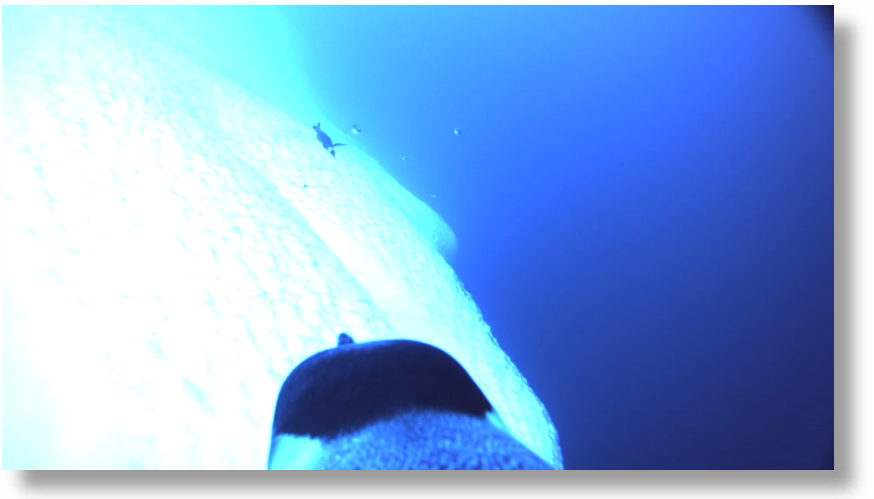

Fig. 4.11.4: Underwater still frame from a CatsCam video showing emperor penguins foraging near the base of an iceberg.

Tab. 4.11.1: Proportion of birds detected during the season 2024/25 from the different groups of marking

Year of marking	**2017/18**	**2018/19**	**2019/20**	**2020/21**	**2021/22**	**2022/23**	**2023/24**	**2024/25**
Marked as juvenile	3/300	10/300	4/300	0	1/300	0/300	0/300	5/300
Marked as adult	2/25	0/20	0	0	0/24	0/1	0	0/18

Data management

Phenology data, Capture-Mark-Recapture, the composition of stomach contents and the mineralogical composition of the gastroliths will be published in AWI's PANGAEA repository after analyses completion of the analysis, as it was previously done for the at-sea objectives published in 2022 (e.g. https://doi.pangaea.de/10.1594/PANGAEA.913447 ; https://www.movebank.org/cms/panel_embedded_movebank_webapp?gwt_fragment=page=studies,path=study1322558986).

Any other data will be submitted to an appropriate long-term archive that provides unique and stable identifiers for the datasets and allows open online access to the data.

This expedition was supported by the Helmholtz Research Programme "Changing Earth – Sustaining our Future" Topic 6, Subtopics 1, 2 and 4.

In all publications based on this expedition, the **Grant No. AWI_ANT_14** will be quoted and the following publication will be cited:

Alfred-Wegener-Institut Helmholtz-Zentrum für Polar- und Meeresforschung. (2016a). Neumayer III and Kohnen Station in Antarctica operated by the Alfred Wegener Institute. Journal of large-scale research facilities, 2, A85. http://dx.doi.org/10.17815/jlsrf-2-152.

References

Gutt J, Arndt S, Barnes DKA, Bornemann H, Brey T, Eisen O, Flores H, Griffiths H, Haas C, Hain S, Hattermann T, Held C, Hoppema M, Isla E, Janout M, Le Bohec C, Link H, Mark FC, Moreau S, Trimborn S, van Opzeeland I, Pörtner H-O, Schaafsma F, Teschke K, Tippenhauer S, Van de Putte A, Wege M, Zitterbart D & Piepenburg D (2022) Reviews and syntheses: A framework to observe, understand and project ecosystem response to environmental change in the East Antarctic Southern Ocean. Biogeosciences 19:5313–5342. https://doi.org/10.5194/bg-19-5313-2022

Jenouvrier S, Eparvier A, Şen B, Ventura F, Che-Castaldo C, Holland M, Landrum L, Krumhardt K, Garnier J, Delord K, Barbraud C & Trathan (2025) Living with uncertainty: Using multi-model large ensembles to assess emperor penguin extinction risk for the IUCN Red List. Biological Conservation 305:111037. https://doi.org/10.1016/j.biocon.2025.111037

LaRue M, Iles D, Labrousse S, Fretwell P, Ortega D, Devane E, Horstman B, Viollat L, Foster-Dyer R, Le Bohec C, Zitterbart D, Houstin A, Richter S, Winter A, Wienecke B, Salas L, Nixon M, Barbraud C, Kooymann G, Ponganis P, Ainley D, Trathan P & Jenouvrier S (2024) Advances in remote sensing of emperor penguins: first multi-year time series documenting trends in the global population. Proceedings of the Royal Society B: Biological Science 291:20232067. https://doi.org/10.1098/rspb.2023.2067

Le Scornec E, Allain J, Bardon G, Barracho T, Chatelain N, Delord K, Filippi D, Ribout C, Le Bohec C & Barbraud C (2025) Intrinsic and extrinsic drivers of juvenile survival in emperor penguins. Polar Biology 48(2):41. https://doi.org/10.1007/s00300-025-03369-7

Trathan PN, Wienecke B, Barbraud C, Jenouvrier S, Kooyman G, Le Bohec C, Ainley DG, Ancel A, Zitterbart DP, Chown SL, LaRue M, Cristofari R, Younger J, Clucas G, Bost C-A, Brown JA, Gillett HJ & Fretwell PT (2020) The emperor penguin - Vulnerable to projected rates of warming and sea ice loss, Biological Conservation 241:108216. https://doi.org/10.1016/j.biocon.2019.108216

Winterl A, Richter S, Houstin A, Barracho T, Boureau M, Cornec C, Couet D, Cristofari R, Eiselt C, Fabry B, Krellenstein A, Mark C, Mainka A, Ménard D, Morinay J, Pottier S, Schloesing E, Le Bohec C & Zitterbart DP (2024) Remote sensing of emperor penguin abundance and breeding success. Nature Communications 15(1):4419. https://doi.org/10.1038/s41467-024-48239-8

4.12 NODEMPICE-NM 2024 – Environmental Seismology for Emperor Penguin Behaviour and Population Monitoring

Andrey Jakovlev[1], Amelie Nüsse[1]
not in the field: Dimitri Zigone[1], Céline Le Bohec[2,3], Olaf Eisen*[6,7], Vera Schlindwein[6,7], Daniel Zitterbart[4,5], Stefanie Arndt[6], Christian Haas[6,7]
* olaf.eisen@awi.de

[1]FR.EOST/ITES
[2]FR.CNRS
[3]MC.CSM
[4]EDU.WHOI
[5]DE.FAU
[6]DE.AWI
[7]DE.UNI-Bremen

Grant-No. AWI_ANT_17

Objectives

Current climate change projections indicate that rising temperatures and changing wind patterns will have a negative impact on sea ice (Meehl et al. 2019; Alkama et al. 2020) on which emperor penguins breed. In this context of habitat loss for the species, some studies indicate that emperor penguin populations will decline by more than 50% during the current century (see the synthesis by Trathan et al. 2020, of which two members of the project are part). NODEMPICE is part of the recent development of "environmental seismology", which provides new observables and proxies for the monitoring of environmental processes in the context of climate change (e.g., Larose et al. 2015). We want to employ related seismic techniques to identify sea-ice characteristics which also might be felt by penguins. First, icequakes from cracks display a characteristic frequency in the 10s to 100s or Hz range, which depends on the ice thickness. Second, lower-frequency modes of elastic sea ice motion might also depend on ice thickness and potentially be felt by the animals. Key questions are: What is the distribution of the mechanical properties of ice (sea and land)? How do they change both spatially and over time? How do animal colonies respond (finely - behavioral responses of an individual, a group of penguins called a "huddle", and the colony) to these characteristics and their variations? Are there any particular characteristics of sea ice (which may be related to site configuration, e.g., anchorage to islands, mainland, ice shelf rifts, icebergs) that are critical to the selection of emperor penguin breeding sites (e.g., compromise between sea ice stability, protection from prevailing winds, distance to feeding sites)?

The NODEMPICE-NM project can be broken down into two operational phases in the field at *Neumayer Station III*. In phase I we will deploy a network of miniaturized "Node" seismometers over several weeks, on a few sites around and on the nesting sites (note that the penguin colonies are mobile, that is, they can move several meters or even hundreds of meters during a day) to investigate feasibility. In phase II we plan to repeat the operation, with the same design, over a three-year period at both *Dumont d'Urville Station* (DDU) and *Neumayer Station III* (NMIII) sites, in order to integrate interannual seasonal environmental variability in our models and to detect interannual changes and local trends in the physical and biological properties of our systems. Deployment will be on winter sea ice in May/June and retrieval in October/November before break-up.

The fieldwork described in this report is a contribution to phase I at *Neumayer Station III*.

Fieldwork

The recording systems consisted of SmartSolo seismic nodes (a sealed housing consisting of a 3-component geophone, battery, GPS receiver and data storage). The systems were deployed as listed in Table 1. After formation of the Emperor Penguin colony in Atka Bay the stations were deployed in two groups in front of the colony (01X and 02X). The array set-up consisted of five nodes each (station number 01 to 05 for each array), approximately oriented in a square of some 100 m side length with one node at each corner and one in the center. In order to avoid artifacts for data processing from regular deployment positions the sides of the square and the angles were not exactly 100 m long and not 90°. The deployment took place on 8 July 2024. All nodes were removed on 5 August 2024.

On the day of deployment, there was hardly any snow on the sea ice. Most of the sea ice around the colony was directly at the surface. Therefore, it was quite tricky to find a place where the SmartSolos could be completely covered by snow (to reduce wind noise). Thus almost all of the nodes were installed with the spikes directly touching the ice. Although this is advantageous for signal recording, this caused problems with the retrieval of the nodes. Especially in the western part of the network, near the edge of the shelf, considerable snow accumulation of roughly 2-metre-thick occurred. As was described in the previous years' reports, this led to the two instruments (locations 01X04 and 01X05) being flooded (see photos). The 01X05 node was covered by around 50 cm of water, while the 01X04 was mostly in slushy ice rather than water. Also, at location 01x04, one of the two bamboo poles (reaching above the surface by about 1.5 m) used to mark the node location was completely covered in snow. This made it quite difficult to relocate the node. Luckily, the top of the pole was only about 10 cm below the surface.

To avoid this problem in the future, we suggest not putting the instruments on the ice surface, especially in areas where considerable snow accumulation can be expected because of the prevailing wind direction. In any case, longer poles are required close to the ice shelf edge.

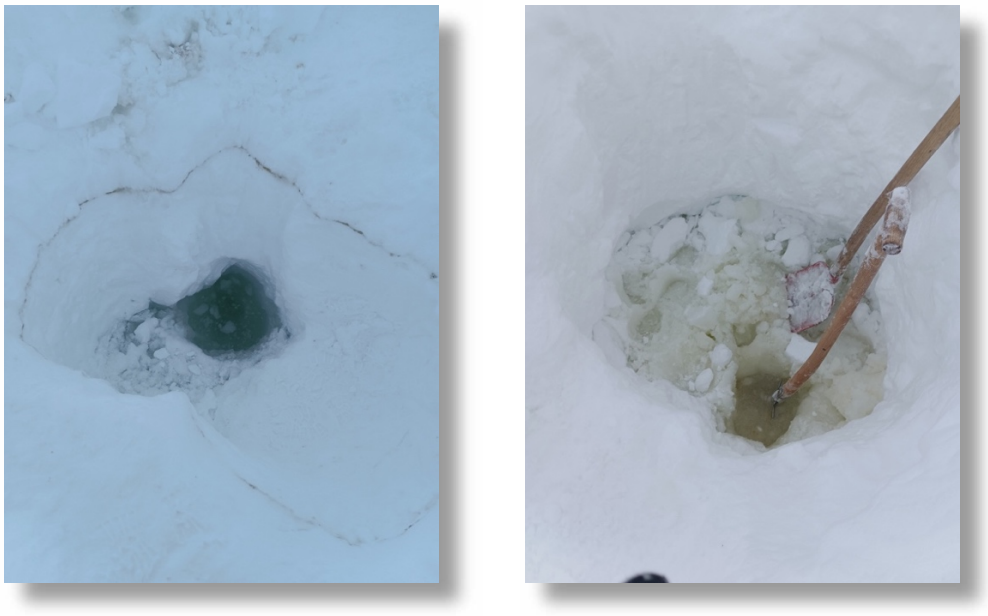

Fig. 4.12.1: Nodes in flooded snow on sea ice in August 2024 at stations 01X05 (left) and 01X04 (right)

Tab. 4.12.1: Deployment times and positions of the SmartSolo nodes in winter season 2024

Station	SNR	Start Date	Start Time UTC	Latitude °	Longitude °
01X01	453014635	08.07.24	12:31:49	-70.61786962	-8,15535975
01X02	453017994	08.07.24	12:51:19	-70.61698834	-8,15598615
01X03	453016587	08.07.24	13:10:13	-70.61752457	-8,15278318
01X04	453017843	08.07.24	13:37:37	-70.6187353	-8,15575662
01X05	453016737	08.07.24	13:51:46	-70.61818001	-8,15792521
02X01	453018377	08.07.24	14:38:37	-70.61819013	-8,11709004
02X02	453017770	08.07.24	14:51:44	-70.61719048	-8,11607495
02X03	453018231	08.07.24	15:03:53	-70.61821958	-8,11435563
02X04	453016608	08.07.24	15:16:22	-70.61897739	-8,11798809
02X05	453017962	08.07.24	15:31:23	-70.61803602	-8,11942271

Preliminary results

Since the start of the NODEMPICE project, we performed three deployments at *Dumont d'Urville Station* (DDU). The first two experiments occurred in 2022 and 2023 were design to test the instruments and the protocols of installation along with the best parametrization for the seismic instruments. The actual sciences experiments started in 2023 with a deployment of 3 antennas of five nodes each deployed at three different locations near DDU.

At Atka Bay (NMIII), following the deployment with different systems in the years 2022 and 2023 (Data Cubes), the winter 2024 was the first deployment of SmartSolos at Atka Bay. The data analysis with a total size of some 50 GB is still in progress.

Data management

The seismic data will be published through GEOSCOPE.

This expedition was supported by the Helmholtz Research Programme "Changing Earth – Sustaining our Future" Topic 6, Subtopics 1, 2 and 4.

In all publications based on this expedition, the **Grant No. AWI_ANT_17** will be quoted and the following publication will be cited:

Alfred-Wegener-Institut Helmholtz-Zentrum für Polar- und Meeresforschung. (2016a). *Neumayer III and Kohnen Station* in Antarctica operated by the Alfred Wegener Institute. Journal of large-scale research facilities, 2, A85. http://dx.doi.org/10.17815/jlsrf-2-152.

References

Alkama R, Koffi EN, Vavrus SJ, Diehl T, Francis JA, Stroeve J, Forzieri G, Vihma T & Cescatti A (2020) Wind amplifies the polar sea ice retreat, Environmental Research Letters 15:124022. https://doi.org/10.1088/1748-9326/abc379

Larose E, Carrière S, Voisin C, Bottelin P, Baillet L, Guéguen P, Walter F, Jongmans D, Guillier B, Garambois S, Gimbert F & Massey C. (2015) Environmental seismology: What can we learn on earth surface processes with ambient noise? Journal of Applied Geophysics 116:62–74. https://doi.org/10.1016/j.jappgeo.2015.02.001

Meehl GA, Arblaster JM, Chung CTY, Holland MM, DuVivier A, Thompson L, Yang D & Bitz CM (2019) Sustained ocean changes contributed to sudden Antarctic sea ice retreat in late 2016, Nature Communications 10:14. https://doi.org/10.1038/s41467-018-07865-9

4.13 WSPR RADIO Beacon at *Neumayer Station III* for Evaluation of Southern Hemisphere Radio Propagation

Michael Hartje[1] [1]DE.HS-Bremen
not in the field: Sören Peik[1]

Grant-No. AWI_ANT_15

Objectives

The objective of this project is to gain more knowledge about the propagation of radio waves in the ionosphere at Antarctic latitudes and at frequencies between 100 KHz and 50 MHz. This is achieved by about 2000 amateur radio stations (also called “ham radio”) spread over the globe. These stations transmit beacon signals or/and receive them from other stations, generating so-called “spots”. These spots are reported into an open web-based database system, also known as “WSPR-Net”. The beacon messages use a standardized format called “propagation reporter protocol”, which has been developed and introduced in 2008 by Joe Taylor, amateur radio call sign K1JT, physicist and Nobel Laureate. Because seasonal propagation situations south of the tropic were scarce to date, a WSPR (Weak Signal Propagation Reporter) beacon station was installed at *Neumayer Station III* in 2018.

The project was initially intended to last for one year, but extended to a full 11-year sunspot cycle until 2030. These years of high activities of the sunspot shows interesting changes of the propagation over the Ionosphere.

The project is funded by the investigating institution as well as by DARC (German Amateur Radio Club) and supported by several private individuals highly dedicated to amateur radio and to research projects. The receivers at *Neumayer Station III* / SPUSO (Air chemistry observatory) are operating autonomously with special decoder programs reporting the mean of the relative signal-to-noise ratio (SNR) during receiving intervals.

Fieldwork

Both the transmitter and the receivers are operated remotely and function autonomously. In the event of a deviation from the expected results, the remote-control operator first attempts to identify and resolve the cause. If the issue persists, an on-site evaluation may provide further insight into the possible technical malfunction.

The enhancement of technical equipment is prepared in Germany and shipped with the vessel *Polarstern*. The summer technical team replaces the prepared equipment, if needed.

Michael Hartje (PI) was on site for the first time this summer season for another project. This also allowed more complex checks of the transmitter and receiver to be carried out during his free time. This meant that more complex checks and measurements could be carried out and implemented directly in changes to the system.

An examination of the antenna for the transmitter on the station showed that the vertical antenna was defective. The vertical antenna could be replaced directly together with the technical team on site, as a repair was not possible.

Among his findings was a defect in the long-wire antenna installed on the roof. Measurements indicated a malfunctioning input transformer, which was subsequently replaced, effectively resolving the problem.

In addition, a new wire antenna was planned as an off-centre fed dipole, OCFD, with a total length of 40 m and erected and measured on the roof of the building. This antenna serves as a test for a further developed method (FST4W) for Doppler analysis of the ionospheric layers along the propagation path and as spare antenna.

Interference Analysis

At the SPUSO, the interference situation and the reception situation were analysed and revised. For this purpose, measuring devices in the SPUSO were switched off individually or, after all devices in the SPUSO had been switched off completely, all devices were switched on individually and one after the other in order to determine the contribution to the interference level. It was found that a large number of very simple sources of interference were created by computer power supplies of individual measuring devices. However, it was not possible to replace these with better devices during the analysis, so that it can now be stated that the high interference levels measured at the SPUSO are related to and caused by an unmistakably large number of measuring devices in the SPUSO.

An inspection of the antenna connections revealed that an unexplained deviation in the reception levels of the two triangular loops, observed repeatedly throughout the year, was likely caused by swapped cable connections during maintenance work performed the previous year. This issue has now been corrected.

Various investigations into the sources of interference and the decoupling to the receivers were used to simplify the connection. Unfortunately, decoupling by means of a common mode choke on the cable did not bring the expected measurable improvement.

Despite many investigations and individual processing of the individual suspected sources of interference, it was established on site that the interference generated in the SPUSO by a large number of devices could not be identified individually with reasonable effort.

It was established that the measuring devices and components and systems set up by various scientific institutions in the past were all together responsible for the high interference levels. It was possible to identify individual devices, some of which contributed up to +10 dB to the interference level. The level of +10 dB corresponds to increase ten times the Radio disturbance power.

Even if they were to comply with the standards for the industrial environment, a measurement in the frequency range above 50 kHz with high sensitivity is impaired by the residual radiation. On the other hand, this use of components and systems is understandable, as sufficient or very good EMC always requires greater effort and expertise before procurement and when setting up the measurement systems and integrating them into the SPUSO.

Therefore, arrangements had been made to install EMC measures on both sides of the supply cable to the SPUSO.

Measurements were first taken of the current interference level on the SPUSO cable, then the EMC filter measures were installed by the technical Team and a new measurement was taken.

The measurements were carried out late in the evening during non-working hours so as not to affect the regular work.

Receiver of WSPR Spots

The receiving system at SPUSO until 2025 February consists of three receivers, all of which support remote configuration. Two receivers are permanently set to continuously monitor 8 amateur radio bands in the range 1.8 to 14 MHz and 7 to 50 MHz. The receivers also decode all received transmissions and send them to the database at wsprnet.org. From there, the information can be analyzed according to various aspects in a special evaluation tool at the webpage wspr.live.

The receiving antennas were moved up in February 2024. The receiver was switched off during the 14 days. After that, the antenna connections for the two loops were apparently swapped. However, this only became apparent during the inspection in January 2025.

To improve the stability of the receivers, the entire system was replaced with a new receiver. This enables observation from 100 KHz to 60 MHz with one receiver. At the same time, all bands can be decoded according to the protocols of WSPR, FT8, FT4 and FST4W as well as other protocols. Although this step changes the reception technology, it has the advantage of a clear simplification and a significant expansion of the evaluation options.

Below is a contribution to this report by Gwyn Griffith, which explains some preliminary results of evaluations of the new receiver.

Preliminary (expected) results

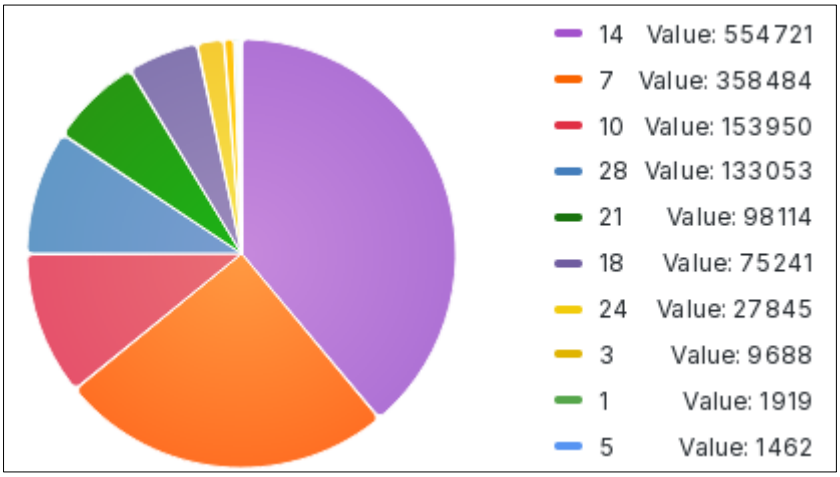

Fig. 4.13.1: Distribution of the spot numbers received on all bands with both receivers

Figure 4.13.1 shows the distribution of 1,414,477 spots received on both receivers over the year 2024. This is comparable to the number of spots in 2023. Last year, most spots are received on 7 MHz and now on 14 MHz. As depicted in Figure 4.13.1, the main bands are 14 and 7 MHz. But the higher bands (18 to 28 MHz) received a quarter of all spots. Compared to

last year, we observed 3 times more spots on 14 MHz and 2 times more on 28 MHz – a good indicator for the ionosphere activity during 2024.

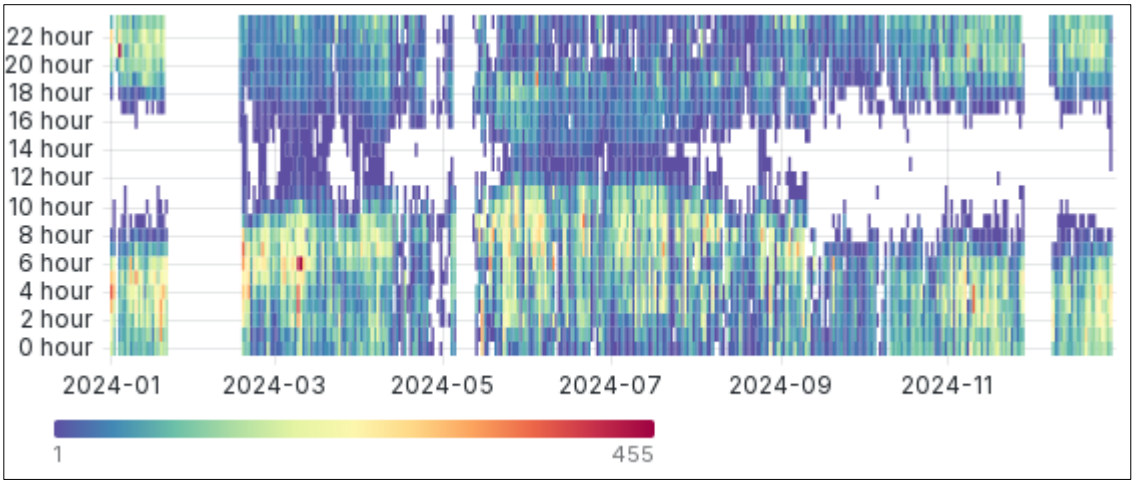

Fig. 4.13.2: Distribution of the received spots over the daytime and the year of from 1 January to 31 December 2024 on the lower bands at SPUSO

Figure 4.13.2 shows the distribution of spots for the lower bands during the time-of-day. It clearly shows the planed downtime until end of February as well as more unplanned downtime in May and in December. It is also noticeable that more spots were received in individual hours between 0 and 10 a.m. than between 6 p.m. and midnight. This can be attributed to the fact that ionospheric conditions for the lower bands are particularly favourable for the propagation of signals from many transmitting stations in North America and Europe during twilight and darkness on the transmission path. It can also be seen that the ionosphere only reaches its particularly favourable properties in the second part of the night and into the morning.

New receiver with Doppler shift measurement extension

As a side effect of the newly installed receiver in the SPUSO, further investigations can be carried out. An example of this is the report of a preliminary investigation prepared by Gwyn Griffith, which was kindly prepared and made available for this contribution to the BzPM as follows.

The installation of an RX888 Mk II Software Defined Receiver (SDR) at *Neumayer Station III* enables simultaneous decoding of WSPR/FST4W transmissions on all amateur bands 1.8 MHz to 28 MHz as well as acquiring Doppler and amplitude information on nine frequencies 2.5 MHz to 25 MHz from standard time stations WWV/WWVH and CHU. This preliminary note is an example of the new capability for Doppler and amplitude from these time stations. The WsprDaemon reporting program (https://github.com/rrobinett/wsprdaemon) for the RX888 sends data to the HamSCI Personal Space Weather Station (PSWS) Control Centre at the University of Alabama. Daily quick-look spectrograms and amplitude time series are available the following day via a browser for registered users (https://pswsnetwork.caps.ua.edu). A subset from 3.33 MHz to 14.67 MHz is shown in Figure 4.13.3. These plots are invaluable for checking technical performance and ensuring absence of interference. Over time, they will

build up interpretive experience, for example, on the times bands open and close, why some frequencies show considerable spectral spread (fuzzy traces) at times while others have narrow spectra with sharp traces, and which Doppler variations are associated with diurnal sunset/sunrise and which with large-scale wave structures.

While the quick-look plots are useful, a link on the PSWS graphics page allows data for that day to be downloaded in digital_RF format (https://github.com/MITHaystack/digital_rf) for further analysis. As an example, a preliminary analysis from the digital data for 24-25 February 2025 on 15 MHz from WWV, a US-Transmitter for time and frequency standard, has been conducted. The date was chosen because quick-look 14 MHz WsprSonde data to California had shown interesting post-sunset Doppler variations. As the quick-look WWV spectrogram showed a unimodal spectrum, albeit wide at times, the Doppler shift and spread were calculated using time-domain complex autocorrelation algorithms (see Warde & Torres 2013). This approach gave a Doppler resolution of 16 MHz every one minute.

Figure 4.13.4a shows the Doppler shift, which can be interpreted in conjunction with the frequency spread (Fig. 4.13.4b) and the signal level (Fig. 4.13.4c). The 10 kW effective radiated power of WWV meant there was sufficient signal level for Doppler estimates to capture the early stages of the post-sunset rise in height of reflection. Specifically, the record in Figure 4.13.4a began with Doppler becoming increasingly negative. The change occurred smoothly, with no large perturbations. As negative Doppler decreased perturbations appeared.

The frequency spread in Figure 4.13.4b, initially decreased as signal level rose, reaching a minimum at ~01:00 UTC, with the rise coinciding with a step increase in signal level and a change in Doppler shift with the start of the wave train. There is considerable potential for investigation in the time-series structure of these three parameters.

Comparison of Doppler shifts on two paths by two methods: WsprSonde and WWV

Figure 4.13.5a shows the great circle paths between *Neumayer Station III* and KFS (for WsprSonde 262˚) and WWV to *Neumayer Station III* (280˚). For the comparative Doppler plot, Figure 4.13.5b, linear interpolation was applied over seven gaps in the four-minute interval WsprSonde data. The overall visual agreement was surprisingly strong. Only between 04:30 UTC and 05:30 UTC there was substantive sustained divergence. We observed also differences in detail for the wave structure. But, at four-minute time resolution, there was no discernible difference in phase for the wave structures observable for the two paths and two techniques. At zero lag the correlation coefficient was 0.802, falling to 0.692 and 0.708 at +/- four minutes. Two alternative tentative explanations for further investigation are: a) the large-scale wave structure was a time variation in-place across a spatial scale longer than the path separation or b) it was a travelling wave structure with substantial longitudinal scale moving normal, or very close to normal, to the line joining the areas of ionospheric reflections giving rise to the Doppler shifts. For reference, the paths at separated longitudinally by 2,024 km at the equator.

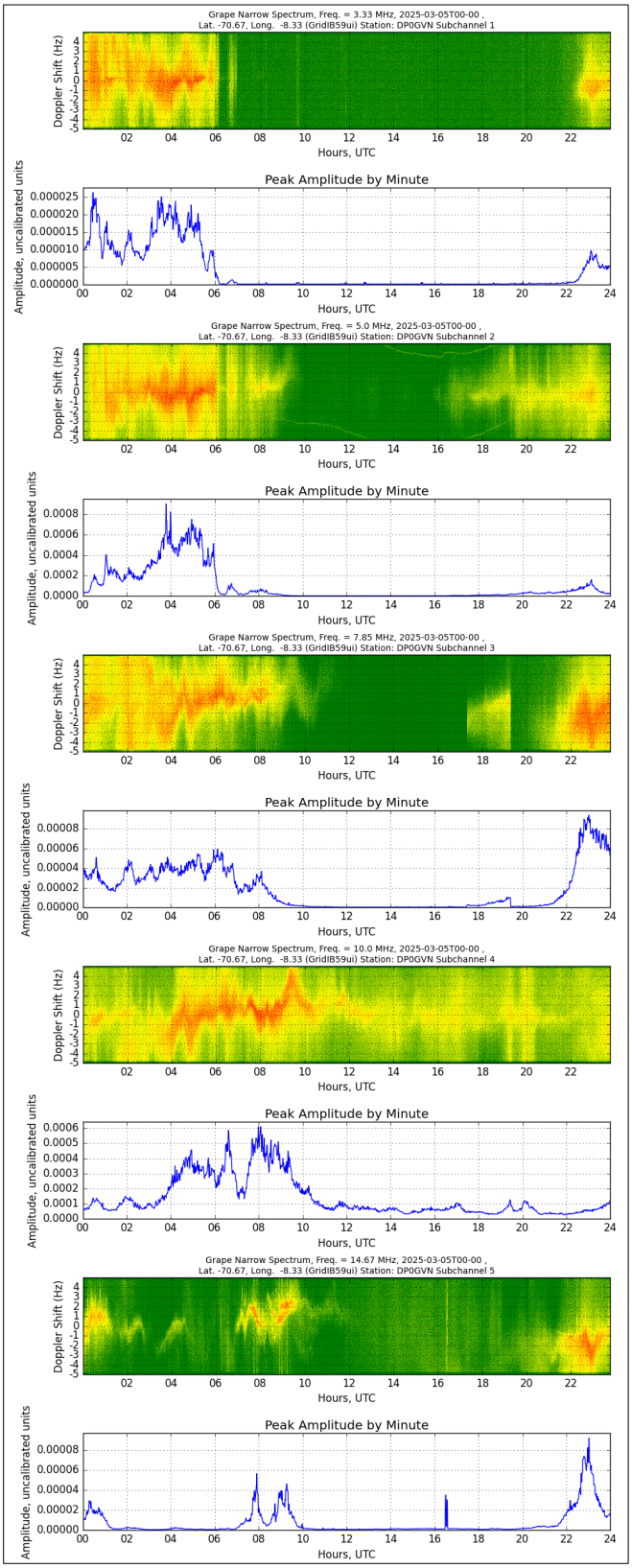

Fig. 4.13.3: Example spectrograms and amplitude time series for transmissions on 5 March 2025 from CHU (Ottawa, Canada) on 3.33 MHz, 7.85 MHz and 14.67 MHz and WWV (Fort Collins, USA) on 5 MHz and 10 MHz received by the RX888 SDR at Neumayer Station III, locally processed by WsprDaemon and ka9q-radio, telemetered to the HamSCI PSWS database and available online the following day

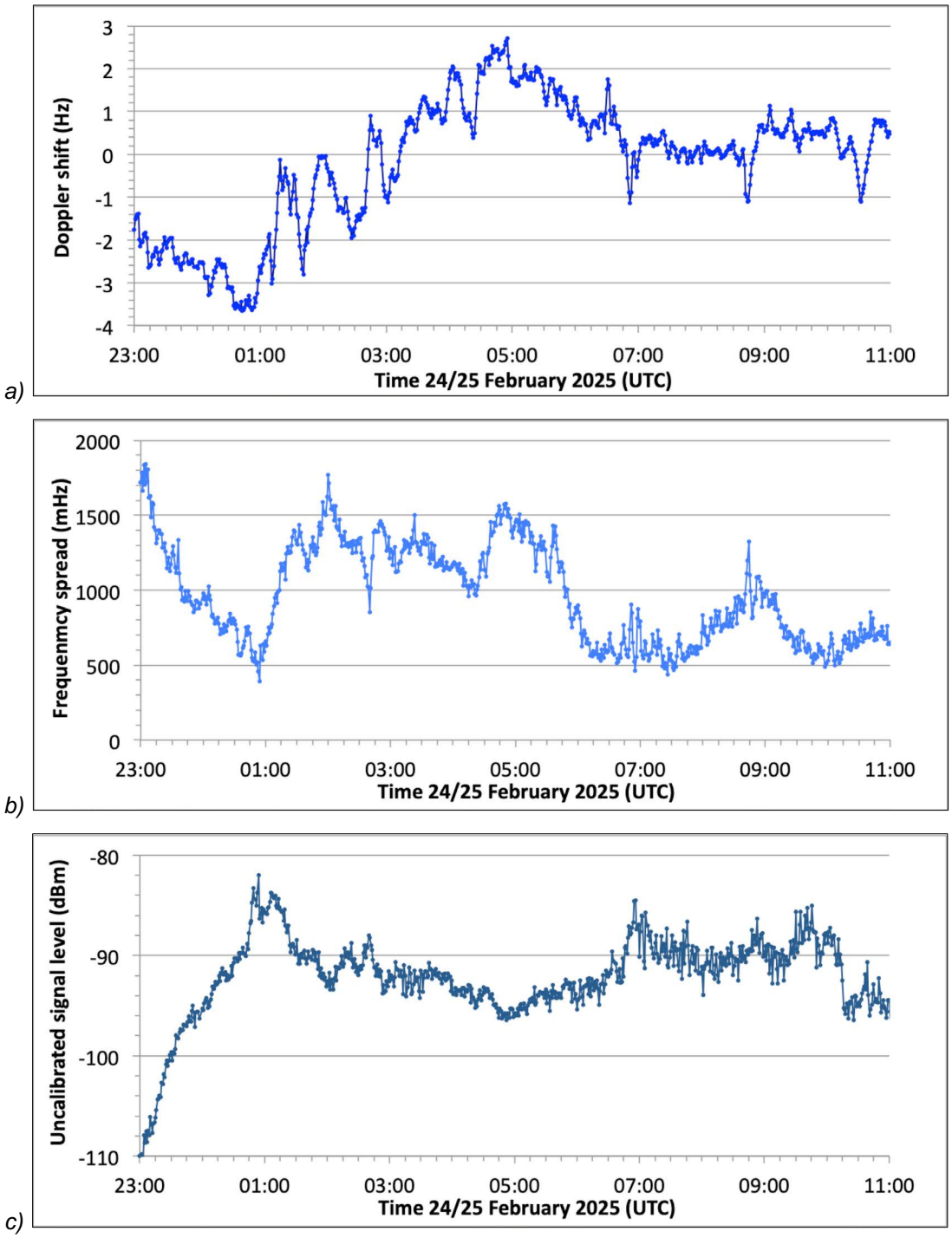

Fig. 4.13.4: Time series of WWV 15 MHz reception by the RX888 Mk II receiver at Neumayer Station III from the digital_RF data from the HamSCI PSWS database for 23 to 24 February 2025, a) Doppler shift and b) frequency spread calculated as first and second moments using a time-domain complex autocorrelation algorithm and c) uncalibrated signal level.

a) 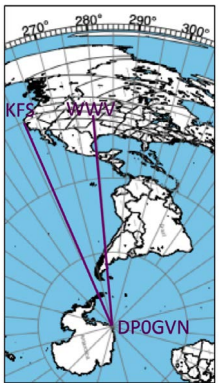

b) 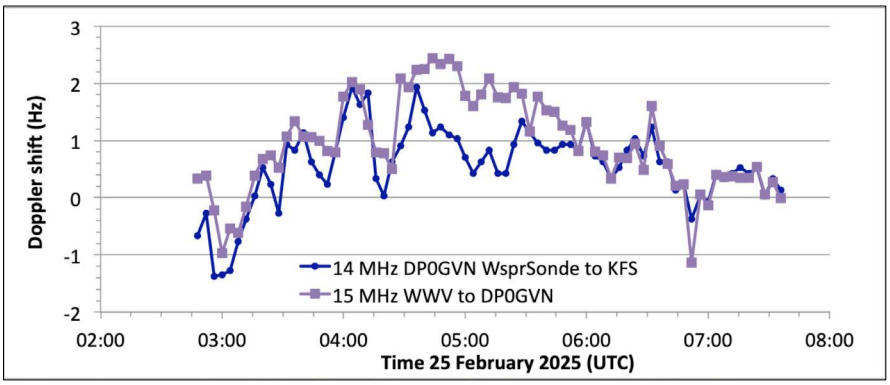

Fig. 4.14.5a) Map showing the great circle paths to KFS and WWV over which Doppler measurements at 14 MHz (WsprSonde with 1 W) and 15 MHz (WWV with 10 kW) were made, b) the Doppler measurements showing good agreement for the overall pattern and, until 04:30 UTC, during a large scale wave structure.

WSPR Transmitter at Neumayer Station III

Operation of the WSPR transmitter experienced some issues again during this year. The wire antenna had to be taken out of operation in mid-February due to poor performance, which suggested of some kind damage. Fortunately, this was fixed before the winter season began, allowing us to resume nominal operation at 10 April. Then, on 28 October, reception reports suddenly stopped. It quickly became clear that this was a transmitter issue. After further analysis, it was determined that the transmitter's final power amplifier stage had failed following five years of nearly continuous operation.

The failed component could be identified and a replacement part was sent to the station. Thanks to the great work of the station staff the power amplifier could be fixed by January 2025.

Data Analysis

Although we experienced interrupted operation, a substantial amount of data was still gathered. The total number of reception reports reached approximately 1.12 million, close to the Figure for 2022, a year almost unaffected by outages. Due to the technical issues the number of transmitted messages dropped by 28% to almost 188,000.

The nonetheless high number of reception reports indicates that radio propagation conditions were very favourable, once again surpassing those of the previous year. All reception reports are provided by a worldwide automated system designed to monitor radio propagation, which is established and operated by the global community of radio amateurs.

The gathered data indicate that the 11-year solar activity cycle reached its maximum in late 2024. However, this is not yet confirmed, as historically the month of maximum is determined by smoothing monthly sunspot numbers over a 13-month period (red curve in Fig. 4.13.6). therefore, it can take up to a year until the maximum becomes clearly visible in the figures (Fig. 4.13.6).

If the maximum gets confirmed the ascending phase of cycle 25 would have had a duration of almost five years. This is about half a year less than its two predecessors but more than a year longer than cycles 21 and 22 between 1976 and 1996. The ascending phase is usually shorter than the descending phase and there is a correlation between the maximum solar activity level and this duration: The stronger a cycle the faster it reaches its maximum.

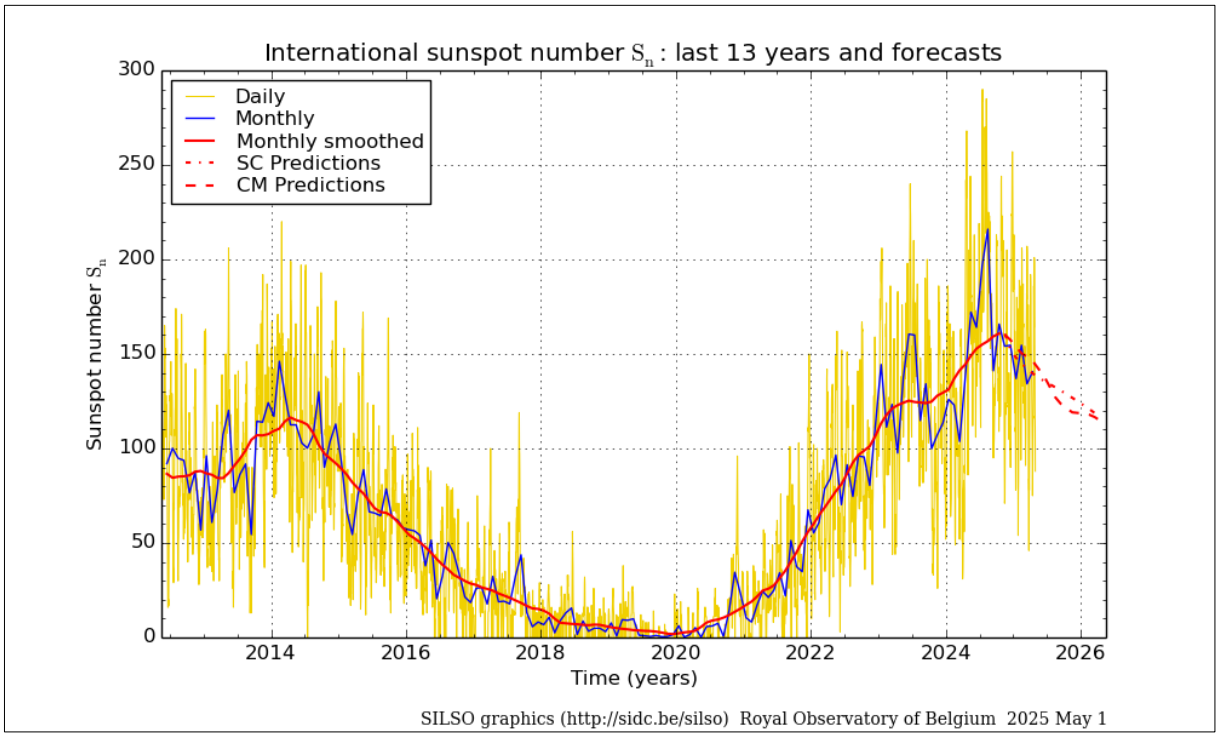

Fig. 4.13.6: Development of Smoothed Sunspot Number (SSN) during cycle 24 and 25
Source: WDC-SILSO, Royal Observatory of Belgium, Brussels, *https://www.sidc.be/SILSO/dayssnplot*

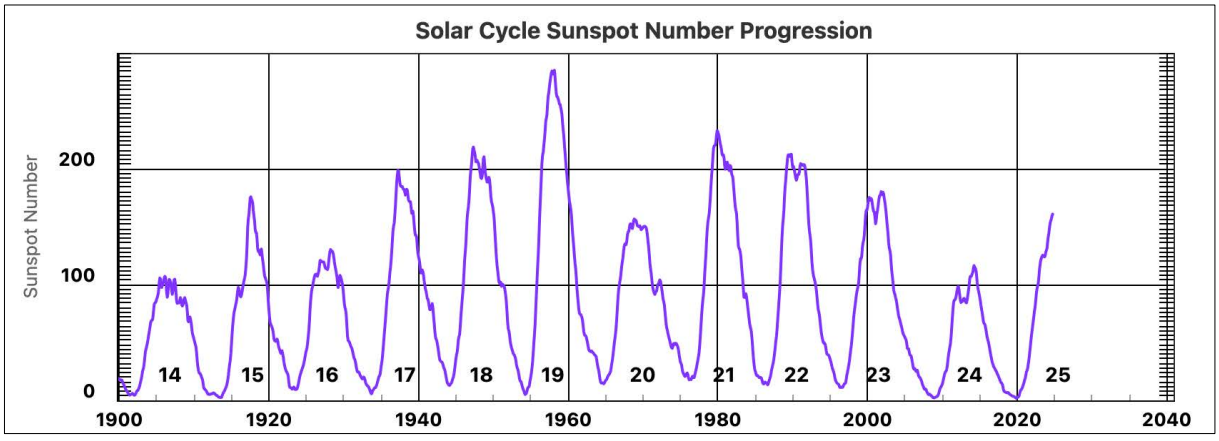

Fig. 4.13.7: Development if SSN since the year 1900
Source: NOAA SWPC https://www.swpc.noaa.gov/products/solar-cycle-progression

The maximum turns out to have a higher level than expected by most experts. Forecasts had called for a maximum comparable to the predecessor cycle which was the weakest cycle in 100 years. It peaked in April 2014 at a smoothed sunspot number (SSN) of 116. Preliminary calculations show that in October 2024 the SSN had already exceeded 160. While still being below the long-running average of 179 but is an indication that there will be no prolonged phase of weak solar activity cycles. This is illustrated in Figure 4.13.7 which shows the development of SSN since 1900.

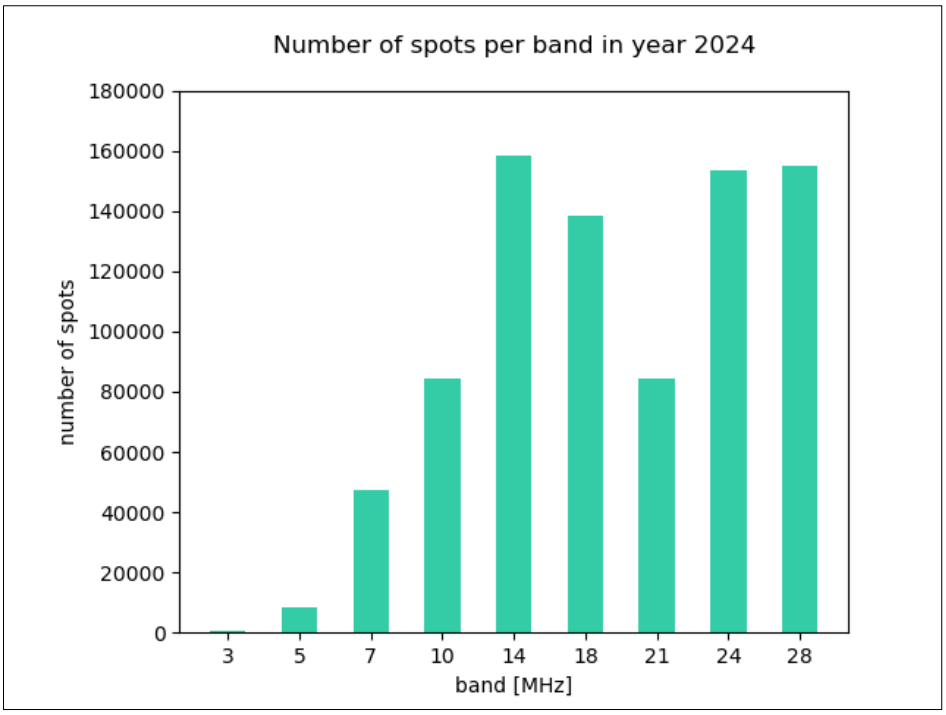

Fig. 4.13.8: Total number of spots on each band during 2014. Numbers are lower than expected from February to April and November to December due to outages.

Looking at the data gathered during 2024 most reception reports were received for the upper shortwave bands between 14 and 30 MHz (Fig. 4.13.8). Compared to 2023 we again see many successful receptions on the highest band (28 MHz), which is typical for solar maximum.

There is a noticeable increase on 14 MHz which is mostly caused by improved night-time performance (often all-day round) during summer season in the southern hemisphere (Fig. 4.13.9). This is a direct consequence of the higher level of ionisation in the ionosphere near solar maximum. The reduced value for 21 MHz is due to poor performance of the long wire antenna on this band.

Figure 4.13.10 shows the distribution of the receiving stations on the upper bands. As a special feature, the reception locations of the research vessel *Polarstern* in the Arctic Ocean near the North Pole, as well as a large research cruise between the Australia and the Canary Islands are also clearly recognizable here. The route of the *Polarstern* is shown like a string of pearls. The interruptions are caused by the time-of-day-dependent transfer conditions in the ionosphere and thus mark the daily route of the *Polarstern*.

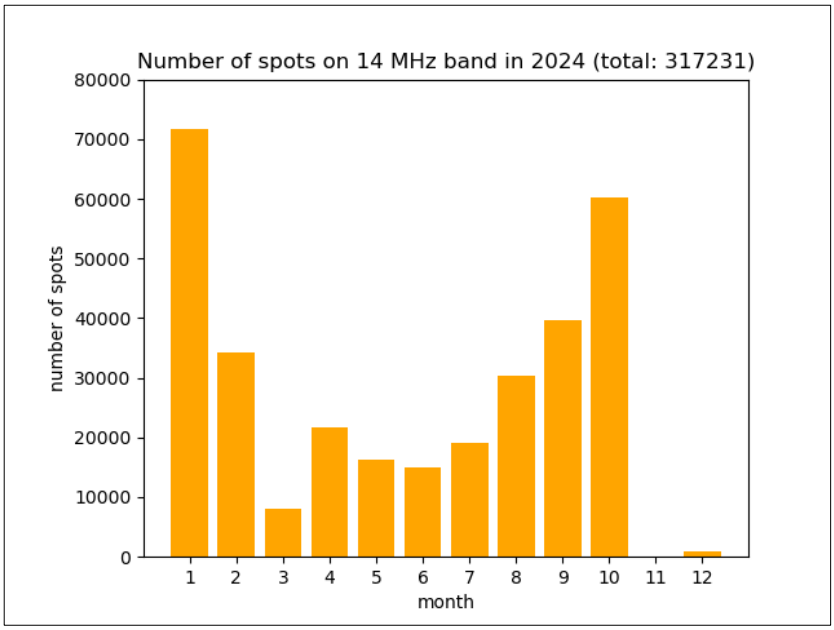

Fig. 4.13.9: Number of spots by month for the 14 MHz band. Clearly visible is the outage at the end of the year, also February to April numbers are reduced.

Fig. 4.13.10: locations of the receivers during 2024 on the higher bands

Additional Transmitter Extension Wsprsonde 8

International discussion of the research results at the *Neumayer Station III* gave led to the idea of supplementing the WSPR transmitter, with a special transmitter utilizing a new, highly precise protocol. This new method makes it possible to investigate deviations in frequency on the transmission path through the ionosphere to the receiver. Deviations of a few MHz due to Doppler shifts indicate that the propagation path has shortened or lengthened. For this purpose, the FST4W protocol is used for transmissions to many receivers in the northern hemisphere.

Figure 4.13.11 shows the WSPR-Transmitter (Version 2.1) in the lower silver case and new wsprsonde 8, upper blue case. On the top of the blue case the power combiner for 8 bands (top in the middle), a Raspberry Pi as gateway to intranet (upper left) and a Leo Bodnar GPSDO (upper right) is shown.

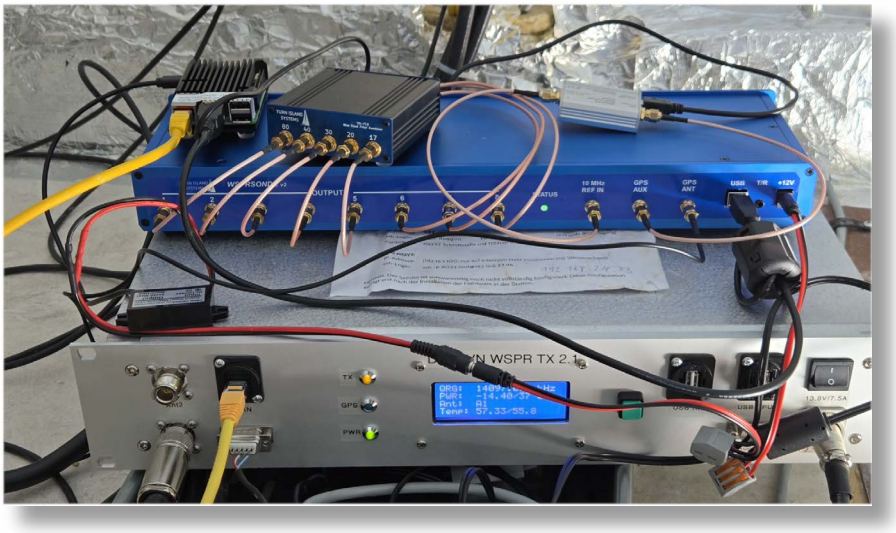

Fig. 4.13.11: In the station upper deck installed WSPR-Transmitter (below, large silver unit) with the new multiband extension unit "wsprsonde 8" for FST4W-Emission (upper blue unit)

Fig. 4.13.12: The Üwi communication engineer, Alexander Schegber, was climbing up the antenna mast to repair the vertical antenna and mount the OCFD-antenna

Data management

The data generated from the beacon receiver is saved locally on a network storage at *Neumayer Station III* as well as on a worldwide database called “wsprnet.org”. This offers worldwide and very established access via a web interface. Both offer archive functions as well as basic evaluation functionality. In addition, a new API-based access to the database has been developed and is used by several other websites via https://wspr.live .

The wsprnet.org archive collects all received spot reports worldwide since 2008. In June 2025, about 9.7 billion spot reports are stored. All spots can be downloaded with free access, compiled on a monthly basis, to a compressed CSV-file. In addition, noise measurement results and locally stored results are available on the server at *Neumayer Station III*. In addition, there are some web pages available now, which have access to a specialized database of the total dataset of spots since 2008 (https://wspr.live/gui).

In all publications based on this expedition, the **Grant No. AWI_ANT_15** will be quoted and the following publication will be cited:

Alfred-Wegener-Institut Helmholtz-Zentrum für Polar- und Meeresforschung. (2016a). Neumayer III and Kohnen Station in Antarctica operated by the Alfred Wegener Institute. Journal of large-scale research facilities, 2, A85. http://dx.doi.org/10.17815/jlsrf-2-152

Acknowledgements

The authors are grateful to many voluntary supporters in this project. Our warm thanks go to the radio amateurs Dipl. Ing. Rainer Englert and the IT-Specialist and space weather specialist Christian Reiber from DARC for setting up and remotely operating the transmitter hardware. Christian Reiber prepared the drafting the last part of the report on the work and propagation interpretation results about the transmitter and the transmitters spot evaluation. Many thanks have to be addressed to Paul Elliot and Rob Robinet and unnamed other experts, who prepared and sent the new multiband beacon transmitter wsprsonde 8 and the new receiver so, that it could be installed in February 2025 at the Station and in the SPUSO. Special thanks for discussion and preliminary evaluations goes to Gwyn Griffith, who wrote a contribution for this report about the new opportunities. Special thanks go also to Felix Riess, Jörg Lauer and Alexander Schegber and several researchers at *Neumayer Station III*, unknown to us, who set up and repaired the antennas and commissioned the transmitter and receiver systems on-site with untiring commitment.

References

Warde DA & Torres SM (2013) The autocorrelation spectral density for Doppler-weather-radar signal analysis. IEEE Transactions on Geoscience and Remote Sensing 52: 508–518.

4.14 MICA-S – Magnetic Induction Coil Array - South

Jölund Asseng[1], Amelie Nüsse[1], Andrey Jakovlev[1], Jürgen Matzka[2]
not in the field: Khan-Hyuk Kim[3], Tanja Fromm[1], Hyomin Kim[4], Marc Lessard[5], H.-J. Kwon[6]

[1]DE.AWI
[2]DE.GFZ
[3]KR.KHU
[4]EDU.NJIT
[5]EDU.UNH
[6]KR.KOPRI

Grant-No. AWI_ANT_9

Objectives

MICA-S continuously observes geomagnetic pulsations at *Neumayer Station III*. The geomagnetic latitude of *Neumayer Station III* is ideally suited to investigate so-called electromagnetic ion cyclotron (EMIC) waves near the plasmapause by observing these pulsations. EMIC waves are naturally occurring electromagnetic waves in the near-Earth space that can cause loss processes for particles in the Earth's radiation belts as well as the ring current and are therefore relevant for space radiation processes and risks to spacecraft. They are studied by ground and satellite magnetometers and often in conjunction with each other. Both fluxgate and induction magnetometers can be used, but the latter are preferred. Therefore, the MICA-S induction magnetometer at *Neumayer Station III* is relevant for scientific satellite missions like ESA's Swarm mission, NASA's Van Allen Probes, or JAXA's ARASE (ERG) satellite. Also of great importance is a coordinated ground observation effort at both hemispheres and especially at high latitudes.

Fieldwork

During 2024, the MICA-S data acquisition was running without major problems. After strong winds, the flags, which are used to mark the position of the MICA-S, have been checked.

New snow constantly accumulates on top of the instrument pit, which therefore becomes deeper over time. Once a year, we remove the upper layer of snow from the wooden plates on top of the pit and either reinstall the cover at snow surface or move the instrument into a new pit close to the surface. In the summer season 2022/23 the cover of the magnetometer has been indirectly raised by installing a new, second cover at the surface. The second cover provides additional protection of down falling snow onto the instrument when opening the pit. Since then, only the second cover has been reinstalled on the snow surface each year. In the summer season 2024/25 the second cover of the magnetometer has been raised at 17 February 2025. The two covers are now separated by approx. 3m.

Due to the ice shelf movement of approximately 154 m per year, the location of the pit also changes. At 27 January 2024 it was located at S70° 40.416' W8° 16.603', at 17 February 2025 it was located at S70° 40.332' W8° 16.668'.

Preliminary results

Figure 4.14.1 shows an example of geomagnetic pulsations at *Neumayer Station III* (VNA) and other high latitude stations. It demonstrates both the quality of the data from the instrument installed at *Neumayer Station III* and shows that the signal is to some extent coherent with that at other stations in Antarctica and the Arctic, capturing important wave activities peculiar at certain geomagnetic latitudes.

Since its installation in January 2018, results from MICA-S have been published by Kim et al. (2020), Kim et al. (2021) and Salzano et al. (2022).

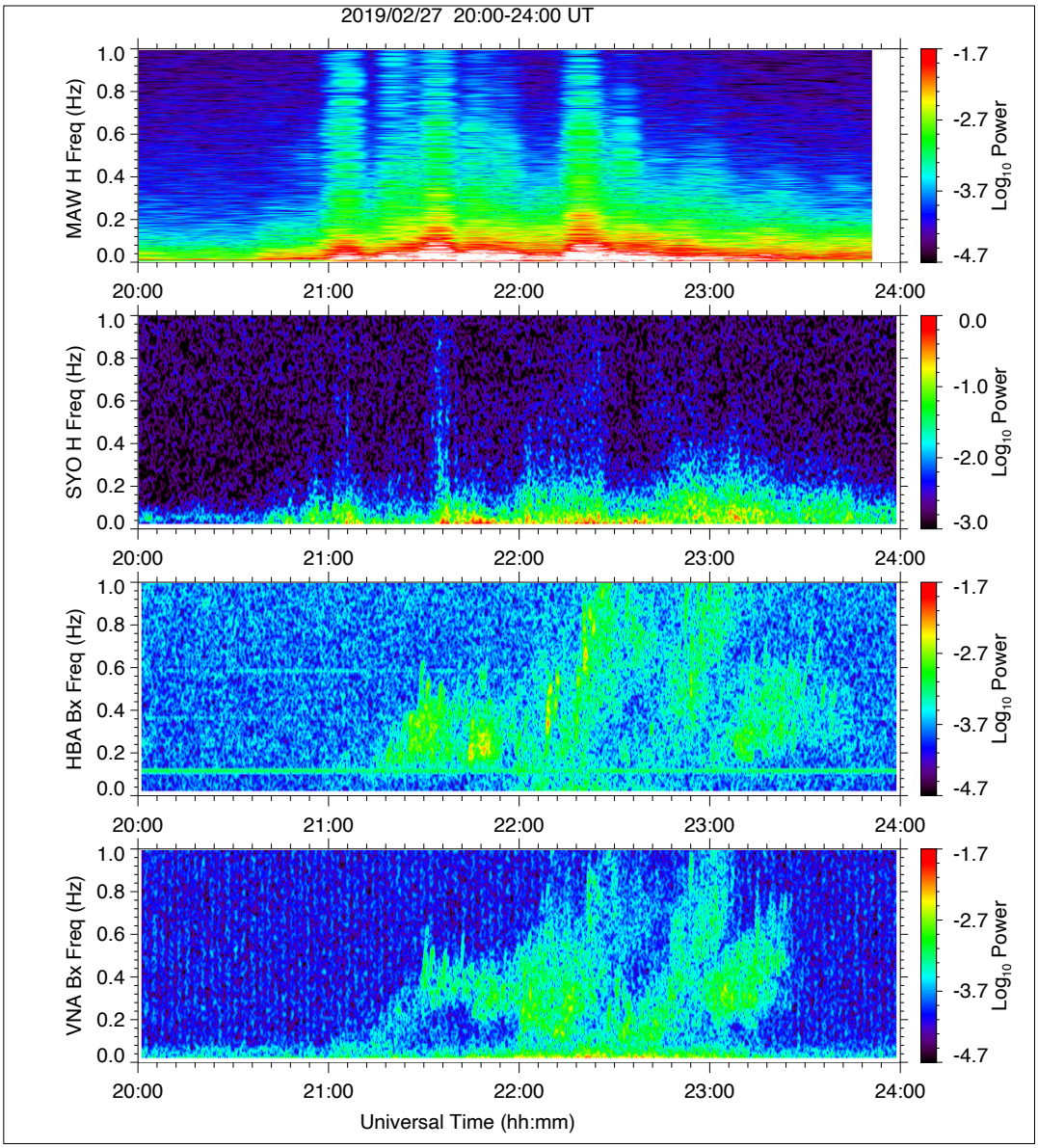

Fig. 4.14.1: Geomagnetic spectrograms for 27 February 2019 using data from Antarctic stations Mawson (MAW), Syowa (SYO), Halley Research Station (HBA), and Neumayer Station III (VNA). Intervals of Pulsations of Diminishing Periods (IPDPs), a subtype of EMIC waves, are observed at HBA and VNA (-62.2 and -60.6 CGM lat; Salzano et al, 2022). Near-simultaneous Pi1Bs are observed at MAW and SYO (-70.4 and -66.5 CGM lat).

Data management

Data (plots and cdf-files) is currently freely distributed through http://mirl.unh.edu/ulf_status.html. Data will also be curated either at AWI or GFZ and will receive a DOI.

In all publications based on this expedition, the **Grant No. AWI_ANT_9** will be quoted and the following publication will be cited:

Alfred-Wegener-Institut Helmholtz-Zentrum für Polar- und Meeresforschung. (2016). *Neumayer III* and *Kohnen Station* in Antarctica operated by the Alfred Wegener Institute. Journal of large-scale research facilities, 2, A85. doi: 10.17815/jlsrf-2-152.

References

Kim H, Shiokawa K, Park J, Miyoshi Y, Miyashita Y, Stolle C, Kim K-H, Matzka J, Buchert S, Fromm T & Hwang J (2020) Ionospheric Plasma Density Oscillation Related to EMIC Pc1 Waves, Geophysical Research Letters, 47(15). https://doi.org/10.1029/2020GL089000

Kim H, Schiller Q, Engebretson M J, Noh S, Kuzichev I, Lanzerotti LJ, Gerrard A J, Kim K-H, Lessard MR, Spence HE, Lee D-Y, Matzk J & Fromm T (2021) Observations of Particle Loss due to Injection-Associated Electromagnetic Ion Cyclotron Waves. Journal of Geophysical Research: Space Physics, 126(2). https://doi.org/10.1029/2020JA028503

Salzano M, Lessard MR, Noh S, Kim H, Waters C, Engebretson MJ, Horne R, Clilverd M, Kadokura A, Tanaka Y, Kim K-H, Matzka J, Fromm T, Goldstein J & Kim MJ (2022) Modeling the Effects of Drift Shell Splitting in Two Case Studies of Simultaneous Observations of Substorm-Driven Pi1B and IPDP-Type EMIC Waves, Journal of Geophysical Research: Space Physics, 127(10). https://doi.org/10.1029/2022JA030600

4.15 MAGSI-NEU – Magnetic and Geospace Instrumentation Observations at *Neumayer Station III*

Jürgen Matzka*[1], Jölund Asseng[2], [1]DE.GFZ
Wojciech Miloch[3], Johanna Brehmer-Moltmann[2], [2]DE.AWI
Jozef Müller[2] [3]NO.UIO
not in the field: Yuri Shprits[1], Vera Schlindwein[2], [4]CU.UCA
Emma Spanswick[4]
* Juergen.matzka@gfz.de

Grant-No. AWI_ANT_46

Objectives

The aurora is a natural phenomenon in the upper atmosphere of Earth, at an approximate altitude of 100 km. It is characterized by the luminescent emission of photons originating from excited atoms and molecules, such as atomic oxygen and molecular nitrogen. The excitation occurs as a result of the interaction with energetic charged particles precipitating from Earth's magnetosphere (Thorne et al. 2010). Previous observations have revealed the diverse range of dynamic characteristics exhibited by aurorae. Among these features is the phenomenon known as "auroral breakup", where discrete aurora suddenly and fleetingly expands to encompass the entire sky for a duration of several tens of minutes (Akasofu 1968). This dynamic behavior occurs due to the abrupt release of accumulated energy within the magnetosphere. Subsequent to auroral breakups, diffuse and patch-like aurorae emerge, spanning a wide region from midnight to dawn, occasionally persisting for several hours or even longer periods of time (Jones et al. 2013). Most of these diffuse aurorae exhibit quasi-periodic pulsation, and they are commonly referred to as pulsating aurorae (Johnstone 1978; Hosokawa et al. 2015).

The proximity to the auroral oval of the southern geomagnetic pole make *Neumayer Station III* a prime location to investigate the near-Earth space (also called geospace) in Antarctica. From *Neumayer Station III*, the geomagnetic field lines reach out into the Earth's outer radiation belt. Observations of the geomagnetic field, electromagnetic waves (ULF and VLF (not yet installed and riometer) and optical aurora observations allow us to study physical processes of the aurora and the radiation belts, and their connection to the Earth's atmosphere, in particular, particle precipitation from space into the atmosphere. Observations at *Neumayer Station III* will be perfect to complement similar programs in Antarctica and in particular at *Neumayer Station's III* neighborhood (*Halley, Troll, SANAE*) and in conjunction with magnetic, ionospheric and magnetospheric satellite missions (e.g. ESA's Swarm mission, JAXA's Arase satellite, NASA's THEMIS and MMS). The observations and accompanying research will greatly benefit our understanding of space weather effects that can damage satellites, degrade satellite navigation and communication, and change low Earth satellite orbits due to changing drag. The location of *Neumayer Station III* is ideal due to its geomagnetic latitude just north of the auroral zone, with the auroral oval expanding equatorward over *Neumayer Station III* during geomagnetic activity. The geomagnetic latitude can also be expressed as the L-shell parameter, which is L = 4.2 for *Neumayer Station III* and ideal for radiation belt studies. Additionally, this location is at the edge of the South Atlantic Magnetic Anomaly and the *Neumayer Station III* geomagnetic field measurements are influenced by it.

MAGSI-NEU stands for Magnetic and Geospace Instrumentation Observations at *Neumayer Station III*. MAGSI-NEU, or short MAGSI, adds optical and electromagnetic sensors to complement existing infrastructure for the observation of the ionosphere and upper atmosphere above the station. The new instruments in the 2024/25 season are two all-sky cameras and a riometer operated from a new box about 300 m south of the station building. This box allows for the installation of additional optical and electromagnetic sensors in the future. The existing infrastructure consists of a geomagnetic observatory (INTERMAGNET certified and producing 1-second data), an ultra-low frequency receiver (an induction coil magnetometer with 10 Hz data) and a 50 Hz GNSS receiver. Thus, *Neumayer Station III* now has a well-balanced suite of high-quality, fundamental instruments to observe geospace (including the upper atmosphere, ionosphere and the geomagnetic field) and allows the addition of further, specialized instruments in the future.

Fieldwork

On the platform 300 meters south of the main building an insulated box with approx. 2m x 2m x 3m size was installed in February 2025. The so-called MAGSI-Box (Fig. 4.15.1) has a power and an internet connection to the station building and an uninterruptible power supply (UPS) unit. So far, the MAGSI-box contains 2 all-sky imagers (a Keo Sentry3 deep-cooled EMCCD camera with 6 filters and a Sony camera) and a riometer (HyperSpectralRiometer by University of Calgary) with an external antenna. They started their recordings at the end of February 2025.

The cameras are accompanied by heating systems and fans to avoid water condensation and ice formation in their respective domes, which are the coldest spots in the MAGSI-box. The area of the cameras is separated from the rest of the box by a curtain to minimize light pollution and humidity of personnel performing maintenance and by an electrically conductive curtain to attenuate their electromagnetic signal, which might otherwise interfere with the riometer electronics.

The Keo Sentry3 all-sky-imager has six optical filters:

- OH >790 nm, for air glow in the mesosphere, 60 to 90 km altitude
- 427.8 nm, for purple aurora in 110 km altitude
- 557.7 nm, for green aurora in 150 km altitude
- 630.0 nm, for red, fuzzy Aurora (110 s) and F-region air glow in >200 km altitude
- 844.6 nm, for IR, prompt aurora
- DG3 broadband filter for pulsating aurora

Observations are coordinated with Troll Station, which has some of these filters also installed.

The Sentry camera resides in a BK7 specially manufactured glass dome.

The other camera is a Sony alpha7 II and connected via a Canon EF to Sony E Speed Booster Ultra 0,71 x II to a Canon EF 8-15 mm, f/4L USM fish-eye lense. The Sony is set to produce images every hour in summer and every 10 minutes (or faster) in winter. These color images can be used to investigate aurora and cloud coverage and be used for knowledge transfer into society.

The Sony camera resides in a UV-protected acrylic dome.

Compressed daily videos of the Sony camera images are automatically transferred to AWI and GFZ and visually checked every few days. High resolution images from the Sentry and the Sony can then be downloaded manually for specific events.

The riometer is a UCalgary Hyper Spectral Riometer (HSR) with an SDDR receiver for 5 to 50 MHz. Currently it runs with 11 frequency channels at around 20 MHz, 22 MHz, 24 MHz, and so on, until 40 MHz. In order to avoid local radio disturbances, the channels can be tuned slightly away from the nominal frequency. The antenna is located approx. 140 m SSW of the MAGSI-box (Fig. 4.15.1). The cables to the antenna were buried in a snow trench. Since snow has very little conductivity, there is a rectangular iron grid below the antenna to simulate the electrically conductive Earth. Additionally, in the snow, a number of copper cables were laid out radially from the mast to improve the electric conductivity of the ground below the antenna.

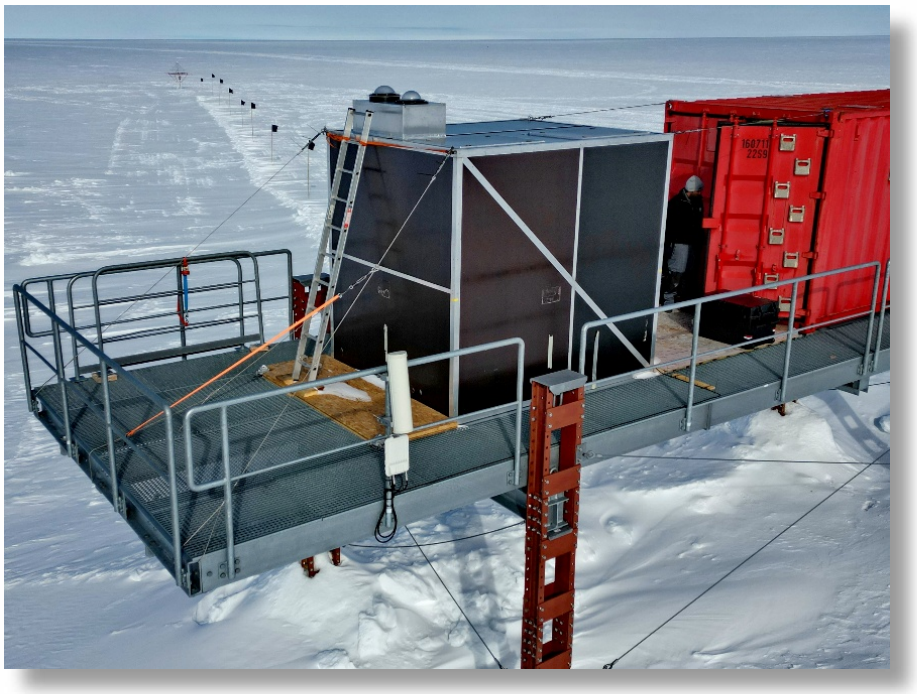

Fig. 4.15.1: MAGSI-box with camera domes on the roof and the riometer antenna in the background.

Preliminary (expected) results

Auroral activity is seen in about a third of the nights. Figures 4.15.2 and 4.15.3 show two examples of aurora images, which were taken by the Sony camera within 20 minutes on 5 April 2025.

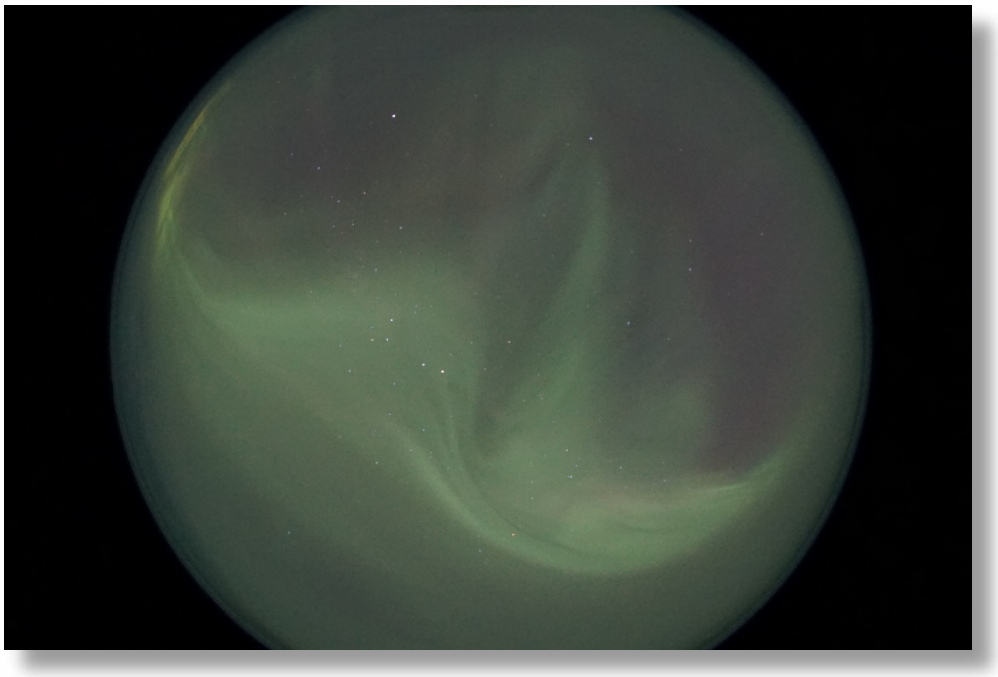

Fig. 4.15.2: Auroral image taken by the Sony camera on 5 April 2025 at 03:41 UTC. North is up; East is on the left.

Fig. 4.15.3: Auroral image taken by the Sony camera on 5 April 2025 at 04:00 UTC. North is up; East is on the left.

As examples for the riometer data, we show daily plots of the Hyper Spectral Riometers at *Neumayer Station III* and Narsarsuaq in south Greenland, which is located at a similar (but

northern) geomagnetic latitude and longitude like *Neumayer Station III* (Fig. 4.15.4). The plotted signal is the power of the received radio signal and the decrease by about 1 dB for about an hour at around 03:30 at *Neumayer Station III* and at Narsrasuaq are absorption events, when the ionized ionosphere above the stations blocks out the galactic radio signal. Note that these plots are raw data, which partly are tuned to avoid local noise sources. Note the different scales for the band_00 (around 30 MHz, black curve) and the other bands.

A next step in the riometer data processing will be further tuning and to determine and subtract a daily quiet curve (aka baseline) from the signals. This work is done at University of Calgary.

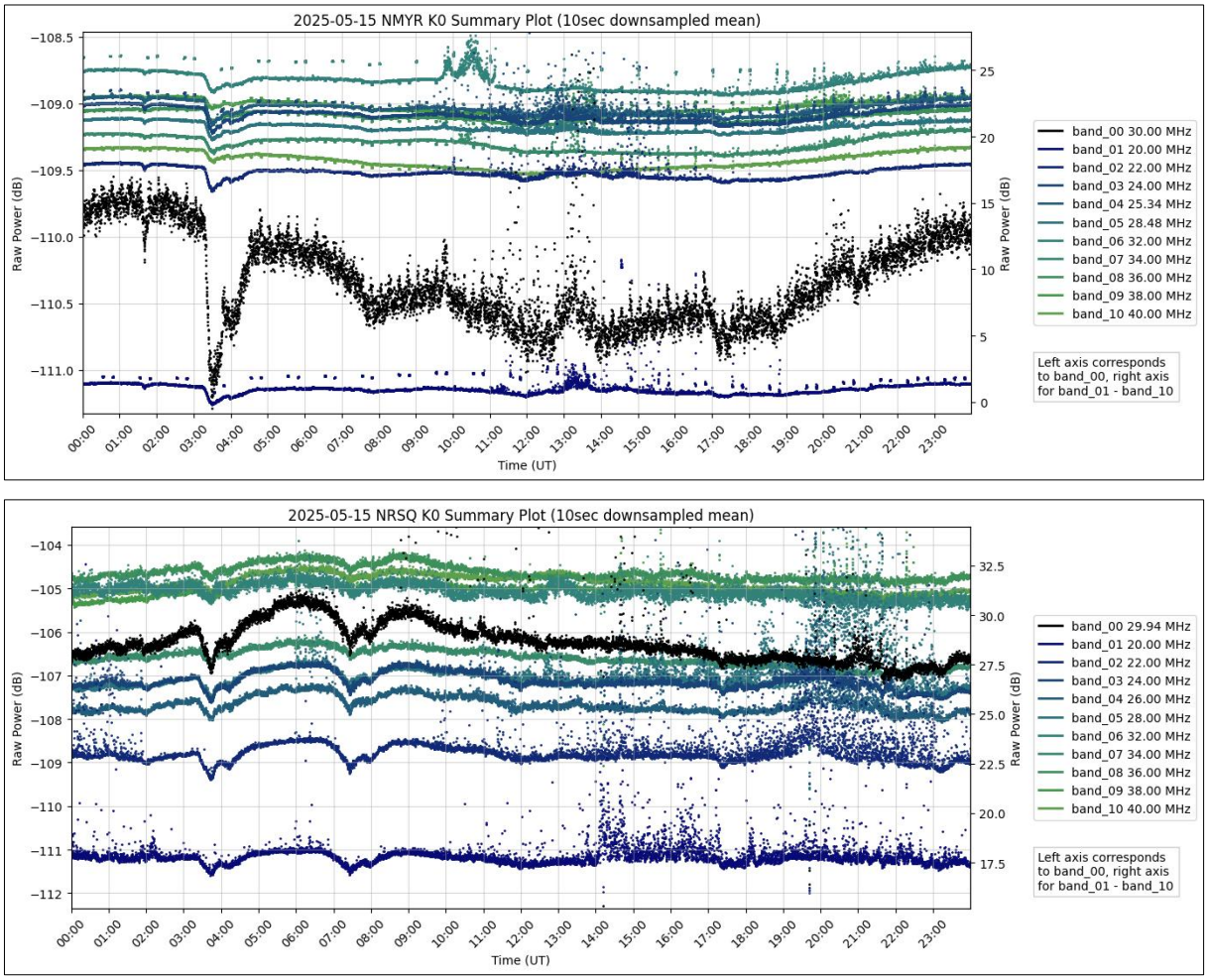

Fig. 4.15.4: Riometer data from Neumayer Station III (Antarctica, previous page) and Narsarsuaq (Greenland, this page) showing an absorption event at around 03:30 UTC on 15 May 2025.

Data management

Environmental data will be archived, published and disseminated according to international standards by the World Data Center PANGAEA Data Publisher for Earth & Environmental Science (https://www.pangaea.de) within two years after the end of the expedition at the latest. By default, the CC-BY license will be applied. Any other data will be submitted to an appropriate

long-term archive that provides unique and stable identifiers for the datasets and allows open online access to the data.

In all publications based on this expedition, the **Grant No. AWI_ANT_46** will be quoted and the following publication will be cited:

Alfred-Wegener-Institut Helmholtz-Zentrum für Polar- und Meeresforschung. (2016). *Neumayer III and Kohnen Station* in Antarctica operated by the Alfred Wegener Institute. Journal of large-scale research facilities, 2, A85. http://dx.doi.org/10.17815/jlsrf-2-152.

References

Akasofu SI (1968) Polar and Magnetospheric Substorms. D. Reidel Publishing Company, Dordrecht

Hosokawa K, Miyoshi Y, Li W (2015) Introduction to special section on pulsating aurora and related magnetospheric phenomena. J. Geophys. Res. Space Phys. 120:5341–5343. https://doi.org/10.1002/2015JA021453

Johnstone AD (1978) Pulsating aurora. Nature 274:119–126. https://doi.org/10.1038/274119a0

Thorne RM, Ni B, Tao X, Horne RB, Meredith NP (2010), Scattering by chorus waves as the dominant cause of diffuse auroral precipitation. Nature 467:943–946. https://doi.org/10.1038/nature09467

Jones SL, Lessard, MR, Rychert K, Spanswick E, Donovan E & Jaynes AN (2013) Persistent, widespread pulsating aurora: A case study. J. Geophys. Res. Space Phys. 118:2998–3006. https://doi.org/10.1002/jgra.50301

4.16 VACCINE – Variation in Antarctic Cloud Condensation Nuclei (CCN) and Ice Nucleating Particle (INP) Concentrations at *Neumayer Station III*

Zsofia Juranyi[2]
not in the field: Silvia Henning[1], Oliver Eckermann[1], Heike Wex[1]

[1]DE.TROPOS
[2]DE.AWI

Grant-No. AWI_ANT_16

Objectives

Despite the progress polar climate research made, poorly understood processes remain, one of those being the aerosol – cloud – climate interaction, which still cannot be modelled with satisfying accuracy. Clouds and their interactions with the climate system are one of the most difficult components to model, especially in the polar regions. This is, among others, due to difficulties in obtaining high-quality measurements. The availability of high-quality measurements is therefore of crucial importance for understanding processes and for driving and / or evaluating atmospheric models. Increasing the available data-base is one of the main objectives of VACCINE. Starting with December 2019, TROPOS continuously performs in-situ Cloud Condensation Nuclei (CCN) and Ice Nucleating Particles (INP) measurements at *Neumayer Station III*. The captured data such as number concentrations, particle hygroscopicity, INP freezing spectra etc. were linked with meteorological information (e.g. back trajectories) and information on the chemical composition of the prevailing aerosol particles for identifying sources of INP and CCN (secondary vs. primary) and transport pathways (local vs. long-range transport) over the full annual cycle. A result of this project will be a deeper understanding about processes dominating the CCN and INP population in Antarctica.

Fieldwork

Starting with the austral summer season in December 2019, CCN-measurements are carried out at the AWI Air Chemistry Observatory with a commercially available CCN instrument (Roberts & Nenes 2005). With the instrument total CCN number concentrations can be determined as function of supersaturation in the range between 0.1 and about 1%. The CCN instrument has been measuring almost continuously since then and has been replaced with a freshly calibrated device beginning of the season 2023/24 to prevent malfunction. However, in the current season 2024/25 some hardware communication issues occurred, and the instrument needs to be replaced, but fortunately no data loss occurred. The daily / weekly on-site maintenance is being carried out by AWI-staff.

Besides CCN also INP sampling was established, using the low volume filter sampling setup available in the AWI Air Chemistry Observatory. These activities aim at the number concentrations of INP in the air, active at temperatures above -25°C. Filter samples are collected on polycarbonate filters and immediately frozen for later analysis in the TROPOS laboratories (Wex et al. 2019). The weekly filter change and handling is done by the AWI-staff, as well. The latest filter samples arrived recently at TROPOS and the analysis is ongoing.

Preliminary results

CCN measurements

The CCN instrument measures CCN number concentrations at 5 different supersaturations. Combined with the particle number size distribution measurements, the particle hygroscopicity can be derived (Petters & Kreidenweis 2007). Running continuously since December 2019 more than five full years of CCN data for *Neumayer Station III* have been gained. Number concentrations in general are low and a clear annual cycle is found for CCN as well as for the total particle number (CN). The latter is similar to results reported for the Belgian *Princess Elisabeth Station*, located 200 km inland in the escarpment zone of Dronning Maud Land at an altitude of 1400 m (Herenz et al. 2019). Lowest number concentrations are observed in austral winter months May to August and highest in austral summer.

INP results

Each filter is analysed with two different freezing arrays (LINA and INDA, Hartmann et al. 2021) covering a wide freezing temperature range. Samples are also heated to 60°C and 90°C to provide information on the proportion of heat-labile ice-active protein. In general, the INP concentrations are very low even compared to other measurements in the southern hemisphere (e.g. Tatzelt et al. 2022; McCluskey et al. 2018) and thus close to the detection limit. Based on a statistical approach that only considers values significantly different from the field blank, an INP parameterisation for the remote region was developed and successfully tested against other Antarctic INP data (Wex et al. 2024). As a preliminary result, only a few samples are ice-active at temperatures above -15°C, and no decrease in ice-activity after heating was observed. This suggests an absence of biological INP sources in the region.

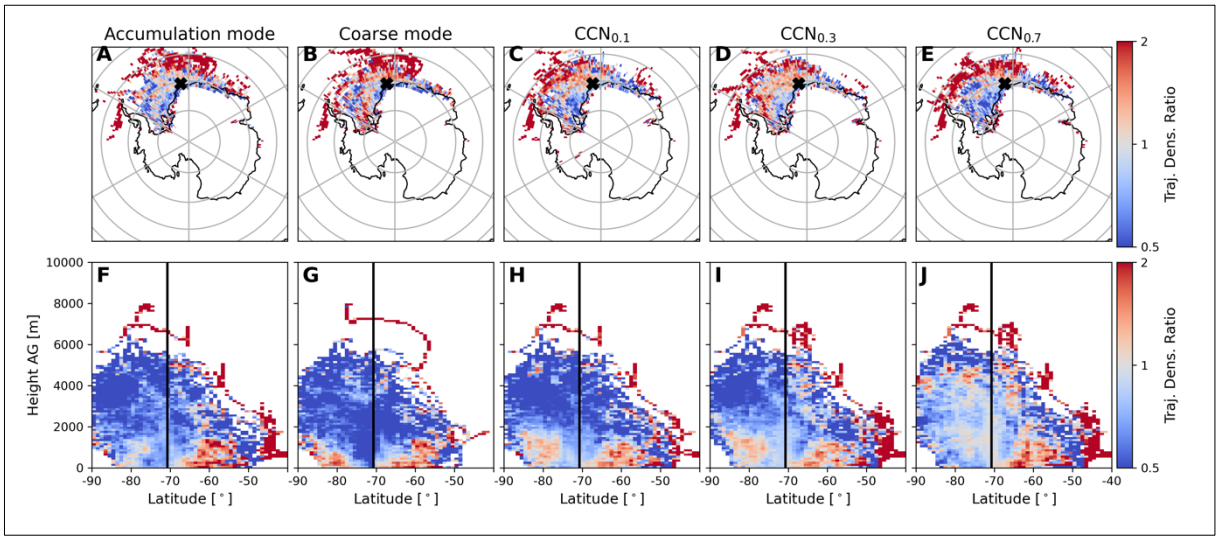

Fig. 4.16.1: Gridded trajectory density ratios (TDRs) and surface contribution for cases of high particle concentration. The particle modes are derived from SMPS+LASX-data and the CCN-concentration from CCNc-data. The selected dates consist of those, where the particle concentration is above the 90th percentile of the running mean. A, B, C, D, E: Surface TDR; F, G, H, I, J: Latitude-height above ground TDR; A, F: Accumulation mode particles; B, G: Coarse mode particles; C, H: $CCN_{0.1}$; D, I: $CCN_{0.3}$; E, J: $CCN_{0.7}$.

Source analysis

All data were analysed using a backward trajectory analysis (Eckermann 2025). The source region analysis of Antarctic aerosol particles identifies the most probable sources of CCN and particles above 65 nm in size (accumulation and coarse modes) in oceanic regions. These regions exhibit areas of high TDR for accumulation and coarse mode particles, as well as for CCN (see Fig. 4.16.1). This is evident in both the spatial distribution of surface TDR and the latitude-height TDR distribution, with high TDR values observed at low altitudes to the north, where the ocean is located. The Master's thesis by Eckermann (2025) also discusses the ocean as a potential source of less hygroscopic particles, INPs and heat-labile INPs. Meanwhile, highly hygroscopic particles appear to originate from inland areas and higher altitudes. The processes behind this, such as photochemistry or transport, are currently under evaluation.

Data management

CCN raw data are transferred daily from the instrument to the data server at Neumayer Station III and from there to the TROPOS server via cronjobs. After their analysis the INP data, will be stored in a long-term archive at TROPOS. Furthermore, the processed CCN data, quality controlled (level 2) data will be archived, published and disseminated according to international standards by the World Data Center PANGAEA Data Publisher for Earth & Environmental Science (https://www.pangaea.de). The INP data are already available on PANGAEA (Eckermann et al. 2024).

SH position was funded by DFG project HE 6770/3-1 within the DFG Priority Program 1158 – Antarctic Research.

In all publications based on this expedition, the **Grant No. AWI_ANT_16** will be quoted and the following publication will be cited:

Alfred-Wegener-Institut Helmholtz-Zentrum für Polar- und Meeresforschung. (2016a). *Neumayer III and Kohnen Station* in Antarctica operated by the Alfred Wegener Institute. Journal of large-scale research facilities, 2, A85. http://dx.doi.org/10.17815/jlsrf-2-152.

Acknowledgement

We thank all overwinterers who collected samples for our project so far, namely M. Schumacher, J. Loftfield, L. Ort, H. Keck, N. Wullenweber, M. Radenz, T. Bösch, L. Weis.

References

Eckermann O (2025) Antarctic particles and where to find them. Master. Faculty of Physics and Earth System Sciences, Leipzig

Eckermann O, Wex H, Juranyi Z, Weller R & Henning S (2024) INP data from Antarctica, Neumayer Station III, during two years [dataset bundled publication]. In: PANGAEA (ed)

Herenz P, Wex H, Mangold A, Laffineur Q, Gorodetskaya IV, Fleming ZL, Panagi M & Stratmann F (2019) CCN measurements at the Princess Elisabeth Antarctica research station during three austral summers. Atmospheric Chemistry and Physics 19:275–294. https://doi.org/10.5194/acp-19-275-2019

Petters MD & Kreidenweis SM (2007) A single parameter representation of hygroscopic growth and cloud condensation nucleus activity. Atmospheric Chemistry and Physics 7:1961–1971.

Roberts GC & Nenes A (2005) A continuous-flow streamwise thermal-gradient CCN chamber for atmospheric measurements. Aerosol Sci Technol 39:206–221.

Tatzelt C, Henning S, Welti A, Baccarini A, Hartmann M, Gysel-Beer M, van Pinxteren M, Modini RL, Schmale J & Stratmann F (2022) Circum-Antarctic abundance and properties of CCN and INP, Atmos. Chem. Phys. https://doi.org/10.5194/acp-2021-700

Wex H, Huang L, Zhang W, Hung H, Traversi R, Becagli S, Sheesley RJ, Moffett CE, Barrett TE, Bossi R, Skov H, Hunerbein A, Lubitz J, Loffler M, Linke O, Hartmann M, Herenz P & Stratmann F (2019) Annual variability of ice-nucleating particle concentrations at different Arctic locations. Atmospheric Chemistry and Physics 19:5293–5311. https://doi.org/10.5194/acp-19-5293-2019

Wex H, Eckermann O, Juranyi Z, Weller R, Mangold A, Overmeiren PV, Zeppenfeld S, van Pinxteren M, Dall'Osto M & Henning S (2024) Antarctica's Unique Atmosphere: Really Low INP concentrations https://doi.org/10.22541/au.172953981.12412340/v1

4.17 SnAcc – Investigating Snowdrifts Around *Neumayer Station III*

Océane Hames[*1,2], Peter Köhler (Logistics)[3], Christian Haas[3], Michael Lehning[*1,2]
*oceane.hames@epfl.ch,
*lehning@slf.ch

[1]CH.SLF
[2]CH.EPFL
[3]DE.AWI

Grant-No. AWI_ANT_27

Outline

The present chapter reports the work achieved during season 2024-2025 for the SnAcc project, which investigates the snow accumulation around the German Antarctic research station *Neumayer Station III*. Details about field work as well as numerical simulations are presented subsequently.

Objectives

Since its inauguration in 2009, the German Antarctic research station *Neumayer Station III* has experienced significant snow accumulation in its direct vicinity. In addition to increasing the work load of the overwintering staff, the deposited snow largely endangers the statics of the station structure. The SnAcc project addresses this issue and aims to define appropriate snow mitigation strategies at *Neumayer Station III* based on the results of a physics-based numerical snow transport model. Numerical simulations enable the testing of various mitigation solutions with minimal effort and resources compared to wind-tunnel experiments. However, prior to its use in decision making processes, the model needs to be compared to field observations to verify the accuracy of the produced results.

Fieldwork

Numerical simulations of snowdrifts around *Neumayer Station III* were conducted and compared to snow depth measurements taken in June 2009 after the inauguration of the station building (Hames et al., 2025). However, this comparison could only be qualitative (deposition locations) due to the multi-month period of accumulation represented by the measurements and their poor accuracy and resolution. Thus, there is a need for precise snow accumulation measurements at *Neumayer Station III* that could be quantitatively compared to numerical results.

Conducting snow accumulation measurements in the *Neumayer Station III* surroundings would constitute a valuable basis to validate our snow transport model. However, such measurements should be taken during the austral winter when human disturbance on the snow distribution is at its minimum (limited snow removal). For this reason, the field work related to SnAcc is mostly achieved by the station overwinterers. It consists of using a terrestrial laser scanner (TLS) to capture the surface topography around *Neumayer Station III* at a given point in time (Prokop et al., 2008). By conducting successive scans, one can assess the changes in snow distribution (accumulation, erosion) that occurred over the time period between the two scans (Sommer et al., 2018; Hames et al., 2022).

The topography scans are conducted with the RIEGL VZ-6000 (RIEGL, 2020), well suited for the survey of icy and snowy terrain. This device produces three-dimensional (3D) point clouds through the reflection of its laser pulse against surrounding objects. To create a local coordinate reference system (CRS) and tie all the scans together, cylinder reflectors are placed on the building and on the neighbouring structures. Figure 4.17.1 illustrates the TLS (left) and cylinder reflectors (right) employed for the snow accumulation measurements.

Fig. 4.17.1: Left: Terrestrial laser scanner RIEGL VZ-6000 used for the snow topography measurements around Neumayer Station III. Right: Cylinder reflector used as tie point for the local reference coordinate system of the scans.

TLS measurements are conducted from several positions around the station structure to obtain a complete scan of the neighbouring surface. Roof-based positions supplement the ground-based ones to limit the shadowing of the scans by the topography and other obstacles. The snowdrifts that formed over time on the East, North-West and South-West sides are used as scanning positions because they are higher than the adjacent terrain and reduce the shadowing in the measurements. Once the scans are acquired from the various positions, they are aligned and integrated using a system of reflectors strategically distributed across the building and its surroundings. An overview of the scanning positions used for the data acquisition is given in Figure 4.17.2.

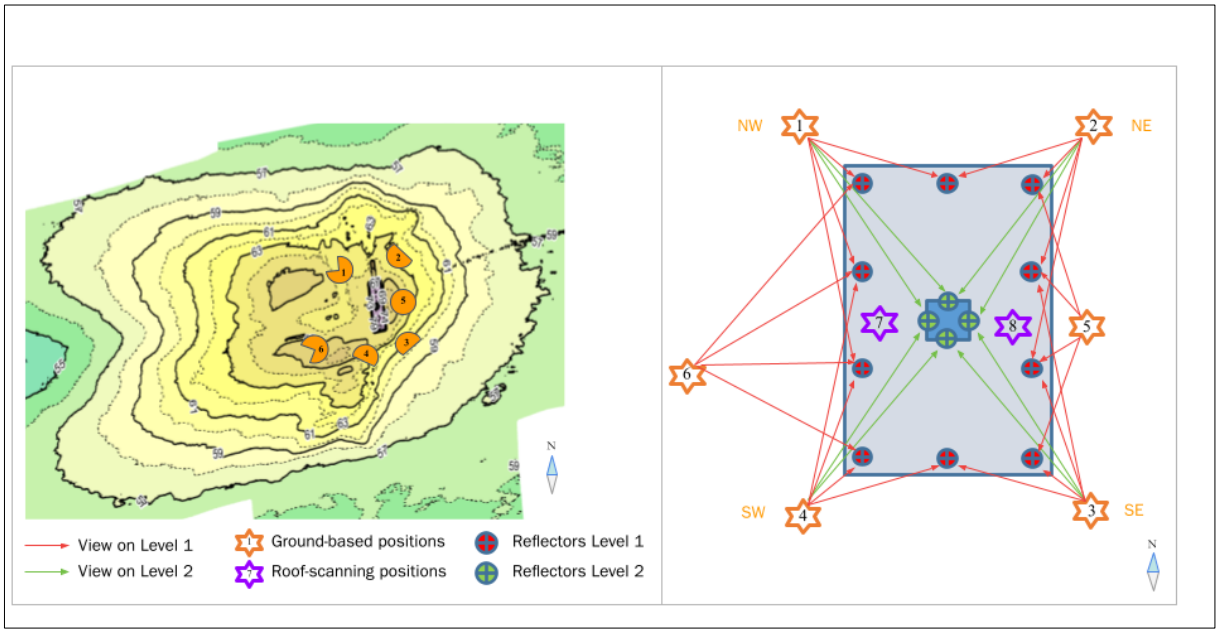

Fig. 4.17.2: Left: Snow surface topography and ground-based scanning positions at the Neumayer Station III. The orange circles show the panoramic view covered by the scans. Right: Reflector and scanning positions (ground- and roof-based) defined for the snow accumulation measurement set-up.

To adequately compare field observations and numerical results, the two successive scans should be conducted around a defined, distinguishable storm event (pre- and post-storm scans). The snow model employed in SnAcc (Hames et al., 2022) simulates the snow redistribution associated with a specific wind speed and direction. Thus, short storm events with homogeneous weather conditions constitute an ideal dataset for model-measurement comparison. The difference between post-storm and pre-storm scans yields the snow depth redistribution associated with that given storm, which can be compared to snow mass distribution results produced by the numerical model.

Test measurements were carried out during the 2022/23 and 2023/24 seasons to develop the laser scanning and stitching methodology. In October and November 2023, two measurement campaigns were conducted to evaluate the suitability of the scan settings (e.g., resolution, duration). Scans were performed from multiple positions, using different combinations of horizontal and vertical resolutions as well as laser pulse repetition rates to determine the optimal configuration. These measurements enabled improvements to the stitching procedure and clarified that precise reflector identification was not critical. A balance had to be found between scan quality (high resolution) and acquisition time. The scan settings selected based on the 2023 test measurements are summarized in Table 4.17.1 and were employed for the 2024 campaign.

Tab. 4.17.1: Settings of the RIEGL VZ-6000 chosen for the snow accumulation measurements at *Neumayer Station III*.

Parameter	Unit	Value
Laser pulse repetition rate	kHz	300
Horizontal resolution	°	0.02
Vertical resolution	°	0.02

The measurement concept and TLS settings were extensively studied during the post-processing of the scans acquired at the end of 2023. In May 2024, measurement attempts were conducted, but the very low temperatures caused issues with the scanner, leading to a postponement of the measurements until the austral spring. In October 2024, the milder temperatures allowed the overwinterers to take full scans of the area surrounding *Neumayer Station III* on 22 October (pre-storm) and 31 October (post-storm). Although the measurements from the roof-based scanning positions were difficult to integrate within the rest of the scans due to a lack of tie points, the results are convicting and could capture the snow accumulation occurring after a storm of 9 days by substracting the pre-storm from the post-storm scans.

Preliminary (expected) results

An example of scan measurement (pre-storm) from the East and West sides is shown in Figures 4.17.3 and 4.17.4, respectively.

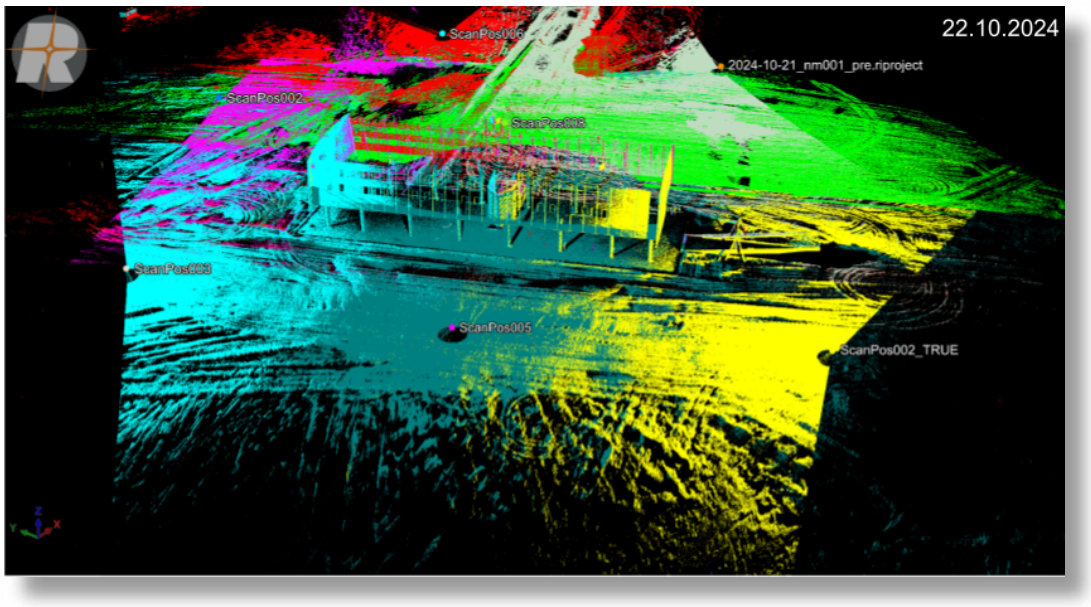

Fig. 4.17.2: East side view of the pre-storm measurement on 22 October 2024. The different colours correspond to scans taken from various positions, as described earlier.

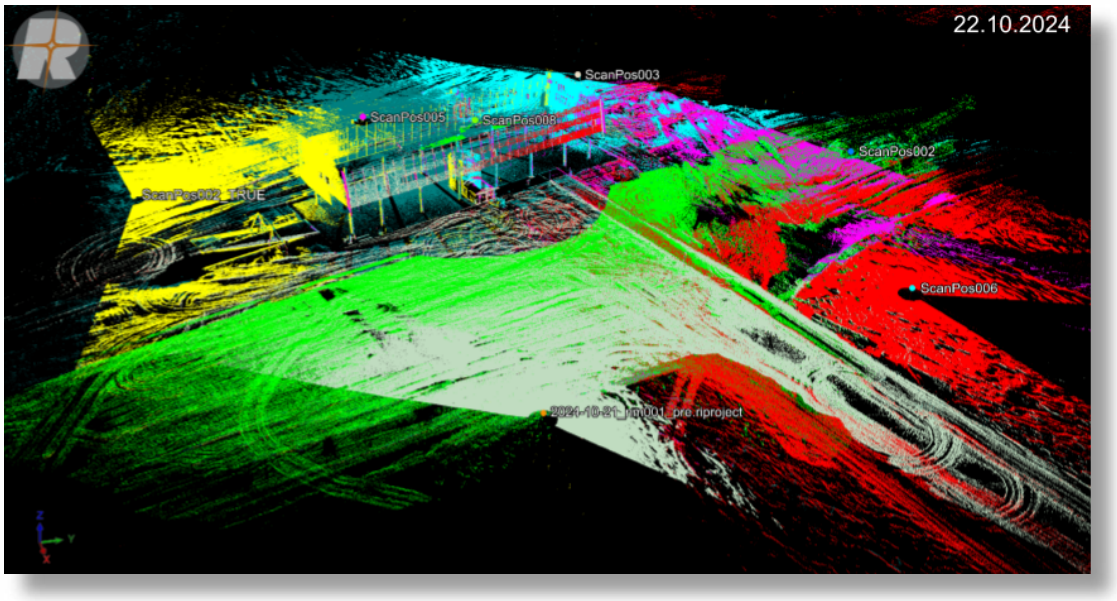

Fig. 4.17.3: West side view of the pre-storm measurement on 22 October 2024. The different colours correspond to scans taken from various positions, as described earlier.

The different colours represent scans acquired from various positions, which were integrated into a common coordinate reference system defined by reflectors placed on the building. Overall, surface coverage around the station is satisfactory; however, the presence of sastrugi on the snow surface introduces small-scale shadowing effects in the scans, visible as black stripes. Portions of the area near the ramp were not fully captured, likely due to the ramp obstructing the scanner's line of sight. While the stitching process between scans has been largely successful, it still requires refinement. In particular, the absence of a fine reflector search–omitted due to time constraints–reduces the positional accuracy of tie points, necessitating further adjustments using the Multi Station Adjustment tool in RiSCAN PRO (RIEGL, 2025). Similar observations apply to the post-storm dataset.

Subtracting the pre-storm elevation data from the post-storm dataset reveals the total snow depth changes that occurred during the period between the two measurements. According to observations from the overwintering team, strong winds accompanied by snowfall between 22 and 31 October led to significant snow accumulation on the eastern side of the station. This accumulation is clearly captured in the data, as illustrated in Figure 4.17.5. The blue point cloud represents the reference baseline (pre-storm scan), while the white point cloud corresponds to the post-storm scan. A marked increase in snow accumulation is evident on the eastern side of the station, highlighting the obstructing effect of the building–particularly the staircase–on the snow-laden airflow.

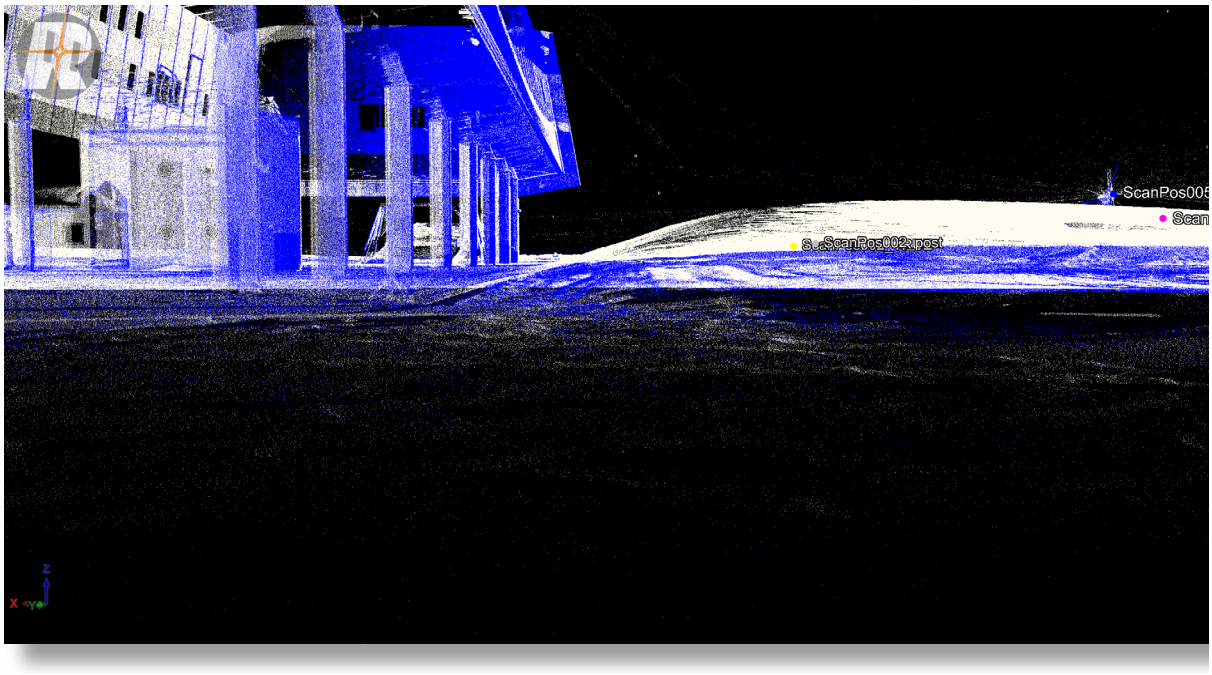

Fig. 4.17.4: Snow accumulation between 22 and 31 October 2024 that occurred at the East side of Neumayer Station III. The blue point cloud corresponds to the pre-storm scan, while the white point cloud corresponds to the surface elevation measured after the storm.

The two datasets require further post-processing, including the removal of structures located above the snow surface and refinement of the stitching accuracy between scan positions collected during the same campaign. The ultimate objective is to generate a map of snow elevation changes during the storm period, free of points corresponding to non-snow objects. Once this is achieved, the resulting snow depth change map will be used to evaluate snow accumulation and distribution patterns around *Neumayer Station III* under specific forcing conditions. This will provide a foundation for numerical model validation and support a deeper understanding of the drifting snow processes occurring in the vicinity of the station's structure.

Data management

The terrestrial laser scanning data will be submitted to EnviDat (https://www.envidat.ch/#/), which is an appropriate long-term archive that provides unique and stable identifiers for the datasets and allows open online access to the data.

In all publications based on this expedition, the **Grant No. AWI_ANT_27** will be quoted and the following publication will be cited:

Alfred-Wegener-Institut Helmholtz-Zentrum für Polar- und Meeresforschung. (2016a). *Neumayer III* and *Kohnen Station* in Antarctica operated by the Alfred Wegener Institute. Journal of large-scale research facilities, 2, A85. http://dx.doi.org/10.17815/jlsrf-2-152.

References

Hames O, Jafari M, Wagner DN, Raphael I, Clemens-Sewall D, Polashenski C, Shupe MD, Schneebeli M & Lehning M (2022) Modeling the small-scale deposition of snow onto structured Arctic sea ice during a MOSAiC storm using snowBedFoam 1.0. Geosci. Model Dev. 15:6429–6449. https//doi.org/10.5194/gmd-15-6429-2022

Hames O, Jafari M, Köhler P, Haas C & Lehning M (2025) Governing processes of structure-borne snowdrifts: A case study at Neumayer station III. Journal of Geophysical Research: Earth Surface, 130:e2024JF008180. https://doi.org/10.1029/2024JF008180

Prokop A, Schirmer M, Rub M, Lehning M & Stocker M (2008) A comparison of measurement methods: terrestrial laser scanning, tachymetry and snow probing for the determination of the spatial snow-depth distribution on slopes. Annals of Glaciology. 49:210–216. https://doi.org/10.3189/172756408787814726

RIEGL Laser Measurement Systems (2020) RIEGL VZ-6000, 3D Ultra Long Range Terrestrial Laser Scanner with Online Waveform Processing. Accessible at: http://www.riegl.com/uploads/tx_pxpriegldownloads/RIEGL_VZ-6000_Datasheet_2020-09-14.pdf (Last access: 16 May 2025)

RIEGL Laser Measurement Systems (2025) RiSCAN PRO (2.16) [Software]. RIEGL Laser Measurement Systems. Accessible at: http://www.riegl.com/products/software-packages/riscan-pro (Last access: 16 May 2025)

Sommer C, Wever N, Fierz C & Lehning M (2018) Investigation of a wind-packing event in Queen Maud Land, Antarctica. The Cryosphere 12:2923–2939. https://doi.org/10.5194/tc-12-2923-2018

4.18 ZeroPolAr – Incentives for a Zero-Pollution Ambition for Antarctica

Anja Weber[1]
Not in the field: Anette Küster[2]*, Jan Koschorreck[2], Zhiyong Xie[3]
* Anette.Kuester@uba.de

[1]DE.AWI
[2]DE.UBA
[3]DE.HEREON

Grant-No. AWI_ANT_26

Outline

This project focuses on investigating Persistent Organic Pollutants (POPs) and the Chemicals of Emerging Concern (CECs) in Antarctic ecosystems to protect the fragile polar environment. Based at the German Antarctic *Neumayer Station III*, this project involves systematic screening of POPs and CECs in environmental and biota samples. By analyzing their concentrations and temporal trends, the research aims to identify contamination sources, evaluate bioaccumulation in penguin, assess ecological risks, and support evidence-based chemical regulation. The collected data will contribute to international monitoring efforts, such as those under SCAR, and to inform stakeholders to moderate anthropogenic impacts on Antarctica.

Objectives

Early studies by the German Environmental Specimen Bank revealed the presence of flame-retardant chemicals in Antarctic fish samples (Dreyer et al. 2019), demonstrating the long-range transport potential of persistent organic pollutants – a key criterion under the Stockholm Convention. Emerging evidence suggests accelerated pollutant accumulation in polar organisms due to climate-driven ice melt and subsequent remobilization of historically regulated contaminants. However, systematic chemical monitoring remains inadequate, particularly in Antarctica (Umweltbundesamt 2020; Xie et al. 2020), despite being critical for ecosystem protection and global chemicals management.

To address these gaps, the UBA has initiated an international research project synthesizing pollutant data from Antarctic Treaty states. The project aims to establish a comprehensive concept for a polar environmental monitoring programme (POLEMP), developing standardized protocols for tracking chemical pollution in Antarctica. The proposed monitoring programme will systematically track the occurrence and temporal trends of organic pollutants in Antarctica, building upon established frameworks such as the Arctic Monitoring and Assessment Programme (AMAP), the Antarctic Monitoring and Assessment Program (AnMAP), and the United Nations Environment Programme (UNEP). This approach includes Antarctic sample analysis to develop standardized protocols for data collection and laboratory assessment, ensuring methodological consistency and comparability.

The project will synthesize current Antarctic pollution data for submission to SCAR's ImPACT Action Group and Stockholm Convention bodies. Strategic knowledge exchange will be facilitated through international workshops (2024, 2026), with findings disseminated via open-access platforms to maximize scientific and policy impact. This initiative represents a critical step toward evidence-based polar protection and global chemicals management.

Environmental sampling within ZeroPolAr is intended as a pilot study for a collection of Antarctic samples as a building block for a structured chemical monitoring.

The following research questions are to be answered within the framework of the project:

1. Characterize polar-region pollution loads by identifying chemicals with long-range transport potential into Antarctica using environmental samples such as samples from the emperor penguin colony near *Neumayer-Station III* sampled in a non-destructive manner.
2. Assess climate change impacts on pollutant dynamics in polar regions, focusing on bioaccumulation along food webs, to evaluate ecosystem resilience under increasing anthropogenic and climatic pressures.
3. Evaluate the feasibility of establishing a systematic Antarctic specimen archive for long-term environmental monitoring, adhering to German Environmental Specimen Bank protocols.

Fieldwork

Samples of the Antarctic Ecosystem were collected on-site near the German research facility *Neumayer-Station III* 15 abandoned eggs from the emperor penguin colony in Atka Bay were collected and brought to *Neumayer-Station III* in the project year 2023 and 2024 (Tab. 4.18.1). Following non-destructive assessment of developmental status through X-ray scanning at the station, the eggs were then transported back to Bremerhaven via a ferry in March 2025, and then send to Fraunhofer Institute for Molecular Biology and Applied Ecology (IME), where they are prepared following the protocol of German ESB. Homogenised penguin egg samples will be further distributed to Hereon and MINJIE for analysing legacy persistent organic pollutants and CECs. PFAS, selected elements and isotopes are analysed at IME. The remaining sample material will be archived at German ESB.

Tab. 4.18.1: Information of penguin egg samples collected from the emperor penguin colony, Atka Bay, 2024

Penguin egg No.	Weight (g)	Remark
1	429	Whole egg, one big crack, Intact
2	549	Whole egg, one big crack, Intact
3	198	Half egg, shell broken, only yolk
4	471	Whole egg, one big crack, Intact
5	453	Whole egg, flawless
6	390	Whole egg, flawless
7	408	Whole egg, flawless
8	483	Whole egg, broken shell
9	406	Whole egg, one big crack, Intact
10	438	Whole egg, flawless
11	444	Whole egg, broken shell
12	185	Half egg, broken shell
13	438	Whole egg, flawless
14	394	Whole egg, flawless
15	396	Whole egg, flawless

Preliminary (expected) results

This study demonstrates the successful opportunistic collection, storage at *Neumayer Station III*, and subsequent transport of Antarctic samples to German ESB at Fraunhofer IME. Emperor penguin egg samples serve as key indicators for assessing the feasibility of establishing an Antarctic ESB under the German Environment Agency (UBA) initiative.

Penguin egg samples will be analyzed in the analytical laboratories at Hereon, MINJIE and IME using advanced analytical tools, e.g. GC-MS/MS, GC-QTOF-MS, LC-MS/MS, and LC-QTOF-MS/MS for legacy POPs and CECs. Analytical results will reveal the occurrence and distribution of POPs and CECs in penguin eggs, reflecting bioaccumulation patterns and potential toxic risks to Antarctic biota. Both targeted and nontarget analyses will identify unknown substances and transformation products of chemical contaminants. These data will clarify the biomagnification potential of EOCs across Antarctic food webs and assess their ecological impacts on penguins and other endemic species.

Chemicals of emerging concern in Penguin eggs

Phthalate esters (DMP, DEP, DiBP, DnBP, BBP, DCHP, DEHP, DOP), organophosphate esters (TEP, TPrP, TiBP, TnBP, TCEP, TCIPP, TDCIPP, TPhP, EHDPP, TEHP, TCBP) and synthetic musk fragrances (HHCB, AHTN) were detected in most penguin egg samples analysed (Fig. 4.18.1). Among these contaminants, DEHP emerged as the most predominant compound, a finding consistent with its extensive use in plastic manufacturing, industrial applications, and consumer products. Notably elevated concentrations of DnBP, TEHP and TBCP were observed in some samples, suggesting potential point sources of contamination. The presence of synthetic musks (HHCB and AHTN) in penguin eggs is particularly significant, as it indicates either long-range environmental transport of these compounds or direct input from personal care products used by tourists visiting penguin habitats.

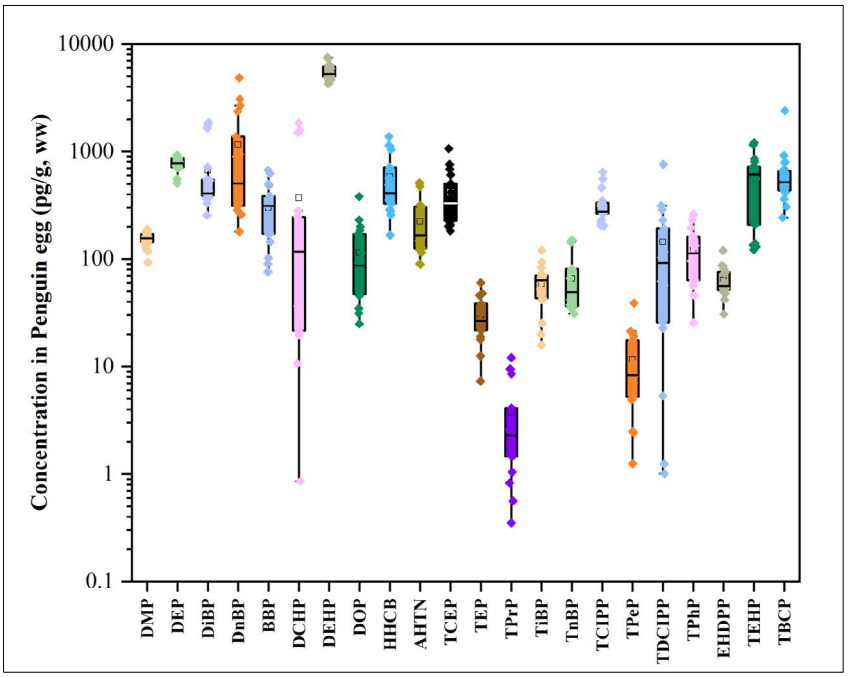

Fig. 4.18.1: Concentration ranges of PAEs, OPE and synthetic musk fragrances measured in the penguin eggs collected in Antarctica.

The detection of these contaminants raises important environmental health concerns. DEHP and DnBP are known endocrine disruptors, while certain organophosphate esters like TDCIPP and TCIPP have been identified as potential carcinogens. These findings emphasize the need for comprehensive monitoring programmes to track chemical pathways and implement targeted source control measures to protect Antarctica.

Data management

Environmental data will be archived, published and disseminated according to international standards by the World Data Center PANGAEA Data Publisher for Earth & Environmental Science (https://www.pangaea.de) within two years after the end of the expedition at the latest. By default, the CC-BY license will be applied.

Data will also be submitted to the long-term archive of the Information System Umweltprobenbank (IS UPB) with a web-based data portal and webpage (www.umweltprobenbank.de) that provides unique and stable identifiers for the datasets and allows open online access to the data.

Any other data will be submitted to an appropriate long-term archive that provides unique and stable identifiers for the datasets and allows open online access to the data.

This expedition was supported by the Helmholtz Research Programme “Changing Earth – Sustaining our Future” Topic 4, Subtopic 4.1.

In all publications based on this expedition, the **Grant No. AWI_ANT_26** will be quoted and the following publication will be cited:

Alfred-Wegener-Institut Helmholtz-Zentrum für Polar- und Meeresforschung. (2016a). *Neumayer III and Kohnen Station* in Antarctica operated by the Alfred Wegener Institute. Journal of large-scale research facilities, 2, A85. http://dx.doi.org/10.17815/jlsrf-2-152.

References

Dreyer A, Neugebauer F, Lohmann N, Rüdel H, Teubner D, Grotti M, Rauert C & Koschorreck J (2019) Recent findings of halogenated flame retardants (HFR) in the German and Polar environment. Environmental Pollution 253:850–863. https://doi.org/10.1016/j.envpol.2019.07.070

POLEMP Project: Developing a concept for a Polar Environmental Monitoring Program | Umweltbundesamt.

Umweltbundesamt 2020. Schwerpunkt 1-2020: PFAS. Came to stay. 48S. What Matters 1-2020: PFAS. Came to stay. | Umweltbundesamt.

Xie ZY, Zhang P, Wu ZL, Zhang S, Wei LJ, Mi LJ, Kuester A, Gandrass J, Ebinghaus R, Yang RQ, Wang Z & Mi WY (2022) Legacy and emerging organic contaminants in the polar regions. Sci. Total Environ. 835. http://dx.doi.org/10.1016/j.scitotenv.2022.155376

4.19 Helikite Tethered Balloon Deployment Under ORACLES Project

Michael Lonardi[1], Yolanda Temel[1] [1]CH.EPFL
not in the field: Julia Schmale*[1]
* julia.schmale@epfl.ch

Grant-No. AWI_ANT_47

Outline

The ORACLES project aims at better understanding aerosol-cloud interactions and cloud radiative effects in coastal Antarctica. In this framework, a tethered balloon platform was operated in the vicinity of *Neumayer Station III* between December 2024 and February 2025. The system collected more than 130 vertical profiles of key atmospheric variables, focusing on thermodynamics, aerosol particle concentrations, and filters samples for chemical analyses.

Objectives

The ORACLES project aims to pursue five objectives:

1. Acquire unprecedented vertically-resolved observations of aerosol-cloud interactions.
2. Use molecular-level atmospheric chemical information for source identification of cloud particles.
3. Fill the gap of missing vertical thermodynamic profiles and cloud properties.
4. Upscale the in-situ measurements to the whole of Antarctica with a chemical transport model based on enhanced process understanding.
5. Simulate the impact of aerosol-cloud interactions on Antarctica's surface radiation budget.

In particular, objectives 1 – 3 are to be achieved primarily with data obtained with *in-situ* observations at *Neumayer Station III*, while objectives 4 and 5 are supported by the field measurements but are mainly model-oriented.

Fieldwork

The centerpiece of the field deployment was the operation of a tethered balloon setup ("Helikite") to profile the lower troposphere. The system consists of a Helium filled balloon, a payload setup comprising several miniaturized instruments for atmospheric measurements, an electrically operated winch that controls the vertical movement of the balloon, and a computer to monitor the system's telemetry (Pohorsky et al., 2024). Figure 4.19.1 displays the Helikite setup.

Fig. 4.19.1: Helikite take off on a clear sky day. The white payload box and the tethersonde are attached to the system. Y. Temel controls the balloon ascent speed operating one of the electrical winches fixed to the Lehman sledges. (Photo: M. Lonardi).

The instrumental payload consists of a combination of a tethersonde, a condensation particle counter (CPC3007), a miniaturized scanning electrical mobility sizer (mSEMS), a portable optical particle spectrometer (POPS), a miniaturized cloud droplet analyzer (mCDA), a Sonic anemometer, an 8-channel filter sampler for aerosol particles (FILT), and a tiny autonomous portable infrared radiometer (TAPIR). These instruments provide measurements of thermodynamic conditions, aerosol particle total concentration and size distribution, cloud droplet size distribution, brightness temperature, and samples for chemical analyses. The specific instrumental configuration was decided on a flight-by-flight base, in accordance to the wind conditions and the cloud cover.

During the campaign, two different balloons were operated. A smaller setup (24 m^3 Helikite with a 900 m tether on one winch) was brought in with the field team, and a larger setup (64 m^3 Helikte with 1,000 m of tether splitted on 2 winches), arrived with *Polarstern*. The larger system is able to lift a heavier payload, i.e., carry more instruments, which results in more complete observations of the atmosphere, however it was not possible to airfreight it due to its bulkiness.

The field team arrived at the station on 17 December 2024. In the following days, a Lehman sledge was fitted to anchor and operate the 24 m^3 tethered balloon, and was placed near the former Eden ramp site, approx. 300 m South of *Neumayer Station III*. The balloon was inflated and the full system was tested for integrity first in calm and then strong (10 m/s) wind

conditions, while the scientific payload was assembled inside the station. Scientific flights began on 22 December, and a full list is provided in the following Table 4.19.1.

Tab. 4.19.1: List of Helikite flights during the field season. Note that flights 0 – 44 were performed with the 24 m^3 system, 45 – 68 with the 64 m^3 system. Flights 0, 14, and 51 were technical flights with no aerosol measurements. The value for the maximum altitude was obtained from the raw data and a correction up to ±20 m may be applied. All times are in UTC.

Flight number	Date	Code	Max altitude [m]	Take off time	Landing time	Flight duration
0	2024-12-21	A	20	14:33	16:20	01:47
1	2024-12-22	A	93	10:54	11:18	00:24
2	2024-12-22	B	225	11:23	11:58	00:35
3	2024-12-22	C	447	14:27	15:47	01:20
4	2024-12-23	A	365	09:19	10:32	01:13
5	2024-12-23	B	444	10:58	11:56	00:58
6	2024-12-23	C	406	14:07	15:04	00:57
7	2024-12-23	D	535	15:28	17:03	01:35
8	2024-12-27	A	430	09:59	10:57	00:58
9	2024-12-27	B	402	11:08	12:11	01:03
10	2024-12-27	C	325	14:29	15:22	00:53
11	2024-12-27	D	516	16:02	16:43	00:41
12	2024-12-30	A	333	09:00	09:31	00:31
13	2024-12-30	B	478	09:36	10:30	00:54
14	2024-12-30	C	10	10:37	10:46	00:09
15	2024-12-30	D	200	11:00	11:29	00:29
16	2024-12-31	A	275	09:20	10:25	01:05
17	2024-12-31	B	410	10:27	11:41	01:14
18	2025-01-02	A	348	16:36	17:42	01:06
19	2025-01-03	A	438	09:52	11:09	01:17
20	2025-01-03	B	300	13:32	15:39	02:07
21	2025-01-03	C	471	16:08	17:07	00:59
22	2025-01-05	A	194	14:37	15:03	00:26
23	2025-01-06	A	511	09:54	11:05	01:11
24	2025-01-06	B	303	11:25	13:53	02:28
25	2025-01-06	C	392	14:18	15:20	01:02
26	2025-01-06	D	250	15:24	15:59	00:35
27	2025-01-06	E	360	16:22	17:41	01:19
28	2025-01-09	A	479	09:50	10:56	01:06
29	2025-01-09	B	356	11:21	13:54	02:33
30	2025-01-09	C	488	14:15	15:29	01:14
31	2025-01-10	A	352	15:53	16:52	00:59
32	2025-01-16	A	587	15:43	16:57	01:14
33	2025-01-16	B	170	17:10	17:33	00:23

Flight number	Date	Code	Max altitude [m]	Take off time	Landing time	Flight duration
34	2025-01-16	C	240	17:36	19:18	01:42
35	2025-01-17	A	340	20:16	20:38	00:22
36	2025-01-17	B	333	20:41	20:54	00:13
37	2025-01-17	C	328	20:59	21:12	00:13
38	2025-01-17	D	150	21:23	21:53	00:30
39	2025-01-17	E	172	21:53	22:14	00:21
40	2025-01-17	F	129	22:18	22:41	00:23
41	2025-01-18	A	342	09:56	10:12	00:16
42	2025-01-18	B	403	11:01	11:50	00:49
43	2025-01-18	C	119	11:58	12:08	00:10
44	2025-01-18	D	344	13:44	16:17	02:33
45	2025-01-27	A	853	18:28	19:32	01:04
46	2025-01-28	A	617	19:07	20:20	01:13
47	2025-01-28	B	544	20:51	21:50	00:59
48	2025-02-03	A	640	14:02	16:58	02:56
49	2025-02-04	A	420	10:46	12:21	01:35
50	2025-02-06	A	927	14:41	16:52	02:11
51	2025-02-06	B	944	17:26	17:56	00:30
52	2025-02-07	A	484	11:03	13:04	02:01
53	2025-02-07	B	400	22:39	00:32	01:53
54	2025-02-08	A	591	14:50	16:59	02:09
55	2025-02-08	B	606	17:33	18:37	01:04
56	2025-02-08	C	555	19:46	21:30	01:44
57	2025-02-10	A	335	11:34	13:33	01:59
58	2025-02-11	A	605	14:38	16:56	02:18
59	2025-02-12	A	573	08:03	10:10	02:07
60	2025-02-12	B	566	10:48	12:14	01:26
61	2025-02-13	A	595	14:20	16:14	01:54
62	2025-02-13	B	310	16:28	16:57	00:29
63	2025-02-14	A	654	11:04	11:48	00:44
64	2025-02-14	B	636	11:56	12:28	00:32
65	2025-02-14	C	638	12:33	13:04	00:31
66	2025-02-14	D	697	16:23	17:44	01:21
67	2025-02-14	E	767	18:40	19:15	00:35
68	2025-02-15	A	420	09:49	11:19	01:30

When not in operation, the balloon was secured to the heavy Lehman sledge with multiple ropes and parked hovering at approximately 10 m altitude. For safety reasons, the 24 m^3 balloon was stored underneath the station when strong winds were forecasted for the following day. During the strong wind periods, the field team primarily performed data analysis and maintenance on the instrumental payload. In early January, the AWI technical team built a

container shelter to house the incoming larger 64 m^3 balloon. Since 7 January, the balloon was stored in this location in case of strong winds. Figure 4.19.2 displays the container shelter.

Fig. 4.19.2: The container shelter and the 64 m^3 Helikite. (Photo: Y. Temel).

After the arrival of *Polarstern*, the 24 m^3 Helikite was deflated and the larger 64 m^3 system was operated. An additional Lehman sledge was prepared, in order to accommodate the second winch necessary for this system, and laboratory work was performed at the station to transition to a larger payload box.

In the evening of 30 January 2025, the 64 m^3 Helikite deflated due to the inner shell being ripped by the wind. The balloon was brought inside, checked for integrity, and it was decided to substitute the broken shell with a new one. Measurement operations were resumed on 3 February.

After the last flight on 15 February, the system was deflated and stored in the EPFL container, now located on top of the Eden platform. The container shelter was dismantled by the technical team, and all the material, including the Lehman sledges, was placed in the winter storage.

The instrumental payload and the broken shell were transported back to Europe, while the rest of the material remained on site for a follow up campaign in the upcoming 2025/26 season.

Preliminary (expected) results

The tethered balloon systems were on site for 56 days, with 28 days of measurements providing a total of 69 flights (66 science flights and 3 technical flights). Of these, 45 were obtained with the 24 m^3 Helikite (approximately 3/day), and 24 with the 64 m^3 setup (approximately 2/day). The main reasons of the apparent performance decrease for the larger system are the complexity of its payload, which caused a longer preparation time on the ground, and the manoeuvrability of the balloon, which required both operators to focus on the hardware during the setup phase, postponing software initializations and therefore take-off.

The typical maximum height for the flights was between 300 – 500 m for the smaller system, with the balloon lift being the limiting factor, and between 500 – 700 m for the larger Helikite, which was constrained by the length of its 1,000 m tether. Warmer days with cloudless conditions and weak wind provided the best flight conditions in terms of maximum flight height. The enhanced vertical range of the 64 m^3 system proved to be crucial, substantially increasing the overall number of clouds reached by the Helikite. This resulted in 9 flights reaching or profiling through a cloud, with additional 8 flights stopping below cloud base. In comparison, two thirds of the flights with the 24 m^3 were performed in cloudy conditions, but none of them reached cloud base. However, 6 flights surveyed a fog layer that was not predicted by the weather forecast.

Helikite flights were performed under various thermodynamic conditions. Figure 4.19.3 showcases an overview of 33 flights of aerosol total concentration obtained with the CPC3007 instrument, classified based on the wind direction. An abundance of data points can be seen for the concentrations between 200 – 500 cm^{-3}, with little to no variation in the vertical component. These profiles are attributed to background conditions, and potentially indicate that only the wind direction, i.e., source region, is not a strong factor controlling the particle total concentrations at this site. However, it should be noted that particle concentrations for the accumulation mode (not shown) seem to relate to northerly direction as a source of larger particles, in agreement with the expected abundance of sea salt and secondary marine particles coming from the ocean. The rest of the profiles displays variations likely caused by the overlap of two distinct airmasses, as also suggested by different wind directions over the vertical component during the same profile, or by the advection of newly formed particles.

Figure 4.19.4 showcases times series from an example flight obtained on 8 February. In particular, the flight pattern is displayed, as well as the particle size distributions and total particle concentrations from the mSEMS and the POPS. Measurements of thermodynamic variables, droplet size distribution, and brightness temperature, are available but not shown.

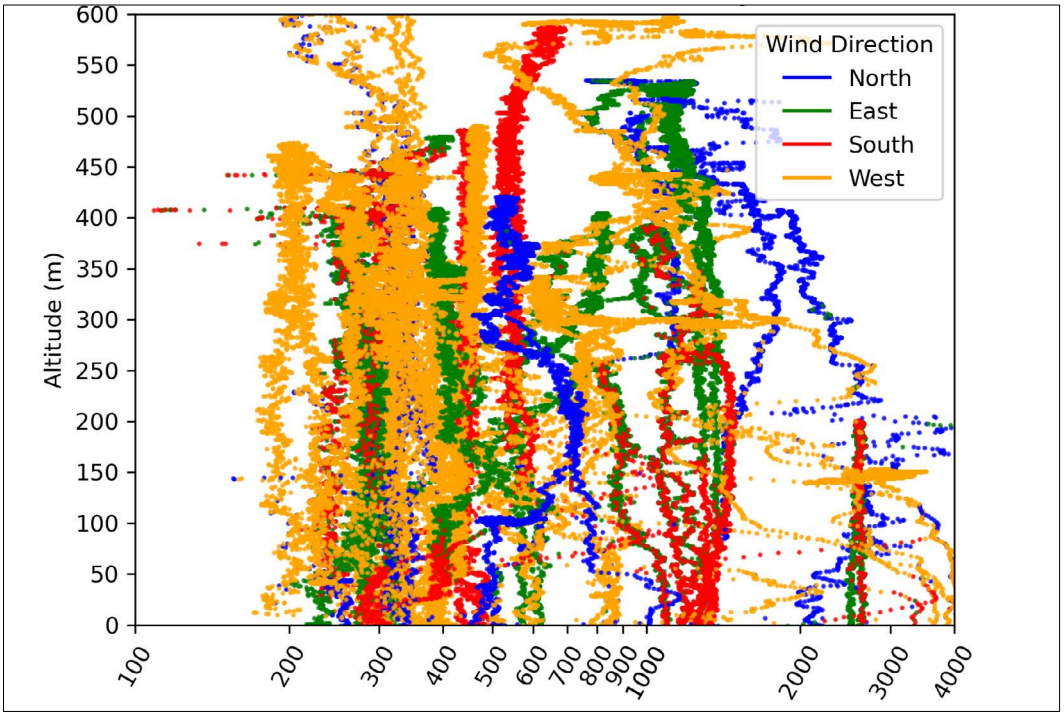

Fig. 4.19.3: Vertical profiles of aerosol particle total concentrations of particles larger than 10 nm. Each data point is color-coded based on the wind direction. The x-axis scale is logarithmic. All data are raw values.

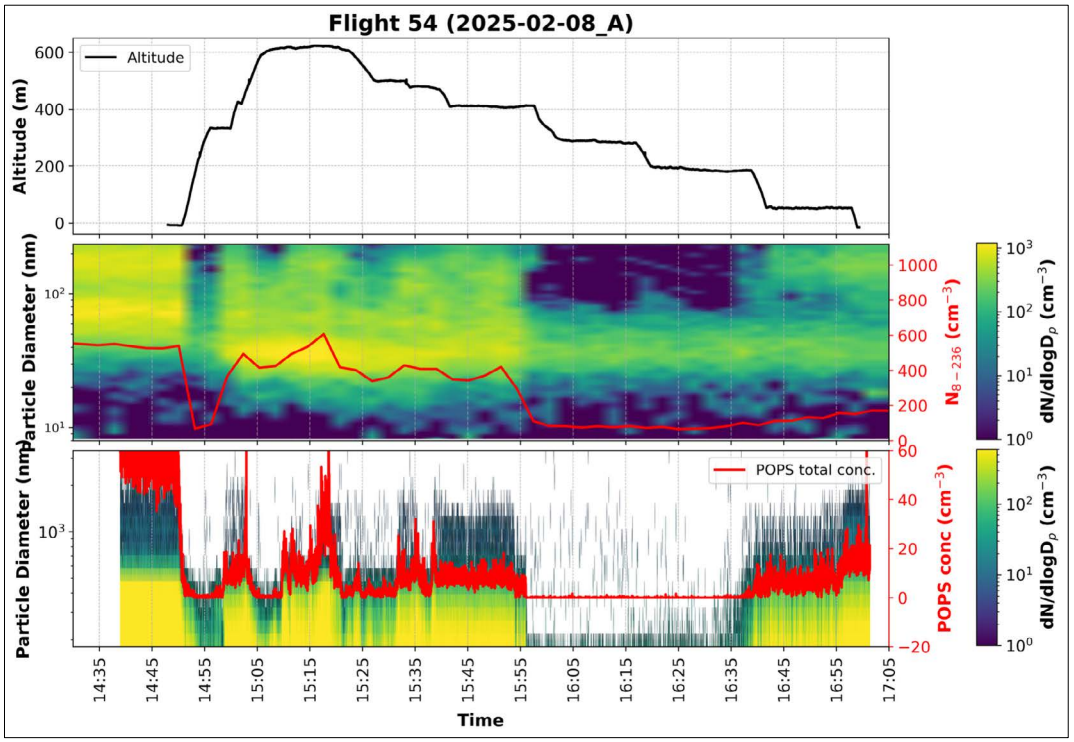

Fig. 4.19.4: Time series of altitude (upper panel), total particle concentration and size distribution for the 8 – 236 nm size range (central panel), and particle total concentration and size distribution for the 183 – 3,300 nm range (lower panel). All data are raw values.

In the upper panel, the altitude above surface shows a quick ascent, with a short stop at about 300 m to concatenate the second tether. After reaching a maximum height of 600 m, the balloon hovers at a fixed height for approximately 15 minutes. This stop allows to average the aerosol particle concentrations, obtaining a more robust representation of the particle size distribution. A stepwise descent was adopted for the same reason, with steps of 100 m down to the surface.

The particle size distributions in the central and lower panel show distinct features for the layers crossed during the flight. Near the surface, a particle concentration of 400 cm^{-3} is observed, with an abundance of Aitken mode particles with a diameter between 70 – 90 nm, and a second peak in the accumulation mode particles with diameters between 150 – 200 nm. The Helikite enters a cloud shortly after take-off, resulting in a 0 cm^{-3} concentration of accumulation mode particles (at around 14:55). Once the helikite crossed cloud top at 300 m altitude, the total concentration is again 400 cm^{-3}. Here the size distribution peaks at 30 nm, with relatively low concentrations in the accumulation mode. During the descent, all the aerosol layers are crossed again, with a slight vertical displacement of the cloud.

The overall concentration of 400 cm^{-3} above and below the cloud suggests a single air mass in which a cloud layer had developed. Aloft, the airmass is characterized by a peak in the Aitken mode particles. In the cloud, the accumulation mode particles get activated as droplets, therefore the remaining particle concentration displays only an Aitken mode peak. When the droplets evaporate, they dry and only the aerosol particles remain. These particles grew inside the cloud, and now display a distinct peak in the accumulation mode. The combined presence of both an Aitken mode and an accumulation mode peak with a Hoppel minimum in between is an indication of aerosol processing by the cloud.

Fig. 4.19.5: Y. Temel prepares a filter. (Photo: M. Lonardi).

A total of 32 filter samples for chemical analysis were also collected during the field deployment, 16 at surface level and 16 during the Helikite flights. Given the low particle concentrations at the site, the filter sampler had to run for approximately one hour to make sure enough particles deposit on the membrane. For the surface measurements, the payload, comprising the filter and the rest of the aerosol setup, was positioned at the Eden platform, with the inlet pointing towards the incoming wind. For the balloon-borne measurements, the Helikite typically hovered at a selected altitude level (typically the maximum reachable height) for the necessary time. However, for technical necessities, the sampling was often performed during a descending scan through a layer identified during the ascent profile. Figure 4.19.5 shows the delicate handling of the filters. These filters will be analyzed to obtain detailed information about the chemical composition of the sampled particles. Organic functional groups, such as alkanes, carboxylic acids, hydroxyl and carbonyl groups, as well as species like ammonium and sulphate can be quantified

The dataset includes filters obtained in cloudless conditions, in or near clouds, and in fog, additionally covering all the principal wind directions. In addition to the filters for chemical analyses, 10 more filters were collected with a small portable setup installed at surface level for sampling times of approximately 3 days: 5 filters for scanning electron microscopy (SEM) and transmission electron microscopy (TEM), and 5 for ice nucleating particles (INP) analysis.

Overall, the dataset obtained through the Heliktie deployment at *Neumayer Station III* constitutes a first solid step for the overall achievement of the project goals of ORACLES. The analysis of the measurements and the filter samples will additionally provide useful insights for the scientific planning of the follow up field campaign in the upcoming Antarctic summer season.

- In summary, the following has been achieved:
- 132 measurements profiles have been obtained through 66 scientific flights, reaching altitudes between 300 – 900 m, and covering various thermodynamic conditions and cloud scenarios, in fulfilment of Objective 3.
- Cloud cases have been investigated with a combination of aerosol and cloud probes, enabling us to tackle the analysis of aerosol-cloud interaction needed for Objective 1.
- 42 filters have been collected and successfully transported back to EPFL, where they will be subject to chemical analyses to complete Objective 2.

In addition to these, long-standing observations performed at *Neumayer Station III* will be used to characterize the synoptic and local meteorological conditions, and to validate the profile measurements. The synergy between Helikite vertical profiles and surface-based observations, *in situ* and remote sensing, is expected to yield substantial results that will help understanding the aerosol-cloud interactions and cloud-radiative effects in coastal Antarctica.

Data management

Environmental data will be archived, published and disseminated according to international standards by the World Data Center PANGAEA Data Publisher for Earth & Environmental Science (https://www.pangaea.de) within two years after the end of the expedition at the latest. By default, the CC-BY license will be applied.

This expedition was supported by the SNSF Consolidator grant ORACLES (no. TMCG-2_213771).

In all publications based on this expedition, the **Grant No. AWI_ANT_47** will be quoted and the following publication will be cited:

Alfred-Wegener-Institut Helmholtz-Zentrum für Polar- und Meeresforschung. (2016a). *Neumayer III and Kohnen Station* in Antarctica operated by the Alfred Wegener Institute. Journal of large-scale research facilities, 2, A85. http://dx.doi.org/10.17815/jlsrf-2-152.

References

Pohorsky R, Baccarini A, Tolu J, Winke LH & Schmale J (2024) Modular Multiplatform Compatible Air Measurement System (MoMuCAMS): a new modular platform for boundary layer aerosol and trace gas vertical measurements in extreme environments. Atmospheric Measurement Techniques 17:731–754. https://doi.org/10.5194/amt-17-731-2024

4.20 SEAEIS II – Seals and Cryobenthic Communities at the Ekström Ice Shelf II

Christoph Held[1]; Henning Schröder[1], Horst Bornemann[1]

[1]DE.AWI

Grant-No. AWI_ANT_25

Outline

SEAIs and cryobenthic communities at the Ekström Ice Shelf II (SEAEIS II) is a follow-up of the *Seals at the Drescher Inlet* (SEADI) project carried out from *Neumayer Station III* as part of the ANT-Land 2015/2016 and PS96 *Polarstern* campaigns (Bornemann et al. 2016), it complements expedition PS129 with *Polarstern* in 2021 (Flores et al. 2023), extends the previous SEAEIS campaign in 2022/2023 (Bornemann et al. 2024), and refers to preceding campaigns at Drescher Inlet in 2003/04 (Plötz et al. 2005) and Atka Bay in 2008 (Naito et al. 2010). In doing so, SEAEIS II applies biologging technologies for studying the foraging ecology of Weddell seals with a direct link to ROV-borne investigations of the cryobenthic communities beneath the Ekström Ice Shelf at Atka Bay. For further details see Bornemann et al. (2024).

Objectives

SEAEIS II focuses on the foraging ecology of Weddell seals (*Leptonychotes weddellii*) and the shelf-ice associated cryobenthic communities. Data obtained from seal-borne 3D-multi-channel data loggers and cameras deployed during earlier expeditions to the Drescher Inlet in 2003/2004 (PS65) documented that Weddell seals dived along the steep cliffs of the shelf ice and made foraging excursions under the ice shelf (Liebsch et al. 2007; Watanabe et al. 2006). The seal-borne images and dive data led to the discovery of a hitherto unknown cryobenthic community of marine invertebrates, presumably isopods (Antarcturidae, Austrarcturellidae), and potentially anthozoans (*Edwardsiella* spp., *cf*. Daly et al. 2013), being attached head-down to the underside of the floating ice shelf at depths of 130-150 m (Watanabe et al. 2006). These “hanging gardens” may represent an attractive food horizon, where seals could benefit from a local hotspot of high biological activity in addition to the seafloor at 450 m depth. These particular findings also explain the trimodal distribution of dive depths of Weddell seals known from earlier investigations during PS65, PS48, PS34, PS20, PS17 (Plötz et al. 2005, 1999, 1997, 1994, 1991). A synoptic field study on Weddell seals at Atka Bay (*Neumayer Station II*) during austral spring 2008 (ANT-Land_2002-2009_ATKA) showed, however, only a bimodal distribution in dive depths and feeding events of Weddell seals with an increased feeding rate likely on smaller prey items in the pelagic realm (Naito et al. 2010). A number of seals undertook dives to shallower depths between 70 and 80 m to the sea floor and close to the ice shelf edge and along an iceberg stranded inside the Atka Bay, and supported our hypothesis of shelf ice associated foraging (McIntyre et al. 2013; Naito et al. 2010).

Underwater video-footage taken during a re-assessment at Drescher Inlet during PS96 in combination with ANT-Land 2015/2016 showed that the cryobenthic isopod crustaceans populate the underside of floating shelf ice in dense aggregations (average: 25 adults/m^2), and at different life stages at depths around 80 m (Bornemann et al. 2016). The filter-feeding crustaceans could be identified as *Antarcturus* cf. *spinacoronatus*. Molecular barcoding

demonstrates that (1) males, ovigerous females and juveniles sampled from the cryobenthic community belonged to the same species, thus proving that the population under the shelf ice is self-sustained and (2) that the same species occurs in nearby benthic communities, albeit abundances on the seabed are about 5 orders of magnitude lower. The aggregations of juveniles concentrated inside depressions of the scallop textured shelf ice underside, with adults on ridges. This suggests the importance of hydrographic conditions across the scallop structure in association with melting ice surfaces. Microturbulences may bring plankton particles within reach of juveniles (<1 cm). Data from earlier expeditions show that Weddell seals feed in depths corresponding to the occurrence of the cryobenthic isopods (70 – 150 m), possibly feeding on the isopods themselves or their associated fish fauna (Plötz et al. 2001).

Although the underside of the ice shelves is considered to be a cold-spot in species richness and abundance and, thus, traditionally not considered as a habitat (Gutt & Dieckmann 2020), the question whether the occurrence of cryo-benthos is representative for the far-ranging high Antarctic ice shelves or limited to certain spots is open, and factors contributing to its existence and its stability over time are unexplored. In particular questions towards species composition, horizontal extent and nutrient supply of the fauna inhabiting the underside of the ice shelf are still open and call for additional investigations to further our understanding of bentho-pelagic coupling processes. In view of the vast but almost entirely unsampled habitat of >1.5 million square km in the entire Southern Ocean, knowledge on the magnitude of the carbon stored in cryo-benthos is a significant gap in our knowledge of the Southern Ocean food web. We therefore initiated SEAEIS at Atka Bay as synoptic study to investigate the underside of the floating ice shelf tongue of the Ekström Ice Shelf with instrumented “camera-seals” and an ROV to be deployed from the fast ice within the bay.

During the first SEAEIS campaign at Atka Bay we found cryo-benthic filter feeding *Antarcturus* cf. *spinacoronatus* occurring as singletons or pairs, as well as other evertebrates (*Amphipoda*, *Pteropoda*, *Polychaeta*, *Aega antarctica*, nemertid worms), and fishes (*Pagothenia borchgrevinki*) at the shelf ice either grounded or floating. Here, Weddell seals dived in corresponding depths either around 50 m or at the seafloor ranging from 70 – 200 m, likely as a result of concentration of prey in these depths. However, we could not detect any shelf ice associated foraging activity of the seals on the footage.

SEAEIS II focuses to enlarge the data set generated by the preceding SEAEIS campaign, i.e. extend the cryobenthic species inventory as well as the ROV- and seal-borne video footage at different locations within the Atka Bay. A detailed description of the bay’s physical (bathymetry, hydrography) and biological environment (benthos, abundant fish and evertebrate fauna, emperor penguins and seabirds as well as seals and whales) can be found in Bornemann et al. (2024).

Fieldwork

Summary and itinerary

The SEAEIS team travelled from Bremen (1 November 2024) via Oslo, Prague, Abuja and Cape Town (2 November – 7 November 2024) with NPI-F1 (Boeing 737 8 MAX) operated by Czech Air Smartwings to the Norwegian research station *Troll* (7 November – 8 November 2024) and arrived at *Neumayer Station III* with a subsequent feeder flight (DC-3 Basler) operated by White Desert on 08.11.2024. The field work was conducted pursuant to the AWI-UBA protocol to mitigate the Highly Pathogenic Avian Influenza (HPAI) (see Annex, green section).

The good weather conditions made it possible to carry out a reconnaissance visit on the sea ice of the Atka Bay immediately after arrival. In the course of several reconnaissance trips by Skidoo and Nansen sledge along the tidal cracks of the sea ice and in the vicinity of grounded icebergs, about 80 adult Weddell seals were counted within the ice-covered Atka Bay in early November. These were mainly female seals with their pups, which were set before the arrival of the SEAEIS team. The animals initially aggregated in groups of up to 15 mother-pup pairs along cracks in the fast ice, some of which separated by more than 10 km to each other. After weaning, the group size of these aggregations increased slightly towards the end of December when the disintegration of the fast ice began along the outer fringes of the bay ice contour. Seal species other than Weddell seals were not encountered on the fast ice. A comprehensive bay-wide count taken by the AFIN team in 2023 arrived at ca 130 adult Weddell seals and 40 pups (M. Neudert & J. Asseng pers. com.), whereas our opportunistic counts in 2024/2025 only matched with about half of the population, likely as a result of different sea ice conditions and resulting distributions of seals around stranded icebergs, of which only a fraction could be visited (Fig. 4.20.1a).

The field work was conducted pursuant to the AWI-UBA protocol to mitigate the Highly Pathogenic Avian Influenza (HPAI) *cf*. Guidelines with respect to Highly Pathogenic Avian Influenza (HPAI) in Antarctica and the Southern Ocean (AWI-UBA 2024). Work on the sea ice continued until 3 January 2025; afterwards access to the sea ice was restricted for safety reasons in view of the anticipated ice break-up. The SEAEIS team then dealt with data inventory and processing and cargo arrangements. The team departed from *Neumayer Station III* in different ways, i.e. via NPI-F3 (H. Schröder) on 17 December, WD13 (C. Held) on 11 January 2025, both via feeder-flights with a DC-3 Basler operated by White Desert to the Norwegian *Troll* Station (H. Schröder) and *Wolf's Fang* (C. Held), from where the return flights to Cape Town were made with NPI-F3 (Boeing 737 8 Max) operated by Smartwings on 13 December 2024 and WD13 (Airbus A340-300) operated by White Desert on 16 January 2025. H. Bornemann left via *Polarstern* expedition PS146 on 11 January 2025.

Skidoo operation

The SEAEIS team visited the seals on the sea ice and the ROV deployment sites with three skidoos, to each of which one sledge with expedition equipment including emergency equipment were attached. Over the entire project period, the SEAEIS team spent a total of 300 hours on the ice during 44 working days and made about 2,500 km by Skidoo. As a rule, the trips started during the morning hours (UTC) and lasted until the late afternoon/early evening hours in order to ensure the probability of encounter according to the seals' diurnal rhythm when searching the sea ice. Table 4.20.1 shows the quantity structure of the travel distances and the duration of the work assignments on the ice; Figure 4.20.1b shows the corresponding routes travelled to the work sites (denoted with trivial designations) within Atka Bay.

Tab. 4.20.1: Data on the total skidoo deployments and distances covered during the Seals and cryobenthic communities at the Ekström Ice Shelf II (SEAEIS II) project of the ANT-Land 2024/25 expedition at *Neumayer Station III* from 8 November 2024 – 11 January 2025. The place names given are trivial designations that only serve to facilitate the orientation of the expedition participants.

Action	**Date**	**Time (Start)**	**Time (End)**	**Latitude**	**Longitude**	**Distance**	**Purpose** Destination
[No]	*[yyyy-mm-dd]*	*[hh:mm]*	*[hh:mm]*	*[deg]*	*[deg]*	*[km]*	*[trivial #]*
01	2024-11-09	11:30	19:00	-70.60468	-7.96918	49	**REC** U-Turn Eisberg
02	2024-11-10	10:00	17:00	-70.60468	-7.96918	39	**REC** U-Turn Eisberg
03	2024-11-11	10:30	17:30	-70.60468	-7.96918	39	**REC** U-Turn Eisberg
04	2024-11-12	12:30	19:00	-70.60468	-7.96918	39	**ROV** U-Turn Eisberg
05	2024-11-13	13:30	21:00	-70.60468	-7.96918	39	**ROV** U-Turn Eisberg
06	2024-11-15	10:30	20:30	-70.57112	-7.45690	86	**REC** Fischmaul Inlet
07	2024-11-16	11:30		-70.57112	-7.45690		**ROV** Fischmaul Inlet
			19:15	-70.56585	-7.70237	85	**REC** Sealers Cave
08	2024-11-17	10:30	15:15	-70.61169	-7.90389	35	**SEA** U-Turn Eisberg
09	2024-11-18	11:30	19:15	-70.60468	-7.96918	39	**ROV** U-Turn Eisberg
10	2024-11-19	10:15	19:30	-70.57112	-7.45690	85	**REC** Fischmaul Inlet
11	2024-11-20	10:15		-70.61169	-7.90389		**SEA** U-Turn Eisberg
			19:30	-70.57112	-7.45690	85	**ROV** Fischmaul Inlet
12	2024-11-21	10:00	20:00	-70.57112	-7.45690	85	**ROV** Fischmaul Inlet
13	2024-11-22	11:30	18:00	-70.57170	-7.46275	85	**SEA** Fischmaul Inlet
14	2024-11-23	09:00	16:00	-70.53106	-8.20058	60	**REC** Bloody Harry's Hole
15	2024-11-28	10:00		-70.61169	-7.90389		**REC** U-Turn Eisberg
			14:30	-70.53106	-8.20058	47	Bloody Harry's Hole
16	2024-11-29	11:15	14:00	-70.61169	-7.90389	35	**REC** U-Turn Icebergs
17	2024-11-30	10:30		-70.61178	-7.90391		**SEA** Fischmaul Inlet
				-70.62735	7.49177		**REC** Christina Crack

Action	Date	Time (Start)	Time (End)	Latitude	Longitude	Distance	Purpose Destination
[No]	*[yyyy-mm-dd]*	*[hh:mm]*	*[hh:mm]*	*[deg]*	*[deg]*	*[km]*	*[trivial #]*
			19:15	-70.61169	-7.90389	95	**REC** U-Turn Eisberg
18	2024-12-01	11:15	14:45	-70.53106	-8.20058	38	**ROV** Bloody Harry's Hole
19	2024-12-01	15:15	18:30	-70.61169	-7.90389	85	**REC** U-Turn Eisberg via Rums Geb.
20	2024-12-02	09:30	18:15	-70.53106	-8.20058	38	**ROV** Bloody Harry's Hole
21	2024-12-03	11:30		-70.55665	-8.07250	16	**SEA** Jenny's Pool
			17:45	-70.53106	-8.20058	28	**SEA** Bloody Harry's Hole
22	2024-12-04	10:45	17:30	-70.60468	-7.96981	39	**ROV** U-Turn Eisberg
23	2024-12-05	10:30		-70.55665	-8.07250		**ROV** Jenny's Pool
			19:30	-70.53106	-8.20058	44	**ROV** Bloody Harry's Hole
24	2024-12-09	10:30	17:30	-70.53106	-8.20058	38	**ROV** Bloody Harry's Hole
25	2024-12-10	10:45	18:00	-70.60468	-7.96981	39	**ROV** U-Turn Eisberg
26	2024-12-11	10:15	21:30	-70.61178	-7.90391	79	**ROV** Fischmaul Inlet
27	2024-12-12	14:15	21:30	-70.60468	-7.96981	39	**ROV** U-Turn Eisberg
28	2024-12-17	09:30	11:30	-70.53106	-8.20058	38	**REC** Bloody Harry's Hole
29	2024-12-18	08:30		-70.53106	-8.20058	19	**REC** Bloody Harry's Hole
			17:30	-70.61178	-7.90391	155	**SEA** Fischmaul Inlet
30	2024-12-19	08:15	14:00	-70.53106	-8.20058	38	**SEA** Bloody Harry's Hole
31	2024-12-20	09:30	11:30	-70.53106	-8.20058	38	**SEA FIS** Bloody Harry's Hole
32	2024-12-21	09:45	13:30	-70.53106	-8.20058	38	**SEA** Bloody Harry's Hole
33	2024-12-22	09:30		-70.53106	-8.20058		**SEA FIS** Bloody Harry's Hole
				-70.55665	-8.07250		**SCA** Rums Gebirge
			16:00	-70.61169	-7.90389	65	**REC** U-Turn Eisberg
34	2024-12-23	08:30	15:00	-70.61178	-7.90391	86	**SCA** Fischmaul Inlet

Action	Date	Time (Start)	Time (End)	Latitude	Longitude	Distance	Purpose Destination
[No]	*[yyyy-mm-dd]*	*[hh:mm]*	*[hh:mm]*	*[deg]*	*[deg]*	*[km]*	*[trivial #]*
35	2024-12-25	11:30		-70.53106	-8.20058		**FIS** Bloody Harry's Hole
				-70.55665	-8.07250		**REC** Rums Gebirge
			14:15	-71.00761	-8.12105	40	**SCA** Süd-Eisberge
36	2024-12-26	09:00		-70.53106	-8.20058		**FIS** Bloody Harry's Hole
			15:30	-70.55665	-8.07250	58	**REC** Rums Gebirge
37	2024-12-27	09:15		-70.53106	-8.20058		**REC** Bloody Harry's Hole
				-70.55665	-8.07250		**REC** Rums Gebirge
			16:00	-70.61169	-7.90389	65	**SCA** U-Turn Eisberg
38	2024-12-28	09:15		-70.61178	-7.90389		**SEA** U-Turn Eisberg
				-70.60969	-7.88989		**SCA** Dover Cliffs
				-70.55665	-8.07250		**REC** Rums Gebirge
			16:00	-70.53106	-8.20058	65	**REC** Bloody Harry's Hole
39	2024-12-29	09:00		-70.53106	-8.20058		**SCA REC** Bloody Harry's H.
			17:30	-70.53106	-8.20058	64	**SEA SCA FIS** Bloody Harry's H.
40	2024-12-30	9:00		-70.53106	-8.20058		**REC FIS** Bloody Harry's Hole
			16:30	-70.60733	-8.10831	91	**SCA** Aurelia Crack
41	2024-12-31	11:00		-70.53106	-8.20058		**REC** Bloody Harry's Hole
				-70.61169	-7.90389		**SEA** U-Turn Eisberg
				-70.55665	-8.07250		**REC** Rums Gebirge
			16:00	-70.53106	-8.20058	68	**REC** Bloody Harry's Hole
42	2025-01-01	11:00	18:00	-70.53106	-8.20058		**REC** Bloody Harry's Hole
				-70.53106	-8.20058		**REC** Bloody Harry's Hole
				-70.59394	-8.10756	80	**SCA** Eisberg Pingi Rampe
43	2025-01-02	09:30	11:30	-70.53106	-8.20058	38	**REC** Bloody Harry's Hole

Action	Date	Time (Start)	Time (End)	Latitude	Longitude	Distance	Purpose Destination
[No]	*[yyyy-mm-dd]*	*[hh:mm]*	*[hh:mm]*	*[deg]*	*[deg]*	*[km]*	*[trivial #]*
44	2025-01-03	09:30		-70.53106	-8.20058		**REC** Bloody Harry's Hole
			16:30	-70.53106	-8.20058	76	**REC** Bloody Harry's Hole

FIS = fish trap
REC = reconnaissance
ROV = ROV work
SCA = scat sampling
SEA = seal work

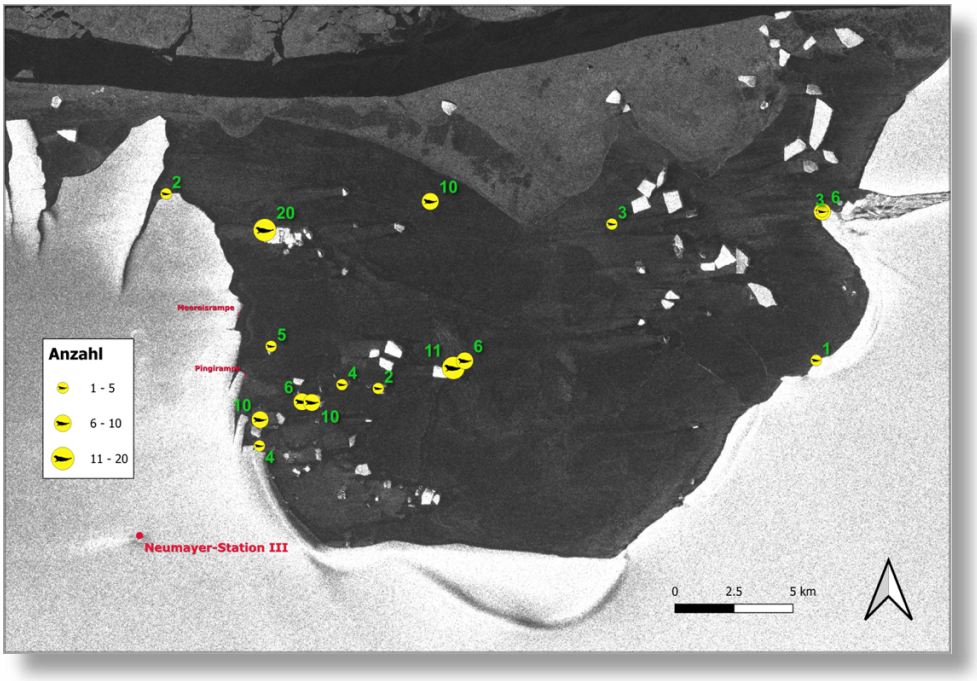

Fig. 4.20.1a: Map of Atka Bay with seal encounters from 10 – 30 November 2024 during the "Seals and cryobenthic communities at the Ekström Ice Shelf II" (SEAEIS II) project of the ANT-Land 2024/25 expedition campaign at Neumayer Station III from 8 November 2024 – 11 January 2025. Image: Sentinal1 (high res S1_EW_IW_combined, 2024-11-20; modified and GPS-Data implementation Jölund Asseng, AWI.

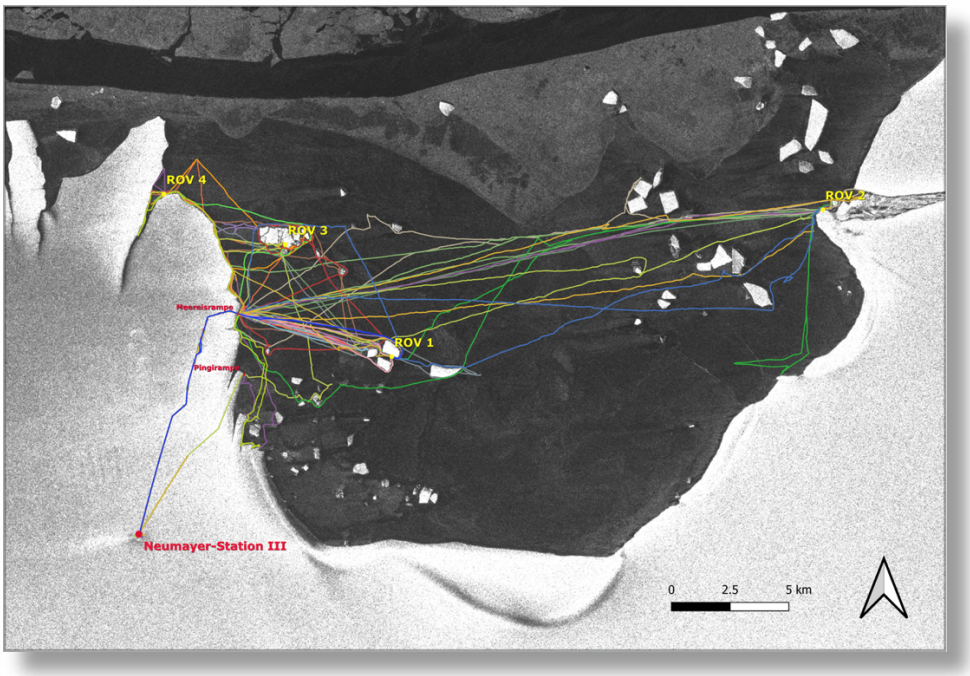

Fig. 4.20.1b: Map of Atka Bay and the locations visited during the "Seals and cryobenthic communities at the Ekström Ice Shelf II" (SEAEIS II) project of the ANT-Land 2024/25 expedition campaign at Neumayer Station III from 8 November 2024 – 11 January 2025. The place names given are trivial designations that only serve to facilitate orientation for the expedition participants. Image: Sentinal1 (high res S1_EW_IW_combined, 2024-11-20; modified and GPS-Data implementation Henning Schröder, AWI.

Work on Weddell seals

For the purpose of instrumentation with video-camera loggers, the seals needed to be anaesthetized following protocols as described in Bornemann et al. (1998) and Bornemann & Plötz (1993). Drugs were initially administered intramuscularly (i.m.) by remote injection using blowpipe darts. Follow-up doses were usually given by manual i.m. injection. The seals were immobilized using a ketamine/xylazine combination that was complemented by diazepam if necessary (see PANGAEA for the dose regime involved the aforementioned drugs). Depending on the course of the immobilisation, dosages were individually adjusted and complemented by the same drugs to maintain or extend the immobilisation period on demand. Atipamezol was used to reverse the xylazine component in the xylazine/ketamine immobilisation. The seals' standard length and girth were measured as immobilisation procedures allowed. All procedures were carried out pursuant to the SCAR Code of Conduct for Animal Experiments, and were approved by the German Federal Environmental Agency (Umweltbundesamt) and the Federal Agency for Nature Conservation (Bundesamt für Naturschutz) under the German acts implementing the Protocol of Environmental Protection to the Antarctic Treaty (Az II 2.3 –94033/257) and the Convention for the Conservation of Antarctic Seals (3.48.50 Bornemann).

During the ice work from 9 November 2024 – 3 January 2025, a total of 9 Weddell seals were immobilised (anaesthetised) in order to deploy infrared underwater video cameras (Little Leonardo, Japan; *cf*. Naito et al. 2013; Watanabe et al. 2006, 2003) in order to provide footage of their foraging behaviour and to investigate whether the seals' foraging excursions reach out

along and underneath shelf ice. Whisker and hair samples were taken for post hoc stable isotope analyses; 4 of the aforementioned seals were adult, non-lactating females and 5 were adult male seals (see Tab. 4.20.2). Figure 4.20.2 shows a Weddell seal male with camera logger.

Fig. 4.20.2: Weddell seal with infrared camera logger. Seals and cryobenthic communities at the Ekström Ice Shelf II (SEAEIS II) project of the ANT-Land 2024/25 expedition at Neumayer Station III from 8 November 2024 – 11 January 2025 (Photo: Horst Bornemann, AWI)

All immobilisations showed the broad spectrum of individual reactions to the applied dosages. Seal numbers 03, 04, 05 and 08 were anaesthetised repeatedly at intervals between 3 and 14 days post deployment; a total of 16 immobilisations were administered (see Tab. 4.20.2). In 3 cases, a sufficiently deep anaesthesia could not be induced. Here, the work was not pursued further and therefore no sampling or instrumentation was carried out. One seal died in narcosis as a result of irreversible apnoea and hyperthermia.

The immobilisations for deployments or retrievals lasted on average 1:03 hours (period between first injection to induce and last injection to reverse the immobilisation) including a standardised observation time of at least 20 minutes after the first injection until the anaesthesia took full effect and plus a standardised observation time of at least 20 minutes after the last injection until awakening from the anaesthesia. The total time including the follow-up observation time was 1:23 hours on average (Tab. 4.20.3).

Data could be recorded from four of the seals fitted with infrared underwater cameras after recovery of the devices. In two cases, the devices remained on the animal as the devices could not be recovered during the phase of incipient sea ice break-up. The gauze mat used to attach the camera loggers will fall off the animals' hair during the annual moult at around February,

limiting the period during which the gauze mats and cameras remain on the animals to a maximum of another 6 – 8 weeks after the end of the project.

Faecal samples from Weddell seals were collected to determine their prey spectrum post hoc using molecular biological analyses. Another analytical aspect is dedicated to the quantification of the iron content in seal faeces, the release of which in the sea has a fertilising effect on phytoplankton. As a limiting element, iron is essential for the photosynthesis of phytoplankton and thus also for CO_2 binding in the ocean. Marine phytoplankton in turn forms the basis of the food web, which is directly linked to the marine mammal and seabird populations via krill and fish. However, the magnitude and importance of animal iron sources for phytoplankton productivity are unclear and will be further analysed by Scarlett Trimborn (AWI) on the basis of the collected samples.

Information on the place and time of the work performed on the animals, the duration of anaesthesia, the total duration of the examination, size and sex of the animals as well as the equipment with infrared camera loggers are summarised in Tables 4.20.2, 4.20.3 and 4.20.4.

Tab. 4.20.2: Data on immobilisations of 9 adult Weddell seals (*Leptonychotes weddellii*) within the project Seals and cryobenthic communities at the Ekström Ice Shelf II (SEAEIS II) of the expedition ANT-Land 2024/25 at *Neumayer Station III* from 8 November 2024 – 11 January 2025.

Weddell seal			**DateTTime**	**Latitude**	**Longitude**	**Length**	**Girth**
[No]	*Sex*	*Treatment [No]*	*[yyyy-mm-ddThh:mm]*	*[deg]*	*[deg]*	*[mm]*	*[mm]*
01	F	1	2024-11-16T16:12	-70.61169	-7.90389	*	*
02	F	1	2024-11-16T17:15	-70.61169	-7.90389	*	*
03	F	1	2024-11-17T11:40	-70.61169	-7.90389	2280	1770
03	F	2	2024-11-20T11:02	-70.61169	-7.90389	n.t.	n.t.
04	M	1	2024-11-22T11:22	-70.57112	-7.45690	n.t.	n.t.
04	M	2	2024-11-30T13:30	-70.57112	-7.45690	n.t.	n.t.
03	F	3	2024-12-03T13:20	-70.55665	-8.07250	n.t.	n.t.
05	M	1	2024-12-03T15:00	-70.53106	-8.20058	2720	1910
04	M	3	2024-12-18T11:10	-70.57112	-7.45690	2720	1740
05	M	2	2024-12-19T09:10	-70.53106	-8.20058	n.t.	n.t.
06	F	1	2024-12-20T10:15	-70.53106	-8.20058	*	*
07	M	1	2024-12-21T10:30	-70.53106	-8.20058	2600	1930
05	M	3	2024-12-22T11:00	-70.53106	-8.20058	n.t.	n.t.
08	M	1	2024-12-28T10:15	-70.61169	-7.90389	2890	2010
09	M	1	2024-12-29T14:42	-70.53106	-8.20058	2750	1750
08	M	2	2024-12-31T13:05	-70.61169	-7.90389	n.t.	n.t.

F **=** female
M = male
n.t = not taken
* = no sufficient immobilization

Tab. 4.20.3: Data on immobilisation, sampling and instrumentation of 9 adult Weddell seals as part of the Seals and cryobenthic communities at the Ekström Ice Shelf II (SEAEIS II) project of the ANT-Land 2024/25 expedition at *Neumayer Station III* from 8 November 2024 – 11 January 2025.

Seal	**Immobilisation**		**Sampling**				**Device**
	Duration	*Full procedure*					
No	*[hh:mm]*	*[hh:mm]*	*Blood*	*Vibrissae*	*Hair*	*Faeces*	*[#]*
01	**	**					**
02	**	**					**
03	01:10	01:30		x	x		IR-CAM
03	00:50	01:10					IR-CAM
04	00:50	01:10					IR-CAM
04	**	**					--
03	00:45	01:05					*
05	01:10	01:30		x	x		IR-CAM
04	01:50	02:10		x	x		*
05	00:45	01:05					IR-CAM
06	01:00	01:20				x	**
07	01:25	01:45		x	x		IR-CAM
05	01:10	01:30					*
08	01:00	01:20		x	x		IR-CAM
09	01:08	01:28		x	x		IR-CAM
08	00:55	01:15					*
Average	**01:03**	**01:23**					

IR-CAM = Infrared-camera logger
* = depth of immobilisation insufficient
** = only retrieval of IR-CAM
*** = died in narcosis
-- = no retrieval possible

Tab. 4.20.4: Data on collections of faecal samples within the project Seals and cryobenthic communities at the Ekström Ice Shelf II (SEAEIS II) of the expedition ANT-Land 2024/25 at *Neumayer Station III* from 8 November 2024 – 11 January 2025.

Sample	**Seal**	**Date**	**Latitude**	**Longitude**	**Sample**
No	*Nr.*	*[yyyy-mm-dd]*	*[deg]*	*[Grad]*	*[#]*
01	06	2024-12-20	-70.53106	-8.20058	x
02	K1	2024-12-22	-70.55278	-8.03653	x[1,2]
03	K2	2024-12-22	-70.56128	-8.03316	x[1,2]
04	K3	2024-12-23	-70.55372	-7.99419	x[1,2]
05	K4	2024-12-23	-70.56717	-7.78597	x[1,2]
06	K5	2024-12-23	-70.55841	-7.67803	x[1,2]
07	K6	2024-12-23	-70.56792	-7.44436	x[1,2]
08	K7	2024-12-23	-70.59897	-8.10986	x[1]

Sample	Seal	Date	Latitude	Longitude	Sample
No	*Nr.*	*[yyyy-mm-dd]*	*[deg]*	*[Grad]*	*[#]*
09	K8	2024-12-23	-70.59897	-8.10986	x[1]
10	K9	2024-12-25	-70.61186	-8.04253	x[1,2]
11	K10	2024-12-25	-71.01186	-8.12106	x[1,2]
12	K11	2024-12-27	-71.93347	-8.12219	x[1,2]
13	K12	2024-12-27	-71.00511	-8.01222	x[1,2]
14	K13	2024-12-28	-70.61008	-7.97644	x[1]
15	K14	2024-12-28	-70.61000	-7.93911	x[1]
16	K15	2024-12-28	-70.61617	-7.83861	x[1]
17	K16	2024-12-28	-70.61200	-7.92761	x[1]
18	K17	2024-12-28	-70.59966	-7.98522	x[1]
19	K18	2024-12-29	-70.53106	-8.20058	x[1]
20	K19	2024-12-29	-70.53106	-8.20058	x[1]
21	K20	2024-12-30	-70.56036	-8.07913	x[1]
22	K21	2024-12-30	-70.60733	-8.10831	x[1]
23	K22	2024-12-31	-70.53106	-8.20058	x[1]
24	K23	2024-12-31	-70.61169	-7.90389	x[1]
25	K24	2025-01-01	-70.59394	-8.10756	x[1]

K = unknown seal

x1 = sample for genetic analysis

x2 = sample for iron analysis

Making of ice holes

In the course of the campaign, 4 deployment sites for the ROV were explored. In one case, the hole was made with a chain saw, in two cases by hand saws (“Fin saw”), and one open pool provided natural access. The ice holes were kept open and maintained as needed in the course of the ROV deployments (see Fig. 4.20.3). The highly compacted platelet ice floating in the ice holes was removed with buckets (“Schlagpütz”) and a scoop. Depending on the thickness of the ice and the thickness of the platelet-ice layer, it took three people about one to three days to create an ice hole on a crack in the immediate vicinity of the ice shelf edge. However, the success of the subsequent ROV deployment depends on the fact that underwater ice pressing with multi-layered uplift of floes has not occurred in the course of sea ice formation, that the further aggregation of platelet ice at the once opened ice hole is low or that larger accumulations can be bypassed with the ROV. These conditions can only be determined empirically. At a distance of about 50 – 100 m from the ice shelf edge, these would be much safer for deploying, manoeuvring and recovering the submersible as well as setting up the ROV control station and winch, and would be more promising in terms of the expected data yield. At this distance from the ice shelf edge, however, the consolidated sea ice is about 3 m thick. The underlying platelet ice aggregations accumulate to about 7 m, and in individual cases platelet ice thicknesses of up to 16 m have been observed in the eastern part of Atka Bay. Such ice thicknesses cannot be managed without special mechanical equipment with an adequate amount of work and time to deploy an ROV. The creation of ice holes at a greater distance from tidal cracks would also make it possible to use equipment that is lowered into the water column in the manner of a plumb bob (CTD, fish traps, fishing rods, hydrophones).

With a view to future operations and the support of the Neumayer technical team, the creation of a fifth ice hole was therefore trialled using the Neumayer's Yanmar mini excavator with a 90 cm auger drill and two drill extensions of meter each to test the mechanical creation of a hole in the sea ice. It turned out that one metre of snow cover and around 2.3 m of sea ice could be drilled through without any problems and the excavated material could be lifted out of the hole with the auger drill. As the amount of water in the excavation increased, the crushed ice and platelet ice was removed with the 70 cm excavator bucket, after which the water was completely cleared of ice with the Atlantica B platelet ice pump. Including the travelling time of the mini-excavator to the site, it took two and a half hours to create the ice hole until the ROV was ready for use. Based on our experience of creating the ice hole at the U-Turn iceberg (western Atka Bay), we estimate the time required to use a chainsaw and manually remove the ice under otherwise similar conditions to be at least seven days with three people. For future operations, it is being considered to keep the Argo vehicle currently parked in the port warehouse with its pontoon skid for transporting the mini excavator on the sea ice at *Neumayer Station III*.

Particularly against the background of future systematic, comparative sampling along different depth horizons of the ice shelf of Atka Bay and neighbouring inlets, the availability of the aforementioned mechanical equipment at *Neumayer Station III* would be desirable in order to be able to collect and analyse data and samples on a sufficient scale. This is the only way to determine with the necessary statistical precision which species occur under the ice shelf and what their spatial distribution looks like (patchiness, abundance, estimated total biomass, etc.). Both are indispensable for modelling the carbon cycle in order to be able to meaningfully determine the magnitude of the cryobenthos in the carbon and energy flux. The collection of invertebrate samples and fish for a genetic investigation of the cryobenthic species inventory is essential to investigate species identity, phylogenetic position and population genetic links in comparison with conspecifics from the adjacent benthos. For future time series and potential deployments of underwater robotics and landers, it would be indispensable to have the appropriate equipment for an efficient creation of ice holes available on site. Figure 4.20.3 illustrates work and gear to create an ice hole. The future assistance of drilling hardware would permit establishing holes a bit farther away from tidal cracks and thus grounded icebergs or shelf ice cliffs, thereby improving the work safety and permitting systematic surveys independent of the existence of conveniently located and sized tidal cracks.

ROV setup

Two BlueROV (bluerobotics, US) were assembled and customized by Geo-Engenieering.org, Bremen and IGP Meerestechnik, Hamburg, Germany, used in varying technical configurations (Tab. 4.20.5); one of the ROVs was originally considered redundant as back up in case of critical damages.

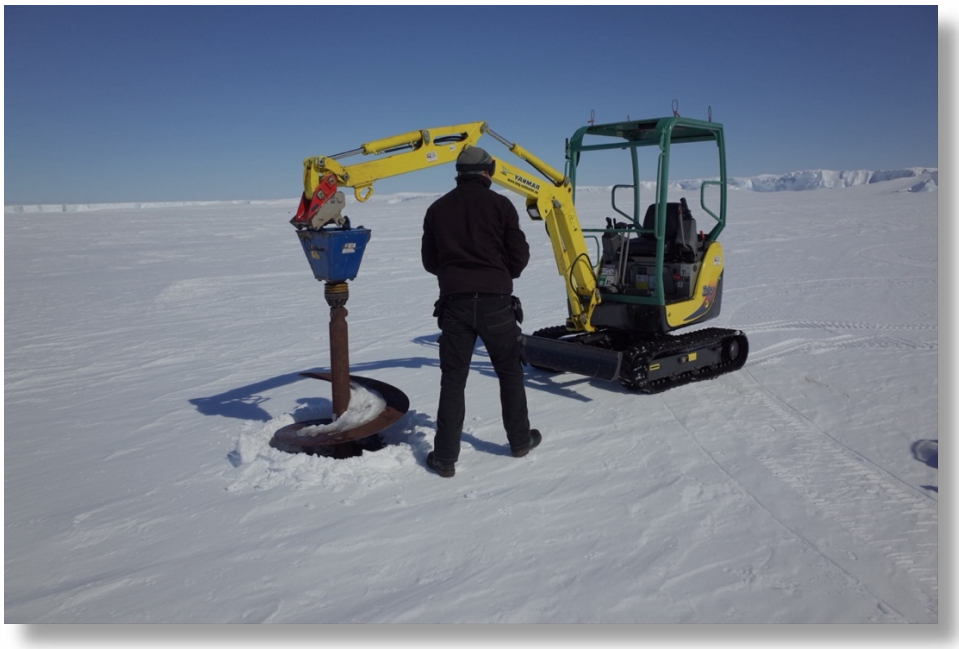

Fig. 4.20.3: Set-up of the working site to create an ice hole by means of an excavator (Photo: Horst Bornemann, AWI) within the Seals and cryobenthic communities at the Ekström Ice Shelf II (SEAEIS II) project of the ANT-Land 2024/25 expedition at Neumayer Station III from 8 November 2024 – 11 January 2025. See Bornemann et al. (2024) for an image of a manually made ice hole.

The ROV setup consists of two racks of which the technical equipment combined different constellations as outlined in Table 4.20.5, the Full HD ROV video camera (1920x1080) in the front transmitted the signal to the control laptop on the surface via the tether and was recorded there and one GoPro Hero 8 camera (4K), which did not and recorded locally on a micro-SD card. The cameras were complemented by two parallel green laser points providing reference scales of 50 cm on the videos. Illumination is ensured by four white LED lights (each 1500 lumen, color temperature 5700 Kelvin) in the front. A sampling box, a so-called slurp gun was attached to the underside and front side of the ROV respectively to obtain invertebrate specimens for *post hoc* morphological and genetic investigations. Water samples for environmental DNA were taken by means of a pump, activated by a manipulator, and samples stored into a Niskin bottle. Setting out and retrieval of the ROV was achieved manually, and spooling of the 450 (4 x twisted pair) and 600 m (1 x twisted pair) alternating ROV cables was done by a hand winch, which was placed on a sledge or the back of a skidoo next to the ice hole. Only very few of the dives of the ROV turned out to be close or even beyond its operational technical specifications, and hence required intensive technical support and maintenance before and after each dive. As a result, these dives needed to be aborted prematurely due to various technical malfunctions. The successful dive operations under the ice shelf provided high resolution footage and samples of the under-shelf ice community at depths between 0 and 230 m. Table 4.20.5 provides all data on the deployments of ROV and its customized technical specifications.

Sonars were not used for navigation, since the ROV could be driven under visual control between the deployment sites at the tide gaps to and along the contours of the ice walls due to the good visibility conditions (visibility under water 40 m and more). Figures 4.20.4 illustrates the ROV at one of the ice holes and the cockpit setup to manoeuvre the ROV remotely.

Fig. 4.20.4: ROV setup with sledge-mounted cockpit (top) and cabled ROV (bottom) for the Seals and cryobenthic communities at the Ekström Ice Shelf II (SEAEIS II) project of the ANT-Land 2024/2025 expedition at Neumayer Station III (Photo: Horst Bornemann, AWI).

Tab. 4.20.5 (see end of chapter): Technical configurations of the ROV within the Seals and cryobenthic communities at the Ekström Ice Shelf II (SEAEIS II) project of the ANT-Land 2024/25 expedition at *Neumayer Station III* from 8 November 2024 – 11 January 2025. Deployments were counted separately if ROV configuration, deployment location or date changed.

ROV operation and cryobenthic work implementation

The SEAEIS team conducted ROV operations on a regular basis at 3 deployment sites on the and eastern and western shelf ice contour of Atka Bay and on grounded icebergs to secure extensive video and sample material (see Fig. 4.20.1b for locations). A fourth location was only visited once. Weddell seals were instrumented with camera loggers at each location. Vibrissae, hair and faecal samples were collected in order to map the diving behaviour and diet of the animals in the context of the topography and fauna documented with the ROV. At the western ROV location, fish traps were laid out.

Deployment of fish traps

At the western deployment site of the ROV, a fish trap was deployed several times at the level of a platelet ice aggregation on the vertical ice shelf flank (approx. 40 m) at a distance of approx. 10 m. The traps stayed for up to 4 consecutive days, and were successfully recovered but did not provide catches, likely due to a distance too far from the platelet ice layer.

Preliminary (expected) results

Work on Weddell seals

In total, six seals were fitted either once or multiple times with a total of 12 camera loggers, of which 9 camera loggers could be retrieved. The camera loggers yielded a total of 140 gigabytes of infrared video recordings, 6 megabytes of dive depth data and 660 megabytes of acceleration data records. In addition to the imaging information, the infrared camera logger data obtained includes data on the animals' diving depth, acceleration measurements during swimming and feeding, and water temperature, and helps to supplement and update previous assumptions about the animals' underwater foraging. The data sets are subject to visual analyses in Bremerhaven. For the analysis a computer program was written to evaluate the video data sets from both seals and ROV, which makes it possible to visualise video recordings in connection with recorded measurement values and to comment on or index them in the sense of a finding aid. In this way, the recorded videos can be analysed with the best possible level of detail. Table 4.20.6 provides the entire information for all camera deployments and retrievals. In addition, two vibrissae as well as hair were collected from each of the seals that got a successful immobilisation (Tab. 4.20.3, 4.20.4). Hair and vibrissae will be used for analyses of stable isotopes. From hair and whiskers, indications of short to medium-term, cumulative, retrospective prey spectra can be obtained by (component-specific) isotope analysis (*cf*. Brault et al. 2019; Goetz et al. 2017; Beltran et al. 2015; Lewis et al. 2006). All samples were stored at -20°C, and will be returned with *Polarstern* expeditions PS146 and PS147 to the AWI in Bremerhaven for analyses.

The entire field work was conducted pursuant to the AWI-UBA protocol to mitigate the Highly Pathogenic Avian Influenza (HPAI). From all seals which got camera deployments nasal swabs were taken and underwent PCR tests at *Neumayer Station III*. None of which detected HPAI. All faecal samples taken for iron analysis were tested as well, and none was positive. All faecal samples for molecular analyses were stored in DNA/RNA shield faecal collection tubes. These tubes are designed for the collection and preservation of nucleic acids from stool specimens and take a microbial snapshot of a sample while inactivating viruses, and hence making the samples safe for transport.

Tab. 4.20.6: Deployment and retrieval information for all seal camera loggers used on Weddell seals (Leptonychotes weddellii) within the Seals and cryobenthic communities at the Ekström Ice Shelf II (SEAEIS II) project of the ANT-Land 2024/25 expedition at *Neumayer Station III* from 8 November 2024 – 11 January 2025.

Event	DateTTime deployment	Latitude	Longitude	Location	Procedure	DVL	Date Start	Time Start	Loggertimer	Depth trigger
[#]	*[yyyy-mm-ddThh:mm]*	*[Deg]*	*[Deg]*	*[#]*	*[n]*	*[ID]*	*[yyyy-mm-dd]*	*[hh:mm]*	*[h]*	*[m]*
NEU2024_wed_a_f_03	2024-11-17T11:50	-70.61169	-7.90389	U-Turn seal group	1	23036	2024-11-17	08:15	36	20
						23037	2024-11-17	08:25	72	20
NEU2024_wed_a_m_04	2024-11-22T12:45	-70.57112	-7.45690	Fischmaul Inlet	1	20018	2024-11-22	09:05	36	20
NEU2024_wed_a_f_03	2024-11-20T10:40	-70.61169	-7.90389	U-Turn seal group	2	20040	2024-11-20	07:55	36	20
						23038	2024-11-20	08:05	72	20
NEU2024_wed_a_m_05	2024-12-03T15:00	-70.53106	-8.20058	Bloody Harry's Hole	1	22026	2024-12-03	11:05	36	20
NEU2004_wed_a_m_05	2024-12-19T09:10	-70.53106	-8.20058	Bloody Harry'y Hole	2	23036	2024-12-21	06:45	36	20
NEU2004_wed_a_m_07	2024-12-21T10:30	-70.53106	-8.20058	Bloody Harry'y Hole	1	23037	2024-12-21	05:55	36	20
						23038	2024-12-21	06:05	72	20
NEU2004_wed_a_m_08	2024-12-28T10:15	-70.61169	-7.90389	U-Turn seal group	1	23036	2024-12-28	06:15	36	20
						24040	2024-12-28	06:25	72	20
NEU2004_wed_a_m_09	2024-12-29T14:42	-70.53106	-8.20058	Bloody Harry'y Hole	1	20018	2024-12-29	06:20	36	20

Event	DateTTime retrieval	Latitude	Longitude	Location	Deployment	DVL	Video	Depth	Acceleration	Comment
[#]	*[yyyy-mm-ddThh:mm]*	*[Deg]*	*[Deg]*	*[#]*	*[#]*	*[ID]*	*[GB]*	*[MB]*	*[MB]*	*[#]*
NEU2024_wed_a_f_03	2024-11-20T10:40:00	-70.61169	-7.90389	U-Turn seal group	Head; left	23036	18.30	0.73	83.30	
					Head; right	23037	22.20	0.72	83.80	data invalid
NEU2024_wed_a_m_04	2024-12-18T11:10:00	-70.57112	-7.45690	Fischmaul Inlet	Head; middle	20018	11.32	0.72	84.20	
										no deployment
NEU2024_wed_a_f_03	2024-12-03T13:20:00	-70.55665	-8.07250	Rums Gebirge	Head; left	20040	16.20	0.73	82.48	
					Head; right	23038	14.80	0.73	79.95	data invalid
NEU2024_wed_a_m_05	2024-12-19T09:10:00	-70.53106	-8.20058	Bloody Harry's Hole	Head; left	22026				data retrieval pending
NEU2004_wed_a_m_05	2024-12-22T11:00:00	-70.53106	-8.20058	Bloody Harry's Hole	Head; left	23036	15.20	0.74	83.60	
NEU2004_wed_a_m_07					Head; left	23037				no retrieval
					Head; right	23038				no retrieval
NEU2004_wed_a_m_08	2024-12-31T13:05:00	-70.61169	-7.90389	U-Turn seal group	Head; left	23036	20.10	0.73	81.64	
					Head; right	24040	17.90	0.73	81.38	
NEU2004_wed_a_m_09					Head; middle	20018				no retrieval
										no 2nd deployment

data valid
data or unit lost
data invalid

ROV operation and cryobenthic work implementation

During 15 ROV missions, 50 dives of about 1 – 1.5 hours each were conducted at depths between 10 and 230 metres along the flanks of the ice shelf or grounded and decaying iceberg (Tab. 4.20.5 & 4.20.7). A total of 550 Gigabyte of video footage was recorded. To evaluate the video data sets from the ROV and seals, a Python script was written at Neumayer that makes it possible to visualise video recordings in connection with recorded measurement values and thus facilitate and improve their evaluability. In this way, the recorded videos can be analysed with the best possible level of detail. The occurrence of ice fish, ctenophores, amphipods, isopods, pelagic bryozoans, and the benthos, which was partly disturbed by the influence of icebergs at the iceberg ROV-sites or undisturbed at the shelf ice ROV-sites were documented (Tab. 4.20.5 & Tab. 4.20.7). In addition, depths as to which platelet layers of ice and meteoric ice as a result of platelet ice aggregation beneath shelf ice reached, the surface structure of the ice and the benthos on the seafloor were documented.

The comprehensive inventory of samples (dead or alive, Tab. 4.20.5 & 4.20.7) yielded three samples with icefishes (*Pagothenia borchgrevinki* and a yet undetermined species), two samples with Isopods of the genus *Antarcturus*, two samples with pelagic bryozoans (Bryozoa), and one sample each containing krill (*Euphausea sp.*), several species of amphipods (Amphipoda), one polychaete worm (Polychaeta, Terebellida), one nematode

worm (Nematoda), as well as one crinoid (Crinoidea), and 32 water samples for environmental DNA (eDNA) analyses.

ROV dives reaching the seabed showed a rather undisturbed benthos rich in species as expected for the region, with dense occurrences of bryozoans (Bryozoa), sea cucumbers (Holothuroidea), glass sponges (Hexactinellida), and fish.

Documentation of ROV-borne samples

In addition to the video footage taken during the ROV dives, all specimen sampled by ROV (see below) were photographed and preserved in ethanol or frozen for later molecular biological and further taxonomic analyses at the AWI in Bremerhaven. Figure 4.20.5 exemplifies a selection of taxa from Atka Bay. All images were taken with an Olympus OM1 digital camera equipped with a 60mm f2.8 macro lens using one or two Olympus FL300 flash units for illumination, occasionally also an LED constant light source (BigBlue VTL800P) was used for this purpose. Various samplings yielded live catches of isopods (*Antarcturus* spp.), amphipods of various species and icefish (*Pagothenia borchgrevinki*),

Fig. 4.20.5: Selected representatives of ice-associated fauna collected with the ROV in Atka Bay within the Seals and cryobenthic communities at the Ekström Ice Shelf II (SEAEIS II) project of the ANT-Land 2024/25 expedition at Neumayer Station III from 8 November 2024 – 11 January 2025. (Photo: Horst Bornemann, AWI)

Tab. 4.20.7: ROV deployments and sampling of species within the Seals and cryobenthic communities at the Ekström Ice Shelf II (SEAEIS II) project during the ANT-Land 2024/25 expedition at *Neumayer Station III* from 8 November 2024 – 11 January 2025. Deployments were counted separately when the ROV configuration, deployment location or date changed.

ROV	Date	Time *Start*	Time *End*	Latitude	Longitude	Dives	Samples	
No	*yyyy-mm-dd*	*hh:mm*	*hh:mm*	*[Deg]*	*[Deg]*	*[n]*	*Species*	*No [n]*
01	2024-11-12	14:50	16:25	-70.60468	-7.96918	2		
02	2024-11-13	14:30	18:45	-70.60468	-7.96918	3	I	<15
03	2024-11-16	13:30	15:50	-70.60468	-7.96918	3		
04	2024-11-18	13:20	17:10	-70.60468	-7.96918	2		
05	2024-11-20	14:50	16:20	-70.57112	-7.45690	1		
06	2024-11-21	13:05	17:00	-70.57112	-7.45690	2	I	<10
07	2024-12-01	11:00	11:30	-70.53106	-8.20058	1		
08	2024-12-02	11:42	12:39	-70.53106	-8.20058	4	I, W	>10, 4
09	2024-12-04	11:15	15:55	-70.60468	-7.96918	2	W	1
10	2024-12-05	10:30	14:30	-70.55665	-8.07250	1	Nd	1
11	2024-12-05	15:00	18:30	-70.53106	-8.20058	3		
12	2024-12-09	11:55	16:05	-70.53106	-8.20058	9	F, W	1, 9
13	2024-12-10	11:55	16:28	-70.60468	-7.96918	10	W	8
14	2024-12-11	13:40	18:25	-70.57112	-7.45690	5	A, B, C, K, P, W	5, 1, 1, 2, 5, 5
15	2024-12-12	16:10	19:14	-70.60468	-7.96918	4	F, W	2, 4

A = Amphipod
B = Bryozoa
C = Crinoid
F = Fish
I = Isopod
K = Krill
M = Mollusc
Nd = Nematode worm
P = Polychaet worm
W = Environmental DNA (eDNA)

Data management

Environmental data will be archived, published and disseminated according to international standards by the World Data Center PANGAEA Data Publisher for Earth & Environmental Science (https://www.pangaea.de) within two years after the end of the expedition at the latest, and will be attributed to a consistent project label denoted as “Marine Mammal Tracking” (MMT). By default, the CC-BY license will be applied.

Species barcodes derived from genetic analyses will be deposited in the barcode of life database (www.barcodeoflife.org) and BOLD database and linked to from the SEAEIS II project page in PANGAEA.

Any other data will be submitted to an appropriate long-term archive that provides unique and stable identifiers for the datasets and allows open online access to the data.

This expedition was supported by the Helmholtz Research Programme “Changing Earth – Sustaining our Future” Topic 6, Subtopic 1.

In all publications based on this expedition, the **Grant No. AWI_ANT_25** will be quoted and the following publication will be cited:

Alfred-Wegener-Institut Helmholtz-Zentrum für Polar- und Meeresforschung. (2016a). *Neumayer III and Kohnen Station* in Antarctica operated by the Alfred Wegener Institute. Journal of large-scale research facilities, 2, A85. http://dx.doi.org/10.17815/jlsrf-2-152.

References

Alfred-Wegener-Institut Helmholtz-Zentrum für Polar- und Meeresforschung (2016a) Neumayer III and Kohnen Station in Antarctica operated by the Alfred Wegener Institute. Journal of large-scale research facilities 2:A85. http://dx.doi.org/10.17815/jlsrf-2–152

Alfred-Wegener-Institut Helmholtz-Zentrum für Polar- und Meeresforschung & Umwelt Bundesamt (2024) Guidelines with respect to Highly Pathogenic Avian Influenza (HPAI) in Antarctica and the Southern Ocean (Aug. 2024), 21 pp.

Beltran RS, Conolly Sadou MC, Condit R, Peterson SH, Reichmuth C & Costa DP (2015) Fine-scale whisker growth measurements can reveal temporal foraging patterns from stable isotope signatures. Marine Ecology Progress Series 523:243–253.

Bornemann H, Schröder H & Held C (2024) Seals and cryo-benthic communities at the Ekström Ice Shelf (SEAEIS). Pp 141 – 164 in: Regnery J, Matz T, Köhler P & Wesche C. Expeditions to Antarctica: ANT-Land 2022/23 NEUMAYER STATION III, Kohnen Station and Field Campaigns. Berichte zur Polar- und Meeresforschung = Reports on polar and marine research, Bremerhaven, Alfred-Wegener-Institut Helmholtz-Zentrum für Polar- und Meeresforschung 784, 217 pp.

Bornemann H, Held C, Nachtsheim D, Owsianowski N, Richter C & Steinmetz R (2016) Seal research at the Drescher Inlet (SEADI). Pp 116 – 129 in: Schröder M (ed) The Expedition PS96 of the Research Vessel POLARSTERN to the southern Weddell Sea in 2015/2016, Berichte zur Polar- und Meeresforschung = Reports on polar and marine research, Bremerhaven, Alfred Wegener Institute for Polar and Marine Research 700, 142 pp.

Bornemann H & Plötz J (1993) A field method for immobilizing Weddell seals. Wildlife Society Bulletin 21:437–441.

Bornemann H, Mohr E, Plötz J & Krause G (1998) The tide as zeitgeber for Weddell seals, Polar Biology 20:396–403.

Bornemann H, Hindell MA, Steinhage D & Wesche C (2019) SEAEIS seal census survey at Atka Bay during campaign NEU2018. Alfred Wegener Institute, Helmholtz Centre for Polar and Marine Research, Bremerhaven, PANGAEA, https://doi.org/10.1594/PANGAEA.904314

Bornemann H, Schröder H & Held C (2023) Immobilisation dose rates for Weddell seals during expedition NEU2022. PANGAEA, https://doi.org/10.1594/PANGAEA.955098

Brault EK, Koch PL, Costa DP, McCarthy MD, Hückstädt LA, Goetz KT, McMahon KW, Goebel ME, Karlsson O, Teilmann J, Harkonen T & Harding KC (2019) Trophic position and foraging ecology of Ross, Weddell, and crabeater seals revealed by compound-specific isotope analysis. Marine Ecology Progress Series 611:1–18.

Daly M, Rack F & Zook R (2013) *Edwardsiella andrillae*, a new species of sea anemone from Antarctic Ice. PLoS ONE 8(12):e83476. https://doi.org/10.1371/journal.pone.0083476

Liebsch N, Wilson RP, Bornemann H, Adelung D & Plötz J (2007) Mouthing off about fish capture: jaw movements in pinnipeds reveal the real secrets of ingestion. Deep Sea Research II 54:256–269.

Flores H, van de Putte A, Kühn S, Held C, Bach M, Barnes D, van Dorssen M, Fey B, Meijboom A, Vortkamp M, Schaafsma F & Stefels J (2023) EWOS II. Pp 151 – 195 in: Hoppema M (ed) The Expedition PS129 of the Research Vessel POLARSTERN to the Weddell Sea in 2022, Berichte zur Polar- und Meeresforschung = Reports on polar and marine research, Bremerhaven, Alfred Wegener Institute for Polar and Marine Research 218, 142 pp.

Goetz K, Burns JM, Hückstädt LA, Shero MR & Costa DP (2017) Temporal variation in isotopic composition and diet of Weddell seals in the western Ross Sea. Deep-Sea Research II 140:36–44.

Gutt J & Dieckmann G (2021) The Southern Ocean: an extreme environment or just home of unique ecosystems? Pp 218–233 in: di Prisco G, Edwards H, Elster J & Huiskes A (eds) Life in extreme environments – Insights in biological capability, Ecological Reviews, Cambridge, Cambridge University Press, 394 pp. https://doi.org/10.1017/9781108683319

Hückstädt LA, Burns JM, Koch PL, McDonald BI, Crocker DE & Costa DP (2012) Diet of a specialist in a changing environment: the crabeater seal along the Western Antarctic Peninsula. Marine Ecology Progress Series 455:287–301.

McIntyre T, Stansfield LS, Bornemann H, Plötz J & Bester MN (2013) Hydrographic influences on the summer dive behaviour of Weddell seals (*Leptonychotes weddellii*) in Atka Bay, Antarctica, Polar Biology 36:1693–1700. https://www.doi.org/10.1007/s00300-013-1384-7

Naito Y, Costa DP, Adachi T, Robinson PW, Fowler M, & Takahashi A (2013) Unravelling the mysteries of a mesopelagic diet: a large apex predator specializes on small prey. Polar Science 4(2):309–316. https:/doi.org/10.1111/1365-2435.12083

Naito Y, Bornemann H, Takahashi A, McIntyre T & Plötz J (2010) Fine scale feeding behaviour of Weddell seals measured by mandible accelerometer. Polar Science 4(2):309–316.

Newsome SD, Clementz MT & Koch PL (2010) Using stable isotope biogeochemistry to study marine mammal ecology. Marine Mammal Science 26:509–572.

Plötz J, Bornemann H, Pütz K & Steinmetz R (1991) Investigations in penguins and seals at the Drescher Inlet, Riiser-Larsen ice shelf. Pp 41–46 in: Miller H & Oerter H (eds) Die Expedition Antarktis VIII mit FS „Polarstern“ 1989/90. Berichte zur Polarforschung 86.

Plötz J, Bornemann H, Pütz K, Steinmetz R & Ulbricht J (1994) Investigations in penguins and seals at the Drescher Inlet, Vestkapp. Pp 112–118 in: Miller H & Oerter H (eds) Die Expedition Antarktis X mit FS „Polarstern“ 1992. Berichte zur Polarforschung 152.

Plötz J, Bornemann H, Gleitz M & Günther S (1997) Biological investigations at the Drescher Inlet – sea ice communities and Weddell seals. Pp 61–66 in: Jokat W & Oerter H (eds) Die Expedition Antarktis XII mit FS „Polarstern“ 1992. Berichte zur Polarforschung 219.

Plötz J & Bornemann H (1999) Diving and foraging behaviour of Weddell seals. Pp 95–98 in: Arntz W & Gutt J (eds) The expedition ANTARKTIS XV/3 (EASIZ II) of RV “Polarstern” in 1998. Reports on Polar Research 301.

Plötz J, Bornemann H, Knust R, Schröder A & Bester M (2001) Foraging behaviour of Weddell seals, and its ecological implications. Polar Biology 24:901–909.

Plötz J, Bornemann H, Liebsch N & Watanabe Y (2005) Foraging Ecology of Weddell seals. Pp 63–67 in: Arntz W & Brey T (eds) The expedition ANTARKTIS XXI/2 (BENDEX) of RV “Polarstern” in 2003/04. Reports on Polar and Marine Research 503.

Wägele JW (1987) The Feeding Mechanism of *Antarcturus* and a Redescription of *A. spinacoronatus* Schultz, 1978 (Crustacea: Isopoda: Valvifera). Philosophical Transactions of the Royal Society B: Biological Sciences 316(1180):429–458.

Watanabe Y, Mitani Y, Sato K, Cameron MF & Naito Y (2003) Dive depths of Weddell seals in relation to vertical prey distribution as estimated by image data. Marine Ecology Progress Series 252:283–288.

Watanabe Y, Bornemann H, Liebsch N, Plötz J, Sato K, Naito Y & Miyazaki N (2006) Seal-mounted camera detect invertebrate fauna underneath Antarctic ice shelf. Marine Ecology-Progress Series 309:297–300.

Tab. 4.20.5: Technical configurations of the ROV within the Seals and cryobenthic communities at the Ekström Ice Shelf II (SEAEIS II) project of the ANT-Land 2024/25 expedition at *Neumayer Station III* from 8 November 2024 – 11 January 2025. Deployments were counted separately if ROV configuration, deployment location or date changed.

ROV	Date	Time Start	Time End	BlueROV Cam	Latitude	Longitude	Max Depth	Laser	Lamp	2nd Cam	2nd Cam	Water sampler	Sampling slurp gun	Tether	Comment	Observations & sampling
[#]	[yyyy-mm-dd]	[hh:mm]	[hh:mm]	[file name]	[Deg]	[Deg]	[m]	[n]	[n]	[Type]	[file name]	[Model No.]	[Model No.]	[#]	[#]	[#]
1	2024-11-12	14:50	14:55	2024-11-12_14.52.20.mp4	-70.60468	-7.96918	154	2	4	none	none	none	none	8-wire cable	Successful test dive, 1 lamp water intrusion, cable to full length under stranded iceberg	Crinoid spp. Edwardsiella, Pagothenia borchgrevinki, sponges
1	2024-11-12	15:12	16:25	2024-11-12_15.07.11.mp4 2024-11-12_15.21.25.mp4 2024-11-12_15.36.07.mp4 2024-11-12_15.42.09.mp4	-70.60468	-7.96918	154	2	4	none	none	none	none	8-wire cable	Successful test dive, 1 lamp water intrusion, cable to full length under stranded iceberg, video footage of the dive are split into several files	Crinoid spp. Edwardsiella, Pagothenia borchgrevinki, sponges
	2024-11-12	17:26	17:42	none	-70.60468	-7.96918	154	2	4	GoPro	GX010013.MP4	none	none	8-wire cable	Successful dive to seabed and under stranded iceberg, video footage only from GoPro camera, timestamp of GoPro incorrect, uncertain start time, video length is 16min	Crinoid spp. Edwardsiella, Pagothenia borchgrevinki, sponges
2	2024-11-13	15:30	15:55	2024-11-13_15.30.20.mp4 2024-11-13_15.44.58.mp4	-70.60468	-7.96918	53	2	4	GoPro	time-lapse single images	none	none	2-wire cable	Successful dive, video footage of the dive are split into several files, GoPro timestamp is plus 01:01:20 [hh:mm:ss] compared to BlueROV timestamp	Antarcturids of different life stages in groups (n = 6) of 10 - 20 individuals in 20 - 60 m in platelet ice
2	2024-11-13	16:11	16:33	2024-11-13_16.11.39.mp4	-70.60468	-7.96918	53	2	4	GoPro	time-lapse single images	none	none	2-wire cable	Successful dive, GoPro timestamp is plus 01:01:20 [hh:mm:ss] compared to BlueROV timestamp	Antarcturids of different life stages in groups (n = 6) of 10 - 20 individuals in 20 - 60 m in platelet ice

ROV	Date	Time Start	Time End	BlueROV Cam	Latitude	Longitude	Max Depth	Laser	Lamp	2nd Cam	2nd Cam	Water sampler	Sampling slurp gun	Tether	Comment	Observations & sampling
[#]	[yyyy-mm-dd]	[hh:mm]	[hh:mm]	[file name]	[Deg]	[Deg]	[m]	[n]	[n]	[Type]	[file name]	[Model No.]	[Model No.]	[#]	[#]	[#]
2	2024-11-13	17:05	18:47	2024-11-13_17.05.03.mp4 2024-11-13_17.25.53.mp4 2024-11-13_18.12.20.mp4	-70.60468	-7.96918	86	2	4	GoPro	time-lapse single images	none	none	2-wire cable	Successful dive, video footage of the dive are split into several files, GoPro timestamp is plus 01:01:20 [hh:mm:ss] compared to BlueROV timestamp	Antarcturids of different life stages in groups (n = 6) of 10 - 20 individuals in 20 - 60 m in platelet ice, Antarcturid **sampling**
3	2024-11-16	13:35	13:50	2024-11-16_13.30.30.mp4 2024-11-16_13.49.15.mp4	-70.60468	-7.96918	33	2	4	none		none	none	2-wire cable	Contact lost, premature termination, video footage of the dive are split into several files	none
3	2024-11-16	14:08	14:09	2024-11-16_14.07.21.mp4	-70.60468	-7.96918	12	2	4	none		none	none	2-wire cable	Contact lost, premature termination	none
3	2024-11-16	14:38	16:12	2024-11-16_14.37.43.mp4 2024-11-16_14.41.56.mp4 2024-11-16_14.47.01.mp4 2024-11-16_14.50.09.mp4 2024-11-16_14.51.42.mp4	-70.60468	-7.96918	38	2	4	GoPro	time-lapse single images	none	none	2-wire cable	Contact lost, premature termination, two additional ascents during the dive, video footage of the dive are split into several files, GoPro timestamp is plus 01:01:20 [hh:mm:ss] compared to BlueROV timestamp	none
4	2024-11-18	13:22	14:50	2024-11-18_13.22.16.mp4 2024-11-18_14.11.57.mp4 2024-11-18_14.41.05.mp4	-70.60468	-7.96918	121	2	4	GoPro	time-lapse single images	none	none	8-wire cable	Successful dive, video footage of the dive are split into several files, GoPro timestamp is plus 01:01:20 [hh:mm:ss] compared to	Pagothenia borchgrevinki (n ~ 100), polychaets in shelf ice, fish of unknown species

ROV [#]	Date [yyyy-mm-dd]	Time Start [hh:mm]	Time End [hh:mm]	BlueROV Cam [file name]	Latitude [Deg]	Longitude [Deg]	Max Depth [m]	Laser [n]	Lamp [n]	2nd Cam [Type]	2nd Cam [file name]	Water sampler [Model No.]	Sampling slurp gun [Model No.]	Tether [#]	Comment [#]	Observations & sampling [#]
															BlueROV timestamp	
4	2024-11-18	15:30	17:05	2024-11-18_15.29.51.mp4 2024-11-18_16.30.57.mp4 2024-11-18_17.06.01.mp4	-70.60468	-7.96918	153	2	4	GoPro	time-lapse single images	none	none	8-wire cable	Successful dive, video footage of the dive are split into several files, GoPro timestamp is plus 01:01:20 [hh:mm:ss] compared to BlueROV timestamp	Pagothenia borchgrevinki (n ~ 100), polychaets in shelf ice, fish of unknown species
5	2024-11-20	14:55	16:20	2024-11-20_14.52.08.mp4 2024-11-20_15.20.33.mp4 2024-11-20_15.55.28.mp4 2024-11-20_16.11.42.mp4 2024-11-20_16.14.04.mp4 2024-11-20_16.16.01.mp4	70.57112	-7.45690	113	2	4	GoPro	time-lapse single images	none	none	8-wire cable	Successful dive, video footage of the dive are split into several files, GoPro timestamp is plus 01:01:20 [hh:mm:ss] compared to BlueROV timestamp	Antarcturids of different life stages in groups of 10 - 20 individuals in platelet ice, P. borchgrevinki, fish of unknow species, octopode
6	2024-11-21	13:05	14:38	2024-11-21_13.00.51.mp4 2024-11-21_14.06.59.mp4 2024-11-21_14.25.44.mp4	70.57112	-7.45690	60	2	4	GoPro	time-lapse single images	none	none	8-wire cable	Successful dive, video footage of the dive are split into several files, GoPro timestamp is plus 01:01:20 [hh:mm:ss] compared to BlueROV timestamp	Antarcturids of different life stages in groups of 10 - 20 individuals in platelet ice, P. borchgrevinki, fishes, pantopodes, spheres of unknown species

ROV	Date	Time Start	Time End	BlueROV Cam	Latitude	Longitude	Max Depth	Laser	Lamp	2nd Cam	2nd Cam	Water sampler	Sampling slurp gun	Tether	Comment	Observations & sampling
[#]	[yyyy-mm-dd]	[hh:mm]	[hh:mm]	[file name]	[Deg]	[Deg]	[m]	[n]	[n]	[Type]	[file name]	[Model No.]	[Model No.]	[#]	[#]	[#]
6	2024-11-21	15:11	16:56	2024-11-21_15.10.45.mp4 2024-11-21_15.17.50.mp4 2024-11-21_15.23.23.mp4 2024-11-21_16.03.36.mp4 2024-11-21_16.36.11.mp4 2024-11-21_16.51.49.mp4	70.57112	-7.45690	107	2	4	GoPro	time-lapse single images	none	none	8-wire cable	Successful dive, video footage of the dive are split into several files, GoPro timestamp is plus 01:01:20 [hh:mm:ss] compared to BlueROV timestamp, one ROV camera video file corrupted	Antarcturids of different life stages in groups of 10 - 20 individuals in platelet ice, P. borchgrevinki, fishes, pantopodes, spheres of unknown species
7	2024-12-01	12:00	12:30	none	-70.53106	-8.20058	0	2	4	none		AWI-WS & GREIFER	none	8-wire cable	Contact lost, premature termination	none
8	2024-12-02	11:30	12:50	2024-12-02_11.21.07.mp4 2024-12-02_12.45.37.mp4	-70.53106	-8.20058	100	2	4	GoPro	GX012636.MP4	AWI-WS & GREIFER	none	8-wire cable	Successful dive, video footage of the dive are split into several files	Water **sampling**
8	2024-12-02	13:30	14:06	2024-12-02_13.29.27.mp4	-70.53106	-8.20058	30	2	4	GoPro	GX012637.MP4	AWI-WS & GREIFER	none	8-wire cable	Successful dive	Antarcturids in groups of >10; adults and offspring, fishes and Aega - **sampling** Antarcturids (n > 10), water sampling, Edwardsiella; water **sampling** in Antarcturid cavity
8	2024-12-02	14:30	14:40	2024-12-02_14.26.56.mp4	-70.53106	-8.20058	46	2	4	GoPro	GX012638.MP4	AWI-WS & GREIFER	none	8-wire cable	Successful dive	
8	2024-12-02	15:05	16:25	2024-12-02_15.02.11.mp4	-70.53106	-8.20058	83	2	4	GoPro	GX012639.MP4	AWI-WS & GREIFER	none	8-wire cable	Successful dive	Water **sampling** under Edwardsiella

ROV	Date	Time Start	Time End	BlueROV Cam	Latitude	Longitude	Max Depth	Laser	Lamp	2nd Cam	2nd Cam	Water sampler	Sampling slurp gun	Tether	Comment	Observations & sampling
[#]	[yyyy-mm-dd]	[hh:mm]	[hh:mm]	[file name]	[Deg]	[Deg]	[m]	[n]	[n]	[Type]	[file name]	[Model No.]	[Model No.]	[#]	[#]	[#]
9	2024-12-04	12:53	14:22	2024-12-04_12.51.58.mp4	-70.60468	-7.96918	153	2	4	GoPro	GX012642.MP4 GX022642.MP4	AWI-WS & GREIFER	none	2-wire cable	Successful dive	School of Pleuragramma antarcticum (n > 50) hunting; groundling line visted
9	2024-12-04	15:02	15:55	2024-12-04_15.01.31.mp4 2024-12-04_15.37.45.mp4 2024-12-04_15.41.31.mp4	-70.60468	-7.96918	153	2	4	GoPro	GX012643.MP4	AWI-WS & GREIFER	none	2-wire cable	Successful dive, contact lost during ascent in second dive, premature termination, video footage of the dive are split into several files, full video footage on GoPro video file	Pleuragramma antarcticum (n > 50), water **sampling** along grounding line over sponges
10	2024-12-05	12:25	13:16	2024-12-05_12.19.49.mp4	-70.55665	-8.13850	101	2	4	GoPro	GX012644.MP4	AWI-WS & GREIFER	none	8-wire cable	Successful dive through labyrinthic and narrow seal cave	Fishes
11	2024-12-05	15:25	15:45	2024-12-05_15.25.30.mp4	70.53106	-8.20058	45	2	4	GoPro	GX012645.MP4	AWI-WS & GREIFER	none	8-wire cable	Successful dive; AWI-WS blocked, timestamp of GoPro incorrect	Fishes, jelly fish, antarcturids, nemertid worm in platelet ice
11	2024-12-05	16:01	16:41	2024-12-05_16.00.41.mp4	70.53106	-8.20058	80	2	4	GoPro	GX012646.MP4	AWI-WS & GREIFER	none	8-wire cable	Successful dive; AWI-WS blocked	Antarcturids, fishes
11	2024-12-05	16:54	17:40	2024-12-05_16.54.24.mp4	70.53106	-8.20058	236	2	4	GoPro	GX012648.MP4	AWI-WS & GREIFER	none	8-wire cable	Successful dive; AWI-WS blocked, GoPro camera video file corrupted	Sponges, Crinoids, Bryozoans, spheres of unknown origin; rich, undisturbed benthos

ROV	Date	Time Start	Time End	BlueROV Cam	Latitude	Longitude	Max Depth	Laser	Lamp	2nd Cam	2nd Cam	Water sampler	Sampling slurp gun	Tether	Comment	Observations & sampling
[#]	[yyyy-mm-dd]	[hh:mm]	[hh:mm]	[file name]	[Deg]	[Deg]	[m]	[n]	[n]	[Type]	[file name]	[Model No.]	[Model No.]	[#]	[#]	[#]
12	2024-12-09	11:55	12:13	2024-12-09_11.47.16.mp4	70.53106	-8.20058	80	2	4	GoPro	GX012649.MP4	AWI-WS & GREIFER	5	8-wire cable	Successful dive, timestamp of GoPro incorrect	Water **sampling**
12	2024-12-09	12:20	12:31	2024-12-09_12.18.22.mp4	70.53106	-8.20058	39	2	4	GoPro	GX012650.MP4	AWI-WS & GREIFER	5	8-wire cable	Successful dive, timestamp of GoPro incorrect	Water **sampling**
12	2024-12-09	12:35	12:47	2024-12-09_12.34.44.mp4	70.53106	-8.20058	39	2	4	GoPro	GX012651.MP4	AWI-WS & GREIFER	5	8-wire cable	Successful dive, timestamp of GoPro incorrect	Water **sampling**
12	2024-12-09	12:52	13:07	2024-12-09_12.51.21.mp4	70.53106	-8.20058	70	2	4	GoPro	GX012652.MP4	AWI-WS & GREIFER	5	8-wire cable	Successful dive, timestamp of GoPro incorrect	Water **sampling**; fisch **sampling**
12	2024-12-09	13:19	13:38	2024-12-09_13.18.37.mp4	70.53106	-8.20058	62	2	4	GoPro	GX012653.MP4	AWI-WS & GREIFER	5	8-wire cable	Successful dive, timestamp of GoPro incorrect	Water **sampling**
12	2024-12-09	14:17	14:40	2024-12-09_14.14.15.mp4	70.53106	-8.20058	50	2	4	GoPro	GX012654.MP4	AWI-WS & GREIFER	5	8-wire cable	Successful dive, timestamp of GoPro incorrect	Water **sampling**
12	2024-12-09	14:46	15:09	2024-12-09_14.46.10.mp4	70.53106	-8.20058	40	2	4	GoPro	GX012655.MP4	AWI-WS & GREIFER	5	8-wire cable	Successful dive, timestamp of GoPro incorrect	Water **sampling**
12	2024-12-09	15:19	15:35	2024-12-09_15.17.14.mp4	70.53106	-8.20058	21	2	4	GoPro	GX012656.MP4	AWI-WS & GREIFER	5	8-wire cable	Successful dive, timestamp of GoPro incorrect	Water **sampling**; fish **sampling**

ROV	Date	Time Start	Time End	BlueROV Cam	Latitude	Longitude	Max Depth	Laser	Lamp	2nd Cam	2nd Cam	Water sampler	Sampling slurp gun	Tether	Comment	Observations & sampling
[#]	[yyyy-mm-dd]	[hh:mm]	[hh:mm]	[file name]	[Deg]	[Deg]	[m]	[n]	[n]	[Type]	[file name]	[Model No.]	[Model No.]	[#]	[#]	[#]
12	2024-12-09	15:43	15:56	2024-12-09_15.41.05.mp4	70.53106	-8.20058	12	3	4	GoPro	GX012657.MP4	AWI-WS & GREIFER	5	8-wire cable	Successful dive, timestamp of GoPro incorrect	Water **sampling**
13	2024-12-10	11:53	12:30	2024-12-10_11.52.27.mp4	-70.60468	-7.96918	55	2	4	GoPro	GX012658.MP4	AWI-WS & GREIFER	5	8-wire cable	Compass failure; premature termination, one additional ascent during the dive, timestamp of GoPro incorrect	none
13	2024-12-10	12:46	13:19	2024-12-10_12.45.32.mp4	-70.60468	-7.96918	33	2	4	GoPro	GX012659.MP4	AWI-WS & GREIFER	5	8-wire cable	Successful dive, timestamp of GoPro incorrect	Water **sampling**
13	2024-12-10	13:48	14:00	2024-12-10_13.47.33.mp4	-70.60468	-7.96918	20	2	4	GoPro	GX012660.MP4	AWI-WS & GREIFER	5	8-wire cable	Successful dive, timestamp of GoPro incorrect	Water **sampling**
13	2024-12-10	14:03	14:24	2024-12-10_14.03.01.mp4	-70.60468	-7.96918	30	2	4	GoPro	GX012661.MP4	AWI-WS & GREIFER	5	8-wire cable	Successful dive, timestamp of GoPro incorrect	Water **sampling**
13	2024-12-10	14:28	14:40	2024-12-10_14.27.09.mp4	-70.60468	-7.96918	41	2	4	GoPro	GX012662.MP4	AWI-WS & GREIFER	5	8-wire cable	Successful dive, timestamp of GoPro incorrect	Water sampler not active
13	2024-12-10	14:49	14:57	2024-12-10_14.48.09.mp4	-70.60468	-7.96918	40	2	4	GoPro	GX012663.MP4	AWI-WS & GREIFER	5	8-wire cable	Successful dive, timestamp of GoPro incorrect	Water **sampling**
13	2024-12-10	15:00	15:10	2024-12-10_14.59.48.mp4	-70.60468	-7.96918	50	2	4	GoPro	GX012664.MP4	AWI-WS & GREIFER	5	8-wire cable	Successful dive, timestamp of GoPro incorrect	Water **sampling**

ROV	Date	Time Start	Time End	BlueROV Cam	Latitude	Longitude	Max Depth	Laser	Lamp	2nd Cam	2nd Cam	Water sampler	Sampling slurp gun	Tether	Comment	Observations & sampling
[#]	[yyyy-mm-dd]	[hh:mm]	[hh:mm]	[file name]	[Deg]	[Deg]	[m]	[n]	[n]	[Type]	[file name]	[Model No.]	[Model No.]	[#]	[#]	[#]
13	2024-12-10	15:17	15:32	2024-12-10_15.17.29.mp4	-70.60468	-7.96918	60	2	4	GoPro	GX012665.MP4	AWI-WS & GREIFER	5	8-wire cable	Successful dive, timestamp of GoPro incorrect	Water **sampling**
13	2024-12-10	15:37	15:52	2024-12-10_15.37.09.mp4	-70.60468	-7.96918	130	2	4	GoPro	GX012666.MP4	AWI-WS & GREIFER	5	8-wire cable	Successful dive, timestamp of GoPro incorrect	Water **sampling**
13	2024-12-10	15:58	16:22	2024-12-10_15.59.40.mp4	-70.60468	-7.96918	152	2	4	GoPro	GX012667.MP4	AWI-WS & GREIFER	5	8-wire cable	Successful dive, timestamp of GoPro incorrect	Water **sampling**
14	2024-12-11	13:40	14:55	2024-12-11_13.35.29.mp4 2024-12-11_13.53.45.mp4 2024-12-11_14.08.00.mp4 2024-12-11_14.28.10.mp4 2024-12-11_14.51.25.mp4	70.57112	-7.45690	106	2	4	GoPro	GX012668.MP4 GX022668.MP4	AWI-WS & GREIFER	5	8-wire cable	Successful dive, video footage of the dive are split into several files, timestamp of GoPro incorrect	Water **sampling**, Krill sampling, Polychaet
14	2024-12-11	15:20	15:50	2024-12-11_15.16.26.mp4 2024-12-11_15.37.59.mp4	70.57112	-7.45690	58	2	4	GoPro	GX012669.MP4	AWI-WS & GREIFER	5	2-wire cable	Successful dive, timestamp of GoPro incorrect	Water **sampling**, Amphipode sampling
14	2024-12-11	16:05	16:45	2024-12-11_16.04.29.mp4 2024-12-11_16.33.09.mp4 2024-12-11_16.42.42.mp4	70.57112	-7.45690	107	2	4	GoPro	GX012670.MP4	AWI-WS & GREIFER	5	2-wire cable	Successful dive; slow reaction of ROV, timestamp of GoPro incorrect	Water **sampling,** Bryozoe **sampling**, Amphipode **sampling**; Antarcturids in patches of 100
14	2024-12-11	17:00	17:30	2024-12-11_16.59.51.mp4 2024-12-11_17.09.34.mp4	70.57112	-7.45690	100	2	4	GoPro	GX012671.MP4	AWI-WS & GREIFER	5	8-wire cable	Successful dive, timestamp of GoPro incorrect	Water **sampling**, sphere species sampling; Antarcturids in patches of 100

ROV	Date	Time Start	Time End	BlueROV Cam	Latitude	Longitude	Max Depth	Laser	Lamp	2nd Cam	2nd Cam	Water sampler	Sampling slurp gun	Tether	Comment	Observations & sampling
[#]	[yyyy-mm-dd]	[hh:mm]	[hh:mm]	[file name]	[Deg]	[Deg]	[m]	[n]	[n]	[Type]	[file name]	[Model No.]	[Model No.]	[#]	[#]	[#]
14	2024-12-11	17:48	18:22	2024-12-11_17.48.04.mp4 2024-12-11_18.06.05.mp4	70.57112	-7.45690	98	2	4	GoPro	GX012672.MP4	AWI-WS & GREIFER	5	8-wire cable	Successful dive, timestamp of GoPro incorrect	Water **sampling**, Bryozoe species **sampling**, Crinoid **sampling**, Annelid **sampling**; Antarcturids in patches of 100
15	2024-12-12	16:11	16:59	2024-12-12_16.09.49.mp4	-70.60468	-7.96918	150	2	4	GoPro	GX012673.MP4	AWI-WS & GREIFER	5	8-wire cable	Successful dive, timestamp of GoPro incorrect	Water **sampling**, Fish sampling; Edwardsiella, Polychaets
15	2024-12-12	17:05	17:22	2024-12-12_17.04.36.mp4	-70.60468	-7.96918	80	2	4	GoPro	GX012674.MP4	AWI-WS & GREIFER	5	8-wire cable	Successful dive, timestamp of GoPro incorrect	Water **sampling**, Amphipode sampling
15	2024-12-12	17:50	18:12	2024-12-12_17.48.46.mp4	-70.60468	-7.96918	110	2	4	GoPro	GX012675.MP4	AWI-WS & GREIFER	5	8-wire cable	Successful dive, timestamp of GoPro incorrect	Water **sampling**
15	2024-12-12	18:18	19:12	2024-12-12_18.18.10.mp4	-70.60468	-7.96918	155	2	4	GoPro	GX012676.MP4	AWI-WS & GREIFER	5	8-wire cable	Successful dive, timestamp of GoPro incorrect	Water **sampling**

4.21 RecorD – Recording the Baseline Before the Change: First Steps Towards an Integrated Chemical and Biological Pollution and Effects Assessment off Dronning Maud Land

Sabine Strieben[1], Ute Marx[1], Moritz Kielmann[2]
not in the field: Gesine Witt[2], Sarah Zwicker[3],
Matthias Brenner*[1]
* Matthias.Brenner@awi.de

[1]DE.AWI
[2]DE.HAW
[3]DE.ZMT

Grant-No. AWI_ANT_43

Objectives

With an increase in the global average temperature, a rising number of volatile industrial pollutants emitted in the lower latitudes will undergo prolonged atmospheric long-range transport. Through global distillation, the most persistent pollutants released in the southern hemisphere will eventually deposit in the Antarctic, the southern cold-trap (Wania and Mackay 1993; Kallenborn et al. 2013). At the same time, climate change-induced ocean warming and acidification will accelerate the re-release of a history of sealed contaminants from land and marine-terminating glaciers and sea ice into the Southern Ocean (Ma et al., 2011).

The overarching objective of this proposed project is to **i.** record baseline data on the pollution status and biological responses in the eastern Weddell Sea off Dronning Maud Land. Atka Bay, a representative area for the Eastern Weddell Sea coastal system, has so far recorded only a minor impact from climate change (Corsolini et al. 2017).

We aim to investigate **ii.** the potential for biological accumulation (bioaccumulation) of the pollutants in key compartments of the Antarctic ecosystem during the melting season, when ice-bound pollutants become bioavailable in the water column (Bargagli 2008). For this, the internal concentration of contaminants in the organisms living in the investigated area will be determined using the SPME method (Mayer et al., 2014, Witt et al., 2019).

We further aim to **iii.** establish the SPME method in these hardly accessible areas as time- and cost-efficient analytical methods that could play an essential role in future monitoring and risk assessment approaches in Antarctica (Mayer et al., 2014, Witt et al., 2019).

Since assessing the biological response is an indispensable step in thorough pollution risk assessments, we want to study biomarkers of pollution in one organism, the Antarctic krill (Lehtonen et al. 2006). This project further intends to **iv.** investigate the baseline response and variability of the selected biomarkers under different environmental conditions during the relevant sampling time of the melting season (Hagger et al. 2006; Broeg and Lehtonen 2006).

Finally, we aim to **v.** reach out to other Antarctic research stations to involve their knowledge in the development of this concept and build up a network to further expand the current boundaries of pollution research in Antarctica (Tin et al. 2009; Davies and Vethaak 2012).

General and specific Hypotheses

4. If we combine state-of-the-art analytical measurement methods, which primarily determine the biologically available fraction of POPs, with biomarker analyses, we will obtain a holistic picture of the current pollution situation and the current impacts on the Antarctic ecosystem. This is a prerequisite for assessing future pollution trends in the Antarctic ecosystem in terms of risk to the organisms living there.

   H01: Over the melting season, we expect to see an increase of POP concentrations in the water column, ice, algae and krill/amphipods.

5. By conducting chemical and biological studies of organisms along the food chain, we will determine the body's exposure to contaminants, their potential for bioaccumulation.

   H02: We expect to record bioaccumulation of POP concentrations from algae to krill/amphipods tissue.

6. By applying a biomarker approach, we can describe their pathological effects at the cellular and subcellular levels to detect earliest possible changes and impairments in a timely manner.

   H03: We expect krill/amphipods with high pollutant loads to show an elevation in detoxification responses, e.g. elevation of detoxification enzymes expression.

   H04: We expect krill/amphipods with high pollutant loads to show decreased cellular health, e.g. reduced lysosomal stabilities and increased cellular lipofuscin content.

In studying the contamination load **of pollutants travelling from low to high latitudes and measuring the biological response** to them **changing the environment**, we will address SPP1158 research goals: **Linkages of lower and higher latitudes** in combination with research **Response to Environmental Change**. We will tackle especially the research goals described in the subchapter “3.2.C.3 Anthropogenic Impacts” and the resulting research questions 1 and 2: What is the exposure and response of Antarctic organisms to pollutants, and secondly: What are effects of multiple anthropogenic stressors on Antarctic and Southern Ocean biota.

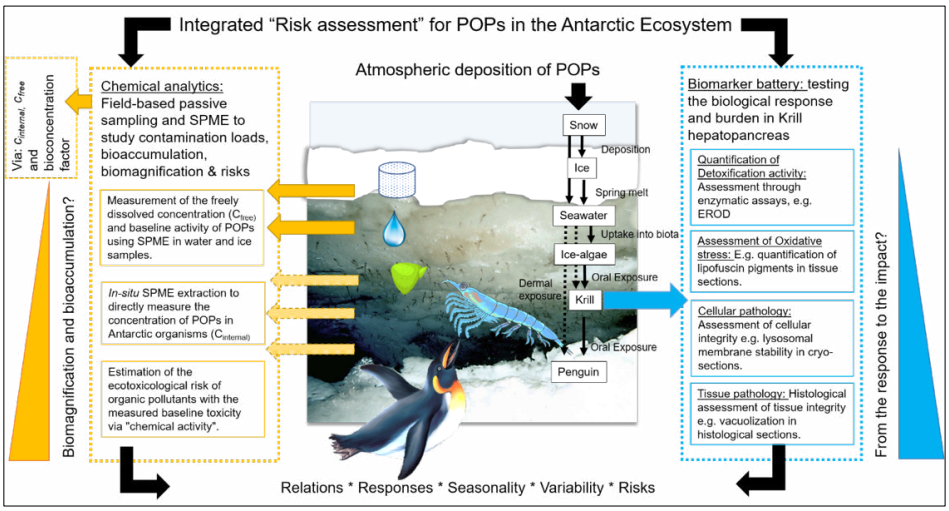

Fig. 4.21.5: Schematic drawing of proposed research project: Integrated risk assessment for POPs in the Antarctic Ecosystem. Containing chemical analytics of biotic and abiotic samples from Ice to Penguin tissue as well as Respone & Impact assessment employing a biomarker approach on Krill/Amphipods tissue samples.

Fieldwork

Summary and itinerary

The RECORD team boarded flight NPI-F1 to Antarctica on 1 November and arrived at *Neumayer Station III* on 8 November 2024.

The first days at the Station began with a safety briefing and guided tour through the building. Because of good weather conditions it was possible to conduct the Skidoo training course and go for a first exploration trip to the sea ice on the day after arrival.

The fieldwork began with selecting a suitable site and attempting to create a sufficiently large ice hole for sampling, as well as for deploying nets and the ROV. Three complete sets of samples, including snow, ice, and water from discrete depths, were collected. Additionally, biota was captured later in the campaign. On-site, the samples were chemically treated and prepared for transport by *Polarstern*. The fieldwork on the ice concluded on January 3, when the sea ice was closed due to the bay's imminent opening. The journey back to Germany commenced on 11 January 2025.

Sampling area, ice hole crafting and sampling

The location for sampling was chosen based on the available data for ice thickness and layered ice at the station. Atka 03 has an ice thickness not exceeding 2 meters and comparatively less flake ice underneath. Additionally, it is reasonably accessible from the station. However, the snow on the ice was about 0.8 meters thick. Initially, creating a large ice hole was challenging. SEAEIS-Team allowed the use of their pre-existing ice hole at the area known as U-Turn (Fig. 4.21.6). This location has nearly the same ice thickness as Atka 03 and not too much flake ice. At U-Turn, the snow layer on the ice was very thin, making the sampling of ice algae possible. No ice algae were observed underneath the ice at Atka 03. The decision was made to use a small single ice core hole at Atka 03 to collect samples for chemical analysis (snow, ice core, water samples) and to collect biota samples (ice algae, amphipods, ROV deployment) at U-Turn. This decision was made because the U-Turn ice hole was created with a regular chainsaw, which might contaminate the surrounding ice, snow, and water with PAHs, which are analytes of interest. However, biota samples caught with traps were not likely to be affected by this. Additionally, ice algae were sampled at a sufficient distance from the original U-Turn ice hole.

Drilling Ice holes

The initial attempts to drill an ice hole at Atka-03 were challenging. The snow was very thick (approximately 0.8 meters), making it labor-intensive to dig a large hole with shovels to reach the ice. Another difficulty was that the drill length exceeded the ice thickness. Initially, the plan was to drill in two steps, but when the ice was penetrated in the second step, the hole filled with water, making it impossible to aim with the drill. The ice was too thick and hard for hand saws. Due to these challenges, the U-Turn ice hole was used to deploy traps and the ROV.

By joining the geoscience team during their ice thickness measurement campaign, new insights were gained. REROD-Team learned to dig small, deep holes in the snow with shovels, which was easier than creating large holes that tended to fill with drifting snow. Further progress was made through discussions with experienced scientists at the station. The new approach was to drill overlapping holes with the ice core drill. The ice was perforated step by step in a circular shape. It was crucial to drill through the ice in one step from the hard ice surface.

The second important factor was the overlap. The overlap needed to be small enough to leave no ice connection between the holes, but not so small that the drill drifted into the next hole. It was necessary to cut through the remaining connections between the cut-out core and the surrounding ice. A long custom ice saw, lent by SEAEIS-Team, was used for this purpose. When the core finally loosened, it was lifted with a tripod and a chain hoist, which was attached to the core with two ice screws. The core was lifted in steps as the layers were broken. This method allowed for the creation of a large hole with approximately 25 holes within one day of work. The flake ice underneath the hole was penetrated with a Niskin bottle and a weight to bring it to the surface. This opened the hole for ROV deployment. The raised flake ice was removed with a shovel and a perforated bucket.

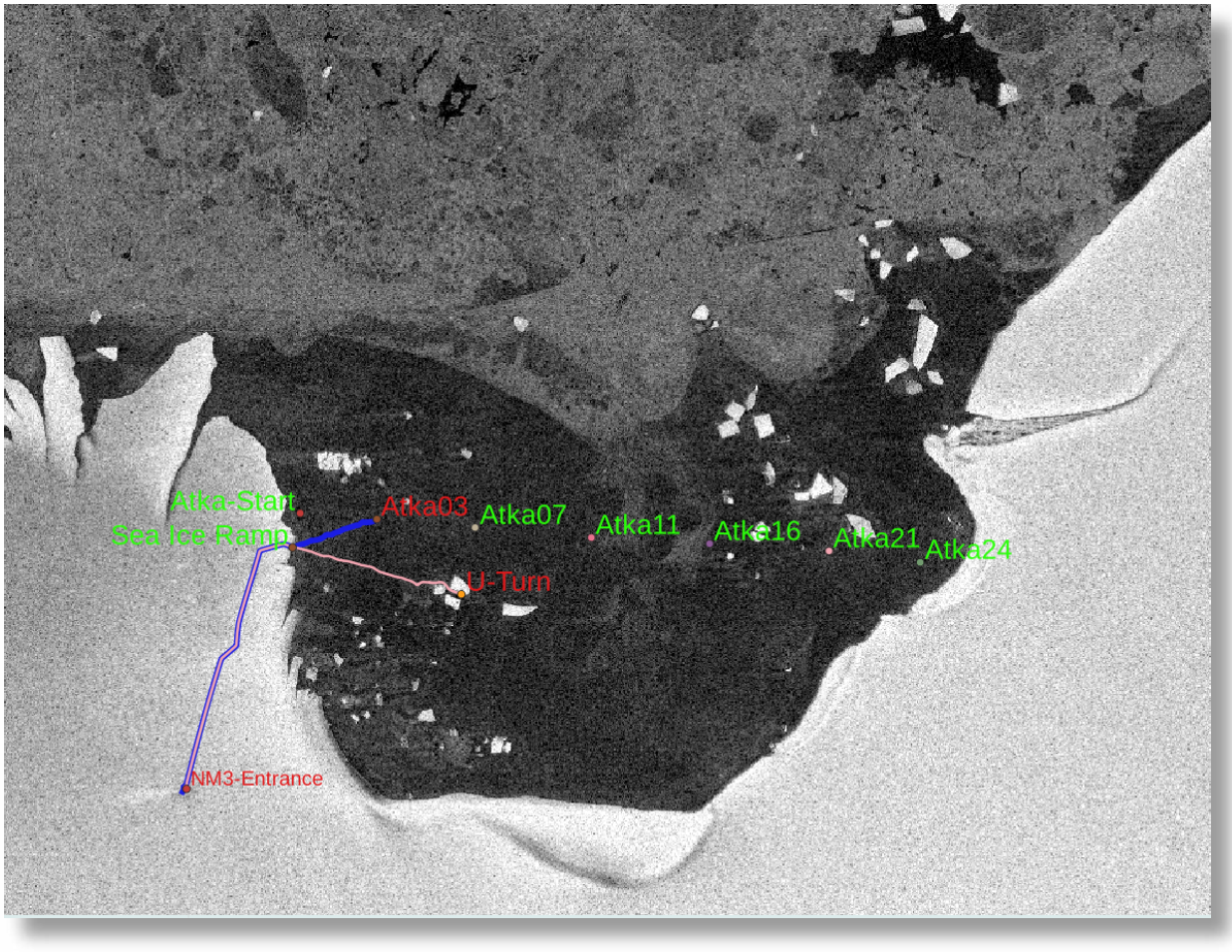

Fig. 4.21.6: Sampling area in Atka Bay on sea ice 2024/25

Reopening of ice holes

The large ice hole at U-Turn was approximately 1 meter by 1 meter. The surface froze between visits (1-3 days) and had to be reopened, as demonstrated by SEAEIS-Team. Initially, the ice surface was penetrated and sawn into pieces with a hand ice saw. Then an ice axe was used to remove the ice pieces from the hole. The thickness varied depending on the temperature and the time between visits. Afterward, newly accumulated flake ice was removed with a shovel and a perforated bucket.

Prevention of freezing

There was an attempt to cover the ice hole with wooden planks to prevent it from closing due to drifting snow on windy or stormy days, and to stop the surface of the water from freezing because of low temperatures. While the planks might prevent these issues, it became apparent that the light shining through the ice hole is needed to attract amphipods to the traps. Therefore, when traps are deployed, covering the hole is not recommended, or a transparent material should be used instead.

ROV Deployment

The ROV (QYSEA FIFISH V-EVO) (Fig. 4.21.7) was deployed at the U-Turn ice hole several times.

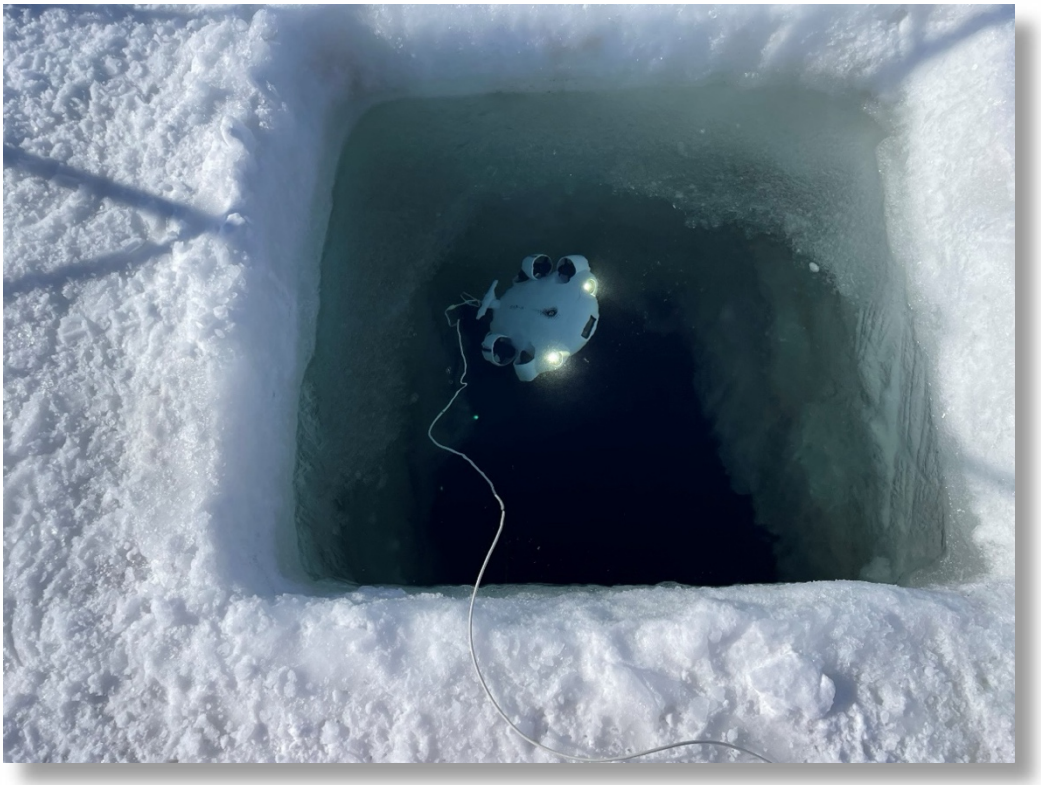

Fig. 4.21.7: ROV at U-Turn ice hole (Photo: Ute Marx, AWI)

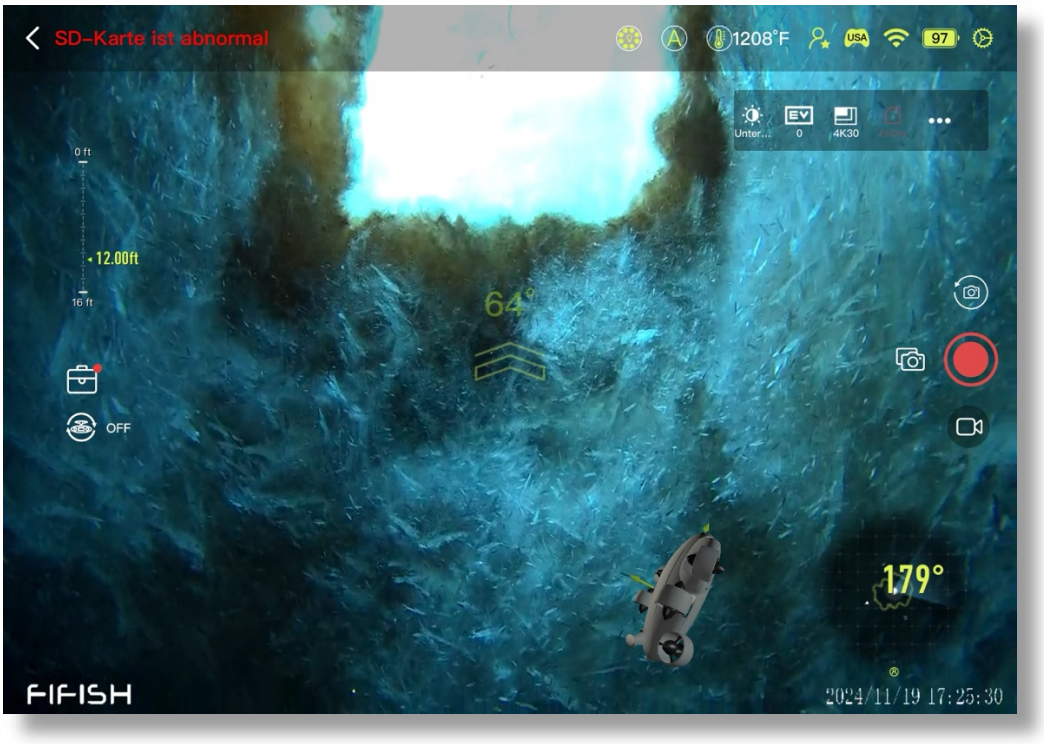

Fig. 4.21.8: Algae layer between flake ice and hard ice at U-Turn ice hole (Photo: Moritz Kielmann, HAW)

Tab. 4.21.1: ROV deployments at Atka Bay

The ROV captured pictures and videos of the ice hole and its surroundings. It was possible to observe the ice algae layer between the hard ice and the flake ice (Fig. 4.21.8). Additionally, Antarctic silverfish (Pleuragramma antarcticum) were visible. The ROV was also used to inspect the position of the traps. Collecting algae with the ROV could not be performed due to the presence of flake ice; therefore, ice cores were taken instead.

ROV	Date	Time	Time	Latitude	Longitude	Ice Hole	Dives
		Start	End				
No	yyyy-mm-dd	hh:mm	hh:mm	hddd° mm.mmm′	hddd° mm.mmm′	Trivial Name	[n]
1	2024-11-17	11:26	11:45	S70° 36.298'	W7° 58.117'	U-Turn	1
2	2024-11-19	17:23	17:50	S70° 36.298'	W7° 58.117'	U-Turn	1
3	2024-12-01	16:32	18:36	S70° 36.298'	W7° 58.117'	U-Turn	2
4	2024-12-23	20:10	20:44	S70° 36.298'	W7° 58.117'	U-Turn new	1

Snow samples

The snow samples were taken several meters away from the Atka-03 ice hole. The sampling area was marked with bamboo stakes to prevent contamination. The surface snow was collected with a stainless-steel shovel. Sufficient snow was gathered to fill two 6.5-liter stainless steel containers for the analysis of PAHs, PCBs, and OCs. Additionally, one 2-liter PP bottle was filled with PFAS samples.

Ice Core samples

Ice samples were taken from ice cores drilled with an ice auger. Only the last 30 centimeters in contact with the sea water were collected. The ice cores were broken into smaller pieces using a stainless-steel shovel, and two 6.5-liter stainless steel containers were filled with the samples.

Water samples

Water samples were collected from discrete depths (1 m, 5 m, 10 m, and 15 m from the water surface level). A Niskin water sampler made from stainless steel was used. The bottle was attached to a steel cable, and a tripod was used to lift and lower the bottle. The bottle was set by pulling the caps from the steel body. After reaching the desired depth, a steel weight (messenger) was sent down the cable to hit the cap and close the bottle with a mechanism. Two liters from each cast were filled into a 6.5-liter stainless steel container for each depth. The bottle was rinsed before each depth.

Ice Algae samples

Ice algae grow beneath the sea ice where it is in contact with sea water. The plan was to collect the ice algae with a net attached to the ROV, as is done in Arctic regions. However, the layered ice prevented this. Thus, ice cores were taken, and the ice algae attached to the ice core were sawed off and collected. This procedure is time-consuming because many ice cores must be drilled to collect enough sample material. Therefore, this work was combined with the crafting of an ice hole to mitigate the effort.

Amphipod samples

During the expedition, amphipods were successfully captured through the drilled ice hole at U-Turn using specially designed traps. The traps were baited with fish that had been previously caught. To ensure effectiveness and prevent the amphipods from escaping during trap retrieval, the baits were wrapped in a net. This method proved efficient in attracting and securing a significant number of amphipods. The samples were collected in Falcon tubes for

chemical analysis. The Falcon tubes were stored in a -20°C environment. The second half of the amphipods were collected in cryo vials and were frozen using dry ice made with CO_2 fire extinguishers. These samples, intended for biological analysis, were stored at -80°C.

Penguin feathers

The penguin feathers were gathered by the MARE and SPOT teams working in the penguin colonies. This innovative approach to sampling feathers for chemical analysis of POPs was developed to overcome obstacles posed by bird flu.

Laboratory work

Bottling the samples

The collected snow, ice, and water samples were brought to the station in 6.5-liter stainless steel containers. The frozen samples were thawed overnight at 20 °C in closed containers. In the laboratory, the samples were decanted from the containers. Each sample was divided into three subsamples with two replicates. The containers were rinsed and dried on the outside to prevent contamination. The subsample bottles were rinsed with acetone and weighed empty. The water was decanted directly from the containers into the bottles, which were rinsed once with sample water. After capping, the bottles were rinsed from the outside with fresh water and dried. The bottles had to be dry on the outside to weigh them in order to determine the exact volume by weight. The samples were bottled for solid-phase extraction into 1-liter brown glass bottles and for stir-bar sorptive extraction in 100-milliliter headspace vials. Additionally, 2 liters of sample were filled into 1-liter and 2-liter bottles for backup and were frozen at the U2 level.

Filtering of the chlorophyll and ice algae samples

The water samples for the chlorophyll determination were drawn through glass fiber filters in the laboratory, as were the ice algae samples from the ice cores. As much volume was passed through glass fiber filters until they blocked, but not over two liters for the water samples. After melting, the ice algae samples were drawn completely through several filters, and the respective volume was noted. The filters were placed in Falcon tubes and stored at -80°C.

Stir bar sorptive extraction

The stir bar sorptive extraction (SBSE) was carried out with magnetic stir bars which were coated with 1 millimeter of silicone (Fig. 4.21.9). These so-called Twisters by Gerstel were placed into the headspace vials. The vials were put on magnetic stirrers and left for 48 hours. During this time, the analytes adsorbed onto the silicone. After that, the Twisters were removed from the vials with a magnetic rod and wrapped in clean aluminum foil for transport. The aluminum foil was wrapped tightly around the Twisters and stored at -20°C.

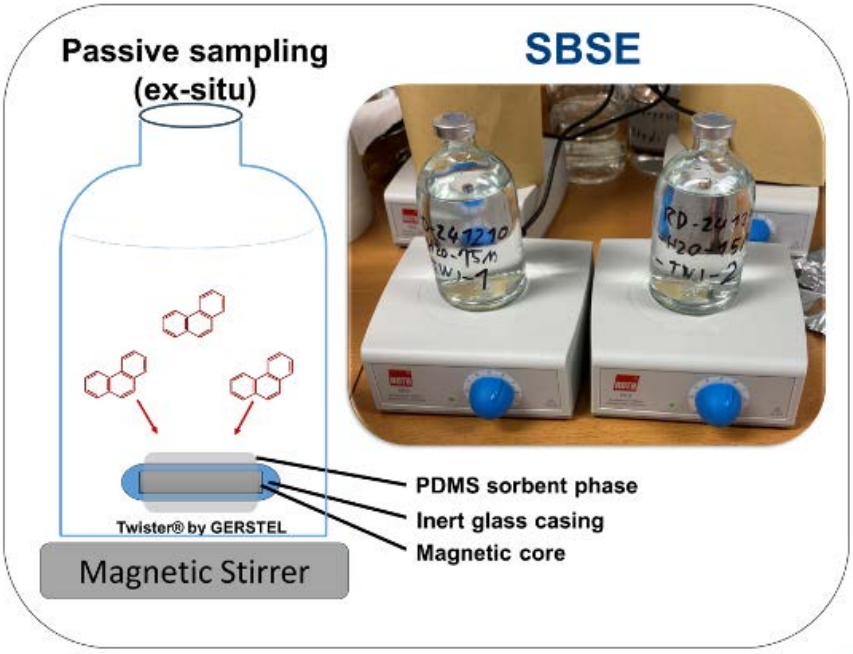

Fig. 4.21.9: Scheme and photo of Stir Bar Sorptive Extraction (SBSE) (Figure/Photo: Moritz Kielmann)

Solid phase extraction

The solid-phase extraction was done with pre-packed columns by Macherey-Nagel. The columns were placed on the manifold (Fig. 4.21.10). Before the extraction, the columns were conditioned with solvents. They were connected to the sample bottle using Teflon tubes. A vacuum pump was initially used to suck the sample from the bottle through the columns. The manifold was positioned lower than the sample bottle to allow the sample to flow by gravity through the columns and into a large bucket. The extraction took several days due to the low throughput. When the sample bottles were empty, the columns were rinsed once with ultra-pure water and dried with the vacuum pump. The columns were then wrapped in clean aluminum foil and stored at -20°C.

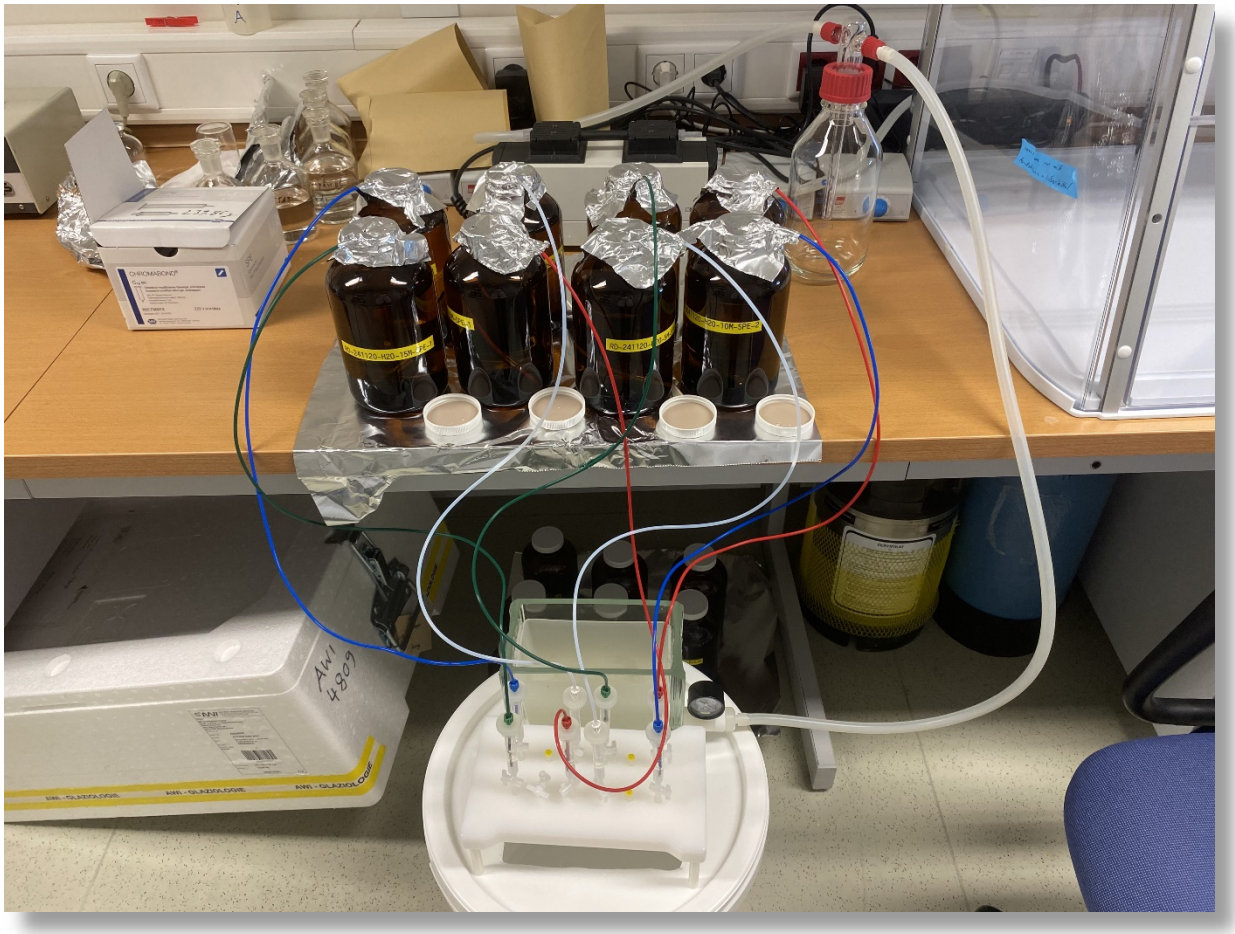

Fig. 4.21.10: Solid phase extraction in the air chemistry laboratory (Photo: Moritz Kielmann, HAW)

Preliminary (expected) results

The samples arrived with the *Polarstern* in April at Bremerhaven. Chemical analysis will start in the summer of 2025. Until then, no statements about the expected results can be made.

Data management

All data collected and generated by the project will be submitted to the central PANGAEA database of SPP 1158. If possible, datasets and results will be published in international (open access) journals, thereby also ensuring scientific credit for the related effort. All samples collected during this project will be listed in a central sample database and stored at the participants' home institutes according to legal requirements, or for at least five years. If not sacrificed during laboratory analysis, the samples will be available for further research on request to the responsible scientist.

Molecular data (DNA and RNA data) will be archived, published and disseminated within one of the repositories of the International Nucleotide Sequence Data Collaboration (INSDC, www.insdc.org) comprising of EMBL-EBI/ENA, GenBank and DDBJ).

Any other data will be submitted to an appropriate long-term archive that provides unique and stable identifiers for the datasets and allows open online access to the data.

This expedition was supported by the Helmholtz Research Programme "Changing Earth – Sustaining our Future" Topic 6, Subtopic 1 and Topic 9, Subtopic 6.

In all publications based on this expedition, the **Grant No. AWI_ANT_43** will be quoted and the following publication will be cited:

Alfred-Wegener-Institut Helmholtz-Zentrum für Polar- und Meeresforschung. (2016a). *Neumayer III and Kohnen Station* in Antarctica operated by the Alfred Wegener Institute. Journal of large-scale research facilities, 2, A85. http://dx.doi.org/10.17815/jlsrf-2-152.

References

Wania F, Mackay D (1993) Global fractionation and cold condensation of low volatility organochlorine compounds in polar regions. Ambio 22(1): 10–18. http://www.jstor.org/stable/4314030

Kallenborn et al. (2013) Long-term monitoring of persistent organic pollutants (POPs) at the Norwegian Troll Station in Dronning Maud Land, Antarctica. Atmos. Chem. Phys. 13(14): 6983–6992. https://doi.org/10.5194/acp-13-6983-2013

Ma et al. (2011) Revolatilization of persistent organic pollutants in the Arctic induced by climate change. Nature Climate Change 1(5): 255–260. https://doi.org/10.1038/nclimate1167

Corsolini et al. (2017) Legacy persistent organic pollutants including PBDEs in the trophic web of the Ross Sea (Antarctica). Chemosphere 185: 699–708. https://doi.org/10.1016/j.chemosphere.2017.07.054

Bargagli (2008) Environmental contamination in Antarctic ecosystems. Science of the Total Environment 400(1–3): 212–226. https://doi.org/10.1016/j.scitotenv.2008.06.062

Mayer et al. (2014) Passive sampling methods for contaminated sediments: Scientific rationale supporting use of freely dissolved concentrations. Integrated Environmental Assessment and Management 10:197–209.

Witt et al. (2019) Assessing PCB pollution in the Baltic Sea- An equilibrium partitioning based study. Chemosphere 191: 886–894.

Lehtonen et al. (2006) The BEEP project in the Baltic Sea: Overview of results and outline for a regional biological effects monitoring strategy. Marine Pollution Bulletin 53(8–9):523–537. https://doi.org/10.1016/j.marpolbul.2006.02.008

Hagger et al. (2006) Biomarkers and integrated environmental risk assessment: Are there more questions than answers? Environmental Toxicology and Chemistry 2(4): 312–329.

Broeg K, Lehtonen K (2006) Indices for the assessment of environmental pollution of the Baltic Sea coasts: Integrated assessment of a multi-biomarker approach. Marine Pollution Bulletin 53(8–9): 508–522. https://doi.org/10.1016/j.marpolbul.2006.02.004

Tin et al. (2009) Review impacts of local human activities on the Antarctic environment. Journal of Environmental Health Science & Engineering 21(1): 3–33.

Davies IM, Vethaak AD (2012) Integrated marine environmental monitoring of chemicals and their effects. ICES COOPERATIVE RESEARCH NO. 315.

4.22 DML-GIA – GNSS Measurements in Dronning Maud Land to Investigate Glacial-Isostatic Adjustment

Jölund Asseng[2] [1]DE.TUDresden
not in the field: Mirko Scheinert*[1], Lutz Eberlein[1] [2]DE.AWI
* Mirko.Scheinert@tu-dresden.de

Grant-No. AWI_ANT_28

Objectives

Quantifying glacial isostatic adjustment (GIA) in Antarctica is crucial for understanding future land- and ice-sheet evolution as well as sea level change, and for correcting estimates of ice-mass change from satellite gravimetry (GRACE). A wide range of GIA models have been developed during recent years adopting different modeling approaches. However, substantial differences between GIA model predictions still remain, regarding both spatial pattern and magnitude of vertical uplift rates as well as the magnitude of the continent-wide GIA mass effect. Geodetic GNSS (Global Navigation Satellite System) observations on bedrock provide direct observables to constrain these models. However, the coverage of permanent and campaign GNSS sites is quite different over Antarctica due to the availability of bedrock outcrops and depending on logistic conditions. In central Dronning Maud Land (DML), East Antarctica, our group started GNSS observation campaigns already in the mid-1990s. The coverage was extended to western DML in 2001/02 and 2004/05. Almost all GNSS sites were set up in the mountain range that stretches nearly parallel to the coast, from Heimefrontfjella over Borgmassivet, Orvinfjella to Wohlthatmassivet, over a distance of more than 1,000 km. Whereas for central DML resulting vertical uplift rates could already be inferred, for western DML this is not the case because only the initial observation campaigns were carried out.

The GNSS measurements during the last seasons (since 2020) are part of the ongoing project “Investigating glacial- isostatic adjustment on basis of geodetic GNSS observation campaigns in Dronning Maud Land, East Antarctica“, funded by the German Research Foundation (SCHE 1426/28-1 and -2). In western DML, additionally to the GNSS campaign measurements two permanently operating GNSS stations were set up, namely at Weigel Nunatak near Kottas Mountains, and at Forstefjell, about 150 km south-east of *Neumayer Station III*. In contrast to campaign sites where only a (long-term) linear trend can be inferred, permanent GNSS recordings allow to also detect periodic signals in coordinate time series (e.g. at annual and semi-annual periods). Both stations are collocated with seismology stations of AWI Geophysics.

In the season 2024/25 the maintenance and data management of both permanent GNSS stations was part of the field work carried out, see overview map in Figure 4.22.1. Furthermore, to optimally use personnel and logistic efforts further tasks were coordinated with other research projects and carried out as following:

- Maintenance of seismology stations of AWI Geophysics (see Chapter 4.3)*;*
- Maintenance of the permanently operating GNSS station at *SVEA* (Sweden).

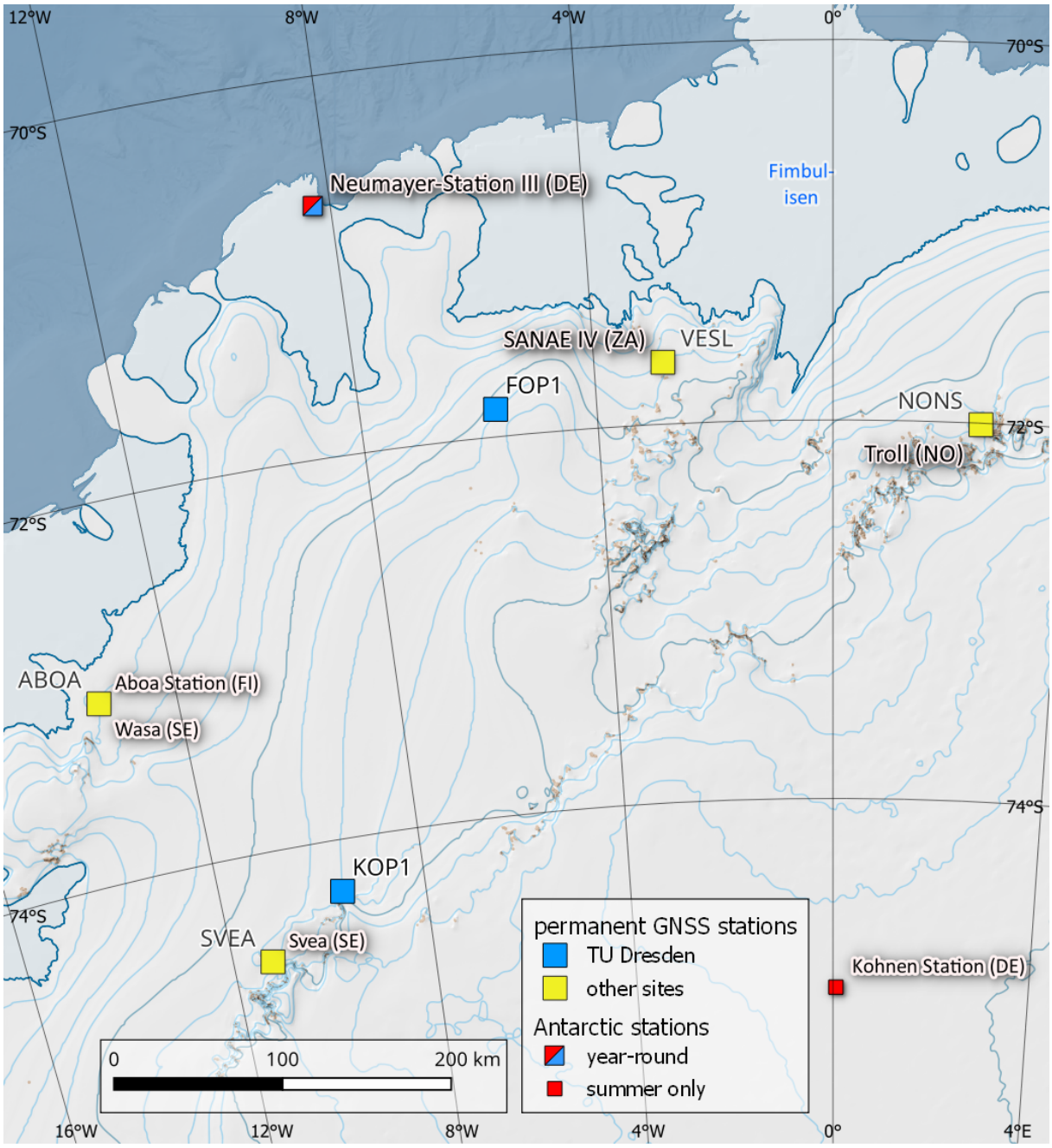

Fig. 4.22.1: Overview map of the working area with Neumayer Station III, the permanent GNSS sites at Forstefjell (FOP1), Weigel Nunatak (KOP1) and SVEA. Also shown are further permanent GNSS sites, operated by other programs (ABOA, VESL and NONS).

Fieldwork

In order to make optimal use of synergies, we cooperated with the AWI Geophysics group. The AWI group led by Jölund Asseng (AWI Geophysics) was in the field and carried out the maintenance work at the AWI seismological stations as well as at the GNSS sites (*cf.* Figs. 4.22.1, 4.22.5 and 4.22.6).

Work at Forstefjell was realized in the period 29 to 31 December 2024. Work at SVEA and Weigel Nunatak was realized on 2 February 2025 and 3 February 2025, respectively. For the travel, the Arctic Trucks were used.

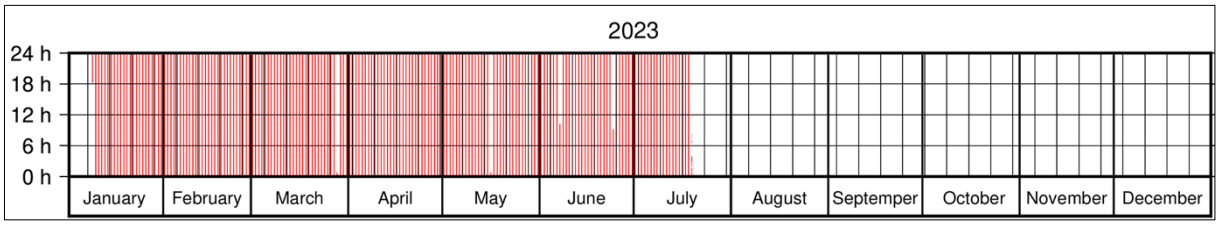

Fig. 4.22.2: Overview of the data recordings at the permanent GNSS site FOP1 (Forstefjell). Each vertical red line denotes one day of recorded data; the length of the line shows the recorded hours per day.

Preliminary (expected) results

All GNSS data will be analyzed at the home institution (post-processing) since precise orbit and clock data as well as observational data of permanent stations of the International GNSS Service are to be incorporated. From the processing we expect to infer precise coordinates (with an accuracy of 2 to 5 mm) and coordinate change rates (with an accuracy of 1 to 2 mm/a).

The data recordings are shown for the period January 2023 to January 2025 for Forstefjell (FOP1, Fig. 4.22.2), Weigel Nunatak (KOP1, Fig. 4.22.3) and SVEA (Fig. 4.22.4). It is clearly visible that all stations failed to record data during the polar winter, although for different time periods, due to low power. For the station at Weigel Nunatak (KOP1) a longer break has to be stated for the austral summer 2023/24. The reason for this has still to be clarified; electrostatic charging can be one possible reason. For the station Forstefjell (FOP1) we received recordings only until mid-July 2023 and no recovery after the polar winter. Also, here electrostatic charging could be one reason.

We are still processing the data. Moreover, the data will be included in a further reprocessing of Antarctic-wide distributed GNSS sites (GIANT-REGAIN project; Buchta et al. 2025), subject to a PhD project to be funded by DFG.

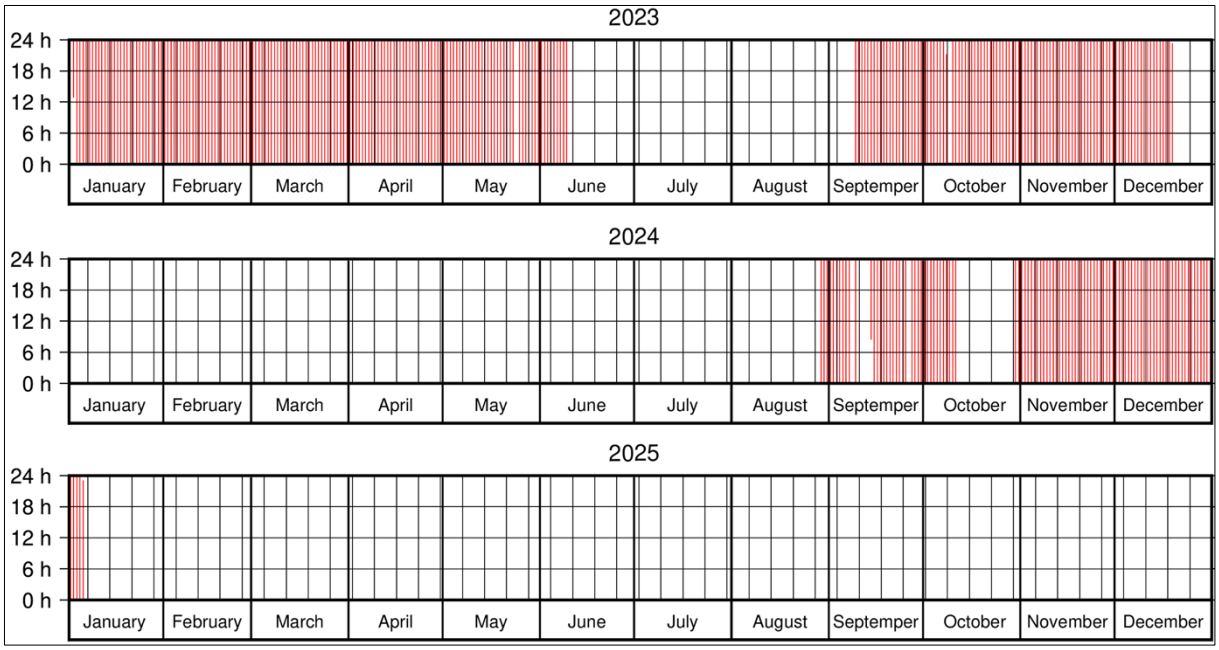

Fig. 4.22.3: Overview of the data recordings at the permanent GNSS site KOP1 (Weigel Nunatak). Each vertical red line denotes one day of recorded data; the length of the line shows the recorded hours per day.

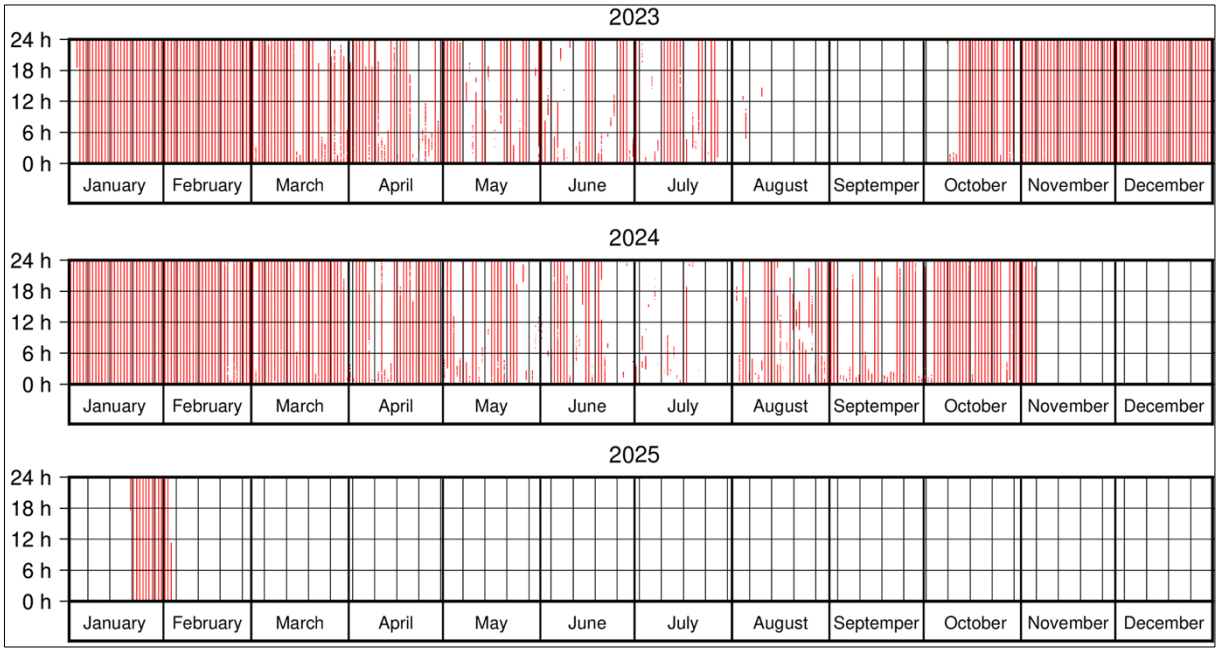

Fig. 4.22.4: Overview of the data recordings at the permanent GNSS site SVEA. Each vertical red line denotes one day of recorded data; the length of the line shows the recorded hours per day.

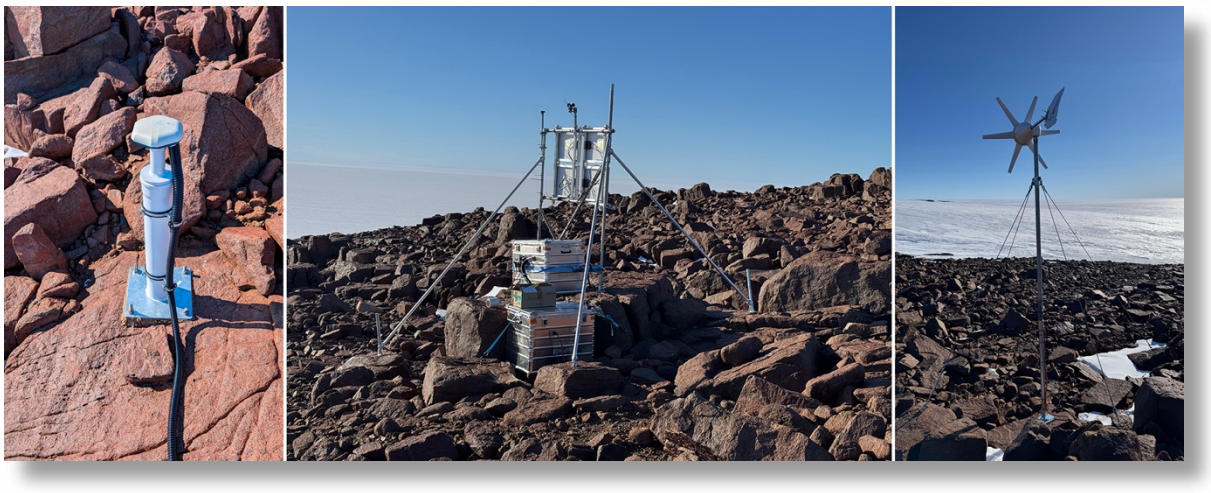

Fig. 4.22.5: GNSS station FOP1 at Forstefjell. Left: GNSS antenna, center: structure with boxes containing GNSS receiver, charge controller, batteries and further electronics, and solar modules; right: wind generator (after it had been repaired).

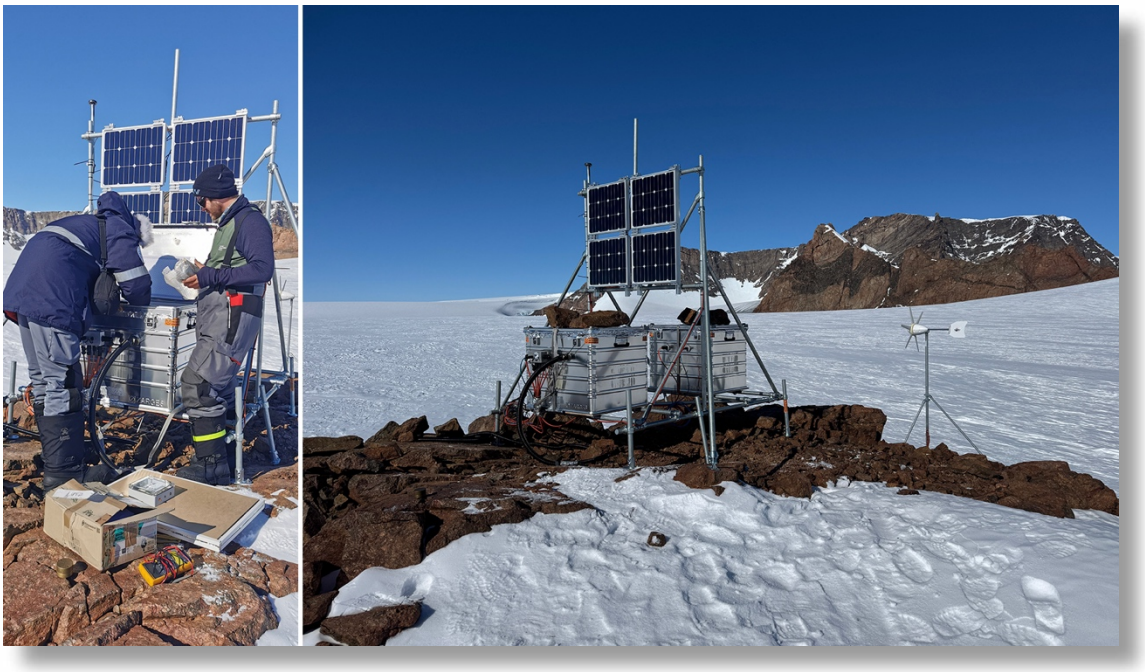

Fig. 4.22 6: GNSS station KOP1 at Weigel Nunatak. Left: During the maintenance work; right: Structure with boxes containing GNSS receiver, charge controller, batteries and further electronics, and solar modules; the wind generator can be seen further downhill to the right.

Data management

Original (raw) GNSS data will be archived at the GNSS database of TU Dresden in conjunction with the SCAR GNSS Database. Final data (processed results) will be published at PANGAEA in conjunction with a scientific publication.

In all publications based on this expedition, the **Grant No. AWI_ANT_28** will be quoted and the following publication will be cited:

Alfred-Wegener-Institut Helmholtz-Zentrum für Polar- und Meeresforschung. (2016a). *Neumayer III and Kohnen Station* in Antarctica operated by the Alfred Wegener Institute. Journal of large-scale research facilities, 2, A85. http://dx.doi.org/10.17815/jlsrf-2-152.

References

Buchta E, Scheinert M, King MA, Wilson T, Koulali A, Clarke PJ, Gómez D, Kendrick E, Knöfel C & Busch P (2025) Advancing geodynamic research in Antarctica: reprocessing GNSS data to infer consistent coordinate time series (GIANT-REGAIN). Earth System Science Data 17:1761–1780. https://doi.org/10.5194/essd-17-1761-2025, 2025.

5. OTHER SCIENTIFIC PROJECTS WITH AWI PARTICIPATION

5.1 Beyond EPICA – Oldest Ice Core

Frank Wilhelms[*1], Julien Westhoff[2], Matthias Hüther[1], Danilo Colino[3], Lisa Ardoin[4], Gianluca Bianchi Fasani[3], Marie Bouchet[5], Massimo Carnevale[3], Ailsa Chung[6], Inès Gay[7], Giulano Guidarelli[3], Manuela Krebs[1], Gunther Lawer[1], Johannes Lemburg[1], Martin Leonhardt[1], Michele Scalet[3], Federico Scoto[8], Barbara Seth[9], Lison Soussaintjean[9];
not in the field: Olivier Alemany[6], Carlo Barbante[8], Melanie Behrens[1], Pierre Henri Blard[4], Grant Boeckmann[2], Justin Chaillot[5], Dorthe Dahl-Jensen[2], Giuliano Dreossi[8], Hubertus Fischer[9], François Fripiat[4], Steffen Bo Hansen[2], Amaelle Landais[5], Maria Hörhold[1], Thom Laepple[1], Robert Mulvaney[10], Saverio Panichi[3], Frédéric Parrenin[6], Catherine Ritz[6], Barbara Stenni[8], Hans Christian Steen-Larsen[11], Jean-Louis Tison[4], Eric Wolff[12], Daniele Zanoni[8]
*frank.wilhelms@awi.de

[1]DE.AWI
[2]DK.PICE
[3]IT.ENEA
[4]BE.ULB
[5]FR.LSCE
[6]FR.IGE
[7]FR.IPEV
[8]IT.ISP-CNR
[9]CH.UNIBE
[10]UK.BAS
[11]NO.UBE
[12]UK.UCAM

Grant-No. AWI_ANT_30

Outline

The Beyond EPICA – oldest ice core project aims at retrieving an ice core spanning the Mid Pleistocene Transition (MPT) back into a 40 kyr cycle dominated climate about 1.2–1.5 Ma ago. The aim of the fourth season is production drilling of up to 900 m under ideal conditions. The recovery of the ice core, which is the meteoric sample for the reconstruction and interpretation of the atmospheric paleo-records, is the basis for the success of the Beyond EPICA– oldest ice project. We report the course of the deep drilling operation during the 2024/25 field campaign, from a depth of 1,836.18 m down to the bed at a preliminary depth of 2799.83 m.

Objectives

The Beyond EPICA field operation at Little Dome C aimed at coring as deep as possible and offered the opportunity to conduct ancillary surface studies. This report summarizes the third deep drilling season 2024/25, where the coring advanced from 1,836.18 m to the bed at a preliminary depth of 2,799.83 m.

Fieldwork

The main group left Europe on 8 November 2024 and stood by for the deployment between 10 to 12 November 2024 in Christchurch, New Zealand. On 12 November 2024 the main group departed Christchurch (NZ) to *Mario Zucchelli Station* (MZS) by Italian LC-130H. The logistic team went by Basler BT-67 to *Dome Concordia Station* (IT/FR) between 29 October and 7 November 2024, where the drilling and science group followed on 13 and 15 November2024, and proceeded after two days to the Little Dome C drilling camp. This resulted in 62 days (17 November 2024 – 18 January 2025) of available time for the drilling operation on site, where the full team could have been present from a logistical point of view for 59 days, as the science party had to leave 15 January 2025 to start closure of the camp. After three days at Little Dome C the team had prepared the core processing and drilling infrastructure, and both drilled and processed the first cores on 20 November 2024.

Putting the core processing operational, comprised getting access to the under-snow core-buffer and core processing line. In the science trench, the DiElectric Profiling (DEP) electronics had to be re-installed from being packed in the +4 °C wintering container and we custom fitted an insulation to electronics box to heat the LCR-meter, thus measuring Inductance (L), Capacitance (C) and Resistance (R) of an electronic circuit, to –35 °C temperature, as the calibration was not satisfactory at the initially found –47 °C ambient temperature in the science trench. The Swiss Saw was equipped with an emergency stop button in an easily accessible position.

The drill trench needed alignment of the logging system, re-installation of the winch- and control electronics of the drill and in relation to the mechanical part mainly preparation of the drill head.

The major upgrade to the science operation on site was the installation of a cavity ring-down spectrometer (PICARRO) in the ITASE (International Trans-Antarctic Scientific Expedition) module, a heated container at Little Dome C. To get the system fully operational took about a week longer till 27 November, when the first sequence was recorded. The sequence matched nicely the EDC99 record. To get a running PICARRO system, components from different European labs were assembled into one system. Auto-samplers were attached to the system and two PICARRO systems were available on site. For remote access form the labs and the PICARRO company back home, we linked the PICARRO spectrometer over the STARLINK system. After plenty of adjustments and calibration we finally ended with a setup, where one PICARRO controlled the auto-sampler and the other one executed the actual measurement. The data were compiled into one dataset with custom written scripts.

Till the end of November, we also covered the entrance to the science trench with a snow wall and removed load from the wooden wall. We trained drillers, loggers and processors and on 25 November 2024 we switched to a drill shift between 08:00 and 24:00 and came into a production mode of drilling with advancement around 30 m or beyond on a normal weekday.

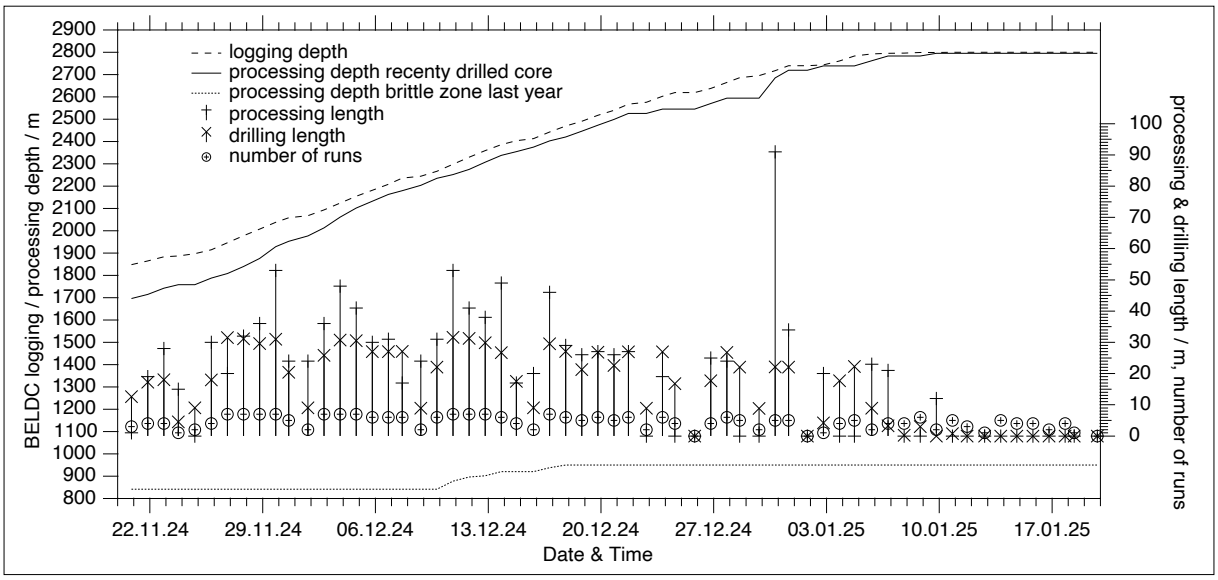

Fig. 5.1.1: Processing compared to logging depth and daily processing and drilling production versus time

The processing started with the 139 m core left at the end of the last season and then followed the freshly drilled core after letting the drill liquid evaporate from the surface for a few days. Around mid-December, we processed the section between 842 m and 950 m, that was left from the brittle zone and stored during the 2023/24 season. The maximum of processing was 91 m, and targeted to use a logistic opportunity for the transport of ice core boxes to *Mario Zuchelli Station.*

The drilling was exceptionally smooth and the just-below 30 m daily production was only interrupted by weekend and holiday rests. There were frequently broken drill parts, including DC-DC power supplies of the electronics, but we were able to prepare at all times enough spare components to just limit the interruption to the time needed for switching the entire components that failed or we judged to need maintenance. Urgent spare parts we did not have on site were provided by *Concordia Station*, ordered and shipped from Christchurch and parts of the dead weights needed for rock-drilling were even pre-manufactured at *Mario Zucchelli Station*. During run 904 on 10 January 2025 we brought up the last ice core with a smooth bottom and without any indication of a core break. The preliminary final loggers' depth was 2,799.83 m, that is corrected to 2,799.85 m after the last cores had been fitted and logged properly. Furthermore, there was silt attached to the surface and we conclude that we reached the underlying bed, or at least approached a boulder that covers the entire cross section of the core. To judge this, we switched the Danish supplied rock drill that already was on site to be deployed the following season.

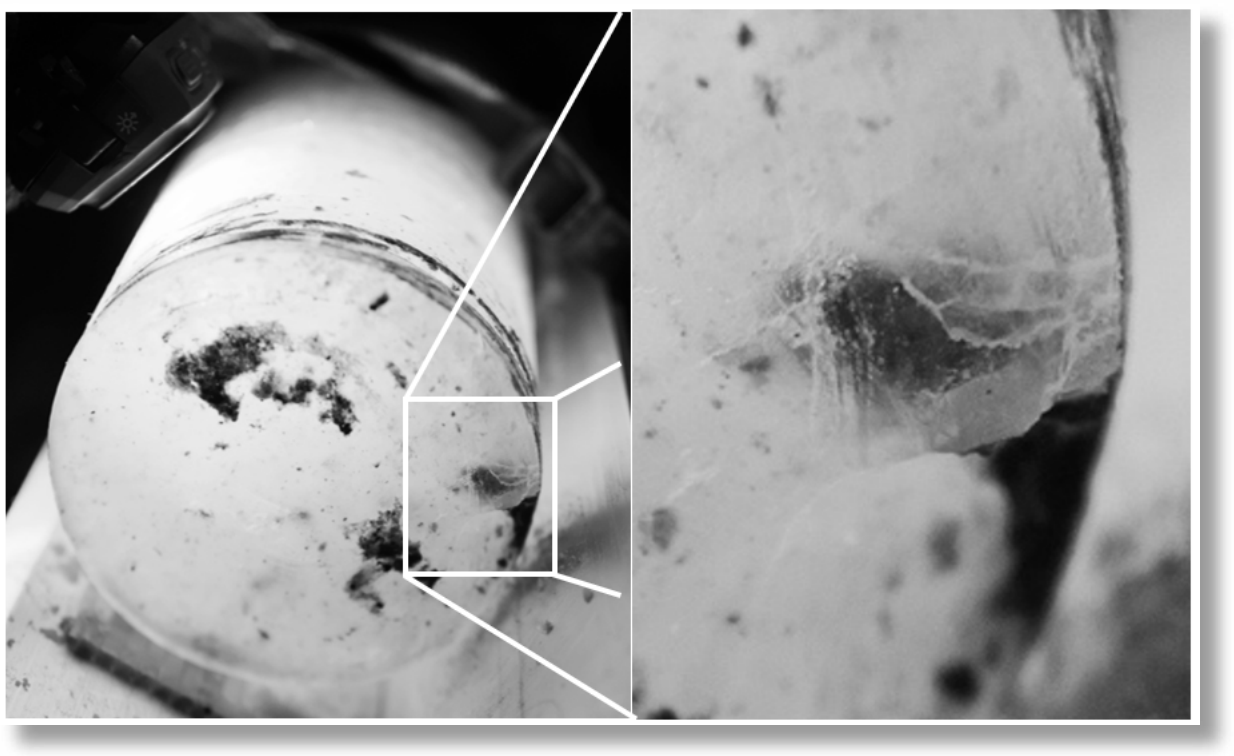

Fig. 5.1.2: Bottom view of the last ice core (bag 2800) brought up during run 904. The preliminary depth of 2,799.83 m was corrected to a final depth of 2,799.85 m after proper fitting and logging. The right image focuses on a core catcher mark that grabbed the core from below, but shows no indication of wedging action for breaking the core. Credit: F. Wilhelms ©PNRA/IPEV

Starting on 10 January 2025 we filtered the hole to clean up for a rock drilling attempt, and switched on 12 January to the rock-drill. This was possible as parts of the rock-drill had already been sent by the Copenhagen group for the planned deployment in the 2025/26 season. The still missing dead weights we manufactured in close cooperation with a team at *Mario Zucchelli Station*, who sent stainless steel parts we welded at Little Dome C and produced two dead weights of about 48 kg each, to be able to increase the weight on bit of the rock drill. We did one run with the Danish set-up of a custom-designed fluid pump attached to the commercial rock-drill, which we supplemented with the dead weights and powered by the drill's electronic-section. We observed very high power-consumption, when we started the motor, which we interpret as icing in the rock-drill's circulation pump. After 1:45 h at the bottom of the hole, we had to stop the motor and let it cool down. From a low idling current, we realized the shear pin to prevent overload of the gear had been broken and pulled up. The drill came to the surface without the outer core barrel, the drill bit and the reamer just above the drill bit. After consulting with experts in commercial mineral exploration equipment, it seems the trapezoidal three-start threads are prone to unscrew themselves. For the fishing operation we started to set the threads with ice and it was not possible to open them even with large pliers. This measure seems to be the appropriate remedy to prevent a similar failure during the course of the upcoming rock drilling operation during the next season. Proper tube wrenches are on the way from Copenhagen to little Dome C for tightening the joints hard without risking to damage them. For the next week, we fished for the left behind rock drill parts. The fishing comprised of cleaning runs just pumping up slush and the deployment of custom designed tools. A fast

assembled tool with seven magnets did not grab the missing parts. During the first fishing run the super-banger type coupling, which is incorporated as a safety feature to be able to unlatch the rock-drill in case the rock-core is too hard to break, disengaged and was left in the hole. During the second fishing run, we managed to re-engage the coupling and bring the drill string to the surface. The coupling has been overworked for the upcoming season and we expect it is much less prone to be accidentally disengaged.

After a custom designed fishing tool with a centering cone and spring-loaded core catchers was manufactured in parallel to the above-described fishing operation, it was deployed and grabbed the core barrel upon its first attempt.

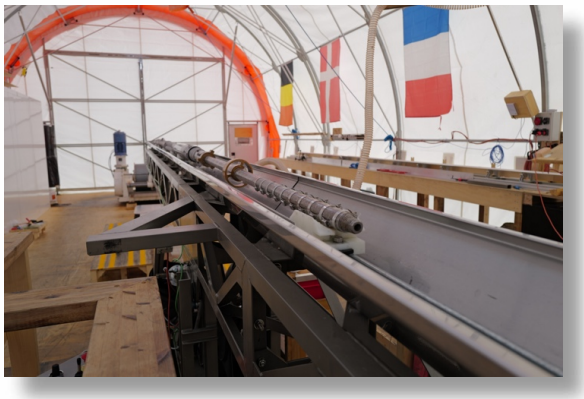

Fig. 5.1.3: The fishing tool with the seven magnets and the centering ring on the tower. Credit: F. Wilhelms ©PNRA/IPEV

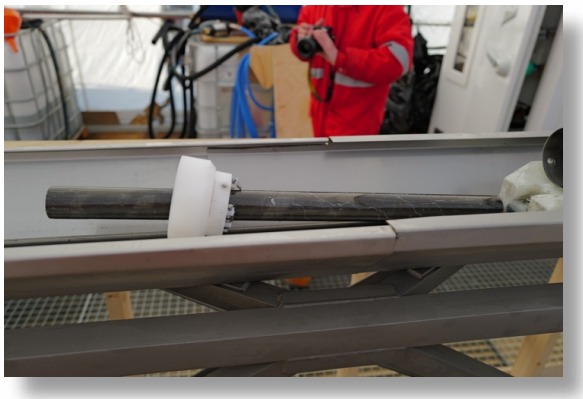

Fig. 5.1.4: The detached fishing tool, with visible arrangement of the core catchers. Credit: F. Wilhelms ©PNRA/IPEV

To our surprise, the drill collar and bit had also disengaged from the outer barrel, and only the core barrel came up to the surface. The drill bit-itself and the drill collar were still in the hole. We undertook further recovery attempts with the conical fishing tool with core catchers. While it seemed to engage, as we pulled 850 daN before the drill moved freely from the bottom of the hole, but this was not sufficient to grab the missing parts.

We machined a further conical tool attached to the rock-drill's outer core barrel with a pin to guide a possibly inclined lower drill-bit-drill-collar section. We did not observe releasing load that would indicate action of the pin and did not manage to screw the missing piece on. Observing the behaviour of the system, we guessed that the missing parts were frozen to the bottom and aligned upright in the middle of the hole. We overworked the three-start thread of the outer barrel to ease initial engagement of the thread and manufactured a guide of the cone to give better centering. Upon the last run of the season on 18 January 2025, we went with three extension rods of the rock-drill, exerted about 400 daN load at the bottom and rotated at different speeds. Although we had no indication of the thread engaging, we had to pull with 830 daN to free the drill from the bottom and finally got all parts up to the surface. When carefully disassembling the drill, we observed that all threaded connections were fully engaged. During the rest of the day, we packed down the drilling and logging infrastructure and closed the LDC camp during the morning of 19 January 2025.

Fig. 5.1.5: Conical tool with pin mounted to outer core barrel of the rock drill.
Credit: F. Wilhelms ©PNRA/IPEV

Fig. 5.1.6: The conical tool moved from the joint, the reamer and the drill head are entirely screwed into position.
Credit: F. Wilhelms ©PNRA/IPEV

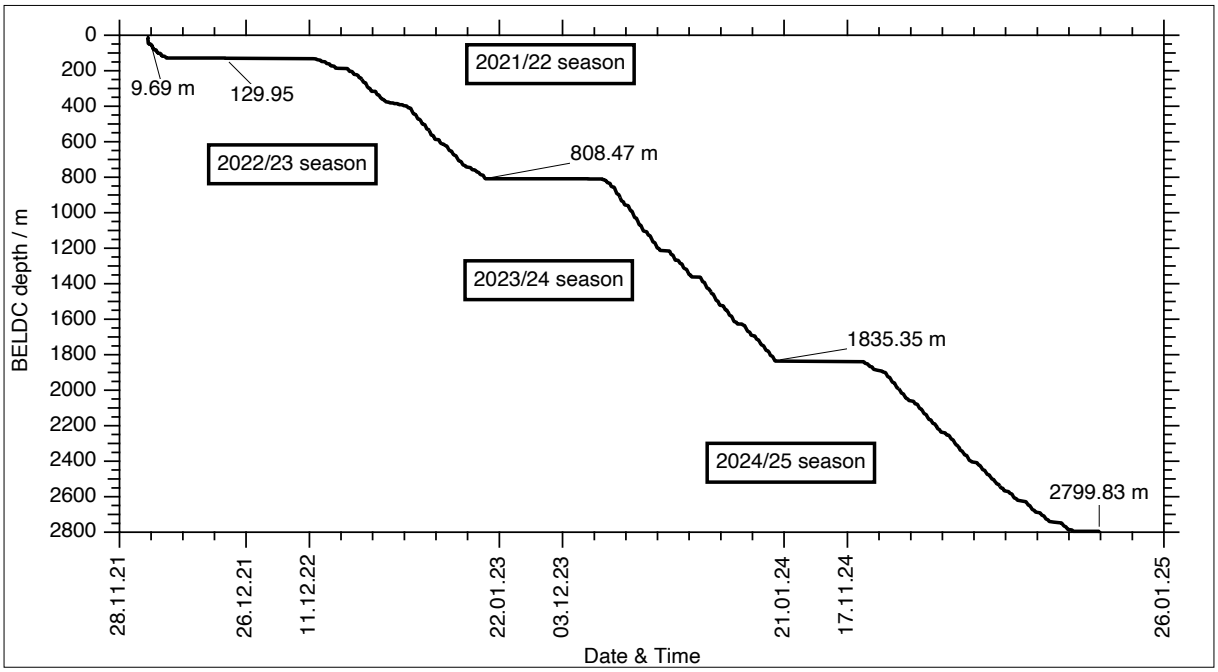

Fig. 5.1.7: Logging depth versus date for the four drilling seasons

According to the amended H2020-proposal MS3.4 (Drill to 2,800 m logging depth (bedrock) (M56), AWI) should be reached at the end of the drilling season. Figure 5.1.7 (BELDC depth vs. Date & Time) illustrates a steep penetration after the 4.5 m version of the drill was running smooth and at the end of the 2024/25 drilling season the project is according to the defined milestones absolutely on track. We also had and initial try with the rock drill and learned plenty of operational improvements for the application of the rock-drill for the first upcoming milestone MS3.6 (Retrieval of the basal ice and possibly bedrock (M68), UCPH), where the basal ice has already been retrieved and MS3.5 (Drilling a replicate core of the oldest ice (M68), UCPH), from a drilling point of view, has to be implemented after the bedrock drilling.

We managed to sample a 50 m trench to study spatial variability, as requested by the stable isotope consortium, and recorded a radar profile between *Concordia Station* and LDC along the flow line with the AWI RAMAC 500 MHz radar, as requested by the geophysics consortium, as ancillary surface programmes.

Federico Scoto left Little Dome C towards *Concordia Station* 14 January 2025 and departed towards *Mario Zucchelli Station* 15 January 2025. The same day Marie Bouchet, Ailsa Chung, Manuela Krebs, Lison Soussaintjean and Julien Westhof moved to *Concorida Station*. 16 January 2025, Federico Scoto left Antarctica to Christchurch. 18 January 2025, Lisa Ardoin, Gunther Lawer and Barbara Seth departed towards *Concordia Station* and were followed the next day by the rest of the team, Danilo Collino, Inès Gay, Matthias Hüther, Johannes Lemburg, Michele Scalet and Frank Wilhelms. Julien Westhoff moved to *Mario Zucchelli Station* on 24 January 2025 and was followed by Matthias Hüther, Manuela Krebs, Gunther Lawer, Johannes Lemburg, Martin Leonhardt, Michele Scalet and Frank Wilhelms on 28 January 2025. The entire group at *Mario Zucchelli Station* left towards *McMurdo Station* on 29 January 2025, where Julien Westhoff immediately proceeded to Christchurch and the rest of the group followd on 1 February 2025. Barbara Seth and Lison Soussaintjean moved from *Concordia Station* to *Casey Station* on 27 January 2025, from where they left Antarctica towards Hobart on 19 February 2025. On 27 January 2025, Lisa Ardoin, Marie Bouchet, Ailsa Chung and Inès Gay went to *Dumont d'Urville Station* and arrived in Hobart onboard *l'Astrolabe on* 6 February 2025. Danilo Colino departed *Mario Zucchelli Station* on 3 February 2025 and ultimately reached Christchurch 4 February 2025.

Fig. 5.1.8: The LDC team celebrating core 2400 on 14 December 2024, the start of the oldest stratigraphic ice ever drilled. FLTR: last row: M. Hüther, B. Seth, J. Westhoff, J. Lemburg, M. Krebs (sitting), L. Ardoin, D. Collino, G. Lawer, M. Scalet, middle row: F. Wilhelms, M. Bouchet, A. Chung, L. Soussaintjean, F. Scoto, front row: M. Leonhardt, I. Gay. Credit: M. Leonhardt ©PNRA/IPEV

Intial logging of the hole during filter runs

The inclination increased from around 4° up to 6° at the bottom of the hole. The inclination around 4° in about 2,300 m depth is in the desirable range to deviate from the hole later, when we will try to replicate the core older than 700 ka.

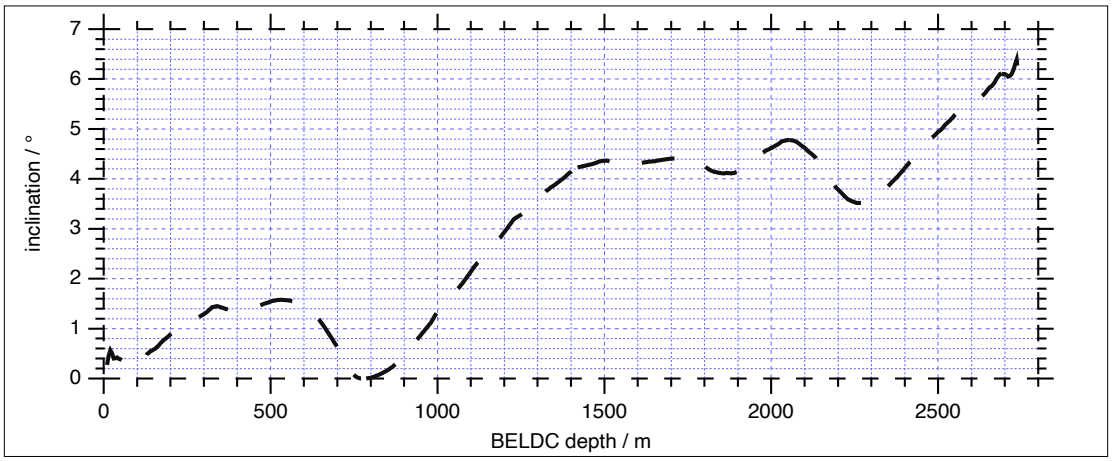

Fig. 5.1.9: Inclination of the hole recorded during the final filter run on 1 January 2025.

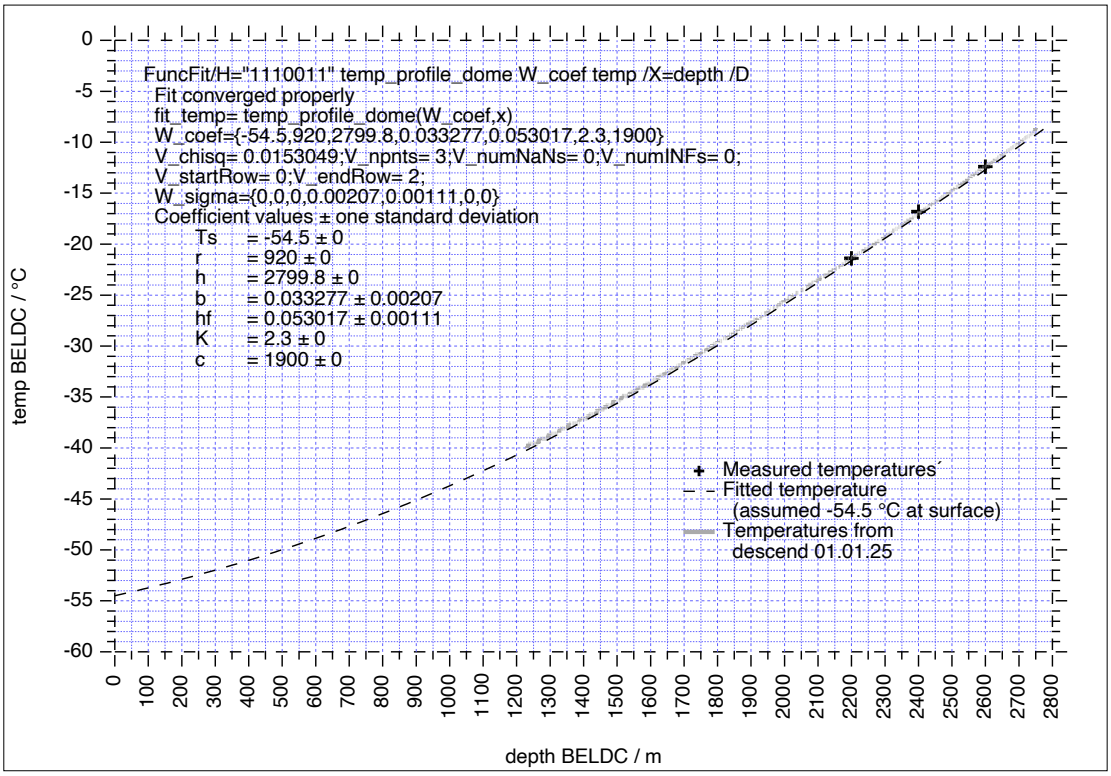

Fig. 5.1.10: The three temperature readings at three different depths logged on 23 December 2024 and temperatures logged on 1 January 2025. The line shows a fitted temperature profile for a Dome position. At the bed, we expect about –8 °C, which is ideal for drilling and close to the requirements below –8 °C, as formulated for the site selection during the pre-site survey. The fitted accumulation rate b = 3.3 cm yr^{-1} and the geothermal heat flux hf = 53 mW m^{-2} are reasonable values.

We recorded the temperature with an EL-USB-1-PRO industrial data logger from Lascar Electronics we had fitted in a custom-built pressure housing and which records above –40 °C. On 23 December 2024 we had parked it at three different depths to estimate the temperature gradient and on 1 January 2025 we recorded the temperature while filtering the hole. The results are consistent with a temperature around –8 °C at the bottom of the hole, which is also predicted by the pre-site survey.

Consumption and supply of drill liquid

The drilling operation consumed during the 2024/25 season 14,165 litres of drill liquid, which is 14.7 litres per drilled metre, where 13.2 litres per metre are needed to geometrically fill the hole. Over the entire drilling this is a consumption of 14.3 litres per drilled metre and an exceptionally good recovery with only 8% loss, that can only be achieved in stable drilling with long runs and effective drill chips handling, also considering that we spun the cuttings over the oldest section to collect them for radio-isotope dating. More than 4,000 litres of Estisol 140 and more than 3,000 litres of Estisol 165 are at Little Dome C, which are sufficient to replicate the oldest ice.

Expected age of the core

To estimate the age of the core, we recorded its dielectric profile (DEP) (Wilhelms, F. et al., 1998, Wilhelms, 2005) already in the field and wiggle matched it to the EPICA Dome C record (Parrenin et al., 2012), which recently received an updated common time scale AICC2023 Bouchet et al., 2023).

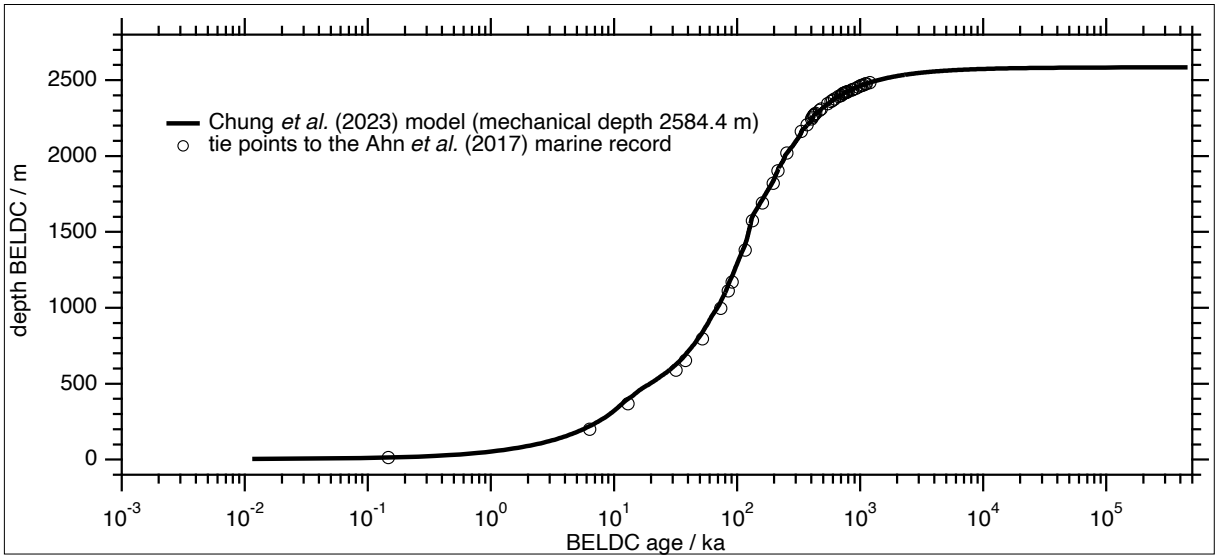

Fig. 5.1.11: The depth age relation for the BELDC core. Shown are the match points for the DEP record to the EPICA (EPICA community members, 2004) DEP record (Parrenin et al., 2012) and the $\delta^{18}O$ record to the Ahn et al. (2017) marine record. The solid line is a run of the Chung model with a mechanical height of 2,584.4 m and the tiepoints to 1.2 Ma.

The ice at 2,404 m is about 700 ka. Below, for which we had no previous ice-core records to match, we wiggle matched the $\delta^{18}O$ record from samples we scraped (shaved) from the surface and already analysed at Little Dome C with marine records (Ahn et al., 2017), the observed record seems to be reliable and better than the targeted minimal resolution of less than 20 ka m^{-1} to at least 1.2 Ma at 2,484 m, but the reliable record likely extending further back in time below. At 2,584 m, the electrical conductivity and stable water isotope records change to a different level. We interpret this lowermost 215 m thick section as unstratified ice. The lowermost five metres above the bed at 2,799.85 m are debris rich basal ice.

Data management

Environmental data will be archived, published and disseminated according to the data management plan of BE-OIC and therefore are in accord with international and European Union standards, most prominently the FAIR principle.

Any other data will be submitted to an appropriate long-term archive that provides unique and stable identifiers for the datasets and allows open online access to the data.

This expedition was supported by the Helmholtz Research Programme "Changing Earth – Sustaining our Future" Topic 2, Subtopic 1.

In all publications based on this expedition, the **Grant No. AWI_ANT_30** will be quoted.

References

Ahn S et al. (2017) A probabilistic Pliocene–Pleistocene stack of benthic δ18O using a profile hidden Markov model, Dynamics and Statistics of the Climate System 2(1)dzx002. https://doi.org/10.1093/climsys/dzx002

Bouchet M et al. (2023) The Antarctic Ice Core Chronology 2023 (AICC2023) chronological framework and associated timescale for the European Project for Ice Coring in Antarctica (EPICA) Dome C ice core. Clim. Past 19:2257–2286. https://doi.org/10.5194/cp-19-2257-2023

Chung A et al. (2023) Stagnant ice and age modelling in the Dome C region, Antarctica. The Cryosphere 17:3461–3483. https://doi.org/10.5194/tc-17-3461-2023

EPICA community members (2004) Eight glacial cycles from an Antarctic ice core. Nature 429:623–628. https://doi.org/10.1038/nature02599

Parrenin F et al. (2012) Volcanic synchronisation between the EPICA Dome C and Vostok ice cores (Antarctica) 0–145 kyr BP, Clim. Past 8:1031–1045. https://doi.org10.5194/cp-8-1031-2012

Wilhelms F et al. (1998) Precise dielectric profiling of ice cores: a new device with improved guarding and its theory. Journal of Glaciology 44(146):171–174. https://doi.org/10.3189/S002214300000246X

Wilhelms F (2005) Explaining the dielectric properties of firn as a density-and-conductivity mixed permittivity (DECOMP). Geophys. Res. Lett. 32:L16501. https://doi.org/10.1029/2005GL022808

5.2 IGIS 2024

Tim Stegmann[1]
Not in the field: Coen Hofstede*[1], Ole Zeising[1];
Olaf Eisen[1,2], Nick Gillett[3]
*coen.hofstede@awi.de

[1]DE.AWI
[2]DE.Uni-Bremen
[3]UK.BAS

Grant-No. AWI_ANT_51

Objectives

In preparation of two planned field seasons at Institute Ice Stream, Antarctica, as part of the research project “IGIS”, AWI employed engineer Tim Stegmann to service the Envirovibe (EV), a seismic vibrator that will overwinter at BAS depot SB9 at the English coast. The EV was used successfully at two consquetive field seasons at Thwaites Glacier (project GHOST, https://thwaitesglacier.org/projects/ghost) as part of the International Thwaites Glacier Collaboration (ITGC) and had overwintered at camp WAIS-divide. The task was to inspect the vehicle for maintenance and perform minor repairs.

IGIS (Impact of deep subglacial Groundwater on Ice Stream flow in West Antarctica) is an international collabarotion (UK, Germany, US) using geophysical methods to locate and model the role subglacial water plays in the dynamic response of Institute Ice Stream that feeds into the Ronne Ice Shelf. AWI’s task will be to collect long (>100km) seismic profiles to determine the subglacial topography and geology. The planned field seasons of IGIS are 2026/27 and 2027/28.

Fieldwork

The initial plan was that BAS would fly personnel via the BAS station Rothera to depot SB9. At the same time BAS transported the EV from WAIS-divide to SB9, this traverse is called “GHOST traverse”. This GHOST traverse should be at SB9 when personnel would arrive there, which would give a total of 3 to 4 weeks to service the EV and support BAS where needed.

As BAS provides the land logistics for the EV until 2028 when IGIS finishes, BAS provided logistics to bring Tim at SB9 via their base Rothera. On 01 December 2024 Tim Stegmann left Germany and arrived at Rothera at 07 December 2024. His return to Germany was on 14 January 2025.

On 21 December 2024 Tim Stegmann arrived at SB9b, a camp close to SB9 and a place the GHOST-traverse would pass by on its way to SB9. The GHOST traverse experienced problems, one of their tracked vehicles broke down. On 03 January GHOST traverse arrived at SB9b with considerable delay where Tim Stegmann was picked up. It was then clear that, due to the delays of the GHOST traverse, there would not be sufficient time for servicing of the EV. Unpacking the EV, necessary for servicing, and packing it for overwintering would take too much time. On 05 January GHOST traverse arrived at SB9. It was possible to get into the EV, and provide us with some quick measurements inside the EV cabin but no servicing was possible.

AWI had a debriefing with Tim Stegmann on 07 April 2025. For the traverses the EV is stored on a Lehmann sled and wrapped in a tarp (fly of a weatherhaven tent). Even for servicing the EV needs to be unwrapped. It is suggested that prefably future servicing should be done in a tent to avoid water intruding in the hydraulic system.

All new equipment, temperature sensor, tools, oil spill tarp, are on site and storded in Zarges box 8033.

Preliminary (expected) results

All things considered, the effort and cost to get personnel at location, the delays land traverses can easily experience, we decided not to send a technician over in 2025/26 but delay servicing of the Vibe until 2026/27 at the start of the field seasons of IGIS.

Tab. 5.2.1: Timeline of servicing season 2024/25

Date	Location	Task	Comment
15 Nov 2024	Bremerhaven	Employment Tim Stegmann as Technician	BAS organizes tickets Hamburg-Antarctica
01 Dec	Hamburg	Departure Antarctica	
07 Dec	Rothera	Arrival at BAS base, courses and helping out	10 days later as planned
21 Dec	SB9b	Arrival at camp close to depot SB9	GHOST traverse has problems
03 Jan 2025	SB9b	Arrival GHOST traverse SB9b	Decision to skip servicing Envirovibe
05 Jan	SB9	Arrival GHOST traverse SB9	
14 Jan	Punta Arenas	Return to Hamburg	
07 April	Bremerhaven	Debriefing servicing season	

Data management

Environmental data will be archived, published and disseminated according to the data management plan of BE-OIC and therefore are in accord with international and European Union standards, most prominently the FAIR principle.

Any other data will be submitted to an appropriate long-term archive that provides unique and stable identifiers for the datasets and allows open online access to the data.

This expedition was supported by the Helmholtz Research Programme "Changing Earth – Sustaining our Future" Topic 2, Subtopic 3.

In all publications based on this expedition, the **Grant No. AWI_ANT_51** will be quoted.

5.3 PolarConnection – Movement Ecology, Diseases Dynamics and Pollutions in Antarctic Breeding Seabirds

Simeon Lisovski*[1], Martha Maria Sander[1], [1]DE.AWI
Thomas Krumpen[1], Christiane Böckel[1] [2]DE.FLI
not in the field: Anne M. Günther[2]
* Simeon.Lisovski@awi.de

Grant-No. AWI_ANT_33

Outline

Migratory birds link ecosystems across the globe. The annual journeys of billions of individuals over vast distances play a crucial role in shaping the dynamics and functioning of ecosystems. The ice-free terrestrial areas of Antarctica are almost exclusively inhabited by migratory seabirds arriving from all oceans, attracted by ideal breeding conditions. The offshore islands of the Antarctic Peninsula serve as key hotspots for nesting seabirds. However, little is currently known about how global and local movement patterns influence ecologically relevant processes–such as the spread and circulation of viruses and pathogens (e.g. highly pathogenic H5N1), or the introduction of environmental pollutants.

Objectives

- Mapping Global Connectivity: Track migratory routes of seabirds traveling to King George Island using geolocators to understand global connectivity patterns.
- Linking Movement with Transmission: Examine the spatial relationships between global migratory networks and the transmission of viruses (including pathogens) and pollutants.
- Local Interaction Networks: Record fine-scale local movement patterns using high-resolution GPS tracking to construct an interaction network within and between seabird species nesting on King George Island.
- Using drones to count seabird population numbers on offshore islands: The use of drones aims to collect scientific data for population surveys of seabirds, through the development of standardized flight plans, and to gather imagery for training AI-based analysis methods, supported by simultaneous ground counts.

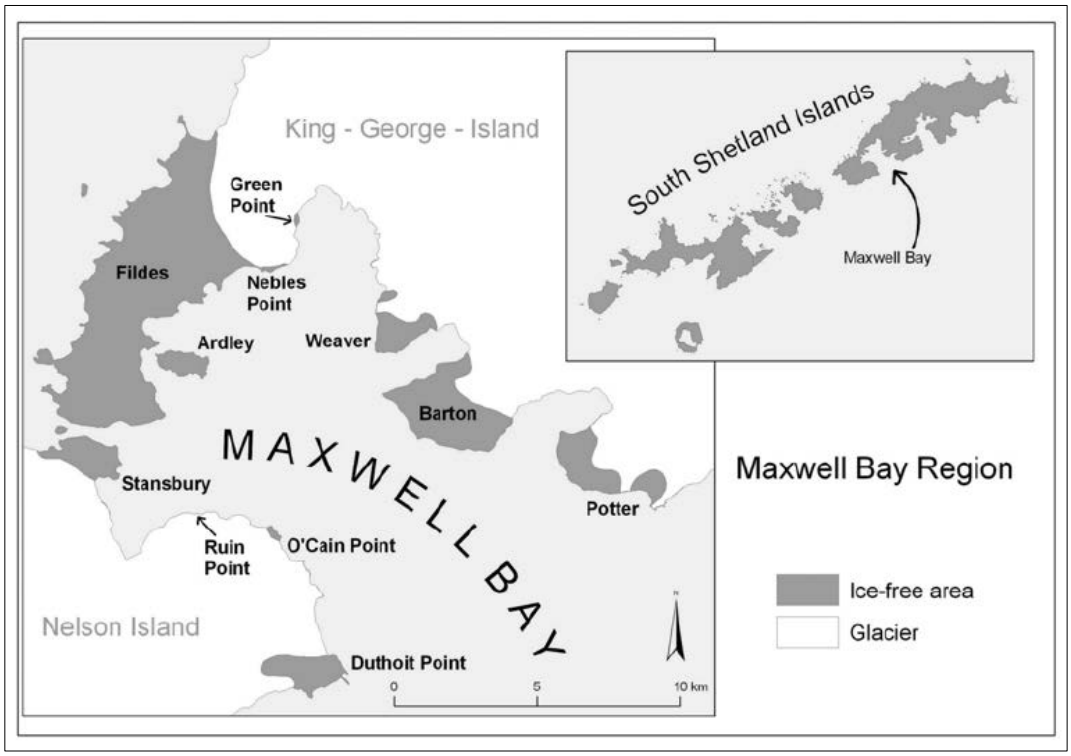

Fig. 5.3.1: King George Island and Nelson Island with the ice-free areas of Maxwell Bay

Fieldwork

During our expedition to King George Island from 18 November 2024 to 20 February 2025 (with no work and people on the ground between 6 December 2024 and 13 January 2025), we conducted extensive fieldwork focused on understanding the movement ecology, health, and potential pathogen dynamics of seabird populations. Our work was carried out primarily on Fildes Peninsula and Ardley Island, within the Antarctic Specially Protected Areas (ASPAs) 125 and 150.

We collected biological samples from a total of 189 live (and 41 dead) seabirds, including 110 Gentoo penguins, 1 Chinstrap penguin, 26 Brown skuas, 27 South polar skuas, 21 Southern giant petrels, 3 Imperial shags, and 1 Kelp gull. From these individuals, we obtained blood, pharyngeal and cloacal swabs, and feather samples for further analysis. In addition, we deployed GPS tags and ARGOS transmitters on Brown (10) and South polar skuas (12), Southern giant petrels (10), and one Kelp gull (1), to track both local and long-distance movements. We also retrieved light-level geolocators from several individuals (10 Brown skuas, 18 South polar skuas, 9 Giant petrels) that had been tagged during previous field seasons.

Capture and handling techniques were tailored to each species to ensure minimal disturbance. Penguins were captured by hand or with a net and were not ringed or tagged, though we applied a new, approved method for blood collection from the back, which proved safer and more effective than the traditional method via foot veins. Skuas were captured using hand techniques or a baited ground snare; we applied metal and colored rings, conducted morphometric measurements, and took biological samples. Southern giant petrels were carefully captured on their nests, with particular attention paid to avoiding disturbance of neighboring breeding pairs. All equipment attached to birds, including transmitters and loggers, adhered to the guideline of being under 5% of the animal's body weight, and all devices were attached using non-invasive, reversible methods.

In terms of disease surveillance during the ongoing highly pathogenic avian influenza H5N1 panzootic, we followed strict safety protocols to collect swab samples from both living and deceased birds.

Fig. 5.3.2: Left: Capture of skuas using a ground snare and sausage bait. Center: GPS tag on a South Polar Skua, attached to the back feathers with duct tape. Right: Banding with metal and color rings; attachment of the GLS logger using two cable ties on the metal ring

We also conducted drone surveys over a Southern giant petrel colony using a DJI Matrice 400 RTK equipped with RGB and thermal infrared sensors. A total of four drone flights were carried out at varying altitudes (60, 90, 120 meters) and times of day to optimize data quality. These flights were designed to test the potential for remote, standardized population counts and to collect imagery for training AI-based counting methods. We monitored all wildlife closely during drone operations and observed minimal disturbance, with only Kelp gulls exhibiting noticeable–but likely curiosity-driven–reactions.

Preliminary (expected) results

Of 15 dead Brown skuas tested, 11 were confirmed positive for H5N1 by the Friedrich-Loeffler-Institut. Other species tested included South polar skuas, Southern giant petrels, Cape petrels, terns, storm petrels, penguins, gulls, and even Antarctic fur seals, with no additional positive results.

The global migration data and the local tracking data show significant differences between species, with South polar skuas migrating into the northern hemisphere (Atlantic and Pacific) and feeding solely on marine food, Brown skuas migrate to the off shores of Patagonia and the River Plata estuary, likely feeding on both marine and terrestrial food. In Antarctica Brown skuas heavily depend on penguins as prey and actively search the shorelines for food. Southern giant petrels remain close to the breeding site during the austral winter. Feeding occurs both at the ocean and on land. These differences may, to some extent, explain the differences in susceptibility to H5N1 and may also define ther differential role in the spread and amplification of the virus.

The (pilot) drone surveys provided first important insights into the best survey height, the time of the day and the required frequency of surveys to detect breeding and filter out non-breeding individuals. Notably the use of thermal infrared showed promising results, however, only if the survey has been conducted shortly after sunrise. During the day, the contrast in temperature between the brids and the environment dissapeared.

Data management

Raw data information and results will be submitted to an appropriate long-term archive upon first pulication of the results, providing unique and stable identifiers for the datasets and allows open online access to the data.

This expedition was supported by the Helmholtz Research Programme “Changing Earth – Sustaining our Future” Topic 5, Subtopic 3.

In all publications based on this expedition, the **Grant No. AWI_ANT_33** will be quoted.

5.4 SIGMA-II – Sediment-RIch Glacial Meltwater Plumes Affecting Benthic-Pelagic Habitats at Recently Deglaciated Coasts of Beagle Channel and King Georg Island, Antarctica

Kerstin Jerosch[1]; Clarissa Vock[1], Grit Steinhöfel[1], Friederike Weith[1]; Rosby Gomez Farfan[2], Mariano Rodriguez[3], Maria Bagur[4], Maria Włodarska-Kowalczuk[5], Piotr Bałazy[5], Rafał Boehnke[5], Katarzyna Błachowiak-Samołyk[5]
*Kerstin.jerosch@awi.de

[1]DE.AWI
[2]PE.UCdS
[3]ARG.IPCA-TDF
[4]ARG.CONICET-CADIC
[5]PL.IOPAN

Grant-No. AWI_ANT_34

Outline

The Southern Patagonia and the West Antarctic Peninsula are remarkable fjord regions of a rich marine ecosystem and dynamic landscape evolution, a process that is strongly driven by the current dramatic glacier retreat. These fjords are influenced by marine-determined glaciers that promote upwelling of nutrient-rich waters, as well as land-terminated glaciers that maintain a stratified water column. In our fieldwork, we employed a range of methods to examine biological, physical, and chemical processes from the glacier front to the deep-water zones at the fjord mouth. We sampled streams in glacier forefields to explore weathering and erosion processes on land. Using Unmanned Airkraft Systems (UAS), known as *drones*, we monitored meltwater plumes in the fjords and conducted water sampling and *in-situ* measurements to assess turbidity and organic carbon content in suspended sediments, which are closely linked to biological activity. Sediment cores were collected to examine sedimentation and diagenetic processes. Scuba divers mapped the community structure of the benthic fauna in kelp forests with photoquadrats and belt transects, providing key insights into distinct ecosystems. Additionally, we investigated the composition and abundance of zooplankton communities in deep fjord water. Through image and spatial analyses, along with geochemical data, our research aims to provide a comprehensive understanding of the marine and benthic dynamics within fjord ecosystems. The gained data hold promises for offering valuable insights into the future of Antarctic and Patagonian fjords.

Objectives

The campaign ANT-Land-SIGMA-II 2024/2025 with leg 1 to the Beagle Channel (10 days ship time) and with leg 2 to King George Island (3 months field work) aimed to spatially assess and quantify the influence of glacial meltwater discharge on marine ecosystems in different fjord environments, in Southern Patagonia and the West Antarctic Peninsula (WAP). The fjord environments are impacted by 1) marine- and land-terminated glaciers, which affects supply of suspended particulate material (SPM) as well as upwelling and stratification of water masses within the fjords and 2) surrounding lithology, which influences nutrient supply and composition of SPM. It is known that glacier retreat leads to an increased supply of SPM to fjords and therefore higher sedimentation rates, which have major effects on the marine and benthic ecosystem causing habit shifts (e.g., Sahade et al. 2015; Breackman et al. 2021; Quartino et al. 2013; Jerosch et al. 2018, 2019).

During leg 1, four fjords in the Beagle Channel (Yendegaia, Alemania, Garibali, Francés) were targeted; leg 2 focused on sampling five fjords at King George Island, West Antarctic Peninsula: Maxwell Bay (Potter Cove/Fourcade Glacier, Marian Cove/Moczydlowski Glacier; Collins Harbour/Polar Friendship Glacier; Admiralty Bay (Lussich Cove/Krak Glacier; Mackellar Inlet/Domeyco Glacier Southern and Northern side) with the following objectives:

- Air-borne UAS-based reflectance georeferenced mapping of meltwater discharge and its distribution within the fjord (meltwater plumes)
- Examining the relationship between air-borne (multispectral) and water-borne data (salinity, temperature, turbidity, suspended particulate matter, oxygen, chlorophyll-a, pH, total organic carbon, geochemistry/stabile isotopes, phytoplankton) for calibration and extrapolation purposes (satellite data)
- Investigating of meltwater streams to examine terrestrial weathering and erosional processes (SPM, TOC and chemical composition of dissolved load)
- Investigating of fjord sediments (deposition mechanism, diagenetic processes, marine foreward versus reverse weathering)
- Investigating the composition and abundance of zooplankton communities in different Patagonian fjord settings
- Mapping of benthic communities along Patagonian fjord axes (photoquadrats and video transects)
- Investigating the effect of meltwater discharge on benthic communities and zooplankton

Air-borne data and water parameters obtained for different fjord settings will be evaluated at AWI (Germany) to assess the distribution and contents of SPM/TOC and its effect on the planktonic and benthic communities in different fjord settings. Multispectral sensors of the DJI P4 Multispectral UAV will be used for the analysis of water turbidity (Fig. 5.4.1A, B). Red wavelengths are applicable for identifying values representing low-turbidity and medium-turbidity waters (<70 FNU) and for identifying red and white sediments in water. High turbidity in water correlates with longer wavelengths such as Red Edge and Near Infrared (Wójcik et al. 2019). Furthermore, we will conduct geochemical analyses (TOC, element composition and Li isotopes) in AWI labs in order to characterize dissolved load and sediment supply to identify chemical and physical processes on land, in the water column and in fjord sediments, taken with the UWITEC corer and YSI Exo2 Sonde (Fig. 5.4.1C, D).

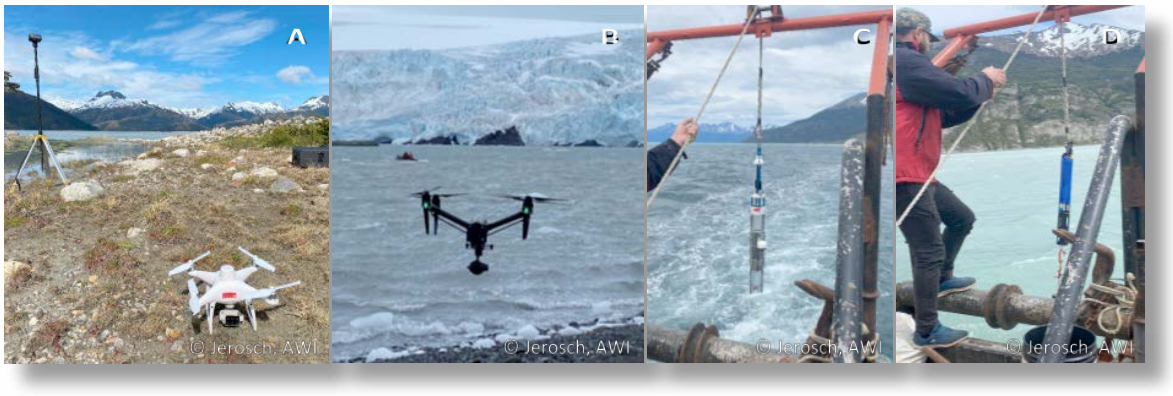

Fig. 5.4.1: A) DJI P4 multispectral (blue, green, red, red edge and near infrared) GNSS Mobile Station ensures precise position data and centimeter-accurate measurements. B) DJI Inspire 2 Zenmuse X5s camera for high resolution RGB (for macroalgae, plume, vegetation mapping) C) UWITEC corer, 60 x 6 cm tubes, for sampling TOC, chlorophyll-a, texture, porewater geochemistry D) YSI Exo2 Sonde for conductivity, temperature, dissolved oxygen, fDOM, pH, turbidity and chlorophyll-a measurements

Furthermore, airborne UAS data have a high potential to contribute to operational monitoring programs and can form useful links between satellite and in-situ observations (De Keukelaere et al. 2023).

The results will be compared with those obtained in King Georg Island during leg 2 of ANT-Land-SIGMA-II 2024/2025 and ANT-Land-SIGMA-I 2022/2023.

The results of ANT-Land-SIGMA-II 2024/2025 (this campaign) will be compared with those of ANT-Land-SIGMA-I 2022/2023 in King Georg Island.

Fieldwork

Field work was conducted along environmental gradients from the glacier front to the deep-water zones at the fjord mouth. Sampling and in-situ measurements were performed either on board of the vessel Huracan, using a zodiak, on land or by scuba diving (Fig. 5.4.2: leg 1, Fig. 5.4.3: leg 2). Air-borne based observation together with water sampling were conducted at the same field stations as zooplankton sampling and mapping of benthic communities if possible. Additional we took sediment cores along the fjord axes and sampled water from terrestrial meltwater streams.

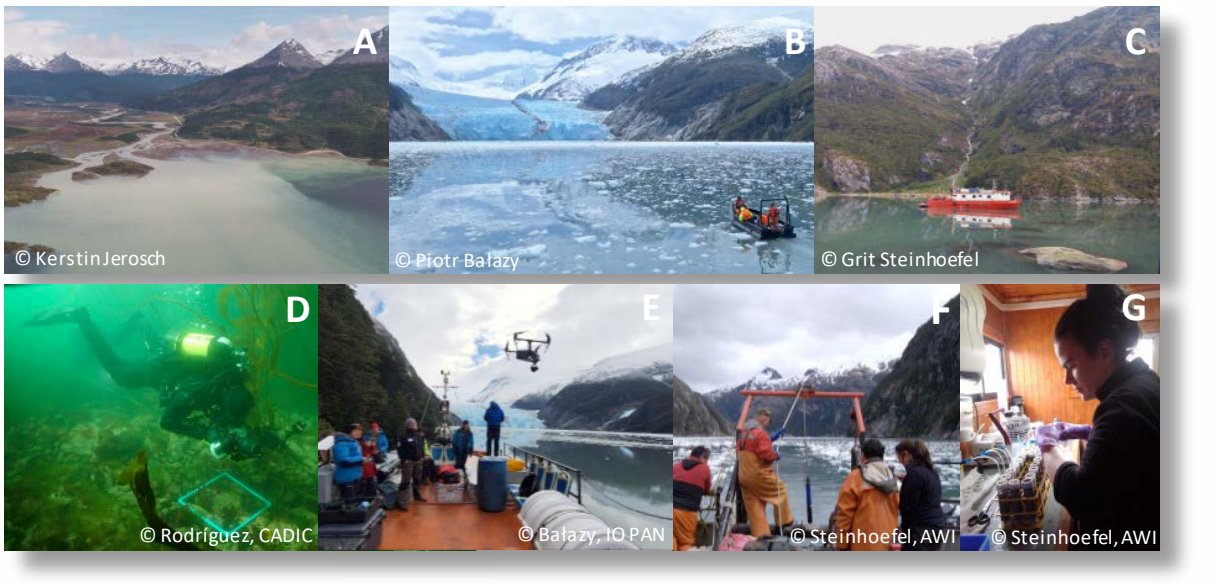

Fig. 5.4.2: Fjord landscapes and examples of field work during ANT-Land-SIGMA-II leg 1: A) Head of Yendegaia fjord dominated by land-terminated glaciers with major meltwater inflow causing sediment plums B) Head of Garibaldi fjord with marine-terminated glacier C) Huracan in the Garibali fjord with inflowing meltwater stream in the background and kelp forests in the shallow water zone D) Mapping of the benthic fauna in kelp forests by scuba diving E) Air-borne UAS-based mapping of meltwater discharge and its distribution within the fjord F) Measuring of water parameters using the CTD YSI Exo2 Sonde G) Extraction of pore water on board

UAS data and water parameters within fjords were obtained as follows: a station consisted of about 3 h UAV missions with a DJI Phantom 4 multispectral (blue, green, red, red edge, and near infrared bands) and a DJI Inspire 2 (high resolution Zenmuse X5s with a standardized Red-Green-Blue colour model (sRGB)). The RTK positioning and the D-RTK 2 Mobile Station provided high precision georeferencing and an independent flight planning system controlled via the DJI GO4 and DJI GS Pro Apps. The missions were accompanied by synchronous in--situ water measurements using a YSI Exo2 Sonde (for conductivity, temperature, dissolved oxygen, dissolved organic matter, pH, turbidity, and chlorophyll-a) from a zodiac. Inside the recorded area five water samples were taken from the surface and one with a Niskin bottle at 10 m depth (Fig. 5.4.3A). Furthermore, one phytoplankton sample were taken from the water column down to 10 m depth.

To investigate fjord sediments, we took two cores at each sampling site two cores using an UWITEC corer (60 x 6 cm) for TOC, chlorophyll-a, texture, porewater, geochemistry analyses (Fig. 5.4.1C, 3D). At the coast, we sampled different types of meltwater streams characterized either by high turbidity caused by subglacial discharge or low turbidity typical for surface glacier melting. Water parameters were determined using the CTD YSI Exo2 Sonde (Fig. 5.4.2: leg 1, Fig. 5.4.3: leg 2). Water samples will be examined for SPM/TOC and chemical composition.

Fig. 5.4.3: ANT-Land-SIGMA-II leg 2 – impression of sampling with different gears on the coast and in the water in front of three glaciers in Admiralty Bay, King George Island, Antarctica: A) Water sampling with a Niskin bottle; B) deployment of YSI Exo 2 sonde in a meltwater stream and C) in a fjord D) Sediment sampling E) Drone missions

Preliminary (expected) results

During the two legs of the campaign to the Beagle Channel (10 days) and King George Island (3 months) we accomplished the forseen program. An overview of the number of samples and the sample site is given in Table 5.4.1 and in Figure 5.4.4.

Tab. 5.4.1: Sample type, purpose and number as well as number of UAS missions during ANT-Land-SIGMA-II. For more detailed information refer to Appendix A4 and A.5.

Device/sample type	Parameter / Purpose	No
EXO2 Deployments	CTD, chlorophyll-a, pH, turbidity, O_2, fDOM	326
Filter (Durapore)	TOC, element composition and Li isotopes	73
Fresh Water	TOC, element composition and Li isotopes	107
Pore water	TOC, element composition and Li isotopes	504
Rocks	TOC, element composition and Li isotopes	43
Sea water	TOC, element composition and Li isotopes	373
Meltwater stream sediment	TOC, element composition and Li isotopes	7
Multispectral UAS missions	turbididy, chlorophyll-a	43
RGB imagery UAS missions	plume extent, macroalgae, vegetation	45
Filter (GF/F)	SPM / TOC (fresh and marine water)	476
UWITECH cores	Texture, Geochemistry, chlorophyll-a, TOC	43

We present the first results of some locations analyzed during the campaign ANT-Land-SIGMA-II (11/2024 – 03/2025): from four glaciers in the Beagle Channel (Garibaldi, Francés, Alemania and Yendegaia Glacier) and from five glaciers of the WAP, King George Island (Domeyko and Krak Glaciers in Admiralty Bay; Fourcade Glacier in Potter Cove, Moczydlowski in Marian Cove and in Polar Friendship Glacier in Collins Harbour).

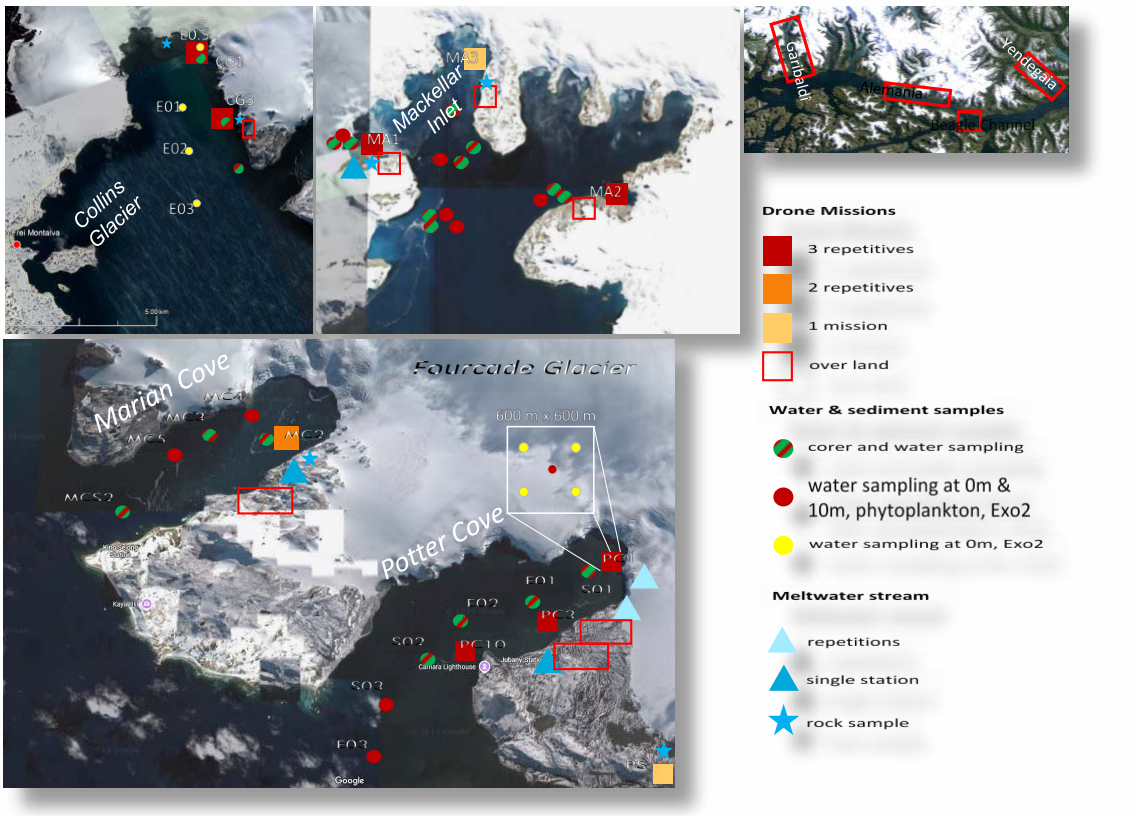

Fig. 5.4.4: ANT-Land-SIGMA-II (11/2024-03/2025) study sites in the Beagle Channel and at King George Island.

Garibaldi Fjord, Collins Harbour, Marian Cove and Admiralty Bay are related to glaciers that are defined as marine-terminating glaciers. Marine-terminating glaciers have a direct impact to coastal circulation due to their direct interaction with ocean waters. Warm ocean currents accelerate submarine melting retreat faster than terrestrial-terminating glaciers through calving. The retreat of marine-terminating glaciers due to climate change has a more pronounced effect on marine circulation, as it directly alters the freshwater balance and heat exchange in the ocean.

The terrestrial-terminating glaciers (Alemania, Francés, Yendegaia and Fourcade) are dominated by high turbidity values mainly at the sea surface down to 5-10 m. Turbidity, caused by suspended sediments in water, significantly influences marine ecosystems, since elevated turbidity reduces light penetration, which can limit photosynthesis in phytoplankton, the foundation of marine food webs. The sedimentation of particles further influences benthic habitats especially for non-mobile filter-feeders such as ascidians. In the Beagle Channel, Alemania Glacier releases high amounts of SPM with cold water to the marine ecosystem.

The Garibaldi Fjord is located in the Chilean territory of the Beagle Channel, shaped by the Garibaldi Glacier, and is surrounded by steep valley walls, dense forests, and active waterfalls. Salinity, temperature and turbidity in Figure 5.4.4 were measured in different distances to the glacier with the multiparametric YSI Exo 2 sonde down to 40 m water depth. The transect from fjord entrance in the South to the fjord head in the North, where the glacier terminates close to the glacier, show the interaction between the meltwater (stratification of salinity, low temperature and high turbidity values at the surface) and fjord's waters. The freshwater layer often carries nutrients and sediments, influencing biological productivity. However, it

also reduces mixing between water layers, which can limit the distribution of oxygen and nutrients in deeper waters. This dynamic plays a critical role in fjord and coastal ecosystems near marine-terminating glaciers.

At King George Island (WAP) we took samples at Krak, Domeyko Glacier, Fourcade, Moczydlowski and Polar Friendship Glaciers. The analysis of the Exo2 data of five glaciers at King George Island revealed significant differences. Krak and Fourcade Glacier show high SPM values, however, they differ clearly in salinity, which reflects the huge amount of meltwater entering into the cove through its large meltwater streams, while Krak Glacier provides the sediment exclusively through sediment release beneath the glacier. Marian Cove and Collins Harbour are comparable in salinity, temperature and turbidity; Mackellar Inlet and Keller Peninsula are both located at Moczydlowski Glacier and vary slightly in the penetration depth of SPM.

The glacial influence in Collins Harbour (Polar Friendship Glacier) and in Marian Cove (Moczydlowski Glacier) is highest close to the glacier fronts. These fjords are comparable deep. Potter Cove (Fourcade Glacier) and Lussich Cove (Krak Glacier) show the highest turbidity values. Potter Cove is characterized by a wide transport of sediments and freshwater into the bay, while in Lussich Cove the high turbidity values are more limited to the area near the fjord head.

Data management

Environmental data will be archived, published and disseminated according to international standards by the World Data Center PANGAEA Data Publisher for Earth & Environmental Science (https://www.pangaea.de) within two years after the end of the expedition at the latest. By default, the CC-BY license will be applied.

Any other data will be submitted to an appropriate long-term archive that provides unique and stable identifiers for the datasets and allows open online access to the data.

The ANT-Land-SIGMA-II expedition was supported by the Helmholtz Research Programme “Changing Earth – Sustaining our Future” Topic 4, Subtopic 2, and was funded by AWI and the EU project CoastCarb (Marie Curie Action RISE, Research and Innovation Staff Exchange, H2020-MCSA-RISE 872690, www.coastcarb.eu).

In all publications based on this expedition, the **Grant-No. AWI_ANT_34** will be quoted.

References

Braeckman U, Pasotti F, Hoffmann R *et al.* (2021) Glacial melt disturbance shifts community metabolism of an Antarctic seafloor ecosystem from net autotrophy to heterotrophy. Commun Biol 4:148. https://doi.org/10.1038/s42003-021-01673-6

De Keukelaere L, Moelans R, Knaeps E, Sterckx S, Reusen I, De Munck D, Simis SGH, Constantinescu AM, Scrieciu A, Katsouras G, Mertens W, Hunter PD, Spyrakos E & Tyler A (2023) Airborne Drones for Water Quality Mapping in Inland, Transitional and Coastal Waters-MapEO Water Data Processing and Validation. Remote Sensing 15 (5):1345. https://doi.org/10.3390/rs15051345

Jerosch K, Pehlke H, Monien P, Scharf F, Weber L, Kuhn G, Braun M & Abele D (2018) Benthic meltwater fjord habitats formed by rapid glacier recession on King George Island, Antarctica. Philos Trans A Math Phys Eng Sci 376:2122. https://doi.org/10.1098/rsta.2017.0178

Jerosch K, Scharf FK, Deregibus D, Campana GL, Zacher K, Pehlke H, Falk U, Hass HC, Quartino ML & Abele D (2019) Ensemble Modeling of Antarctic Macroalgal Habitats Exposed to Glacial Melt in a Polar Fjord. Frontiers in Ecology and Evolution 7: 207. https://doi.org/10.3389/fevo.2019.00207

Sahade R, Lagger C, Torre L, Momo F, Monien P, Schloss I, Barnes DKA, Servetto N, Tarantelli S, Quartino ML, Deregibus D, Campana GL, Latorre GEJ & Momo FR (2013) Evidence of Macroalgal Colonization on Newly Ice-Free Areas following Glacial Retreat in Potter Cove (South Shetland Islands), Antarctica. PLoS ONE 8(3):e58223. https://doi.org/10.1371/journal.pone.0058223

Wójcik KA, Bialik RJ, Osińska M & Figielski M (2019) Investigation of Sediment-Rich Glacial Meltwater Plumes Using a High-Resolution Multispectral Sensor Mounted on an Unmanned Aerial Vehicle. Water 11(11):2405.

A.1 Summary of sampling in the various study areas for further investigations at AWI

Year	Month	Location	Parameter / Purpose	Sample Type (short)	Device	No. of Samples	Total Vol [ml]	Total Weight [g]
2024	12	Admiralty Bay	RGB Imagery	Drone Flights	DJI Inspire 2, Zenmuse 5	14		
2024	12	Admiralty Bay	Multispectral Imagery	Drone Flights	DJI Phantom 4 multispectral	11		
2024	12	Admiralty Bay	CTD, Turbidity, Chlorophyll, pH	EXO2 Deployments	YSI EXO2 Multiparameter Sonde	52		
2024	12	Admiralty Bay	Geochemistry	Filter (Durapore)		8		76
2024	12	Admiralty Bay	SPM / TOC	Filter (GF/F)		89		
2024	12	Admiralty Bay	Geochemistry	Fresh Water		21	2760	
2024	12	Admiralty Bay	Phytoplankton, quantitative	Phytoplankton	Niskin bottle	26	1300	
2024	12	Admiralty Bay	Phytoplankton, qualitative	Phytoplankton	Phytoplankton Net	13	650	
2024	12	Admiralty Bay	Geochemistry	Porewater	UWITEC Corer	94	564	
2024	12	Admiralty Bay	Geochemistry	Rock		6		444
2024	12	Admiralty Bay	Geochemistry	Sea Water		70	1100	
2024	12	Admiralty Bay	Geochemistry	Sea Water	UWITEC Corer	30	300	
2024	12	Admiralty Bay	Texture, Geochemistry, Chlorophyll a, TOC	Sediment	UWITEC Corer	10		3330
2025	1	Potter Cove	RGB Imagery	Drone Flights	DJI Inspire 2, Zenmuse 5	18		
2025	1	Potter Cove	Multispectral Imagery	Drone Flights	DJI Phantom 4 multispectral	13		
2025	1	Potter Cove	CTD, Turbidity, Chlorophyll, pH	EXO2 Deployments	YSI EXO2 Multiparameter Sonde	170		
2025	1	Potter Cove	Geochemistry	Filter (Durapore)		33		
2025	1	Potter Cove	SPM / TOC	Filter (GF/F)		230		
2025	1	Potter Cove	Geochemistry	Fresh Water		55	4120	
2025	1	Potter Cove	Phytoplankton, quantitative	Phytoplankton	Niskin bottle	34	1700	
2025	1	Potter Cove	Phytoplankton, qualitative	Phytoplankton	Phytoplankton Net	17	850	
2025	1	Potter Cove	Geochemistry	Porewater	UWITEC Corer	186	1649	
2025	1	Potter Cove	Geochemistry	Rock		5		700
2025	1	Potter Cove	Geochemistry	Sea Water		64	1120	
2025	1	Potter Cove	Geochemistry	Sea Water	UWITEC Corer	32	320	
2025	1	Potter Cove	Geochemistry	Sediment		3		430
2025	1	Potter Cove	Texture, Geochemistry, Chlorophyll a, TOC	Sediment	UWITEC Corer	8		7950
2025	2	Marian Cove	RGB Imagery	Drone Flights	DJI Inspire 2, Zenmuse 5	4		
2025	2	Marian Cove	Multispectral Imagery	Drone Flights	DJI Phantom 4 multispectral	3		
2025	2	Marian Cove	CTD, Turbidity, Chlorophyll, pH	EXO2 Deployments	YSI EXO2 Multiparameter Sonde	19		
2025	2	Marian Cove	Geochemistry	Filter (Durapore)		11		
2025	2	Marian Cove	SPM / TOC	Filter (GF/F)		33		
2025	2	Marian Cove	Geochemistry	Fresh Water		4	580	
2025	2	Marian Cove	Phytoplankton, quantitative	Phytoplankton	Niskin bottle	16	800	
2025	2	Marian Cove	Phytoplankton, qualitative	Phytoplankton	Phytoplankton Net	8	400	

Year	Month	Location	Parameter / Purpose	Sample Type (short)	Device	No. of Samples	Total Vol [ml]	Total Weight [g]
2025	2	Marian Cove	Geochemistry	Porewater	UWITEC Corer	86	580	
2025	2	Marian Cove	Geochemistry	Rock		2		280
2025	2	Marian Cove	Geochemistry	Sea Water		30	540	
2025	2	Marian Cove	Geochemistry	Sea Water	UWITEC Corer	24	240	
2025	2	Marian Cove	Texture, Geochemistry, Chlorophyll a, TOC	Sediment	UWITEC Corer	6		4930
2025	2	Stranger Point	RGB Imagery	Drone Flights	DJI Inspire 2, Zenmuse 5	2		
2025	2	Stranger Point	Multispectral Imagery	Drone Flights	DJI Phantom 4 multispectral	1		
2025	2	Stranger Point	CTD, Turbidity, Chlorophyll, pH	EXO2 Deployments	YSI EXO2 Multiparameter Sonde	6		
2025	2	Stranger Point	Geochemistry	Filter (Durapore)		1		
2025	2	Stranger Point	SPM / TOC	Filter (GF/F)		8		
2025	2	Stranger Point	Geochemistry	Fresh Water		4	580	
2025	2	Stranger Point	Phytoplankton, quantitative	Phytoplankton	Niskin bottle	2	100	
2025	2	Stranger Point	Phytoplankton, qualitative	Phytoplankton	Phytoplankton Net	1	50	
2025	2	Stranger Point	Geochemistry	Rock		4		560
2025	2	Stranger Point	Geochemistry	Sea Water		8	80	
2025	2	Stranger Point	Geochemistry	Sediment		1	20383	140
2025	2	Collins Harbour	Multispectral Imagery	Drone Flights	DJI Phantom 4 multispectral	7		
2025	2	Collins Harbour	CTD, Turbidity, Chlorophyll, pH	EXO2 Deployments	YSI EXO2 Multiparameter Sonde	38		
2025	2	Collins Harbour	Geochemistry	Filter (Durapore)		6		
2025	2	Collins Harbour	SPM / TOC	Filter (GF/F)		57		
2025	2	Collins Harbour	Geochemistry	Fresh Water		2	290	
2025	2	Collins Harbour	Phytoplankton, quantitative	Phytoplankton	Niskin bottle	22	1100	
2025	2	Collins Harbour	Phytoplankton, qualitative	Phytoplankton	Phytoplankton Net	11	550	
2025	2	Collins Harbour	Geochemistry	Porewater	UWITEC Corer	56	600	
2025	2	Collins Harbour	Geochemistry	Rock		5		500
2025	2	Collins Harbour	Geochemistry	Sea Water		32	480	
2025	2	Collins Harbour	Geochemistry	Sea Water	UWITEC Corer	24	360	
2025	2	Collins Harbour	Texture, Geochemistry, Chlorophyll a, TOC	Sediment	UWITEC Corer	9	840	7000

A.2 Flight information on UAS deployments during SIGMA-II (2024-2025)

Study Area	Station	Repetition	Date	Time start	Time end	Drone used	Height (m)	Conditions
Mackelar Inlet, ECAMP	MA1	1	11.12.2024	10:20	11:30	DJI P4 multispectral	100	windy
Mackelar Inlet, ECAMP	MA1-land	1	11.12.2024	12:00	12:30	DJI P4 multispectral	100	windy
Martel Inlet, Krak Glaciar	MA2	1	15.12.2024	07:45	09:30	DJI P4 multispectral	100	bit cloudy, few wind, some tiny waves
Martel Inlet, Krak Glaciar	MA2	1	15.12.2024	11:00	13:00	DJI Inspire 2	500	sunny, few wind
Martel Inlet, Krak Glaciar	MA2-land	1	15.12.2024	09:40	10:30	DJI P4 multispectral	100	bit cloudy, few wind, some tiny waves
Martel Inlet, Krak Glaciar	MA2-land	1	15.12.2024	11:00	13:00	DJI Inspire 2	500	sunny, few wind
Mackelar Inlet, Keller Peninsula	MA3	1	16.12.2024	09:50	11:30	DJI P4 multispectral	100	cloudy, no wind, no waves but ice on the water
Mackelar Inlet, Keller Peninsula	MA3	1	16.12.2024	12:40	13:10	DJI Inspire 2	500	cloudy, no wind, no waves but ice on the water
Mackelar Inlet, Keller Peninsula	MA3-land	1	16.12.2024	11:33	12:30	DJI P4 multispectral	100	cloudy, no wind
Mackelar Inlet, Keller Peninsula	MA3-land	1	16.12.2024	12:40	13:10	DJI Inspire 2	500	cloudy, no wind
Mackelar Inlet, Keller Peninsula	MA3	2	18.12.2024	10:55	12:40	DJI P4 multispectral	100	after a storm on 17.12.24, sunny, few wind and clouds
Mackelar Inlet, Keller Peninsula	MA3	2	18.12.2024	12:45	13:20	DJI Inspire 2	500	after a storm on 17.12.24, sunny, few wind and clouds
Martel Inlet, Krak Glaciar	MA2	2	18.12.2024	18:00	20:00	DJI P4 multispectral	100	cloudy, windy
Mackelar Inlet, ECAMP	MA1-land	2	21.12.2024	19:20	19:40	DJI Inspire 2	500	sunny, almost no wind
Mackelar Inlet, ECAMP	MA1	2	21.12.2024	19:42	20:50	DJI Inspire 2	500	sunny, almost no wind
Mackelar Inlet, ECAMP	MA1	2	21.12.2024	20:55	22:15	DJI P4 multispectral	100	sunny, almost no wind
Martel Inlet, Krak Glaciar	MA2	3	21.12.2024	14:44	16:50	DJI P4 multispectral	100	cold, some wind, cloudy
Martel Inlet, Krak Glaciar	MA2	3	21.12.2024	17:00	18:10	DJI Inspire 2	500	cold, some wind, cloudy
Mackelar Inlet, ECAMP	MA1	3	22.12.2024	11:27	12:42	DJI P4 multispectral	100	cold, some wind, cloudy, later sunny
Mackelar Inlet, ECAMP	MA1	3	22.12.2024	12:50	13:06	DJI Inspire 2	500	cold, some wind, cloudy, later sunny
Potter Cove, close to glacier	PC3	1	12.01.2025	07:15	09:00	DJI P4 multispectral	100	low wind, cloudy
Potter Cove, close to glacier	PC3	1	12.01.2025	09:00	11:30	DJI Inspire 2	500	low wind, cloudy
Potter Cove, helipuerto	PC10	1	17.01.2025	15:30	17:20	DJI P4 multispectral	100	some wind, cloudy
Potter Cove, helipuerto	PC10	1	17.01.2025	17:20	18:30	DJI Inspire 2	500	some wind, cloudy
Potter Cove_Land1	PC_land1	1	18.01.2025	15:02	17:00	DJI P4 multispectral	100	some wind, cloudy

Study Area	Station	Repetition	Date	Time start	Time end	Drone used	Height (m)	Conditions
Potter Cove_Land1	PC_land1	1	18.01.2025	17:00	18:00	DJI Inspire 2	500	some wind, cloudy
Potter Cove, Cabildo	PC1	2	20.01.2025	10:00	12:00	DJI P4 multispectral	100	windy, sunny, cold
Potter Cove, Cabildo	PC1	2	20.01.2025	12:00	13:00	DJI Inspire 2	500	windy, sunny, cold
Potter Cove, close to glacier	PC3	2	20.01.2025	14:30	16:30	DJI P4 multispectral	100	windy, cloudy
Potter Cove, close to glacier	PC3	2	20.01.2025	16:30	17:30	DJI Inspire 2	500	windy, cloudy
Potter Cove, Cabildo	PC1	2	21.01.2025	09:00	11:00	DJI P4 multispectral	100	low wind, cloudy
Potter Cove, Cabildo	PC1	2	21.01.2025	11:00	12:00	DJI Inspire 2	500	low wind, cloudy
Potter Cove, helipuerto	PC10	2	21.01.2025	14:30	16:00	DJI P4 multispectral	100	very windy
Potter Cove, helipuerto	PC10	2	21.01.2025	16:00	17:00	DJI Inspire 2	360	high reduction due to wind
Marian Cove	MC2	2	25.01.2025	09:30	11:10	DJI P4 multispectral	100	some wind & sun
Marian Cove	MC2-land	1	25.01.2025	11:10	11:30	DJI P4 multispectral	150	obstacle (mountain too high)
Marian Cove	MC2-land	2	25.01.2025	11:30	11:45	DJI P4 multispectral	250	abort, connection difficulties
Marian Cove	MC2	2	25.01.2025	11:45	11:55	DJI Inspire 2	500	abort, clouds too low
Marian Cove	MC2	2	25.01.2025	11:55	12:45	DJI Inspire 2	400	cloudy
Potter Cove_Land2	PC-land2	1	26.01.2025	11:00	13:00	DJI Inspire 2	500	some wind, cloudy
Potter Cove_Land2	PC-land2	1	31.01.2025	11:35	13:30	DJI P4 multispectral	100	some wind, cloudy
Potter Cove, helipuerto	PC10	3	26.01.2025	14:00	15:50	DJI P4 multispectral	100	no wind, cloudy
Potter Cove, helipuerto	PC10	3	26.01.2025	15:50	16:00	DJI Inspire 2	500	no wind, cloudy
Potter Cove, close to glacier	PC3	3	29.01.2025	08:45	10:45	DJI P4 multispectral	100	sunny, no wind
Potter Cove, close to glacier	PC3	3	29.01.2025	10:48	11:45	DJI Inspire 2	500	sunny, no wind
Punta Stranger (PeñonVII)	PS	1	06.02.2025	09:45	12:00	DJI P4 multispectral	100	foggy
Collins Glacier	CG3	1	21.02.2025	16:00	19:00	DJI P4 multispectral	100	weather good
Collins Glacier_Land	CG3-land	1	21.02.2025	19:00	20:00	DJI P4 multispectral	100	weather good, dark at the end
Collins Glacier	CG3	2	25.02.2025	16:20	16:25	DJI P4 multispectral	100	snow, abort
Collins Glacier	CG3	2	26.02.2025	16:30	18:30	DJI P4 multispectral	100	some wind, cloudy
Collins Glacier	CG3	3	27.02.2025	10:30	13:15	DJI P4 multispectral	100	some wind, cloudy
Collins Glacier close to glacier	CG1	3	28.02.2025	14:00	18:00	DJI P4 multispectral	100	windy, cloudy

5.5 Spongescan – Deciphering the Role of Glass Sponges in the Carbon and Silicate Cycle of a Changing Antarctic

Jürgen Laudien*[1], Ian Hawes[2], Erik Wurz[3], [1]DE.AWI
Andreas Schmider-Martínez[4], Rod Budd[5], [2]NZ.UoW
Katherine Rowe[2]; [3]NL.WUR
not in the field: Claudio Richter[1], Ulrike Hanz[1] [4]CHL.UACH
*juergen.laudien@awi.de [5]NZ.NIWA

Grant-No. AWI_ANT_49

Outline

Large glass sponges (class Hexactinellida), which incorporate amorphous hydrated silica into their bodies, play a substantial role in structuring the Antarctic shelf benthos. Hexactinellid-dominated communities are mainly found in productive regions (e.g., coastal polynyas of the Ross Sea and Weddell Sea), but the mechanisms linking production to sponge growth are still unknown. Carbon and silicate likely limit the distribution and growth of these unique glass sponge communities on Antarctic shelves. As most of the Antarctic coastline is rimmed by ice, access by divers is limited. An exception is McMurdo Sound in the Ross Sea which offers diving access to high Antarctic glass sponges at a water depth of <30 m (Fig. 5.5.1).

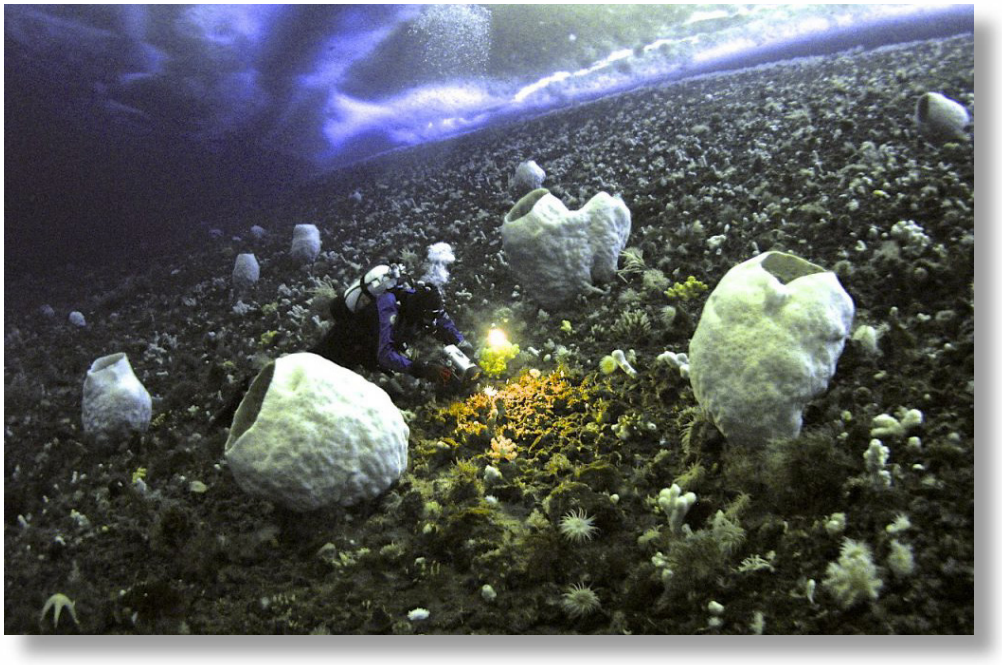

Fig. 5.5.1: Large glass sponges in McMurdo Sound, note the SCUBA diver in between the Hexactinellids

Objectives

The aim of the project was to determine the role of glass sponges in the uptake and cycling of silicate and carbon on a high Antarctic shelf, and to quantify sponge feeding and silicification. Specific objectives were to assess glass sponges' diet, feeding rates and metabolism through in situ measurements combining concentration differences in particulate and solutes (C, N, Si, O_2) between inhalant and exhalent water, with simultaneous measurements of sponge pumping rates to accurately describe the fluxes.

Fieldwork

Dive hole preparation

Fieldwork was carried out in a multinational team, using Scott Base as a basis. We determined in situ the sponge pumping rate. In addition, repeated oceanographic casts were carried out and a CTD and underwater camera installed to assess the environmental conditions near sponge communities.

A ROV survey was carried out and the location with highest densities of large glass sponges (*Anoxycalyx joubini*) depth nearest to the surface (~30 m) was selected as study site (Arrival Heights Dive Site). On 24 October 2024, a chainsaw was used to cut out a rectangular opening measuring 1.7 m by 1.2 m (Fig. 5.5.2). The inside of the hole was cut into squares approximately 25×25cm in size, which extend over the entire depth of the chainsaw blade. It was important that the cuts were vertical so that the blocks would not jam when pulled out. The 'ice pillars' were broken off at their base by levering them aside with a large crowbar. Once loosened, an ice screw was screwed into the top of each block and the blocks were pulled out manually using a rope. The remaining lower 30 cm of the ice layer was left intact so that the hole would not flood while the chainsaw work was carried out. After the last blocks of ice had been removed, a hole was drilled through the last layer of ice with a drill so that the hole was flooded to approx. 25 cm below the top edge. Now an ice melter could be used to remove the remaining ice. This draws seawater out of the hole and passes it through a diesel-powered heat exchanger. The heated water was pumped in a T-shaped spray lance to a series of hot water nozzles, which were placed in the submerged hole and slowly melt the remaining ice. As soon as this had been cut free with the melter, the larger pieces floated up and could be removed. Floating platelet ice was removed with the help of wire nets. For safety reasons, two reserve holes were created parallel to the coast at a distance of approx. 50 metres to the right and left of the main ice hole, over which a heated diving tent was placed.

Fig. 5.5.2: The snow was removed from the ice surface and the ice thickness was determined using a Kovacs drill. A chainsaw was used to cut a rectangular opening measuring 1.7 metres by 1.2 metres into the ice, and the blocks of ice were manually removed from the ice hole. A hole was drilled through the last layer of ice with a drill so that the hole was flooded. An ice melter was used to remove the remaining ice.

Research methods

To obtain data to estimate respiration rate, the silicate and carbon cycle and the pumping capacity of the glass sponges, a lightweight aluminium frame was positioned directly above the sponges (Fig. 5.5.3). In these active suspension feeders, the ambient water is pumped through the body wall into the spongocoel (central cavity of the sponge) and exits the sponge through the osculum. Samples were thus taken in ambient waters surrounding the sponges and in the spongocoel to assess the fluxes of materials between sponges and their environment.

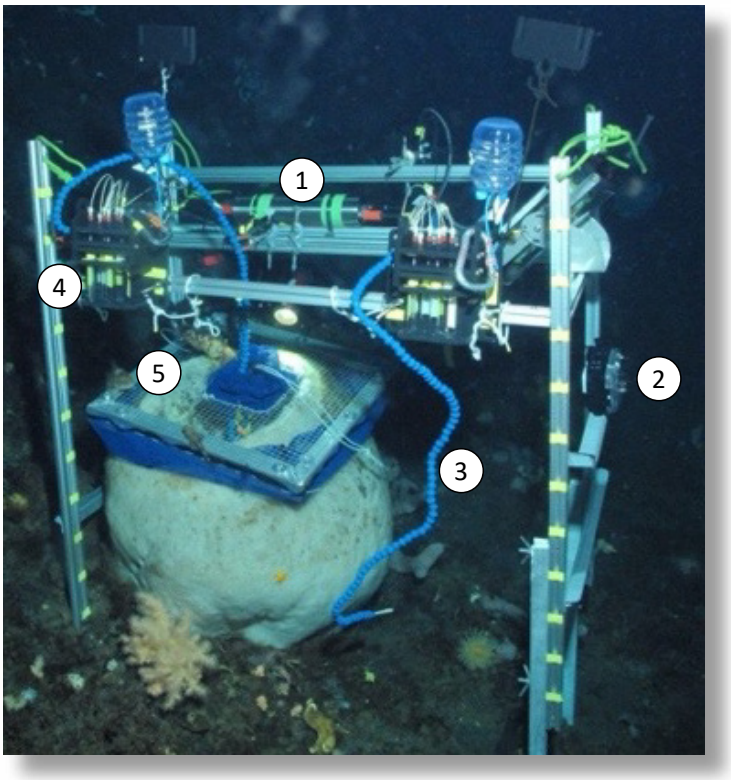

Fig. 5.5.3: Aluminium lightweight frame installed above the 70 cm high Anoxycalyx joubini with installed Firesting-Optode (1), camera and vertical underwater lighting (2), PEEK tube in blue lock-line (3) and Vacu-Sampler (4) with cannulas piercing the membranes of vacuum bottles to collect water samples. The sponge opening was temporarily covered with a net (5) to keep fish away from the central cavity during the measurements.

Firesting optodes were positioned using stand clamps to record the oxygen concentration 20cm deep in the spongocoel and outside the sponge. Water samples were collected using a custom-built 'Vacu-sampler', specially developed by the AWI's scientific workshop. This comprised a series of lengths of PEEK tubing, with an internal diameter of only 0.25 mm, which were positioned either within the inner cavity or outside of the cavity close to the sponges. Tubing was connected to syringe needles, which were individually assigned to 9 ml Vacuett® vials, that had a negative pressure after the air had been sucked out. To activate sampling, the research diver had to press down a holding plate carrying the syringe needles, so that these pierced the septa of the evacuated vials, and the suction effect began to draw water, dropwise, into the vials. In this way, water samples were collected slowly for picoplankton, inorganic

nutrient salts and dissolved organic material, effectively integrating sampling over a 2 hour time interval. An inline GF/F filter installed in front of a Redon bottle under vacuum collected particulate organic material. To determine the uptake of picoplankton, water samples were taken from the immediate vicinity of the sponges within their central habitat, which were then fixed, deep-frozen and sent to the AWI for analysis.

We observed pumping activity of the sponges by suspending a small rotating flow indicator (plastic rotor) in the central cavity of the sponges. Its rotation initially confirmed the pumping activity of the respective test sponge.

Pumping speeds were later determined by particle tracking. For this purpose, video recordings were analysed that were taken at an angle of 90° to the light cone of a diving lamp. The videos clearly showed that illuminated particles left the sponges vertically, while particles in the surrounding water moved horizontally with the current. The speed of the particles could be measured based on their known size ratios and the time.

To investigate flow profiles across sponge openings, we used a curtain made of thin HDPE tubes weighted down with fishing lead, which served to apply a fluorescent dye (Fig. 5.5.4). One research diver used a syringe to inject the fluorescent dye simultaneously through all ten tubes, at intervals, while another diver filmed the rising dye plumes so that the upward speed of the dye solution could be measured later in the video. A flow profile was also determined. These experiments were carried out on two test sponges and a total of 5 ml of 0.1 % fluorescein was released to the environment per sponge individual.

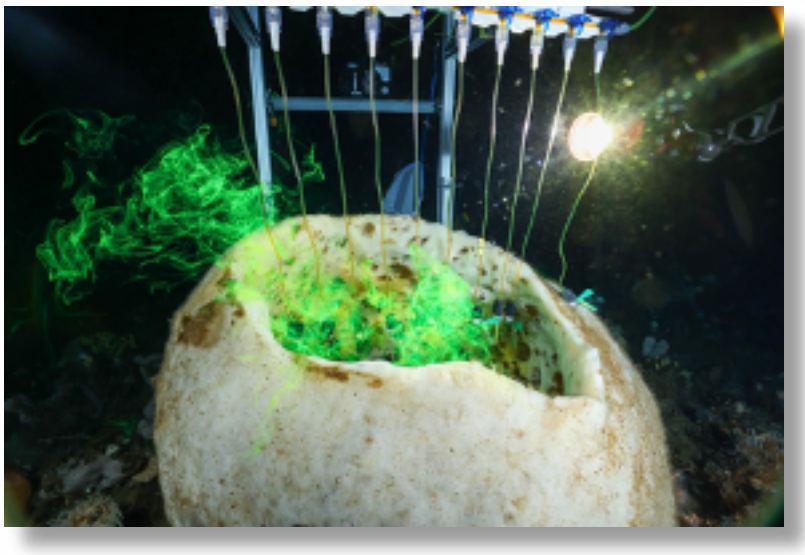

Fig. 5.5.4: To investigate flow profiles across sponge openings, a research diver simultaneously injected fluorescein through ten tubes weighted with clamping lead, while a camera (in the background) filmed the rising dye plumes of the test sponge (Anoxycalyx joubini) at 25 m water depth.

The abundance of glass sponges along bathymetric transects (20 m, 40 m, 60 m, 80 m) was recorded using an ROV (Boxfish). Tissue samples of the sponges were taken with a biopsy tool so that the species identification could be confirmed later.

Tissue samples were taken from four sponges at five different heights by inserting a thin, sharpened metal tube from the inside through the sponge to the outside. The biopsy samples taken were immediately divided into the epidermis of the inner cavity, mesohyl and the epidermis on the outer body wall under clean conditions and then shock-frozen in liquid nitrogen. These samples were used to identify the species by electron microscopy and to characterise the microbiome by PCR and genetic analyses. For bacterial comparison, sediment and water samples were also taken from the environment (using two collapsible canisters connected to a CTD)

To measure the presence and photosynthetic potential of possible benthic and/or symbiotic algae on the epidermis on the outer body wall and inside the body wall, an underwater Pulse Amplitude Modulated fluorometer (DIVING-PAM) was used to estimate chlorophyll fluorescence properties on three of our four test sponges (Fig. 5.5.5). The Diving PAM was used to take two replicate profiles of fluorescence properties at intervals from the base to the apex of each sponge. For each point, the base fluorescence was recorded as an index of biomass, and the variable fluorescence as a measure of instantaneous photosynthetic capacity. A green-brownish plaque was evident on some areas of many of the shallow sponges, and it was recorded if the measurement was taken on green brownish or rather white parts (Fig. 5.5.5). Samples of the plaque were examined microscopically to identify its origin.

Fig. 5.5.5: Scientific diver with underwater fluorometer behind a test sponge (Anoxycalyx joubini) with green-brownish plaque areas in 27 m water depth

A CTD, which was used daily in profile mode, was reprogrammed to mooring mode and installed directly on the bottom at a depth of 25 metres at the end of the expedition (Fig. 5.5.6). A Pi-Cam was attached to the lightweight aluminium frame, which from then on photographed a sponge twice a day in order to observe the mobile fauna visiting the sponge. The requested sediment trap was not installed.

Fig. 5.5.6: Daily measurement of temperature, salinity and pH using Sea Bird CTD

We focussed on sampling four glass sponges. We opted for minimally invasive sampling using biopsy and photogrammetry and therefore did not have to remove the sponges from the ecosystem. To ensure representative sampling, each approximately 70 cm high sponge was biopsied at five different heights using a metal coring tube. The collected tissue samples were immediately flash-frozen in liquid nitrogen.

Biomass estimates were made by determining the ash-free dry mass of a known-volume subsample of the biopsy samples. The mass of the analysed volume is then set in relation to the sponge volume determined by photogrammetry. In addition, the tissue samples will be used to determine the microbiome of the five sponges.

Fig. 5.5.7: (A) 3D model of two glass sponges and associated biota in their natural habitat. Note the orange patches of diatoms on much of the upper surface of the sponge. Model was constructed in Agisoft Metashape based on 97 photographs. (B) A. Schmider preparing biopsy samples, which were immediately frozen in liquid nitrogen in the diving tent and taken to the AWI for analysis.

Preliminary results

The environmental data collected during the *SpongeScan* campaign from 30 October to 12 November 2024 at the site "Arrival Heights Dive Hole" in McMurdo Sound (Ross Sea, Antarctica) have been published (Laudien et al. 2025). Using a CTD in both profiling and moored deployment modes, the dataset includes key oceanographic parameters such as water temperature, conductivity, pressure, oxygen concentration, pH, and salinity, as well as derived values like water depth and density. These measurements provide a detailed characterization of the physicochemical conditions shaping the benthic environment during the Antarctic summer. In particular, the moored CTD deployment enables a better understanding of internal water movements, which are primarily driven by tidal dynamics.

Seawater temperature was recorded every five minutes between October and November 2024 in McMurdo Sound, Ross Sea, Antarctica (Laudien et al. 2025). Measurements were taken at depths ranging from 9.5 to 29 metres to characterize the early summer temperature regime of the benthic community. Data were collected using a HOBO TidbiT v2 underwater data logger with an accuracy of ±0.2 °C. The logger was mounted on the aluminium frame, which was deployed by scientific divers during the study period. These high-resolution temperature recordings provide insights into the thermal environment shaping McMurdo Sound benthic ecosystems in the Antarctic summer.

We confirmed the species identification by scanning electron microscopy (SEM) of sponge spicules from three individuals as the glass sponge *Anoxycalyx (Scolymastra) joubini* (Topsent, 1916), collected in McMurdo Sound, Ross Sea, Antarctica (Schmider-Martínez et al. 2025). The frozen tissue samples were analysed at AWI. In the laboratory, approx. 1 cm^3 thawed tissue was treated with sodium hypochlorite (10 %) at room temperature to dissolve organic material while leaving behind the siliceous spicules. The latter were then washed multiple times with distilled water until neutral pH was reached, followed by a graded ethanol dehydration series (30%, 50%, 70%, 90%, and 100%). After final ethanol washes, the spicules were transferred onto SEM object holders with carbon adhesive, dried at 50 °C, and sputter-coated with gold. Prior to SEM imaging, light microscopy was used to verify the absence of organic residues. The dataset provides high-resolution microstructural data, contributing to the understanding of *A. joubini* spicule morphology and its taxonomic implications.

Analyses of the exhalent water from *Anoxycalyx joubini* revealed a marked decrease in dissolved organic carbon (DOC) concentrations compared to the surrounding ambient water. The sampled individuals showed a reduction of DOC content. These findings suggest active uptake or transformation of organic matter by the sponges. Further analyses of picoplankton in both inhalant and exhalant water are still pending and are expected to provide additional insights into the trophic role of *A. joubini* within the benthic food web.

Contrary to expectations for low microbial abundance (LMA) sponges, we observed no significant net nutrient release or uptake. However, a trend towards NO_3^- release was observed, potentially related to the presence of symbiotic microorganisms. High densities of epizoic diatoms made it difficult to measure the sponge's oxygen consumption, as the algae's oxygen production through photosynthesis counteracts consumption measurements.

The green-brownish plaque was microscopically identified as epizoic mats dominated by benthic pennate diatoms. In situ fluorescence analysis of the sponges using the Diving PAM showed that chlorophyll was detectable on/in the tissues even in areas without visible green-brownish plaque. In order to answer if the fluorescence was generated by benthic diatoms on the epidermis of the outer body wall (benthic diatoms) or inside the tissue by symbiotic algae needs further investigation.

Summary and outlook

The present in situ measurements of inorganic nutrients revealed no ammonium but a significant nitrate efflux, which suggests that microbial nitrification occurs within the sponge holobiont. We did not detect a significant oxygen uptake, which could indicate either a low oxygen demand by the sponge holobiont or oxygen production by associated primary producers, which counteracts the oxygen reduction. These findings underscore that the metabolic processes of the sponge holobiont are not solely driven by the sponge itself but also by its microbiome. To better understand the metabolic interactions, supplementary in situ incubation experiments will be carried out to quantify the metabolic processes and to tease apart primary productivity from oxygen uptake within the sponge holobiont. The close metabolic association between microbial symbionts and the sponge host may provide *A. joubini* with an alternative matter and energy pathway from its microbiome during dark winter months when primary production is limited. Moreover, the matter and energy transfer from the microbiome via the sponges potentially extends into the associated fauna by release of detritus or direct predation on the sponge, thereby acting as a conduit for energy flow into the broader Antarctic benthic food web. Planned stable isotope food web studies aim to clarify and quantify these potential trophic linkages.

Data management

Environmental data are archived (Laudien et al. 2025), published and disseminated according to international standards by the World Data Center PANGAEA Data Publisher for Earth & Environmental Science (https://www.pangaea.de). By default, the CC-BY license will be applied.

Molecular data (DNA and RNA data) will be archived, published and disseminated within one of the repositories of the International Nucleotide Sequence Data Collaboration (INSDC, www.insdc.org) comprising of EMBL-EBI/ENA, GenBank and DDBJ).

Any other data will be submitted to an appropriate long-term archive that provides unique and stable identifiers for the datasets and allows open online access to the data.

This expedition was supported by the Helmholtz Research Programme “Changing Earth – Sustaining our Future” Topic 4, Subtopic 2.

In all publications based on this expedition, the **Grant-No. AWI_ANT_49** will be quoted.

References

Laudien J, Schmider-Martínez A, Hawes I, Wurz E, Rowe K, Budd R, Hanz U, Richter C (2025) Physical oceanography at time series station Arrival Heights Dive Hole, McMurdo Sound, Ross Sea, Antarctica in October/November 2024 [dataset publication series]. PANGAEA, https://doi.pangaea.de/10.1594/PANGAEA.975230

Schmider-Martínez A, Laudien J, Hawes I, Wurz E, Rowe K, Budd R, Hanz U, Richter C (2025) Scanning Electron Microscopy (SEM) Images of Sponge Spicules from *Anoxycalyx (Scolymastra) joubini* (Topsent, 1916) in McMurdo Sound, Ross Sea, Antarctica [dataset]. PANGAEA, https://doi.pangaea.de/10.1594/PANGAEA.979762

APPENDIX

A.1 TEILNEHMENDE INSTITUTE / PARTICIPATING INSTITUTES

A.2 EXPEDITIONSTEILNEHMER:INNEN / EXPEDITION PARTICIPANTS

A.3 LOGISTISCHE UNTERSTÜTZUNG, ÜBERWINTERNDE / LOGISTICS SUPPORT, WINTERING TEAM

A.4 AUTOREN OHNE EXPEDITIONSTEILNAHME/ AUTHORS WITHOUT EXPEDITION PARTICIPATION

A.1 PARTICIPATING INSTITUTES

Affiliation	Address
In the field	
ARG.CONICET-CADIC	Centro Austral de Investigaciones Científicas del Consejo Nacional de Investigaciones Científicas y Técnicas Bernardo Houssay 200 V9410 Ushuaia Tierra del Fuego Argentina
ARG.IPCA-TDF	Universidad Nacional de Tierra del Fuego Fuegia Basket 251 V9410 Ushuaia Tierra del Fuego Argentina
AT.NGF	Nikolaus Geyrhalter Filmproduktion GmbH Hildebrandgasse 26 1180 Wien Austria
BE.FairWind	Fairwind Chaussée de Gilly 299 6220 Fleurus Belgium
BE.ULB	Université Libre de Bruxelles Laboratoire de Glaciologie (GLACIOL) Faculté des Sciences Campus du Solbosch - CP 160/03 Avenue F.D. Roosevelt, 50 1050 Bruxelles Belgium
CH.EPFL	École Polytechnique Fédérale de Lausanne ALPOLE, Route des Ronquos 86 1951 Sion Switzerland

Affiliation	Address
In the field	
CH.UNIBE	Climate and Environmental Physics, Physics Institute & Oeschger Centre for Climate Change Research University of Bern Sidlerstrasse 5 3012 Bern Switzerland
CHL.UACH	Universidad Austral de Chile Avenida Independencia 641 Valdivia, Región de Los Ríos Chile
DE.AWI	Alfred-Wegener-Institut Helmholtz-Zentrum für Polar- und Meeresforschung Postfach 120161 27515 Bremerhaven Germany
DE. BauWerk	BauWerk Sandbergstraße 26 27711 Osterholz-Scharmbeck Germany
DE.BGR	Bundesanstalt für Geowissenschaften und Rohstoffe Stilleweg 2 30655 Hannover Germany
DE.Etteplan	Etteplan Germany GmbH Werkstättenstr. 37 52379 Leverkusen Germany
DE.FAU	Friedrich-Alexander-Universität Erlangen-Nürnberg Henkestraße 91 91052 Erlangen Germany
DE.GFZ	Deutsches GeoForschungsZentrum GFZ Telegrafenberg 14473 Potsdam Germany
DE.HAW	Hochschule für Angewandte Wissenschaften Hamburg Department Umwelttechnik Ulmenliet 20 21033 Hamburg Germany

Affiliation	Address
In the field	
DE.HS-Bremen	Hochschule Bremen Neustadtswall 30 28195 Bremen Germany
DE.LAEISZ	Logistics F. Laeisz GmbH Bartelstraße 1 27570 Bremerhaven Germany
DE.MWB	MWB Elektrotechnik Service GmbH Rudloffstr. 49 27568 Bremerhaven Germany
DK.PICE	Physics of Ice, Climate and Earth Niels Bohr Institute University of Copenhagen Tagensvej 16 2100 Copenhagen OE Denmark
EDU.WHOI	Wood Hole Oceanographic Institution 266 Wood Hole Road Woods Hole MA 02543 USA
FR.IGE	CNRS, Grenoble INP, IRD, et UGA Institut des Géosciences de l'Environnement 54, rue Molière 38400 Saint-Martin d'Hères France
FR.IPEV	French Polar Institute Paul-Émile Victor Technopôle Brest-Iroise CS 60 075 29280 Plouzané France
FR.LSCE	LSCE (Laboratoire des Sciences du Climat et de l'Environnement) CEA Saclay – Orme des Merisiers Bâtiment 714 91191 Gif-sur-Yvette Cedex France
IS.Arctictrucks	Arctic Trucks Polar Kletthális 3 110 Reykjavík Iceland

Affiliation	Address
In the field	
IT.ENEA-BO	ENEA Centro Richerche Brasimone Sezione Ingegneria Sperimentale 40032 Camugnano (Bologna) Italy
IT.ENEA-EI	Italian Armed Forces
IT.ENEA-RO	ENEA – Centro Richerche Casaccia Via Anguillarese, 301 00123 S. Maria di Galeria (Roma) Italy
IT.ENEA-TR	ENEA – Energy Technologies and Renewable Sources Department Ss Ionica 106 75026 Rotondella Italy
IT.ISP-CNR	Institute of Polar Sciences – CNR and Ca' Foscari University of Venice via Torino, 155 30172 Venice-Mestre Italy
MCO.CSM	Centre Scientifique de Monaco 8 Quai Antoine 1er MC 98000 Monaco
NL.WUR	Wageningen University & Research Droevendaalsesteeg 4 6708 PB Wageningen The Netherlands
NO.UIO	Universitetet i Oslo Sem Sælandsvei 24 371 Oslo Norway
NZ.NIWA	National Institute of Water and Atmospheric Research 41 Market Place Viaduct Harbour Auckland Central 1010 New Zealand
NZ.UoW	University of Waikato Te Whare Wānanga o Waikato Gate 1, Knighton Road Hillcrest, Hamilton 3216 New Zealand

Affiliation	Address
In the field	
PE.UCdS	Universidad Cientifica del Sur, Antigua Panamericana Sur 19 Villa EL Salvador 15067 Peru
PL.IOPAN	Institute of Oceanology Polish Academy of Science Powstańców Warszawy 55 81-712 Sopot Poland
UK.Talesmith	Talesmith Audley House 12-12a Margaret Street London W1W8jQ United Kingdom

Affiliation	Address
Not in the field	
ARG.IAA	Instituto Antártico Argentino Av. 25 de Mayo 1147 B1650 Villa Lynch Provincia de Buenos Aires Argentina
BE.ULB	Université Libre de Bruxelles CP 160/03 Avenue F.D. Roosevelt B-1050 Brussels Belgium
CA.SFU	Simon Fraser University School of Interactive Arts and Technology (SIAT) 250 -13450 102 Avenue Surrey, BC, V3T 0A3 Canada
CH.EPFL	Ecole Polytechnique Fédérale de Lausanne EPFL Route cantonale CH-1015 Lausanne Switzerland
CH.EPFL	Ecole Polytechnique Fédérale de Lausanne ALPOLE Route des Ronquos 86 1950 Sion Switzerland

Affiliation	Address
Not in the field	
CH.SLF	WSL Institute for Snow and Avalanche Research SLF Flüelastrasse 11 7260 Davos Dorf Switzerland
CL.IDEAL	Centro de Investigación Dinámica de Ecosistemas Marinos de Altas Latitudes Universidad Austral de Chile Avda. El Bosque 01789 Punta Arenas Magellanes y la Antártica Chilena Chile
CL.INACH	Instituto Antártico Chileno Pl. Benjamín Muñoz Gamero 1055 Punta Arenas Magellanes y la Antártica Chilena Chile
CU.UCA	University of Calgary 2500 University Drive NW Calgary Alberta T2N 1N4 Canada
DE.BCAN	Berlin Center of Advanced Neuroimaging (BCAN) Charité – Universitätsmedizin Berlin Charitéplatz 1 10117 Berlin Germany
DE.CHARITE	Charité Universitätsmedizin Berlin Charitéplatz 1 10117 Berlin Germany
DE.FLI	Friedrich-Loeffler-Institut Federal Research Institute for Animal Health Südufer 10 17493 Greifswald – Insel Riems Germany
DE.HEREON	Helmholtz-Zentrum Hereon Max-Planck-Straße 1 21502 Geesthacht Germany
DE.HS-Bremen	Hochschule Bremen Neustadtswall 30 28195 Bremen Germany

Affiliation	Address
Not in the field	
DE.Med.Uni-Muenchen	Klinikum der Universität München Department of Anesthesiology Marchioninistr. 15 80377 München Germany
DE.MPIB-Berlin	Max-Planck-Institut für Bildungsforschung Lentzallee 94 14195 Berlin Germany
DE.TROPOS	Leibniz Institute for Tropospheric Reseach Permoserstraße 15 04318 Leipzig Germany
DE.TUDresden	Technische Universität Dresden 01062 Dresden
DE.UBA	Umweltbundesamt Wörlitzer Pl. 1 06844 Dessau-Roßlau Germany
DE.UNI-Bremen	Universität Bremen Bibliothekstraße 1 28359 Bremen Germany
DE.UNI-Tuebingen	Eberhard Karls Universität Tübingen Geschwister-Scholl-Platz 72074 Tübingen Germany
DE.ZMT	Leibniz-Zentrum für Marine Tropenforschung Fahrenheitstraße 6 28359 Bremen Germany
EDU.NJIT	New Jersey Institute of Technology Center for Solar-Terrestrial Research New Jersey USA
EDU.UNH	University of New Hampshire Space Science Center Durham New Hampshire USA

Affiliation	Address
Not in the field	
FR.CNRS	Centre National de la recherche scientifique 23 rue Becquerel Bâtiment 60 67087 Strasbourg France
FR.EOST/ITES	ITES - École & observatoire des sciences de la Terre – EOST Université de Strasbourg 67081 Strasbourg Frankreich
KR.KHU	Kyung-Hee University School of Space Research Gyeonggi Korea
KR.KOPRI	Korea Polar Research Institute Division of Polar Climate Sciences Incheon Korea
NO.NPolar	Norwegian Polar Institute Framsenteret Hjalmar Johansens gate 14 9296 Tromsø Norway
NO.UBE	Geofysisk institutt Universitetet i Bergen Bergen Norway
PE.RREE	Ministerio de Relaciones Exteriores Jr. Lampa 580 Lima 15001 Peru
UK.BAS	British Antarctic Survey High Cross Madingley Road Cambridge CB3 0ET United Kingdom
UK.UCAM	University of Cambridge Downing Street Cambridge CB2 3EQ United Kingdom

A.2 EXPEDITION PARTICIPANTS

Name/ Last name	Vorname/ First name	Institut/ Institute	Beruf/ Profession	Fachrichtung/ Discipline
Ardoin	Lisa	BE.ULB	Scientist	Geology
Arlamovsky-Geyrhalter	Adane Nikolaus	AT.NGF	Journalist	Media
Asseng	Jölund	DE.AWI	Technician	Geophysics
Bagur	María	ARG.CONICET-CADIC	Scientist, Scientific Diver	**Biology**
Baille	Loicka	EDU.WHOI	PhD student	Engineering
Bałazy	Piotr	PL.IO PAN	Scientist, Scientific Diver	Biology
Bardon	Gaël	MCO.CSM	Scientist	Biology
Berger	Sebastian	DE.AWI	Engineer	Meteorology
Błachowiak-Samołyk	Katarzyna	PL.IO PAN	Profesor	Biology
Böckel	Christiane	DE.AWI	Scientist	Biology
Boehnke	Rafał	PL.IO PAN	Technician	Biology
Bornemann	Horst	DE.AWI	Scientist	Biology
Bouchet	Marie	FR.LSCE	Scientist	Geology
Budd	Rod	NZ.NIWA	Dive supervisor	Diving
Calek	Oliver	DE.AWI	Engineer	Meteorology
Chung	Ailsa	FR.IGE	Scientist	Geophysics
Eagles	Graeme	DE.AWI	Scientist	Geophysics
Geyrhalter	Nikolaus	AT.NGF	Journalist	Media
Gomez Farfan	Rosby	PER.UCdS	Student	Biology
Grasse	Torsten	DE.BGR	Engineer	Geophysics
Hartje	Michael	DE.HS-Bremen	Scientist	Engineering
Hartmann	Gernot	DE.BGR	Scientist	Geophysics
Hawes	Ian	NZ.UoW	Scientist	Biology
Heitmann	Filip August	DE.AWI	Technician	Glaciology
Held	Christoph	DE.AWI	Scientist	Biology
Helm	Veit	DE.AWI	Scientist	Glaciology
Hobin	Helen	UK.talesmith	Fotograf/in	Media
Hoffmann	Mathias	DE.BGR	Scientist	Geophysics
Houstin	Aymeric	EDU.WHOI	Scientist	Biology
Hüther	Matthias	DE.AWI	Chief Driller	Mechanical Engineering
Jerosch	Kerstin	DE.AWI	Senior Scientist	Biology
Juranyi	Zsofia	DE.AWI	Scientist	other Geosciences

Name/ Last name	**Vorname/ First name**	**Institut/ Institute**	**Beruf/ Profession**	**Fachrichtung/ Discipline**
Kielmann	Moritz	DE.HAW	PhD student	Chemistry
Krebs	Manuela	DE.AWI	Driller	Chemistry
Krumpen	Thomas	DE.AWI	Scientist	Geoscience
Laggner	Sophia Rosa	AT.NGF	Journalist	Media
Laudien	Jürgen	DE.AWI	Scientist	Biology
Lawer	Gunther	DE.AWI	Drill Engineer	Mechanical Engineering
Lemburg	Johannes	DE.AWI	Drill Engineer	Mechanical Engineering
Leonhardt	Martin	DE.AWI	Drill Engineer	Electrical Engineering
Lisovski	Simeon	DE.AWI	Scientist	Geoscience/Bioscience
Lonardi	Michael	CH.EPFL	Scientist	Meteorology
Marx	Ute	DE.AWI	Technician	Biology
Matzka	Jürgen	DE.GFZ	Scientist	Geophysics
McCowen	Pete	UK.talesmith	Photographer	Media
Miloch	Wojciech Jacek	NO.UIO	Scientist	Physics
Paranhos Zitterbart	Daniel	EDU.WHOI	Scientist	Physics
Ponniah	Alex	UK.talesmith	Photographer	Media
Rodriguez	Mariano	ARG.IPCA-TDF	Scientific Diver	Biology
Rowe	Katherine	NZ.UoW	Scientific diver	Diving
Sander	Martha Maria	DE.AWI	Scientist	Biology
Scalet	Michele	IT.ENEA-BO	Camp engineer	Mechanical Engineering
Schmider-Martínez	Andreas	CHL.UACH	Scientist	Biology
Schröder	Henning	DE.AWI	Engineer	Engineering
Schulz	Alexander	DE.AWI	Scientist	Physics
Scoto	Federico	IT.ISP-CNR	Scientist	Glaciology / Geology
Seth	Barbara	CH.UNIBE	Driller	Geology
Soussaintjean	Lison	CH.UNIBE	Driller	Geology
Spiesecke	Stefanie	DE.AWI	Technician	Oceanography
Stegmann	Tim	DE.AWI	Technician	Engineering
Steinhöfel	Grit	DE.AWI	Senior Scientist	Geochemistry
Strieben	Sabine	DE.AWI	Technician	Biology
Temel	Yolanda Riccarda	CH.EPFL	PhD student	Meteorology
Vaibhav	Dev	EDU.WHOI	Engineer	Engineering
Vock	Clarissa	DE.AWI	PhD-Student	Biology
Weith	Friederike	DE.AWI	Scientist	Biology
Westhoff	Julien	DK.PICE	Chief Scientist	Glaciology / Geology
Wilhelms	Frank	DE.AWI	PI in the field	Glaciology / Geophysics
Winterl	Alexander	DE.FAU	PhD student	Physics

Name/ Last name	**Vorname/ First name**	**Institut/ Institute**	**Beruf/ Profession**	**Fachrichtung/ Discipline**
Witte	Marlena	DE.AWI	Other	Media
Włodarska-Kowalczuk	Maria	PL.IO PAN	Profesor, Scientific Diver	Biology
Wurz	Erik	NL.WUR	Scientist	Biology
Zeising	Ole Marten	DE.AWI	Scientist	Glaciology

A.3 LOGISTICS SUPPORT, WINTERING TEAM

Name/ Last name	Vorname/ First name	Institut/ Institute	Beruf/ Profession	Fachrichtung/ Discipline
Alarcón	Emilio	CL.IDEAL	Technician	Biology
Anger	Johann	DE.LAEISZ	Engineer	ÜWI2024
Ascione	Rocco	ENEA-RO	Logistic coordinator / station leader Mario Zucchelli station	Mechanicla engineer
Bello	Cynthia	PER.UCdS	Profesor	Glaciology
Betz	Maximilian	DE.AWI	Engineer	Logistics
Bianchi Fasani	Gianluca	IT.ENEA-RO	Logistic	Geology / Logistics
Boesch	Tim	DE.AWI	Scientist	ÜWI2024
Brehmer-Moltmann	Johanna	DE.AWI	Scientist	ÜWI2025
Carnevale	Massimo	IT.ENEA-TR	Logistic	Technician
Colino	Danilo	IT.ENEA-EI	Camp manager BEOI	Mountain Guide Lieutenant
Conrat Fuentes	Pablo Luis	DE.AWI	Scientist	ÜWI2024
Einarsson	Einar Magnus	IS.Arctictrucks	Technician	Logistics
Espinoza Gallardo	Pablo	CL.INACH	Chief Scientist (Escudero Station)	Biology
Fabian	Laura	DE.LAEISZ	Cook	ÜWI2024
Falkenhahn	Martin	DE.LAEISZ	Technician	Logistics
Gay	Inès	FR.IPEV	Paramedic	Nursing
Gehrmann	Martin	DE.AWI	Engineer	Logistics
Goicoetchea	Pierre	FR.IPEV	Technical manager Concordia station	Marine engineer
Guidarelli	Giulano	IT.ENEA-RO	Logistic	Technician
Gutting	Julia Maria	DE.AWI	Physician	ÜWI2025
Hess	Sebastian	DE.LAEISZ	Technician	Logistics
Hoffmann	Thomas	DE.LAEISZ	Engineer	Logistics
Horn	Alexander	DE.MWB	Technician	Logistics
Hornik	Jonas	DE.LAEISZ	Technician	Logistics
Immoor	Sebastian	DE.AWI	Technician	Logistics
Jensen	Eva	DE.LAEISZ	Housekeeping	Logistics
Kapitel	Christoph	COM.Kässbohrer	Technician	Logistics
Kerschner	Regine	DE.LAEISZ	Engineer	ÜWI2025
Koeppen	Thorben	DE.LAEISZ	Cook	ÜWI2025
Köhler	Peter	DE.AWI	Field Operation Manager	Logistics

Name/ Last name	**Vorname/ First name**	**Institut/ Institute**	**Beruf/ Profession**	**Fachrichtung/ Discipline**
Lauckner	Markus	DE.Etteplan	Engineer	Logistics
Lauer	Jörg Hermann	DE.LAEISZ	Technician	ÜWI2024
Lindner	Florian	DE.MWB	Technician	Logistics
Londoñe	Pablo	PER.RREE	Scientific Coordinator & Chief Scientist Machu Picchu Station (ECAMP)	Biology
López	Andrés	CL.INACH	Deputy Director (INACH)	
Massot	Francisco	ARG.IAA	Chief Scientist (BAC)	Biology
Matz	Thomas	DE.AWI	Field Operation Manager	Logistics
Mitteregger	Christian	DE.LAEISZ	Technician	Logistics
Möller	Thomas	DE.BauWerk	Technician	Logistics
Müller	Jozef	DE.AWI	Scientist	ÜWI2025
Nüsse	Amelie Cathrine	DE.AWI	Scientist	ÜWI2024
Oblender	Andreas	DE.LAEISZ	Technician	Logistics
Pech	Caroline	BE.FairWind	Engineer	Logistics
Petersen	Christoph	DE.AWI	Technician	Logistics
Quartino	María Liliana	ARG.IAA	Logistics Coodinator Carlini Station (BAC);	Biology
Rath	Sönke	DE.LAEISZ	Engineer	Logistics
Regnery	Julia	DE.AWI	Scientist	Logistics
Reich	Stefan	DE.LAEISZ	Technician	Logistics
Riess	Jan Felix	DE.LAEISZ	Inspector	Logistics
Roberto	Molina	CL.INACH	Navigation Escudero	Logistics
Rodriguez	Silvia	ARG.IAA	scientific coordinator BAC; scientist	Logistics BAC
Rohde	Lea Mareile	DE.LAEISZ	Engineer	Logistics
Rotthäuser	Siegfried	DE.IGH	Engineer	Logistics
Ruiz	Eduardo	ARG.IAA	Chief Scientist (BAC)	Oceanography
Sadeghzadeh	Meysam	DE.Etteplan	Engineer	Logistics
Sans Coll	Cristina	DE.AWI	Engineer	Logistics
Scipinotti	Riccardo	ENEA-RO	Logistic coordinator / station leader Concordia station	Electrical engineer
Schengber	Alexander	DE.LAEISZ	Engineer	ÜWI2025
Schenk	Thomas	DE.LAEISZ	Engineer	ÜWI2025
Schötz	Johannes	DE.LAEISZ	Technician	ÜWI2024
Schröder	Christian Daniel	DE.AWI	Scientist	ÜWI2025
Stranzinger	Viktoria	DE.LAEISZ	Cook	Logistics
Trimborn	Klaus	DE.LAEISZ	Technician	Logistics
Trost	Volker	DE.BauWerk	Technician	Logistics
Ulrich	Alejandro	ARG.IAA	Chief Scientist (BAC)	Oceanography
Vásquez	Angélica	CL.IDEAL	Secretarian	Logistics

Name/ Last name	**Vorname/ First name**	**Institut/ Institute**	**Beruf/ Profession**	**Fachrichtung/ Discipline**
Weber	Anja	DE.AWI	Physician	ÜWI2024
Weis	Lukas Michael	DE.AWI	Scientist	ÜWI2025
Wilhelms	Armin	DE.LAEISZ	Technician	Logistics
Witting	Simon	DE.LAEISZ	Technician	Logistics
Yakovlev	Andrey	DE.AWI	Scientist	ÜWI2024

A.4 AUTHORS WITHOUT EXPEDITION PARTICIPATION

Name/ Last name	Vorname/ First name	Institut/ Institute	Beruf/ Profession	Fachrichtung/ Discipline
Alemany	Olivier	FR.IGE	Drill Engineer	Mechanical Engineering
Arndt	Stefanie	DE.AWI/DE.Uni-Hamburg	Professor	Sea Ice Physics
Barbante	Carlo	IT.ISP-CNR	Project Coordinator	Glaciology Geochemistry
Barsby	Poppy	DE.CHARITE	Scientist	Medicine
Behrens	Melanie	DE.AWI	Analytical Engineer	Chemistry
Blard	Pierre Henri	BE.ULB	Scientist	Glaciology Geology
Boeckmann	Grant	DK.PICE	Drill Engineer	Mechanical Engineering
Brauns	Katharina	DE.CHARITE	Scientist	Medicine
Brenner	Matthias	DE.AWI	Scientist	
Burkhardt	Elke	DE.AWI	Scientist	Oceanography
Chaillot	Justin	FR.LSCE	Scientist	Glaciology Physics
Choukér	Alexander	DE.Med.Uni-Muenchen	Scientist	Medicine
Dahl-Jensen	Dorthe	DK.PICE	Scientist	Glaciology Geophysics
Dreossi	Giuliano	IT.ISP-CNR	Analytical Engineer	Chemistry
Drews	Reinhard	DE.UNI-Tuebingen	Scientist	Glaciology
Eberlein	Lutz	DE.TUDresden	Scientist	Geosciences
Eckermann	Oliver	DE.TROPOS	Scientist	Chemistry
Eisen	Olaf	DE.AWI/DE.UNI-Bremen	Professor	Glaciology
Fabry	Ben	DE.FAU	Professor	Physics
Fischer	Hubertus	CH.UNIBE	Scientist	Glaciology Physics
Friedl-Werner	Anika	DE.CHARITE	Scientist	Medicine
Fripiat	François	BE.ULB	Scientist	Glaciology Geology
Fromm	Tanja	DE.AWI	Scientist	Geophysics
Gillet	Nick	UK.BAS	Scientist	Glaciology
Haas	Christian	DE.AWI/DE.Uni-Bremen	Professor	Sea Ice Physics

Name/ Last name	**Vorname/ First name**	**Institut/ Institute**	**Beruf/ Profession**	**Fachrichtung/ Discipline**
Hames	Océane	CH.SLF/EPFL	PhD student	Physics
Hansen	Steffen Bo	DK.PICE	Drill Engineer	Mechanical Engineering
Hanz	Ulrike	DE.AWI	Scientist	Biology
Hattermann	Tore	NO.NPolar	Scientist	Oceanography
Henning	Silvia	DE.TROPOS	Scientist	Chemistry
Hetzer	Stefan	DE.BCAN	Scientist	Medicine
Hörhold	Maria	DE.AWI	Scientist	Glaciology Geophysics
Hofstede	Coen	DE.AWI	Scientist	Glaciology
Hyomin	Kim	EDU.NJIT	Scientist	Geophysics
Kim	Khan-Hyuk	KR.KHU	Scientist	Geophysics
Kühn	Simone	DE.MPIB-Berlin	Scientist	Medicine
Küster	Anette	DE.UBA	Scientist	Biology
Koschorreck	Jan	DE.UBA	Scientist	Chemistry
Kwon	Hyuck-Jin	KR.KOPRI	Scientist	Geophysics
Laepple	Thom	DE.AWI	Scientist	Glaciology Physics
Landais	Amaelle	FR.LSCE	Scientist	Glaciology Physics
Le Bohec	Céline	MC.CSM	Scientist	Biology
Lehning	Michael	CH.SLF/EPFL	Professor	Physics
Lessard	Marc	EDU.UNH	Scientist	Physics
Moser	Dominique	DE.Med.Uni-Muenchen	Scientist	Medicine
Mulvaney	Robert	UK.BAS	Scientist	Glaciology Geophysics
Neudert	Mara	DE.AWI	PhD student	Sea Ice Physics
Panichi	Saverio	IT.ENEA-BO	Camp manager	Glaciology Informatics
Parrenin	Frédéric	FR.IGE	Scientist	Gllaciology Geophysics
Pattyn	Frank	DE.ULB	Scientist	Glaciology
Peik	Sören	DE.HS-Bremen	Scientist	Engineering
Reppert	Valerie	DE.AWI	PhD student	Glaciology
Richter	Claudio	DE.AWI	Scientist	Biology
Richter	Sebastian	DE.FAU	Scientist	Physics
Riecke	Bernhard	CA.SFU	Scientist	Medicine
Ritz	Catherine	FR.IGE	Scientist	Glaciology Geophysics
Scheinert	Mirko	DE.TUDresden	Scientist	Geosciences
Schlindwein	Vera	DE.AWI	Professor	Geophysics
Schmale	Julia	CH.EPFL	Professor	Environmental engineering
Schmithüsen	Holger	DE.AWI	Scientist	Meteorology
Shprits	Yuri	DE.GFZ	Scientist	Geosciences

Name/ Last name	**Vorname/ First name**	**Institut/ Institute**	**Beruf/ Profession**	**Fachrichtung/ Discipline**
Spanswick	Emma	CU.UCA	Scientist	Geosciences
Stahn	Alexander	DE.CHARITE	Scientist	Medicine
Steen-Larsen	Hans Christian	NO.UBE	Scientist	Glaciology Physics
Steinhage	Daniel	DE.AWI	Scientist	Glaciology
Stenni	Barbara	IT.ISP-CNR	Scientist	Glaciology Geochemistry
Thomisch	Karolin	DE.AWI	Scientist	Oceanography
Tison	Jean-Louis	BE.ULB	Scientist	Glaciology Geology
Van Opzeeland	Ilse	DE.AWI	Scientist	Oceanography
Wex	Heike	DE.TROPOS	Scientist	Chemistry
Witt	Gesine	DE.HAW	Scientist	Chemistry
Wolff	Eric	UK.UCAM	Scientist	Glaciology Chemistry
Xie	Zhiyong	DE.HEREON	Scientist	Chemistry
Zanoni	Daniele	IT.ISP-CNR	Scientist	Glaciology Geochemistry
Zigone	Dimitri	FR.EOST/ITES FR.CNRS	Scientist	Geophysics
Zwicker	Sarah	DE.ZMT	PhD student	Environmental Science

Die **Berichte zur Polar- und Meeresforschung** (ISSN 1866-3192) werden beginnend mit dem Band 569 (2008) als Open-Access-Publikation herausgegeben. Ein Verzeichnis aller Bände einschließlich der Druckausgaben (ISSN 1618-3193, Band 377-568, von 2000 bis 2008) sowie der früheren **Berichte zur Polarforschung** (ISSN 0176-5027, Band 1–376, von 1981 bis 2000) befindet sich im electronic Publication Information Center **(ePIC)** des Alfred-Wegener-Instituts, Helmholtz-Zentrum für Polar- und Meeresforschung (AWI); see https://epic.awi.de. Durch Auswahl “Reports on Polar- and Marine Research“ (via “browse”/”type”) wird eine Liste der Publikationen, sortiert nach Bandnummer, innerhalb der absteigenden chronologischen Reihenfolge der Jahrgänge mit Verweis auf das jeweilige pdf-Symbol zum Herunterladen angezeigt.

The **Reports on Polar and Marine Research** (ISSN 1866-3192) are available as open access publications since 2008. A table of all volumes including the printed issues (ISSN 1618-3193, Vol. 377-568, from 2000 until 2008), as well as the earlier **Reports on Polar Research** (ISSN 0176-5027, Vol. 1–376, from 1981 until 2000) is provided by the electronic Publication Information Center **(ePIC)** of the Alfred Wegener Institute, Helmholtz Centre for Polar and Marine Research (AWI); see URL https://epic.awi.de. To generate a list of all Reports, use the URL http://epic.awi.de and select “browse”/”type” to browse ”Reports on Polar and Marine Research”. A chronological list in declining order will be presented, and pdf-icons displayed for downloading.

Zuletzt erschienene Ausgaben:

Recently published issues:

807 (2026) Expeditions to Antarctica: ANT-Land 2024/25 NEUMAYER STATION III, Kohnen Station and Field Campaigns, edited by Julia Regnery, Peter Köhler, Thomas Matz and Christine Wesche

806 (2026) The Expedition PS151 of the Research Vessel POLARSTERN to the Atlantic Ocean in 2025, edited by Karen H. Wiltshire, Peter Croot and Angelika Dummermuth with contributions of the participants

805 (2026) The IsoPerm Project: Expedition to the Klondike (Yukon, Canada) in 2023, edited by Thomas Opel with contributions of the participants

804 (2025) The Expeditions of the Research Vessels LITTORINA, LUDWIG PRANDTL and MYA II to the Elbe River, Elbe Estuary and German Bight in 2024, edited by Ingeborg Bussmann, Eric Achterberg, Holger Brix, Norbert Kamjunke, Björn Raupers and Tina Sanders with contributions of the participants.

803 (2025) The Expedition PS148 of the Research Vessel POLARSTERN to the Arctic Ocean in 2025. Edited by Jennifer Dannheim with contributions of the participants.

802 (2025) Arctic Land Expeditions in Permafrost Research in 2024. Edited by Anne Morgenstern, Lutz Schirrmeister and Milena Gottschalk with contributions of the participants.

801 (2025) The Expedition PS143/2 of the Research Vessel POLARSTERN to the Arctic Ocean in 2024. Edited by Katja Metfies with contributions of the participants.

800 (2025) The Expedition PS143/1 of the Research Vessel POLARSTERN to the Arctic Ocean in 2024. Edited by Frank Wenzhöfer with contributions of the participants.

799 (2025) The Expeditions PS147/1 and PS147/2 of the Research Vessel POLARSTERN to the Atlantic Ocean in 2025. Edited by Yvonne Schulze Tenberge and Björn Fiedler with contributions of the participants.

798 (2025) The Expedition PS146 of the Research Vessel POLARSTERN to the Weddell Sea in 2024/2025. Edited by Olaf Boebel with contributions of the participants.

ALFRED-WEGENER-INSTITUT
HELMHOLTZ-ZENTRUM FÜR POLAR-
UND MEERESFORSCHUNG

BREMERHAVEN

Am Handelshafen 12
27570 Bremerhaven
Telefon 0471 4831-0
Telefax 0471 4831-1149
www.awi.de

HELMHOLTZ